# BAT SWING ANALYSIS IN CRICKET

**Ajay Krishno Sarkar**

**2013**

# Bat Swing Analysis in Cricket

by

**Ajay Krishno Sarkar**

**M. Eng (EEE), Mie University, Japan**

**Griffith School of Engineering**

**Science, Environment, Engineering and Technology**

**Griffith University**

**Submitted in fulfilment of the requirements of the degree of**

**Doctor of Philosophy**

**July 2013**

# ABSTRACT

Technology in sports has had great impact during the last two decades. A lot of time, human power and cost are involved in existing batting research methods. The reliability and usefulness of these outcomes is prone to error and dependent on the human ability. In this project, miniature, inexpensive, user and match-friendly inertial sensors were used to extract the cricket bat swing features. The data was validated through existing tools. The object of this work was to demonstrate that accelerometers offer significant advantages in cricket batting analysis. Experimental and theoretical work involved ball free and ball-hit swing profiles.

Bat swing was analysed using accelerometer sensors and was validated using a rigid pendulum. Good agreement was obtained between the measured angles by inclinometer and static sensor (r=0.99), and between the swing angles estimated from equation and dynamic sensor (r=0.88). Hits on the pivot arm showed the optimum contact location to maximize the energy transfer to the ball. A non-linear pendulum equation with moving pivot was solved numerically to model for swing angles in straight drive. The derived equation showed good agreement with the acceleration data (r=0.91). The effect of initial angular velocity, the radius of rotation and phase angle of the pivot on the acceleration profile were strongly correlated with the maximum acceleration peak (r≡0.99). Repetitive bat swings in a straight drive by a novice batter showed that the bat position and orientation can be identified. The results were validated by video. Sweet-spot impacts from bat-ball contacts in defensive strokes (n=61) by five novice batters were determined by the sensor data. An approximate equation for bat angle (cosine squared function of time) during the straight drive was validated with video (r=0.99). The derived acceleration profile matched to the sensor data. Using Bland Altman covariance correlation, correlation coefficients 0.95 and 0.98 were found individually for each batter and among the batters respectively. The results from this experiment allowed the applied force to be calculated. The effect of back-lift height in defensive stroke over the control of bat alignment in bat-ball contact was investigated. Sensor recorded three amateur batters

defensive strokes (n=30) data revealed a detrimental effect of higher back-lift height in bat alignment. The sensor data and video data for a planar orthodox straight drive was analysed using rigid body dynamics using a decision matrix. The maximum bat acceleration occurs when the radius of rotation is maximized. Video and sensor data showed good matching (r=0.92) and the translational and rotational acceleration components dominate on different parts of bat swing. The relationship between bat and wrist sensors data in defensive strokes (n=5) by five batters (one sub-elite, two amateurs, two novices) was investigated to determined the coupling between the hands and the bat before and after ball-contact. Sub-elite and amateurs data showed that the top hand was more strongly coupled with the bat than the bottom hand (slope>0.64 for top and slope>0.4 for bottom hand of individual regression lines). Other novices showed poor coupling and jarring of hands. A linear relationship (r>0.7) was found between wrists and bat velocities for all batters. Integrating the sensors with wireless connectivity can provide feedback to the coach about the quality of stroke play.

# STATEMENT OF ORIGINALITY

This work has not previously been submitted for a degree or diploma in any university. To the best of my knowledge and belief, the thesis contains no material previously published or written by another person except where due reference is made in the thesis itself.

Ajay Sarkar

5 July 2013

# ACKNOWLEDGEMENTS

# TABLE OF CONTENTS

# LIST OF FIGURES

# LIST OF TABLES

# GLOSSARY AND ACRONYMS

| Terms | Basic Description |
|---|---|
| Anterior-Posterior | The axis is lying in the normal direction of human ambulation. |
| FFT | Fast Fourier Transform, is an algorithm to compute the discrete Fourier transform (DFT) and its inverse. FFT substantially reduces the processing required to perform a Fourier Transform. |
| HD converter | This is software that re-arrange or modify segments of video to form another piece of video. Some of the goals of the conversion are the isolation of desired footage, the arrangement of footage in time to synthesize a new piece of footage etc. |
| ICC | International Cricket Council is an international governing body of  cricket. On 15 June 1909 representatives from England, Australia and South Africa met at Lord's and founded the Imperial Cricket Conference. In 1965, the Imperial Cricket Conference was renamed the International Cricket Conference and new rules adopted to permit the election of countries from outside the Commonwealth. |
| Mediolateral | This is an axis that is perpendicular to the direction of forward and backward movement of an object and the vertical axis. This axis lie left-right to human being. |
| Pixel | It is a physical point in a raster image. Pixels are used to describe the picture elements of video images. The address of a pixel corresponds to its physical coordinates. LCD pixels are manufactured in a two-dimensional grid. |

| | |
|---|---|
| Signal Spikes | The comparatively large upward or downward movement of a value level in a short period. |
| Vertical | This is an axis that is perpendicular to ground or parallel to gravity direction. |

# 1 <u>INTRODUCTION</u>

Research in sport, exercise and related topics has grown enormously over the past 30 years. Spectators used to think that any sporting activities was just for enjoyment, passing leisure time, and keeping the body fit and away from disease. More recently the importance of sporting activities and its associated planning and design is seen as engendering high levels of prestige, entertainment and commercial return to the sport at national and international level. Sports bioengineering is now a popular field of study and research in universities. Many of the courses in this field involve a multidisciplinary study of sport and exercise, crossing the biophysical sciences, social and psychological sciences and the humanities. Alongside the growth of popularity of sport-focus courses, research activity has increased. There are five main areas of research and study in sport and exercise courses: biomechanics, exercise physiology, pedagogy, psychology and sociology. Biomechanics includes kinematics, kinetics, impacts, force, work, energy and power. Exercise physiology considers nutrition and biochemistry, homeostasis muscles, strength and power, energy systems, energy balance and body composition, principles of training, fitness for sport and health, growth, maturation, motor development and learning. Pedagogy deals with physical education, instruction, learning, curriculum, and assessment. Psychology considers motivation, adherence, physical activity and mental health, immediate emotional and affective responses to exercise, coping in sport, experience, leaders and leadership, communication. Finally the area of sociology comprises class, gender, 'race' and ethnicity, disability, the body, identity and globalization. These are many research opportunities aimed at gaining a full understanding of the scientific aspects of sport. In particular this thesis relates to the biomechanics of bat swing in cricket using a novel methodology composed of tiny sensors.

## 1.1 Cricket research

The game of cricket is defined by a set of international rules [1]. It is a striking sport, where the players undertake three activities: bowling, batting and fielding. The match

of this sport is played between two teams of eleven players of each on an oval-shaped grass field. There is a strip of Hundred Turf 22 yards (20.12 m) long in the centre of the field. This is called a cricket pitch and each end of it a set of three tubular stakes are stuck upright in the earth, called "stumps". There are two small pieces of wood, called bails, balanced across the top of each stump set. The set of stumps with bails are called the wicket and a batter stands in front of a wicket with a long wooden bat (the images [2] and dimensions shown in Fig. 1.1). The weight of the bat used in this research was 1.3 kg and the axes referred to bat dimensions (for middle image) are shown in Fig. 1.1. The X-, Y-, and Z-axis are along bat's height, width and normal to the bat hitting face (as shown the blade surface in the first image) respectively. The centre of mass (CoM) of the bat was found at 32.5 cm and its blade was divided into five regions (Toe: 0-11 cm; Bottom: between 11-22 cm; Middle: 22-33 cm; Top: between 33-44cm; Top above: 44-58cm) measured from its end of toe. The height of the bat was 85 cm of which the blade was 58 cm.
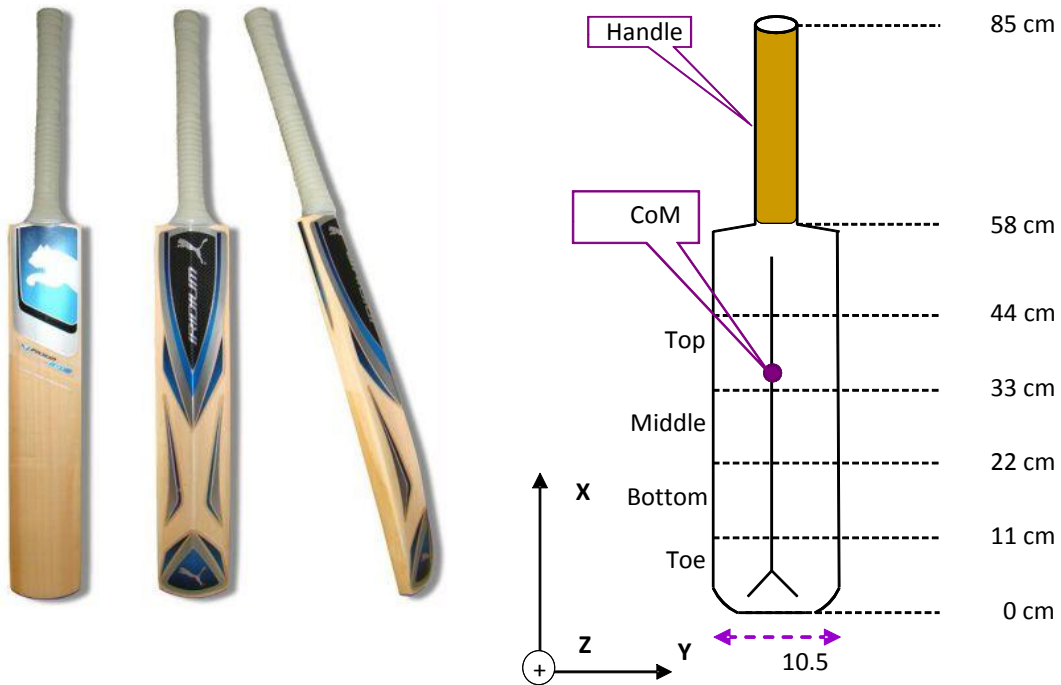


**Fig. 1.1**    Cricket bat images (left) with the view of hitting face, back, side and the dimensions of the bat with the axes definition (right) referred to middle image used in this research. The images are provided from [2] as one of those bats of height 85 cm was used for the experiments. The weight of the bat was 1.3

kg and the centre of mass (CoM) was found at 34.5 cm from the bat toe. The bat's blade of length 58 cm were divided into five regions (Toe: 0-11 cm; Bottom: between 11-22 cm; Middle: 22-33 cm; Top: between 33-44cm; Top above: 44-58cm) measured from its end of toe.

The two batters stand in front of the wickets at either end of the pitch; one who waits for a bowler to bowl the hard, fist-sized ball attempts to hit or defend the ball to score runs or save the wicket of being touched by the ball. The delivery of ball by the bowler towards the stumps is termed bowling. The purpose of bowling is to dismiss the batter by hitting the wicket with the bowled ball or catching the flying ball by the fielders before it touches the ground after being hit. If a ball is blocked by the leg of the batter when likely to hit the wicket, then the batter is out (leg before wicket). But if the batter hits the ball and both of the batters run to the opposite ends of the pitch then a score is made. Multiple runs can be made from one hit. If the fielder throws the ball and it touches at one of the wickets before a running batter crosses a line near the wicket the batter is termed as "run out" [3].

The main activities results in scoring runs by the batters or dismissing. The main competition is mainly more one-to-one (e.g. bowler to batter) in cricket [4]. Over the last several decades much research has concentrated on the performance of batters and bowlers, and less on the fielders.

### 1.1.1 Cricket research endeavours

Cricket research requires well planned multivariate research in order to describe and understand the outcome of training effects in terms of a wide range of mental skills, motor skills and motor fitness. This research answers questions of interest and concern to coaches and players through the following model [5]:

Task 1: The motivation for research-what is the research question?

Task 2: Identify the cause of the problem - more than just technique.

Task 3: Develop technique enhancement.

Task 4: Educate the relevant population (batter, coach, parents, media and other stake holders). Other models expand on this step to include such factors as efficacy of approach in the field setting.

Task 5: Evaluate the effectiveness of the coaching.

Cricket research involves the two main streams of science and technology. Prevailing cricket science research endeavours are more about the key attributes of biomechanics and motor control of cricket skills, the psychology of team dynamics, performance analysis and cricket injuries to meet the physiological and psychological demands of the game [4]. On the other hand, the technological aspects of cricket research focus mainly on injury risk or player performance.

The need for research focusing on biomechanics and motor control, psychology and physiological aspects in cricket science and injury risk or performance varies according to the demand of all three areas of play; bowling, batting and fielding. For instance, the importance of biomechanics and motor control research is very evident in batting and bowling but not so much in the fielding context; even in bowling and batting, the latter demands far more motor control than the former. In fielding, the physiological demand on a slip fielder is less than psychological ones.

As cricket involves an intermittent action by the participants, the research requires the knowledge about the game relating to coordination, control and skills, and evaluating the impact of practising those attributes in training and in match performance. The research should incorporate the study of 'when', 'where' and 'how' in the relationship between perception and action. For instance, research might characterize a good batting technique expressing the optimal position to play the shot, the position of the head, body, and feet, and the swing of the bat at the ball to make fruitful contact; but at the same time it should document the method to accomplish these tasks instinctively and overcome any constraints.

Many of the greater cricket players have exhibited techniques not necessarily matching recommendations in the coaching manuals (Conn, 2009 as in [6]). For

instance, there are a wide variety of different techniques adopted by skilled and lesser-skilled batters to play a particular cricket stroke. Cricket research should therefore formulate techniques and measures for coaching programmes applicable to all the players with different skill playing styles levels.

Cricket research should aim to fill the gap between science and practice, by providing evidence based documents describing the underlying mechanism of the techniques for skill development. A feedback tool for the participant of a performed task can be a vital factor for the cricket research objectives. This tool will allow a novice to develop skills which follow a template. Not only for the coaches and participants, research should focus on educating the parents and media by exploring the social and mental supports for skill development from the root level, in order to identify people with playing potential.

### 1.1.2 Cricket research directions

The following topics of research are being conducted in the science of cricket [5].

(a) Sport and health psychology

Research settings: the development of psychological skills for junior cricketers (Tobin and Gordon as cited in [5]), and 'mental toughness' for high performance batters (Gucciardi and Gordon, 2009 as cited in [5]).

(b) Exercise physiology

Research settings: heat acclimatization/acclimation in preparing high performance batters, fast bowler movement characteristics in a One Day International (1 bowler over 12 matches) (Peterson et al., 2009a as cited in [5]), ground movements and the Twenty20 cricketer (18 batters over 30 innings) (Peterson et al., 2009b as cited in [5]), and preparing cricketers for various match formats (Peterson et al., 2010 as cited in [5]).

(c) Motor learning

Research settings: skill analysis (Renshaw et al., 2007 as cited in [5] – batting against bowler or ball machine), anticipation and batting performance (Weissensteiner et al., 2008 as cited in [5] – skilled and lesser skilled U15, U20 and adult batters completed a temporal occlusion task), learning new skills: talent development programs should avoid the notion of common optimal performance models (Phillips et al., 2010 as cited [5]), and modifying techniques (Elliott & Khangure, 2002; Ranson et al., 2009 as cited in [5]).

(d) Sports medicine

Research settings: the workload and injury (Orchard et al., 2009; Saw et al., 2009 as cited in [5]), and the role of muscle morphology and loading on the bowlers' back (Hides et al., 2007; Visser et al., 2007 as cited in [5]).

(e) Biomechanics

Research settings: performance optimisation; spin bowling (Chin et al., 2009 as cited in [5]), performance optimisation; fast bowling (Middleton et al., in progress as cited in  [5]), lower back injury reduction in male and female fast bowlers (Stuelcken et al., 2010 as cited in [5] – data collected on 26 high-performance female fast bowlers; Portus et al., 2007 as cited in [5]), legality and bowling (ICC approach as cited in [5]).

## 1.1.3 Research methods

The method and tools of data collection, and the data analysis techniques are addressed using several examples outlined in section 1.1.2.

### 1.1.3.1 Methods:

Both qualitative and quantitative methods of research are used in cricket. Historical, comparative, descriptive and evaluation methods are qualitative, while the experimental (also known as cause and effect method) method is quantitative [7].

The **Historical method** deals with the past events in order to establish facts and draw a conclusion; for instance, Gucciardi et al. [8] interviewed eleven Indian and five Australian male cricketers to assess their previous cricket match playing histories in correlation to intelligence, attentional control, resilience and self-belief, with dispositional flow, hardiness, and resilience being positive and athlete burnout negative.

The **Comparative method** employs historical research to compare the present situation and supplies researchers with a natural experiment in which non-essential phenomenon is eliminated by looking at the examples. For instance, Orchard et al. [9] conducted a cohort study for comparing future injury risk between high and low workload bowlers using an annual ongoing injury survey to record injuries in contracted first-class players. The analysis was performed for pace bowlers over the 10 seasons 1998-1999 to 2007-2008 inclusive [9]. The objective of this study was to judge the hypothesis that high bowling workload in cricket leads to increased risk of bowling injury. The findings from this study suggested that high workload resulting in "penalty" may not be fully realized immediately, but may be evident up to a month after the single high overload. This study also disputed that One Day Internationals (ODI) played in Australia have the highest injury incidence of all matches (as reported previously), which is somewhat surprising as bowlers are limited to 10 overs in these matches. However, the comparative method can be conducted at both a macro level (revolutions) and micro level (individual experiences).

The **Description method** deals with observation as a means of collecting data. It seeks to comment on the normal situation and predict the future on the basis of biased questions in interviews, questionnaires and selective observation of events. For instance, Weissensteiner et al. [10] collected data by interviewing three adult cricketers, two adult sub-elite cricketers, five elite coaches and four experienced cricket administrators to generate a conceptual model. A theory was released from the collected data that encapsulated skill components and factors critical to expertise development. It highlighted key factors about the development of expertise in cricket

7

batting and about the transition from "cricket scholar" to "expert". This study reported the co-existence of five key factors which shape the successful progression along the pathway to expertise. Those factors were stated as Socio-Development (Contextual) Factors, Psychological (Cognitive) Factors, Visual Perceptual (Anticipation) Skills, Technical (Motor) Skill, and Intrinsic Motivators.

Outcomes from the **Evaluation method** do not include 'how things are' and 'how they work'; rather they represent meaningful constructions of the things that contribute to the situation. For instance, Christie el al. [11] assessed selected physiological variables including heart rate, ventilation, oxygen uptake and metabolic carbon dioxide production during batting in a simulated high-scoring 1-day cricket game. This study reported that all of the physiological responses increased significantly from the first to the second over while heart rate continued to increase significantly until the end of the third over after which it stabilized. The authors speculated that the factors that affected the heart rate were emotional state and food intake. This study measured mean oxygen uptake during the work bout and increases in breathing frequency. The increased breathing frequency had a greater impact on the ventilation response that increased from the first to the last over. This study demonstrated that the training plays an important role in expertise development although technical skills are still the dominant factors.

In the **Experimental method**, researchers attempt to isolate and control every relevant condition of an event to be investigated to observe the effects. This method is composed of several sub-classes including pre-experimental, true experimental, quasi-experimental, correlation and ex post facto methods.

Assumptions are made in pre-experimental methods despite the lack of control over the variables; for instance, Stuelcken et al. [12] investigated whether there was an association between the movement patterns of the thorax relative to the pelvis during the delivery stride of the bowling action and low back pain in elite female fast bowlers. Collecting three-dimensional trunk kinematic data from different bowling actions and low back pain history of the bowlers, this study documented which action

and related kinematics leads to more back pain. This study sought to provide information for coaches and support staff for a better understanding of female bowling action, and facilitate better screening practices.

In the true experimental method, rigorous checking of the identical nature of groups takes place before testing the influence of a variable under controlled circumstances. For instance, Dias et al. [13] compared the initial movement patterns between elite and amateur batters. This study showed that elite batters had a stable back lift angle during the initial movement, while amateur batters had reduced back lift angle and tended to initiate a second or double back lift prior to final ball contact. This tendency of amateur batters was confirmed by the double peaks in the bat angle profile in back lift time. In addition, they found that amateurs tended to have a higher average back lift angle at all times prior to impact.

In the quasi-experimental method, not all conditions of the true experiments are fulfilled and the shortcomings are identified. For instance, Hides et al. [14] checked the existence of asymmetry of trunk muscles and deficits of motor control among elite cricketers with and without Low Back Pain (LBP). The independent variables in this study were the separate 'groups' (symptomatic and asymptomatic) and 'cricket position' (fast bowler versus the rest of the squad). The dependent variables were the cross-sectional areas (CSA) of the quadratus lumborum (QL), lumbar erector spinae plus multifidus (LES + M) and psoas muscles, the thickness of the internal oblique (IO) and transversus abdominis (TrA) muscles, and the amount of lateral slide of the anterior abdominal fascia. Participants attended a national training camp and MRI (Magnetic Resonance Imaging) and questionnaire assessments were completed in a hospital setting. This study provides evidence of muscle asymmetry and impaired motor control in elite cricketers having LBP, and a motor control approach for rehabilitation was seen to be effective. It also documented new insights into trunk muscle size and function of elite cricketers. This study confessed its inability to comment on cause and effect in relation to trunk muscle asymmetries and LBP. The researchers suggested that future research was required to clarify the complex relationships between pain and pathology and specific muscle adaptation occurring in individual sports so that optimum training techniques, injury prevention and

rehabilitation of sporting injuries could be produced.

The correlation method looks at the cause and effect relationship between two sets of data; for instance, Elliott & Khangure [15] worked to identify the relationship between the incidence of lumber disk degeneration and bowling technique after 3 years of educational intervention. Two groups of fast bowlers from Western Australian fast-bowling development squads participated as subjects and biomechanical data and MRI scans data were gathered for this study. This study reported that the level of shoulder counter rotation was reduced effectively by a 3-year intervention comprising small group coaching and an annual seminar which controlled the level of disk degeneration for young fast bowlers. The Ex post facto method interpreted the cause by observing its effect when reversing the experiment; for instance, Visser et al. [16] attempted to find the physical explanation of the observed correlation of lesions in the L4 pars with the presence of hypertrophy in the contralateral Quandratus Lumborum (QL) muscle in fast bowlers. In this study the amusculoskeletal Finite Element Model (FEM) was developed to assess the potential of the QL to influence the stresses in the pars estimating the forces and moments on the L3 and L4 vertebrae in six postures during fast bowling. By showing the gathered data this study speculated that QL asymmetry might have the potential to reduce the stresses in the pars. However, the authors commented that the relation between QL asymmetry and L4 pars fractures cannot be determined with certainty without having more specific knowledge of fast bowlers' lumbar spine muscle size and activation.

### 1.1.3.2 Data collection and analysis tools:

In qualitative research, most data collection tools are questionnaires, interviews, data archives, past histories etc. However, some technological tools are also involved in a passive way. In quantitative cricket research, most cases utilise technological tools as a central part of the system in a direct way or indirect way. Quantitative research might also require the data collection tools used in qualitative research as an optional method for the validation of the results. Qualitative research sometimes uses technological tools for checking a hypothesis derived from the methodology adopted to validate the data or defining the direction ahead. Qualitative research validates the

results derived from the knowledge and experience of the person who observes and analyses the selected parameters related to a performance, while quantitative research allows validation from a scientific perspective providing numerical results.

Both visual and software tools are being used to collect data in cricket research. Existing visual tools are composed of instruments, materials and human beings which form the protocol of the data collection system which varies according to the research goal and settings required. In quantitative research the visual tools are usually dominated by the technology and its advancement. High-speed film followed by digital video, and more recently passive optical analysis systems (as a supplementation of image-based approaches), such as Vicon, Motion Analysis Corporation etc., active optical analysis systems, such as Optitrack, Skill Technologies, Selspot, MOTECK etc., magnetic-based systems, such as Polhemus-Flock of Birds, etc. are available visual tools. Ball machine, refractive spectacles, markers, specially designed cricket implements and accessories (like bat, ball, helmet, gloves etc.) are also associated with experimental tools. These visual tools are linked to software-based tools developed commercially (like ViconPeak, Ariel, SIMI etc.) or by university students within a research group. The potential and needs of visual tools require storing, indexing and filtering of captured data to measure the kinematic and kinetic signature of a specific performance in cricket. Software associated with visual tools allows the captured image to be converted into two- and three-dimensional coordinates enabling the researcher to extract positional instantaneous.

The data analysis tools used in cricket research are developed from sciences and mathematics, while the interpretation of the results are based on underlying physics phenomenon or existing research evidence. The mathematical analysis requires digitizing the data recorded by the visual tools. Biomechanical models based on vector algebra principles are used to extract the kinematics and kinetics of the variable to be addressed. The branch of biomechanics that describes human motion mainly via image analysis is called kinematics. In cricket, kinematics describes motion in terms of space and time, and it provides information regarding the position and the rate of movement of cricketer limbs or cricket implements (bat and ball)

used. While kinematics describes movement, kinetics explains the cause and effect in movement. Statistical analysis in cricket research is an essential part as multivariate analysis is required for this sport. The accuracy of the results from the data and interpretation depends on the strength of the results from the statistical analysis. For example Portus et al. [17] used Pearson product-moment correlation coefficient tests for the relationship between elbow straightening and ball speed for analysing bowling arm kinematics of elite fast bowlers. Correlation is a popular statistical analysis technique used in cricket research.

**A t-test** tests the null hypothesis about two means; most often, it tests the hypothesis that the two means are equal, or the difference between them is zero. The null hypothesis typically corresponds to a general or default position; for instance, if two means are not equal then the results from t-test can not reject the null hypothesis of no equality between the means (for instance, Pinder et al. [18] compared event initiation, bat height, step length, or angle under bowler and ball machine condition in forward defensive and forward drive in developing cricketers using t-tests).

**A chi-square test** tests a null hypothesis about the relationship between two variables. A t-test requires two variables: one must be categorical and must have exactly two levels, and the other must be quantitative and be estimable by a mean. A chi-square test requires categorical variables, usually only two, but each may have any number of levels (for instance, Elliott et al. [15] used the chi-square test to test for changes in lumber disk degeneration status between two group of bowlers after 3 years of educational intervention).

**ANOVA** generalizes the t-test to more than two groups. ANOVA and MANOVA are non-covariate analyses used to test differences in means (for groups or variables) for statistical significance within one dependent variable and within two or more dependent variables respectively. In these analyses the total variance is partitioned into the component that is caused by true random error (within the group) and the components that are due to differences between means (between groups). These latter variance components are then tested for statistical significance. For instance, Pinder

et al. [19] used separate two-way (experimental task×shot) within subjects ANOVAs with repeated measures for QOC (quality of contact) scores for both experimental tasks ("live" bowler vs. ball machine), and shot type (front and back foot shots) to analyse the movement organization of cricket batter action under distinct experimental task constraints. The statistical significance of a result is the probability that the observed relationship or difference in a sample, occurred by pure chance, and that no such relationship or difference exists. The value of probability within an acceptable range is used to reject the null hypothesis of no differences between means or no relationship between the variables and to accept the alternative hypothesis that the means (in the population) are different from each other or no relationship exists between the variables.

But **ANCOVA** and **MANCOVA** are covariate statistics analyses used for the variables under repeated measurement and seek the relationship between the variables considering the variations among them and within one variable itself. ANCOVA blends ANOVA and regression, where regression is a technique for analysing the relationship between a dependent variable and one or more independent variables. Statistical control for the effect of a continuous variable known as covariates, (ANCOVA) compares the population means of a dependent variable for levels of a categorical independent variable (for instance, Davies et al. [20] used ANCOVA to analyse the relationship between fast-bowling injury and risk factors (bowling workload, bowling technique, fitness, past injury and recurrent injury) on changes in performances in three groups as 'uninjured', 'injured but able to play', 'injured and unable to play' at an elite and junior level). The covariate is a secondary variable that can affect the relationship between the dependent and independent variables of primary interest. MANCOVA deals with multiple numbers of dependent variables unlike ANCOVA which deals with one dependent variable, but allows multiple numbers of independent variables as ANCOVA does.

## 1.2 Bat swing

In bat-ball games, the score or runs needed for the victory in the match comes from

the bat-ball impacts. How well the batter is hitting and directing the balls is important. Leaving the ball i.e. allowing the ball to pass without contact in an efficient way without having any chance of being dismissed (ball contacts the wicket) is also an important skill. For instance, in cricket batting, an attempt to hit a swinging ball may increase the chance of being caught after making accidental contact. In cricket, not only good hitting is the expected action for bat-ball contact but to block the ball in a skilful way to protect the wicket is also important. Skilful blocking against a good quality bowled ball is ensured by good bat-ball contact that directs the ball along the ground or in the gap among the fielders. The ability to hit the ball, block or leave it, relates to the dynamics of bat swing. Sports such as cricket, baseball and golf all require the athlete to have the control and consistency to execute an effective swing to accurately send the ball to a desired location. The sequence of the batter's body movements and pace is a factor that allows the implement to be swung in a smooth motion in the simplest possible arc, and on a path that produces effective speed and ball-contact. The sequences of the movement with the implement are known as phases of bat swing in the swing sports research. Those terminologies are stance and initiation, back-lift, stride and downswing to impact, impact, and follow-through. The next section describes these phases of bat swing and their pictorial view and sequences are shown in Fig. 1.2. Generally these phases relate to a pre-delivery phase, decision making phase and shot execution phase.
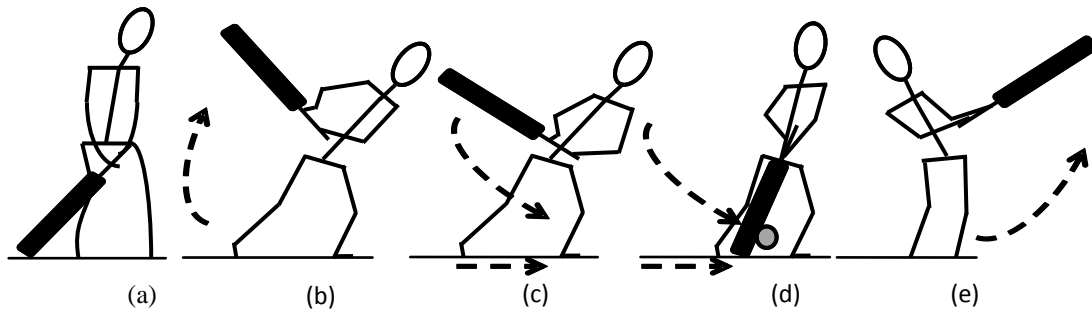


**Fig. 1.2** Different phases of bat swing (from left to right): (a) Stance and initiation, (b) Back-lift, (c) Stride and downswing, (d) Impact, (e) Follow-through.

### 1.2.1 Different phases of bat swing

The phases of bat swing are defined as the sequence of movements (Fig. 1.2). The three phases of batting relate to the interaction between the bowler, ball and batter. These are commonly described as the pre-delivery phase, decision making phase and shot execution phase. These categories of the batting (according to [21]) and the related phases of bat swing are outlined in Table 1.1. The details of each phase of the bat swing are described in the subsequent section. Table 1.1 provides the description of each movement and its interaction with the related swing phases, and batting action (according to [21]).

**Table 1.1** Different phases of bat swing and description of each.

| Phases of bat swing | Category of the phases | Comments |
|---|---|---|
| Stance and initiation | Pre-delivery phase | Stance and initiation starts before the bowler's pre-delivery situation and ends just before start of the delivery. In the pre-delivery phase, the best batters learn lots about the delivery from the bowler's approach. They focus on the bowlers hand holding the ball when the bowler is about to gather. |
| Back-lift | Decision making phase | Decision making starts when the ball is released. The best batters watch the ball from the hand and they are then able to judge the ball trajectory very early and move accordingly. During this cognitive phase batters start back-lift. Open faced back-lift (the face of the bat towards point) is required to increase bat speed. Because closed faced back-lift (the face of the bat towards the ground) will result in slower bat speed. |
| Stride and downswing to impact | Shot execution phase | Shot execution starts from the downswing of the bat from the top of the back-lift. Balance is the key factor; a good balance will |

| | | allow the ball to be hit with power and precision. A good stable base is required to hit the ball and this is achieved by a neat and quick footwork, i. e. stride. |
|---|---|---|
| Impact | Shot execution phase | In impact or bat-ball contact, full phase of the bat should be presented to hit the ball with the middle of the bat. How cleanly the batter strike the ball with the bat during practice is important. The bat speed is critical if power is to be generated. Footwork will provide a good stable base to hit the ball. Good balance is again the key in this phase to hit the ball with power and precision. Regardless of the shot being played batter's head needs to be over the ball on contact. |
| Follow-through | Shot execution phase | Follow-through indicates how well the impact has been conducted. A checked follow-through or incomplete follow-through provide the idea about the forcefulness or dullness of the impact. |

*1.2.1.1 Stance and initiation*

This is the basis of a movement to swing the bat and intercept the ball effectively. The placement of the limbs for posture and balance produce the sequence of movements. Foot, body, head placement, and gripping the implement to generate the desired sequence and swing dynamics, are the important factors of this phase. How well this phase is implemented has a direct effect on the swing parameters and the desired outcome. For instance, in a cricket bat swing, how the batter places the foot in front of the wicket is closely linked with the way power is generated to swing the bat to hit the oncoming ball in the desired direction. If the width of the stance (distance between the feet while the batter waits for the start of bowler's approach) is too wide it will hamper the batter's ability to turn freely and fully; likewise, a stance which is too narrow will result in a lack of stability and balance. Body and head placement are crucial for transferring the weight from the back to front foot or vice-

versa and to judge the oncoming ball-delivery, flight, and length to execute a desired shot. Correct grip on the implement and placing it correctly at this phase ensures that the desired bat swing is executed. For instance, in cricket the distance between the top and bottom hand of the grip, grip force, inclination and the line of the placement of the bat are important.

### 1.2.1.2 Back-lift

The back-lift starts when the batter lifts the bat from the ground in the direction of the oncoming ball. The objective for this phase is to hold a perfectly balanced, powerful position at the top of the swing. The bat's end, the hands, and the shoulders all start in one motion. The weight on the feet in the stance is shifted from front foot to back foot in this phase of bat swing. At the top of back-lift the hands are swung high, and the arms are extended and follow the route of the back-lift plane. The back-lift height (determined by the displacement of the centre of mass of bat horizontally backward and vertically upward as mentioned in Stretch et al. [22]) is important in terms of the stroke to be played. In cricket, to achieve a straight drive bat swing, high back-lift is recommended in order to have more power imparted to the stroke. On the other hand for a defensive stroke, a small back-lift is recommended for making fruitful ball-contact with the bat close to the pad to block or direct the ball along the ground. The ratio of back-lift and downswing speed (discussed next) differentiates the skilled cricket batter from other batter groups. To have the greatest acceleration at the top of the back-lift, batters sometimes shorten their radius (the lever arm) by bending the right elbow during back-lift.

### 1.2.1.3 Stride and downswing

The downswing of bat starts at the top of the back-lift, in the same plane as back-lift together with a stride of the batter. The downswing direction is opposite to back-lift as the weight on the back foot in the back-lift is shifted to the front foot. Ideally the hands and arms move the bat, as the batter lengthens the lever arm to increase the speed. This is because when the downswing is inaugurated, the upper part of the body, the shoulder, arms and hands flow easily into swing and so the speed of the

17

bat's toe increases with gravity. To intercept the oncoming ball, the batter commences a stride with a downswing of the bat. Researchers have worked on the commencement of stride and its length and the ratio of the back-lift and downswing to investigate the effect of bowling (batting against a ''real'' bowler and a bowling machine) on the information-movement couplings of experienced batters on the basis of the oncoming ball delivery and flight assessment skills [23].

*1.2.1.4 Impact*

The main goal of an impact is to maximize the energy imparted to the ball; that is the swing style of the bat should maximize energy transfer from the batter's arm to the ball. The quality of the impact is the most important factor for a desired goal of hitting the ball for scoring runs or to block it to save the wicket. Research on ball-contact has been to quantify its quality according to the contact location in the bat [24], [25], bat vibration [26], pre-impact bat and post-impact ball velocity [27], and how the batter directs the ball after contact [24], [25], [28]. However, it is said in the literature that a fruitful contact with higher bat horizontal velocities can be characterized by the nature of follow-through (discussed next) after the contact [22]. The bat continues to swing smoothly after ball contact "follow-through".

*1.2.1.5 Follow-through*

Immediately following the impact, the follow-through phase starts and ends with the bat swing. In this phase of bat swing, the bat and batter both move in the same direction while a successful ball-contact is made. A complete follow-through ensures a fruitful ball-contact and reduces the dangers of decelerating at impact, and the possibility of injury. Researchers [28] are using follow-through to qualify the ball-contact by assessing its degree of extension whether complete, partial or no follow-through, during a stroke played by the batter.

## 1.2.2 Bat swing research

Maximum energy is imparted to the ball from the batter when almost none is retained

in the arm or bat/club/racket. The underlying physics of the bat swing and the bat/ball interaction are important to finding the mechanics for more effective bat-ball contact. As swinging an implement in a sporting environment involves motion in three dimensions, the measurement is complicated and not easily reproducible. The net force and moment imparted to the grip by the batter can be determined from the angular and linear velocity of the bat mass (work by Cross [29]), and was used in an inverse dynamics model of the baseball bat (work by Shapiro [30]). To estimate how the mass distribution of the bat influences the bat swing speed Koenig et al. [31] measured the bat dynamics projected on the horizontal plane. Mackenzie [32] used a four-segment (torso, upper arm, forearm, and club), three-dimensional forward dynamics model to investigate how the motion of the golf club is influenced by the position of the club relative to the golfer's swing plane for squaring the clubface for impact and delivery of the club head to the ball. Sawicki et al. [33] used models (including the dependence of the coefficient of restitution, pitched ball angle on speed) for the pitch, batting, and post-impact flight phases of a baseball to find swing parameters (undercut distance, bat swing angle, bat and ball speed, bat and ball spin, wind speed, bat-ball coefficient of friction) that produce maximum range and their model incorporated experimental lift and drag profiles. Egret et al. [34] investigated the effect of three different golf clubs (driver, five-iron, pitching-wedge) on the kinematic pattern of a golf swing, including shoulder joint rotation angles, hip joint rotational angles, stance, right knee joint flexion, clubhead speed, and movement time for each phase of swing. Delay et al. [35] investigated how the force is controlled for impact movement in golf putting with increased distance targets by an adjustment of the magnitude of the motor command (backswing or back-lift as a function of target distance, downswing amplitudes for keeping movement time constant). Vena et al. [36] worked to indentify the Instantaneous Screw Axis (ISA) of pelvis, shoulder, left arm during downswing phase of golf swing in part 1 study. They tried to compute the magnitude of segment angular velocity relative to segment's ISA, checking whether the segment angular velocity followed the proximal distance sequence of the summation of speeds [37].

Very few cricket researchers have referred to other hitting sports. Stretch et al. [22] investigated the difference between front foot and the forward defensive strokes by analysing the kinematic and kinetic factors involved in those two strokes. They measured the back-lift height, the temporal parameters of commencement of the stride and the downswing of the bat, the front foot placement with respect to ball-contact, front foot stride length, and the back foot drag. They also measured peak bat horizontal velocity at around pre-impact and post-impact points of the ball-contact according to the front ankle, and the difference of the grip forces of the top and bottom hands for the two strokes. Renshaw et al. [23] investigated the initiation of the back-lift, the ratio of back-lift and downswing, the peak bat height, the stride length under two ecological constraints: batting against a bowling machine and against a bowler. Stretch et al. [38] analysed the rebound characteristics of a willow bat measuring the approach and rebound speed of a ball at three speeds levels. Pinder et al. [18] investigated the effect of changing the informational constraints (advanced information sources from a bowler's actions, removal of those sources etc.) on information-movement coupling of skilled cricketers. Measuring the initiation of the backswing, the front foot movement, the downswing and the front foot placement and peak height of the backswing, they differentiated the skills and developing batters on information-movement couplings under bowling machine and bowler conditions. In 2007 Mann et al. [39] evaluated the performance in execution of an interceptive task under different levels of induced myopic blur by estimating the quality of ball–bat contact. Stuelcken et al. [40] conducted the kinematic analysis of front foot off-side drives by nine right-handed, international batsmen to investigate the techniques for playing this drive. They investigated the peak horizontal end point speed of each segment, the front stride and the downswing of the bat, the path of the bat, the timing of the front stride, the trunk alignment relative to ground and the flow of the bat between the backswing and downswing. Taliep et al. [41] compared some selected kinematic variables of the front foot off-drive between skilled and less-skilled batters. They investigated preparatory feet or foot movement, head and batsmen's centre of mass position, shoulder angle, hip angle, and bat angle or bat speed of the two skilled group batters for differences in playing the drive. Mann et al.

[28] investigated interceptive performance (quality of bat–ball contact, forcefulness of bat-swing, and likelihood of dismissal) of skilled batters under each of four systematically varied visual conditions. Muller et al. [42] examined the validity and reliability of categorical tools for assessment of the quality of bat-ball contact by observer categorisation of bat-ball contacts (i.e., good, bad and no contacts) and displacement of the ball from the bat, and categorisation by a trained assistant, and an elite coach. Dias et al. [13] investigated the initial movement differences between elite and amateur batters in terms of perception time, force magnitude and direction, and stability. They classified two batters group by analysing the forward and backward initial movements, average reaction times (ball release to initial movement), and the bat angle in back-lift.

The implication of bat swing research in cricket should address two main themes: the practical applications of the protocols used, and the complete view of the batting stroke being played. The factors that should be derived for training and assessment perspectives must be evaluated, not from just a static position with a 2D view point. The protocols being used in the cricket batting research discussed above have some limitations in practical application in real match conditions due to the bulky, expensive, performance obtrusive technology and the involvement of expert humans for assessment and reliability. The research techniques sometimes miss the fine details of a stroke as attention is focused on certain macro parameters. This is because the descriptive nature of those research outcomes can not provide statistical support. For instance, using video-camera systems (bulky, expensive in nature and not match-friendly) Stretch et al. [22] documented the difference in front foot and forward defensive strokes in terms of kinematic and kinetic parameters involved but did not provide the bat and limbs dynamics in three dimensions to point out the fine signatures of the two strokes needed to address improvements in performance. Cricket researchers also used video-camera systems, and elite coaches or human expert for assessment (e.g. Renshaw et al. [23]; Pinder et al. [18]; Mann et al. [39]; Muller et al. [42]; Dias et al. [13]), but did not provide for the dynamics of the bat and/or limbs in three dimensions as profiles with numerical values of the parameter measured. Moreover, the underlying physics is absent in the descriptive cricket bat

swing literature to explain a motion to extract the key parameters that might be used for performance enhancement.

## 1.3 Thesis motivation and outline

The objective in cricket bat swing research is to observe the accuracy, control and consistency for an expected outcome by either hitting the bowled ball in the intended direction at maximum distance, blocking it, or leaving it pass. The inherent biomechanics of bat swing can address these issues and suggest whether to swing the bat to maximise the energy for maximum distance, to block the ball and direct it along the ground or to leave it with zero chance of being dismissed.

### 1.3.1 The research gaps

In cricket batting research, the main research gaps are in the protocol used and research outcome format. The significant question is how can technology and science be exploited to design a protocol that is match and user-friendly, inexpensive, easy to deploy, and can provide real-time data with numerical description of batter's performance. Cricket batting research uses bulky technology (video-, opto-tracking systems etc.) but is it possible to replace it using miniature technology? With the advancement of technology, it is possible to use tiny sensors to monitor a batting stroke and extract the key features for coaching, assessment and improvement. The wireless sensors can distinguish the phases of bat motion, the three-dimensional position and orientation of bat, and the timing, acceleration and velocity events of bat swing. The recorded digital data in these sensors (bat, and/or limbs of batter) can be used to establish the relationship among the variables (for instance, relations between bat speed, arm speed, arm mass, bat mass, and bat moment of inertia etc.), spatio-temporal identification of the bat posture and ball-contact features like sweet-spot hits identification etc. to extract the key features of the stroke. Real-time information can provide direct feed-back to the batter about the stroke for immediate possible correction. Post-processed information can provide insights for stroke enhancement

and a record of performance for recent, intermediate and long term assessment, and skills comparison.

## 1.3.2 Aims

The use of sensor technology in sports research has grown rapidly, namely tennis (Ahmadi et el. [43]; Ahmadi et el. [44]; Ahmadi et al. [45]), swimming (Davey et al. [46]), cricket bowling (Rowlands et al. [47]; Wixted et al. [48]; Busch et al. [49]), baseball bat swing (King et al. [50]) and bat-ball collision (Fallon et al. [51]), sword swing (James [52]), running (Wixted et al. [53]), Hammer throw (Ohta et al. [54]) etc. But in cricket batting no significant documentation has been released except the work by Busch et al. [55] who checked the possibility of analysing cricket shots using inertial sensors. However, their work did not have any validation by other systems and no mathematical and/or physical approach to explain the results. This dissertation aims to document cricket bat swing parameters extraction using inertial sensors and explain the results in the light of the underlying physics. The prime objective is to extract the spatial and temporal parameters in bat swing relating to bat and limb postures during a batting stroke using inertial sensors. The spatio-temporal parameters relating to bat and limb's postures are explained. The work in this dissertation starts from the straight drive cricket batting stroke. In the coaching documents it is said that "the straight drive is about timing and placement rather than power" [56], so the temporal and spatial parameters of bat and batter limbs during the stroke is important to judge, assess, and extract the key features about the drive. The existing video-and opto-graphy methods suffer from an inability to provide quantitative information of the bat and batter limbs other than the observer's memory. The numerical information could be used in training and assessment for the particular drive improvement and also as a batting template using the drive from an elite batter. To derive the features of a stroke this dissertation reports a methodology and associated protocol using inertial sensors and a related geometry and mathematical model. The existing video-and opto-graphy tools have been used to validate the results. This confirms that tiny sensors are accurate. This dissertation

proposes some sensor-based integrated methodologies and research concepts for future cricket bat swing research.

### 1.3.3 Objectives

Previous research used several approaches to quantify skill levels in batting. Mann et al. [28] suggested simple categorical measures of batting performance (quality of bat-ball contact, forcefulness of bat swing, and likelihood of dismissal). They suggested that future approaches might move beyond these categorical measures because they were limited in their sensitivity to fine changes in batting strategy. They has suggested that modern technology developed tools such as accelerometers and gyroscopes could examine the torque of bat swing, high-speed cameras and force plates to record the time-course of movements, and vibration sensors to evaluate the quality of bat-ball contact. The objective of this dissertation is to use one of the suggested novel tools-, accelerometer sensors, to quantify the phases of the bat swing. Successful coordination and control of a dynamic interceptive action requires the cricketers to place the bat in the right place at right the time (Savelsbergh et al. [57]; Regan [58]; Williams et al. [59]). The notion of quantitatively gauging a cricket bat swing was realized by Stuelcken et al. [40] in their research. They felt batting research needs to determine the path of the bat and the timing and sequencing of body movement of the batters. In line with these suggestions, the objectives of this research is to detect the posture of bat and body sequence in time and three dimensional space in a drive using triaxial sensors. The bat and limbs postures are described in terms of the physics of the swing. In addition the identification and grading of bat-ball contacts using accelerometer sensors was investigated. The outcomes are intended to:

- provide feedback about key signatures of bat swing in a drive for skill assessment

- assess the performance and detection of error, and proving guidelines for correction

- refinement of style comparing with an expert's drive and assessment of improvement.

## 1.3.4 Contributions

Literature on the analysis of cricket bat swing was reviewed. Due to the limited amount of literature available, other implement swing sports including golf, baseball, and tennis were also reviewed. This literature review reported the methodology, results and limitations of existing research and provided a guide for future research. From this review the gaps and future research directions are evaluated and opportunities were selected for this dissertation.

Secondly, a methodology for cricket bat swing analysis using sensors and video, related mathematics and signal processing tools for results interpretation and the statistical tools to validating the strength of interpreted results are reported.

Thirdly, the results gathered from the works for this dissertation have fulfilled some of the gaps in cricket batting research in the followings ways:

(i) The preliminary and trivial experimental results related to accelerometer sensor calibration, synchronization with validation tools, and basic pendulum swings of the sensors were used to assess the use of tiny, inexpensive sensors in swing related parameter extraction. The effect of gravity on different parts of swing and the shortcomings of the sensors to extract velocity and distance related parameters after integration, and solution to the shortcomings are proposed and validated.

(ii) The results from consecutive and repetitive bat swing in straight drive cricket batting can detect the temporal and spatial posture of the bat in straight drives. The justification of the results used physics and video-footage. The tiny sensors are able to detect the timing and placement of the bat useful in assessments and coaching.

(iii) The bat-ball contact acceleration profiles recorded on the wrists and the bat could differentiate different hit regions in the bat and sweet-spots impacts identified.

(iv) The term 'forcefulness' of bat-ball contact is quite descriptive and imprecise in cricket because it lacks of magnitude or measured values. While quantifying the bat elevation angles at the end of straight drive using acceleration peaks, the angles from the experiment was matched with an equation derived angles. To determine the angle using the initial conditions of the drive from video footage, the maximum centripetal force applied by the batter could be determined from the sensor recorded acceleration profiles. The estimation of maximum centripetal force from the sensor profiles provides the insights for numerical measurement of 'forcefulness' assuming good ball contact.

(v) In the defensive stroke the back-lift height affects the control over the bat for novice batters. A higher back-lift resulted in a misalignment of the bat at the time of ball contact. On side and off side defensive strokes were differentiated from the total acceleration profile. The batters showed more control over the bat in the on-side strokes and more energy was imparted to the ball. In addition the on-side strokes showed less twisting of bat during ball contact. This work verified that tiny, inexpensive sensors can be used to extract the key signatures of a defensive stroke.

(vi) While the acceleration profiles from the bat mounted sensors were matched by the video footage calculated (using rigid body dynamics) profiles, the contributions of different acceleration components (rotational, translational, gravitational) at different phases of the drive was determined. To match the sensor to the video profiles, the calculated radius of rotation revealed that the maximum bat swing force in straight shots required maximum swing radius.

 (vii) GRIP by the hands during batting

The correct grip applied by the hands is very crucial for a successful ball contact to prevent twisting of bat. In the literature, it is said that the top hand dominates in the stroke while the bottom hand reinforces the power [56]. The acceleration measurements from the sensors attached to the bat and wrists revealed how the two hands (top and bottom) were coupled to the bat before, during and after the ball-

contact in a defensive stroke. That is, for good ball contact, the bottom hand should be loosened just at the contact and in a stroke the top hand always dominates. The loosened bottom hand allows the fingers and thumb of the bottom hand to act as a shock absorber [56]. The loosened bottom hand at the contact and the top hand dominance before the contact; and just after the contact both hands are strong and equally coupled with the bat. In this way the batter retains control over the bat. It was revealed that just prior to contact, the batter applies an opposite force to stop the bat for minimal contact force. This sequence was confirmed from the minimum velocities of the bat and wrists prior to ball-contact.

Through the various segments of this research some outcomes have been published. Future directions have been established in many cases. The outcomes were published in two peer reviewed journals and one conference proceedings; abstract submitted for ISEA-2014, several prepared for submission. The lists of published and submitted papers are shown below:

A. K. Sarkar, D. A. James, A. W. Busch, D. V. Thiel, "Triaxial accelerometer sensor trials for bat swing interpretation in cricket," *Procedia Engineering,* vol. 13, pp. 232 –237, 2011.

A. K. Sarkar, D. A. James, A. W. Busch, D. V. Thiel, "Cricket Bat Acceleration Profile from Sweet-Spot Impacts," *Procedia Engineering,* vol. 34, pp. 467–472, 2012.

A. K. Sarkar, D. A. James, D. V. Thiel, "Relationship Between Wrist and Bat Acceleration in Cricket Batting," in *Australian Sports Technology Network (QLD) Inaugural Queensland Seminar 2013*, Queensland Sport & Athletics Centre, Brisbane, Australia, 2013, p. 3.

D. V. Thiel, A. K. Sarkar, " Swing profiles in sport: An accelerometer analysis," in ISEA-2014 (Full paper accepted).

### 1.3.5 Chapters

### Chapter (1) Introduction

This current chapter presents a general introduction about the thesis and cricket research (endeavours, direction, methodology adopted so far), bat swing (why research is required, definition of different phases of bat swing in cricket), implement swing research and implication (how and what research on implement swing has been attempted in different sports other than cricket), the motivation of this thesis (the research gaps, aims, objective and contributions by this thesis), and chapter organisation.

### Chapter (2) Literature review

This chapter documents the existing cricket batting research categorized into biomechanics & motor control, ecology & assessment, psychology, morphology & physiology, injuries and implements of batting. The topics addressed, methodology used, outcomes stated, limitations and gaps and future endeavours possible are discussed about those research. Research on other sports that also require implement swinging is reviewed in this chapter. Finally, the literature using accelerometers even if for other sports is reported.

### Chapter (3) Cricket batting strokes: parameters, issues for bat swing research

This chapter starts with the definition of different batting strokes according to the bat swing dynamics. Then some general strategies adopted by the batters to choose a stroke following coaching guidelines are discussed. This chapter defines a safe stroke and how to make it so, also describes some issues of research that could be done to assess a batter's technique. It is said that vertical batting strokes (e.g. drives, defensive strokes) are the basis of all other strokes; this chapter outlines some key features of those strokes according to the batter's limbs and bat position. This chapter also discusses about the data collection methods, limitations and complexity in

existing cricket batting research methodology. The limitations could be solved using sensors.

## Chapter (4) Methodology and Analysis

A novel methodology composed of tiny inertial sensors is introduced. Some examples are provided on how this novel methodology is already being used in variety of sports research other than cricket. The sensor architecture and data collection features are documented along with a discussion of the conversion of data to the world coordinate system for extracting the biomechanical features. This was compared to data extracted by existing systems. The validation method using existing methodological tools is then documented along with the necessary mathematics and analysis. The limitations of how the analysis of extracted sensor data could be prone to error if some aspects are not considered are discussed.

## Chapter (5) Results and discussions

The results from a pendulum swing using the sensors are presented. The static and dynamic position of the sensor during the swing attached to a wooden pendulum was analysed. Static results showed good agreement between the measured angles from sensor data and by an inclinometer as a reference. The swing frequency of the pivot aligned sensor axis acceleration profile showed double frequency of the tangential axis profile. Using Fast Fourier Transform (FFT) the relation between the frequencies of two axes profile was estimated and used later to match the sensor recorded profiles in the swing position with those from pendulum equation imposing initial conditions. Hits on the pivot arm were distinguished using acceleration values. This allows location of the optimal contact location for maximum the energy transfer to the ball.

The nonlinear equation of a pendulum with a moving pivot is solved by an algorithm based on the state vector equation. The bat angle during a straight drive is modelled using the pendulum mechanics. The equation derived profiles and the sensor recorded profiles were compared. The effect of the initial angular velocity, the radius

of rotation, and the pivot phase angle were investigated using the swing profile. The level of the applied force by the batter using the maximum acceleration values is discussed.

The results from consecutive and repetitive bat swing in straight drive cricket are included. The temporal and spatial posture of bat was identified by sensor data and the results were validated by theory and video reference timing. This work was performed to assess the competency and consistency of a batter by using sensor data.

Next, 61 bat-ball contacts in defensive strokes by five novice batter were recorded in bat and wrists mounted sensors. The intention was to categorise the sweet-spots. The experimental results were linked with the more cited definition that the sweet-spot is determined by the batter when the jarring of the hands is small, as measured by the low levels of vibration in the wrist sensors.

The bat angle and the applied force in a straight drive by several batters are reported. In this work, an approximate equation for the bat angle as a function of time (considering implement swing dynamics and constraints in cricket bat swing) during the straight drive is compared with the video derived angles, which showed good agreement. Using the angle equation, the acceleration along the bat length aligned sensors axis was derived and matched with sensor recorded profiles. In this work the angles at the end of a drive was also correlated with the acceleration peaks from 63 swings by seven amateur batters. Using Bland Altman covariance correlation approach correlation coefficients were calculated individually for each batter and among the batters. While the definition of the term 'forcefulness' of batting is quite ambiguous in the literature, the results from this experiment quantified the force applied by the batter.

The effect of back-lift height on bat orientation during ball contact in defensive strokes was determined from sensor recorded data. On and off defensive strokes were discriminated using total acceleration (the vector sum of the measurements from a triaxial accelerometer) recorded in bat mounted sensor. The results in this work

suggest that sensor recorded data could be useful for qualifying bat alignment during ball-contacts in defensive strokes without needing an independent assessor.

The sensor recorded data was validated with the existing video derived data in an orthodox straight drive using rigid body dynamics. Imposing a decision matrix and mathematics related to rigid body dynamics, the video revealed results were matched with that recorded using a sensor. While matching the results from the two systems, the key parameter for maximising the drive and the control force in the straight drive were derived.

In the defensive stroke the relation between bat and wrists accelerations were studied to judge the differences how two hands are coupled with the bat before and after ball-contact. Five batter's defensive strokes (one sub-elite, two amateurs, two novices) acceleration were recorded in bat and wrists mounted sensors. The difference between top and bottom hand in experienced batters were compared with the non-experienced. The correlation between bat and wrists velocities were outlined for all batters' data.

**Chapter (6) Contributions, Conclusions and Future Directions**

This section summarises the conclusions drawn from the thesis work. Opportunities for further research to extend the work reported in this thesis are suggested.

**Chapter (7) Summary**

The key outcomes from this research are summarised.

# 2 <u>LITERATURE REVIEW</u>

Cricket batting research, a dynamic interceptive action, requires a strategic plan [60]. During laboratory or simulation-based studies, the analyses can suffer from limited validity [61], [19], because those studies can not provide natural performance environment. In most of the available cricket batting research reported most focus on the skill acquisition and sport expertise perspective. The constraints requiring sub-second interceptive action motivated the majority of the works. Fewer published studies have been conducted from a biomechanical perspective. Those biomechanical studies provide the insights into the mechanical differences of the front foot defense and drive in vertical batting shots. Horizontal batting strokes such as the cut, pull, and hook have not been studied. Most literature is descriptive in nature, such as [62], [22], [40], [63], [61], and addresses the batting science with very little use of technology. The research can be divided in several categories: biomechanics & motor control, ecology & assessment, psychology, morphology & physiology, injuries and implements of batting. Some literature present reviews of batting research while most have documented empirical findings.

## 2.1 Biomechanics and motor controls

The available research conducted on the biomechanics and motor controls of batting are mainly descriptive. Some researchers noted the need for the integration of biomechanics and motor control together for neuro-motor control or behavioral learning for skill acquisition in batting. Both neuro-motor control and behavioral learning are fundamental to skill assessment and development. The following works, small in number, evaluated the influences of coaching from biomechanics and motor controls perspectives.

**Stretch et al. [22]**

Topic: The kinematic and kinetic factors of playing forward defensive (FD) stroke and front foot off drive (D) in different phases (includes the stance and back-lift, the

stride and downswing, impact, follow-through) of the two strokes. Outcomes were compared with the coaching literature that provided qualitative and quantitative description about these two strokes.

Methodology: Fourteen male cricketers played the two strokes against medium fast bowler. Batting was filmed by a Photosonics 1P 16-mm camera at 100 Hz and the bat was instrumented by two pressure sensors (Motorola MPX 10 GP) to measure the grip force applied by the top and bottom hands of the batter.

Outcomes: Significant differences of the kinematics and kinetics of the body segments between the two strokes during the downswing of the bat, at bat-ball impact and post-impact were revealed. However, similar stance, back-lift, stride and start of the downswing of the bat of two strokes were reported, generally supportive of the coaching literature as stated in the study. The bat was never kept stationary at the top of the back-lift at any level of back-lift, as suggested by Gibson and Adams, 1989 (as stated in [22]); rather, a continuous movement was observed from backswing to the downswing in the strokes.

   Similar grip and stance was reported for both the strokes, with feet were twice the recommended distance apart (0.30± 0.35 m apart) for both (Greig, 1974; Reddick, 1979; Tyson, 1985; MCC, 1987; Khan, 1989 as stated in [22]). The study found that the body's centre of mass was displaced 0.08 m forward of the midpoint between the feet, and towards the line of flight of the ball, because the front shoulder was forward of the front foot (0.08 m) and above the back shoulder (0.07 m). The results for centre of mass placement agrees with the recommendations of the coaching literature (e.g. MCC, 1987 as stated in [22]) and the findings of Elliott et al., 1993 (as stated in [22]) and supports the principle of weight distribution for an expected forward movement.

   The attacking nature of the front foot drive was compared with a forward defensive stroke by observing a higher back-lift (FD = 0.65 m; D = 0.74 m), later commencement of the stride (FD = 0.64 s pre-impact; D = 0.58 s pre-impact) and

downswing of the bat (FD = 0.38s pre-impact; D = 0.36 s pre-impact), a shorter front foot stride (FD = 0.72 m; D = 0.68 m) with the front foot placement taking place later (FD = 0.14 s pre-impact; D = 0.06 s pre-impact), and the back foot dragging further forward at impact (FD = 0.05 m; D = 0.10 m). For front foot drive, significantly greater (P < 0.05) peak bat horizontal velocity at 0.02 s pre-impact (FD = 3.53 ± 3.44 m.s$^{-1}$; D = 11.8 ± 4.61 m.s$^{-1}$) and 0.02 s post-impact (FD = 2.73 ± 2.88 m.s$^{-1}$; D = 11.3 ± 4.21 m.s$^{-1}$) were reported in this study. These findings were described as a result of multi-segmental series of levers like movement of the front upper limb. This study showed this movement in agreement with tennis and baseball research, where greater racket and bat impact speeds were found from the multi-segmental set of levers like movement of the striking limb (Breen, 1967; Milburn, 1982; Shibayama and Ebashi, 1983; Tyson, 1985; Hay and Reid, 1988; Elliott et al., 1989 as stated in [22]). Significantly greater (P < 0.05) bat-ball closing horizontal velocity (FD = 24.2 ± 4.65 m.s$^{-1}$; D = 32.3 ± 5.06 m.s$^{-1}$) and post-impact ball horizontal velocity (FD = 6.85 ± 5.12 m.s$^{-1}$; D = 19.5 ± 2.13 m.s$^{-1}$) was reported for front foot drive than for the forward defensive stroke. Non-significant difference between the two strokes was noticed in this study about the point of bat-ball contact. However, front foot drive ball-contact occurred further behind the front ankle (FD = 0.09 ± 0.17 m; D = 0.20 ± 0.13 m), with the bat more vertical at impact (FD = 62.6 ± 6.53°; D = 77.8 ± 7.05°) compared with defensive stroke. The batters used a longer follow-through with the bat retaining more of its initial horizontal velocity after impact for the drive.

This study found significant differences (P < 0.01) had occurred between the grip forces of the top and bottom hands for both the strokes. The principal kinetic findings about the grip force were that the top hand plays the dominant role during the execution of the strokes with the bottom hand reinforcing it at impact. Grip force patterns for the two strokes was similar during the initial part of each stroke, however the grip force recordings of drive were significantly greater (P < 0.05) at 0.02 s pre-impact (top hand: FD = 129 ± 41.6 N; D = 199 ± 40.9 N; bottom hand: FD = 52.2 ± 16.9 N; D = 91.8 ± 41.1 N), at impact (top hand: FD = 124 ± 29.3 N; D = 158 ± 56.2 N; bottom hand: FD = 67.1 ± 21.5 N; D = 86.2 ± 58.2 N) and 0.02 s post-impact (top

hand: FD = 111 ± 22.2 N; D = 126 ± 28.5 N; bottom hand: FD = 65.5 ± 26.9 N; D = 82.4 ± 28.6 N).

Limitations and gaps in the study: The tools used in the methodology of this study are bulky, expensive and not suitable in real-match condition. Most of the findings are descriptive. The study provides correlative results as opposed to causative phenomenon necessary for designing strategies for skill enhancement on a particular signature of the two strokes addressed. This study documented discrepancies with the coaching literatures about the back toe horizontal movement that occurred forwards before impact, and the point of bat-ball impact that was behind the front pad.

Possible endeavours ahead: The parameters for characterizing two strokes addressed in this study could be find out more precisely or accurately (without encountered with the standard deviation significantly as mentioned by '±' sign after each numerical values) using miniature sensor technology. For instance, inertial sensors could be better in measuring velocity and bat orientation, pressure sensors could be better for grip force measurement than video. The methodology could be made very easy, inexpensive and real-match friendly using wireless sensors. Using skill breakdown the key signatures could be investigated independently to establish the relation between kinematics and kinetic properties and consequences (performance or injury) as 'cause and effect' in a scientific way. Then each key signature could be combined for the stroke enhancement.

**Taliep et al. [41]**

Topic: Comparison of selected kinematic variables (preparatory feet or foot movement, head position, shoulder angle, bat angle or bat speed, hip angle) of the front foot off-drive in skilled and less-skilled cricket batsmen.

Methodology: 10 skilled and 10 less-skilled right-handed batsmen were used as subjects. High-speed digital cameras were used for recording the three-dimensional kinematics during different phases of the drive (stance, top of back-lift, ball release, predicted bat–ball contact, and follow-through.). This study used Oxford Metrics

Vicon motion analysis system composed of six cameras, operating at 120 Hz. 18 retro-reflective spherical markers were placed at the relevant anatomical sites of the batter, those included the centers of the left and right mid-toes, heels, ankles, knees, hips, wrists, elbows, shoulders, sternum, head. Another two reflective markers were placed on the bat, one on the top centre of the blade and the other at the bottom back of the bat. Projected video footage of a medium-fast swing bowler was used to present the visual information of the bowling action to the batter.

Outcomes: This study reported that skilled batsmen could identify the type of delivery bowled by the fact that seventy percent of skilled batsmen had preparatory feet or foot movement before committing to play forward, but only twenty percent of the less-skilled had this movement. During the predicted bat-ball contact the skilled group had the tendency to put their centre of mass further forward by positioning the head further forward of the centre of base point throughout the drive. This allowed them to better lean into the stroke. The less- skilled group did not show this tendency. This study did not find significant differences of shoulder angle, bat angle or bat speed, hip angle during the different phase of the stroke between the two batters groups. However, skilled batsmen showed a tendency of larger hip angle at ball-contact.

Limitations and gaps in the study: The equipment used in the methodology of this study is bulky, expensive, tedious and not match friendly. The report stated that the procedure does not allow ecological validity. Match conditions were simulated by having the batsmen play shadow strokes against filmed deliveries. This methodology provided a safe and controlled environment but it reflected the fact that it was not match friendly. The video cameras revealed kinematics parameters with significant level of standard deviation presented by the values after '±' sign. For instance, the difference in maximum bat angle during back-lift between the skilled and less skilled batsmen was presented as 26.3±16.3º vs. 27.3±12.7º.

Possible endeavours ahead: Miniature sensors could overcome the methodological complexities this study encountered. The precise values of the kinematics parameters

could be made available from the three-dimensional data recorded by the tiny sensors placed in the corresponding limbs and bat in a planned way. Only a portion of batters moved before the ball release. Tri-axial sensors would allow the movement patterns in time and space to be documented. This descriptive study did not explain any of its results in the light of science phenomenon. Tiny sensors might able to state the reason behind a kinematic parameter that could facilitate batter improvement.

**Stuelcken et al. [40]**

Topic: Biomechanical analysis of variables (the front stride and the downswing of the bat, horizontal end point speed of each limb segment, bat path, front foot placement, position of front ankle, the alignment of the trunk relative to ground) in front foot off-side drives that characterize the techniques of elite cricket batters while performing under match conditions. The analyses were conducted in this study to identify the path of the bat during the back-lift and downswing; to quantify the timing and sequencing of events in relation to the top of the back-lift and bat-ball impact; and to assess the movement patterns of elite batters that enable them to successfully intercept the cricket ball.

Methodology: Nine right-handed, international batters' front foot off-side drives in first class and international matches were used for analysis. Two synchronized high-speed video cameras were used to capture the strokes. The movement sequences during the drives were digitized manually at a sampling frequency of 125 Hz using motion analysis software. Each stroke was divided into six phases as the stance and initial movement, back-lift, stride, downswing, impact, and the follow-through.

Outcomes: The delayed front stride and the downswing relate to the ball flight. The peak horizontal velocity of each limb segment occurred almost simultaneously just before the impact. The constraint on upper limb segments adopted by the batter served to enhance stroke accuracy. A distinctively looped bat path was reported. The front ankle position was well inside the line of the ball at impact. The alignment of the trunk relative to ground and the continuous flow of the bat between the

backswing and downswing matched previous findings. The findings in each of the phases were described as follows:

At stance, the knee, hip and shoulder were positioned forward of the back foot, while the front foot knee and shoulder were close to an alignment over that foot. The left hip was behind the left foot and the shoulder was higher than the right shoulder. A better view of the approaching delivery was facilitated by the shoulder alignment that was marginally open: the angle was $26 \pm 7°$ with respect to a straight line running down the pitch, where angles in an anti-clockwise direction are positive. The feet were at a mean distance of $0.46 \pm 0.08$ m apart and the centre of mass of the body was positioned over the midpoint. For the initial movement 77.7% trials had a back foot movement back and across to either the off or leg sides, and 44.4% trials the batters moved both their front and back feet. During this initial phase, the batters did not lift the bat, but maneuvered it into position like a lever. The angle at the wrists and the horizontal distance between the wrists and the centre of mass of the batter were investigated. The angle at both wrists was decreased, with a greater value at the bottom hand (right hand) wrist compared to other wrist. Then the wrists remained close to the centre of mass. This study found the batters had maintained their balance by placing the mass of the bat close to the base of support. The mean distance between the toe of the bat and the mid-point between the centers of each foot was less than $0.85 \pm 0.09$ m in the transverse plane.

At back-lift, the mean height was $1.53 \pm 0.07$ m determined by the vertical displacement of the bat toe. The back elbow (right) was bent more ($59 \pm 12°$) than the front elbow ($109 \pm 8°$). The mean vertical displacement of the left wrist and left elbow was almost identical while the right wrist and the right elbow were different (the wrist was below the elbow by a mean of $0.15 \pm 0.05$ m). During this phase (back-lift) the front shoulder moved downwards from its height in the stance phase leading to trunk alignment at the top of the back-lift of $69 \pm 8°$ relative to the ground. At the top of the back-lift the mean hips angle had increased in the transverse plane, indicating a more open position.

The mean stride time was 0.33 ±0.12 s and the mean stride length was 0.35 ± 0.22 m. At heel strike, the mean angle was 149 ±11° at the front knee before flexing slightly at bat-ball contact into a mean of 147 ±11°.

The mean downswing to impact time was 0.16 ±0.02 s this study documented. The front elbow was extended by a mean of 7 ±20° during this period to be 116 ±20° at impact. During the downswing the shoulders were opened considerably and were at a mean alignment of 40 ± 19° at impact this study found.

At impact, the position of head was marginally behind the point of impact at a mean distance of 0.05 ± 0.16 m and the trunk was aligned at a mean angle of 91 ±8° relative to the ground. The linear speed of the toe of the bat was 16.0  m. s$^{-1}$ and its mean angle relative to ground was 68 ±7° with impact taking place at a distance of 0.22 + 0.16 m behind the front ankle. The angle of the hips continued to increase marginally and the mean distance between the inside of the bat toe and the front ankle was 0.27 ±0.12 m in a plane parallel to the crease at impact.

Most batters 'checked' (i.e. restrained) follow-through rather than finish the stroke with the bat over the shoulder. However, the mean peak speed of the toe of the bat was higher than that reported in previous research ([62], [22]). This indicated that a 'checked' follow-through does not affect the force production adversely.

Limitations and gaps in the study: This study used bulky and expensive technology (two high-speed video cameras). The study did not examine the dynamics of a cricket stroke but only looked at statistical results. It is important to establish how technique might provide improved batting outcomes and develop skill [60].

Possible endeavours ahead: The high speed video technology could be replaced by low cost sensor technology. Multiple sensors might link the movement patterns with motor control theory.

**Kelly et al. [64]**

Topic: A mathematical classification of the Cover Drive and the Forward Defensive

stroke was developed using fuzzy set theory. The classification was based upon the body position and the ball/bat position for developing the fuzzy sets. The mathematically simulated motion of a batter playing a stroke was compared to known strokes. The quality of the stroke was outlined by feedback from the proposed system.

Methodology: Sensors (electromagnetic position sensors, pressure sensors and pressure mats), a motion capture interface known as Polhemus 3space Fastrak unit, and a computer system were used in this work. Position sensors were placed in the bat (one in the middle at the back of the bat), on the feet (one in each), the hands (one in each) and the head. A motion capture system was used to interface the sensors with a computer. Each stroke was divided into three intervals namely, the waiting time, the receiving state, and the playing and follow through. This technique captured the entire stroke from the moment the bowler started the run up until the ball was deflected from the bat and the motion had ended.

Outcomes: The rules for each stroke were obtained by analysing the fuzzy sets for each state of the motion and then combining them. Two levels to the rules were used, the first gave the composition of the fuzzy sets in each temporal state and the second was a combination of the temporal states. The comparison of limb movements and body positioning between the two strokes was carried out by analyzing body position and bat/ball position in different groups. The body position included the head position, hands position, feet position and the weight distribution on the feet. The ball/bat position included the mode of the stroke being played, the flight path of the incoming ball, the bat orientation and the location of the ball contact. The fuzzy sets for each state in a stroke were described. From this the transition from one state to the next was added. The fuzzy set membership values for the cover drive and the forward defensive strokes were outlined.

Limitations and gaps in the study: The observations were made for the fast bowling. Spin bowling was not considered. The authors worked with a coach for the formulating the batting classification scheme. A descriptive classification of cricket

batting strokes based on body positions and bat/ball position was reported, and the membership values for each fuzzy set in two strokes (cover drive and defensive) were used for comparison. .

Possible endeavours ahead: The same fuzzy sets with membership values could be extracted using tiny sensors for the two drives by proper positioning of the sensors in bat and batter limbs. As the sensors are able to record numerical values directly, the dynamics relating to a movement could be made available by post-processing of the data. Real-time processing (i.e., with a few seconds delay) is likely achievable to provide feedback to the athlete.

### Müller et al. [42]

Topic: The validity and intra- and inter-rater reliability of a simple categorical tool to assess the bat-ball contact quality was assessed. The comparisons made were:

   (i) Observer categorisation of bat-ball contacts (i.e., good, bad and no contact) and the displacement of the ball from the bat,

   (ii) Real time 'Live' categorisation of bat-ball contact trials by a trained assistant and re-assessed via a video record,

   (iii) Categorisation of bat-ball contact on the same video record of trials by an elite cricket coach.

Methodology: One right-handed batsman and one right-arm leg spin bowler participated in this study. Both of the batsman and bowler had first-class playing experience. A trained research assistant was involved as an observer/rater and an elite district cricket coach assessed the bat-ball contact. The batter wore PLATO liquid crystal spectacles and received 45 deliveries that were of full length with two variations (either a 'leg-spinner' or a 'wrong-un'). Variations in the quality of bat-ball contacts were achieved with selectively occluding vision of ball flight by the spectacles. Two synchronized Redlake Motion Scope PCI cameras sampling at 250 frames per second were used to capture the strokes from front-on and side-on. A 2.54

41

cm black strip was used on the longitudinal face of the field to aid digitizing the spatial coordinates of the bat and the ball. Another standard 25 Hz VHS camera was positioned at the bowler's end to film the batsman to provide a reliability of rating on two subsequent occasions two weeks apart (for intra-rater reliability) and cross-rating by the elite coach (for inter-rater reliability).

Outcomes: This study found a strong linear correlation (r = 0.74) between categorisations of bat-ball contacts and displacement of the ball from the bat. For intra-rater reliability, a high correlation was found between live to first video (r = 0.96) and live to second video (r = 0.84) assessments. The comparison between the video records also found high intra-rater reliability (r = 0.87). This study documented a high inter-rater correlation between the assistant and the elite coach for the first (r = 0.83) and second (r = 0.96) video assessments. The categorical assessment tool appeared to be reliable when administered on different occasions and by different individuals.

Limitations and gaps in the study: The protocol used in the methodology is bulky (expensive cameras and other instruments). Tiny, inexpensive sensors could replace the video cameras and human observers (which is prone to error due to *subjectivity*). The numerical values obtained from sensor data would provide bat-ball contact assessment and provide another aid for the validity and reliability assessment.

Possible endeavours ahead: Using sensor technology the bat-ball contact reporting could be more reliable keeping aside the involvement of coach and trained assistant. While the existing bat-ball contact assessment was undertaken using the human eye, sensors could identify the exact location of ball-contact in the bat and categorize the bat-ball contact by the energy transfer or interchange between bat and ball.

**Cross [65]**

Topic: The basic mechanics of the swing of a baseball bat was developed to provide a realistic model of the swing. The model was formulated in terms of the forces and torques acting on the bat. The measurements of the forces and torques allowed an

estimation of the velocity of the centre of mass of the bat. This study determined the effects of the force-couple combination on swing of the bat.

Methodology: A video camera mounted about 4 m immediately above the batter's head. The camera was operated at 25 frames/s and software was used to separate the interlaced images of each frame to make the frame rate 50 frames/s.

Outcomes: The model used to calculate the swing of a bat in a two dimensional (x, y) plane was shown in Fig. 2.1 where $\alpha$ is the angle between the applied force $F$ and the longitudinal axis of the bat, and $\beta$ is the angle between this longitudinal axis and the x axis respectively, $d$ is the distance between the bat centre of mass (CM) and the point of application of force ($F$) on the handle. This work constructed the equations of motion in the x-and y-direction and the angular direction using $F$, $\alpha$, $\beta$, $d$, $M$ (mass of the bat), $C$ (couple applied by the batter) and $I_{CM}$ (bat's moment of inertia about an axis through CM). The direction of $\alpha$ was defined as positive when the torque due to $F$ acted in the "wrong" direction. This study stated that the batter exerted a positive couple ($C$) to rotate the bat in the "right" (counter clockwise) direction.
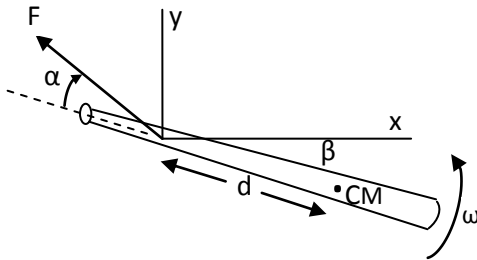


**Fig. 2.1**    Geometry used to calculate the swing of a bat, showing the position of the bat and the direction of the force on the handle near the start of the swing [65].

From the instantaneous bat position in the video footage, the angular velocity ($\omega$), the linear velocity of CM, the radial and tangential components of $F$, torque, $\alpha$ and the couple ($C$) applied by the batter were calculated. The experimental $F$, $\alpha$, and $C$ profiles were compared to the model calculated profiles with good agreement. From the experimental and theoretical results, the author concluded that to start the swing a batter must apply a small positive couple followed by a large negative couple to

complete the swing.

Limitations and gaps in the study: This study used a video camera to extract the bat position in 2 dimensional coordinates. The centre of mass was assumed to rotate in a logarithmical spiral with constant angular acceleration but no supporting evidence was provided. The author noted that this model is unable to completely answer of the questions as to how a batter might maximize the velocity at the impact point, whether maximizing the angular velocity of the bat or maximizing the linear velocity of the centre of mass is important, whether the use of a lighter bat or a bat with a larger moment of inertia is beneficial. The inability of the model to answer those questions was explained by stating that the forces and torques applied to a bat depend on the forces and torques exerted by all of the body segments used by the batter. This was not addressed. That is, the body segments in the body model for the swing were not addressed.

Possible endeavours ahead: The video camera can be replaced by the tiny sensors to extract the spatial and temporal parameters of the bat for the swing model. Various body segments could be included in the model by attaching those sensors in the relevant body segments. The questions stated by the author relating to maximizing the swing velocity could be answered by analysing sensor recorded numerical data.

**Cross et al. [66]**

Topic: The effect of mass and swing-weight on swing speed.

Methodology: In this study six different rods were used: three the same mass but different swing-weight factors and three with the same swing-weight but different mass. All were swung by four male students with maximum effort. Each participant was asked to sit or stand at a selected location and to swing each rod as fast as possible so that the rod would impact a pillow located anteriorly. The forearm of each participant was made approximately horizontal at impact by adjusting the height of the target pillow. Two Qualisys infrared cameras were located approximately 3 m apart in a plane parallel to the sagittal plane and about 4 m from the sagittal plane.

Reflective tape was placed on the elbow, around the wrist, and around each rod at two points. Three-dimensional images of each swing were recorded at 240 frames per second. Each participant swung each rod (in random order) three times, at intervals of about 30 s and through an angle of at least 150º and sometimes up to 240º before striking the pillow. Data files from the two cameras were processed to output centred (x, y, z) coordinates of each marker over selected intervals of time starting from the beginning of each swing and ending just before each rod hit the pillow.

Outcomes: The results from this study showed that the swing speed decreases as Moment Of Inertia (MOI) increases when Mass (*M*) is held constant, regardless of whether the rod is swung by both the upper arm and the forearm or by the forearm alone. This study found results for one participant surprising, indicating that for any given rod, the swing speeds were approximately the same in the seated and standing positions. However, changes in rod MOI had a greater influence on forearm-only swing speeds, because the rod MOI is then a larger fraction of the total moment of inertia about the most proximal axis. In all cases, the lightest rod was swung at approximately the same speed as the intermediate weight rod. Though the results suggested, for example, two participants might benefit by using an intermediate weight racket, on average there was no benefit for any batter in using a light, heavy or intermediate weight racket. An even simpler result was obtained by averaging the swing speeds over all four participants, in which case the maximum linear speed was essentially independent of *M*.

Limitations and gaps in the study: This study used a sixth-order polynomial to fit the data set of the angle of inclination of the forearm and the rod as a function of time. This polynomial fit was required as the video recorded data did not provide smooth data. It is possible that non-uniformity in the swing data is the result of the position of the swung rod relative to video position.

Possible endeavours ahead: It was suggested that racket or bat power should enhance the conclusions. Using tiny sensors the limitations of this study could be overcome as the sensor records continuous and uniform data throughout the swing. The racket or

bat power could also be measured.

**Joseph et al. [67]**

Topic: Techniques of straight hitting the ball at the goal from the top of the shooting circle by fifteen women national hockey players.

Methodology: The hitting motions were videotaped with Panasonic model NVGS150 video camera of frame rate of 50 Hz and shutter speed of 1/250 sec. The camera was set approximately perpendicular to the direction of execution of the skill and the video footage of five repetitions for each individual was captured to analyse various temporal and kinematic parameters of the style using siliconCOACH Pro software.

Outcomes: This study measured the back swing and swing time, knee angles during the swing, contact and follow-through actions and the pattern of movement of the rear foot in the follow through. This study categorized the measured hits into three styles named as Technique-A, Technique-B and Technique-C based on the distinct differences in the movement of the trailing (right) leg in the follow-through.

Technique-A, a movement pattern similar to a running gait was observed. The player maintained a knee angle that facilitated the swing of the stick close to the foot, depending on length of the hockey stick. In the follow through, the right leg was swung forward in a transfer of body weight, which this study stated would reduce the stress on the left knee. A concentric action of the quadriceps propelled the body forward in a gait-like motion.

Technique-B, while setting up for the hit, the body was brought abruptly to halt with the planting of the left leg onto the ground with a rapid eccentric firing from the quadriceps to stabilize the knee angle. The study explained that the left abductors played the role of stabilizers in enabling the knee joint to be stable at the time when the stick contacted the ball. Force was transmitted medially from the lower extremity to contribute to the movement of the ball at strike. The upper trunk contributed only minutely as it did not lean forward instead permit early opening of the left shoulder.

Technique-C, the body was brought abruptly to a halt by planting the left knee onto the ground, which leads to counter-rotatory movements (the swing of the hockey stick and the crossover movement of the right leg) across the left hip which acted as an axis of rotation. The abductors play a dominant role in stabilizing the left lateral knee. This study reported a rapid eccentric action of the left quadriceps groups of muscle and the action remained till the follow through of the stick was completed. Ground reaction forces also pushed the body back.

Limitations and gaps in the study: The video method used in this study might introduce the error in the measurement due to the position of the different limbs and the camera positions. As the camera was fixed the tracking data from the movement of a limb is not uniform, for instance, when the positional height of a limb in the movement plane was the same as the camera height it might result in larger values of the parameter compared to other positional height of that limb. These variations might result from the physical variations in the limbs of different batters that might introduce error as a form of non-uniformity while comparing the batters movement parameters.

Possible endeavours ahead: By employing inertial sensors, the same parameters could be measured and the limitations could be overcome by getting more uniform and continuous data.

**Busch et al. [55]**

Topic: Examined the possibility to estimate the angular velocity and position of the cricket bat and bat twist during a swing using a tri-axial accelerometer.

Methodology: Using bat attached inertial sensors, the ball-contact time, bat twisting and bat tapping prior to swing in off drive, straight drive and on drive performed was recorded. A ball machine was used. Bat swing data under both ball-free and ball machine conditions were recorded.

Outcomes: The time of ball impact were evident by a small dip in the sensor profiles

during the swing. They noted the bat tapping as a small spike just prior to the swing and twisting of the bat from the *y*-axis acceleration profiles. The off drive and on drive shots produced a difference in the bat angle recorded from the *y*-axis acceleration profiles.

Limitations and gaps in the study: This study did not use any validation and refinement techniques for sensor data; just the possibility of using sensors in extracting cricket batting stroke features was reported.

Possible endeavours ahead: Busch et al. [55] concluded that using inertial sensors various key features of a drive such as shot power, shot direction and angle of elevation of the bat during swing could be extracted. They also anticipated future research in verification and refinement of the sensor's data in the light of motion captured data.

### James [52]

Topic: Method of measuring swing path of a sword using sensors that enable the subjects to compare their stroke with a template stroke as a form biofeedback.

Methodology: IMU (Inertial Monitoring Unit) included with tri-axial DC accelerometers, gyroscope and magnetometers with a Bluetooth transceiver and the output displayed on a computer screen.

Outcomes: The subjects improved their learning of a basic skill by following the template.

Limitations and gaps in the study: This work did not use any validation process and did not state the limitations of this method.

Possible endeavours ahead: The same methodology could be used for the cricket bat swing and biofeedback could be made available to the batters with proper validation techniques.

**Weissensteiner et al. [68]**

Topic: Assessment of technical proficiency of skilled and lesser skilled cricket batters performing front foot drives and back foot pull shots against a ball machine in terms of (i) Shot accuracy (ii) Degree of hand-eye coordination (iii) Movement initiation (iv) Swing ratio and (v) Kinematic Sequencing.

Methodology: This study used Gen-locked high-speed Phantom cameras (mid-off and point perspective) at 120Hz. Two digital video cameras (50 Hz) were also used in this study to capture the time of ball release from the balling machine and movement initiation of the batters. One of these two video cameras was positioned above the ball machine and another one on tripod at a mid-off position focusing on the batter. Both cameras were linked together via digital cables through a digital video mixer, digital video recorder (DV Walkman) and viewing monitor to synchronize the time of ball release with the commencement of the batter's backswing.

Outcomes: This study reported that at the early stages of development (ages under 15), the skill groups differed in their technical skills in shot accuracy and quality of bat-ball contact. Skilled batters showed better control over the drive and produced more accurate shots across all bat conditions compared to their lesser skilled counterparts. The skilled adults were much faster than all other groups in regard to initiation of their movement, i.e. commencement of backswing while performing a front foot drive. Skilled batsmen differed in the timing of front foot stabilization according to their age groups in the front foot drives. Across all bat conditions, 55 % of the skilled adult stabilized (i.e. fully planted) their front foot before commencing the downswing of their bat, while lesser skilled do 24 % and the skilled of under 15 years age group do 17.42% of trials.

Limitations and gaps in the study: A methodology with a significant amount of bulky instruments was used. Sensor methodology could make this research protocol simpler in aspects of handling, time synchronizing and data collection.

Possible endeavours ahead: Using sensor methodology this work could be done more precisely, because each sensor has the ability to record data continuously and uniformly.

**Dias et al. [13]**

Topic: Analysis and determination of the differences in the initial movement patterns between elite and amateur batters in terms of perception time, force magnitude and direction, and stability.

Methodology: A 14-camera Cortex Motion Analysis System (200 Hz) was used to capture each of eight batters (recruited from the elite and amateur levels) playing a stroke against 30 deliveries from one of two second grade opening fast bowlers. Each batter was fitted with a 48 retro-reflective marker set. During the stance phase of the stroke the foot placement was made on a separate Kistler (Type 9287B) multi-component force platform for dynamic and quasi-static measurements of body movements. In this study a TeleMyo 2400R Force Transducer was placed on the second finger of the bowling hand to record the time of ball release by the bowler.

Outcomes: Multiple kinematics chains based on the location and orientation of local joint coordinate systems for each body segment according to Grood et al., 1983 (as cited in [13]) was defined in this study. A 16-segment three-dimensional kinematic model of the batter and bat was constructed in MATLAB (Version 7.0, Mathworks, Inc.) from the motion analysis data.

  Two types of initial movement were classified in this study: the forward and backward initial movements, based on the occurrence of the last maximum GRF (Ground Reaction Force) prior to the initiation of the final foot placement. A forward initial movement of the batter was identified if there was a maximum GRF on the front force platform prior to a final back foot plant before impact and conversely a back foot initial movement if there was a maximum GRF on the back force platform prior to a final front foot plant before impact. The front foot initial movement was completed after the ball release and was easily observable during back foot strokes.

The end of the front foot initial movement was reported in this study approximately at the time of maximum GRF through the back foot. Conversely, the opposite applied for the back foot initial movement. Batters with a front foot initial movement had an advantage when playing front foot shots, since their weight was transferred onto the back foot and the front foot was moving forwards before the ball was released. However, when playing back (i.e. not moving forward) these batters tended to rapidly bring their front foot down and jump onto the back foot. Conversely, during back foot strokes, the batter with the back foot initial movement was able to easily shift weight onto the back foot by stepping backwards.

Elite batters had a stable back lift angle during the initial movement, while amateur batters reduced their back lift angle. Hence, amateur batters tended to initiate a second or double back lift prior to final ball contact, which was seen as a second peak during the back-lifting time. In addition, this work found that the amateur tended to have a higher average back lift angle at all times prior to impact.

This work concluded in the way that, considering the initial movement as an important determinant of footwork, elite batters might be utilizing more effective initial movement patterns to promote efficient footwork compared to amateurs.

Limitations and gaps in the study: From the motion analysis data a kinetic model was constructed to observe the peaks and initial movement patterns of the batters. Use of bulky technological tools and the efforts in analysis required for forming the model made the methodology quite cumbersome and complex.

Possible endeavours ahead:  The limitations of this study could be eliminated by tiny sensor methodology that can provide the movement data as a sequence of kinematic chain by the accelerations profiles from the sensor recorded data directly. Then complexity in analysis for model formulation and use of bulky tools could be bypassed using sensors.

**Ohta et al. [54]**

Topic: Establish a method for measuring rotational movement (measuring forces and joint torques) and biofeedback training system of hammer throwers during their training.

Methodology: This work used a system integrating small accelerometer sensors, signal processing, short-range wireless transmission, wearable data-logger and biofeedback training system.

Outcomes: The high accuracy of the developed system was stated while the angular velocity and angular acceleration were compared with that measured by gyro sensors.

Limitations and gaps in the study: This study did not use any validation techniques using existing video or motion capture tools over the sensors system, rather one type of sensor data were compared to the other type. This study confessed that the high accuracy stated in the result was dependent on the fact that the both sensors did not have same error.

Possible endeavours ahead: The errors could be checked by the video or motion capture systems.

**Beek et al. [69]**

Topic: A case for long-route modeling in studying the control of interceptive actions with discussing several limitations of short-route attempts to directly model the dynamical mapping of perceptual variables onto motor variables.

Methodology: Two classes of dynamic models for the control of interceptive actions were distinguished in this work; called short-route and long-route (see Fig. 2.2). This work critically evaluated three short-route models that were being pursued in the study of interceptive actions.

Outcomes: This study documented that Warren, 1988 and Schöner, 1994 (as cited in [69]) described the Short-route models as how perceptual and motor variables are coupled to each other dynamically, thus constituting particular perception–

movement dynamics in the form of a dynamical control law.
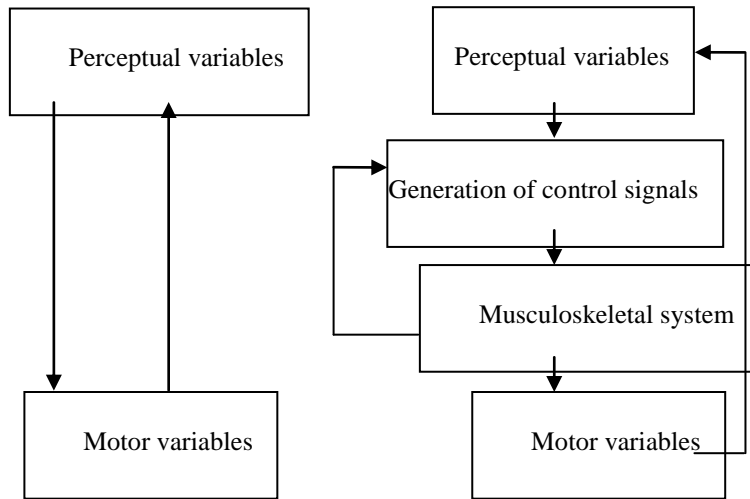


**Fig. 2.2** (a) 'Short-route' models address the coupling between perceptual variables and motor variables at a behavioural level through dynamical equations of motion (left figure); (b) 'Long-route' models specifically address how the information carried by perceptual variables is transformed into appropriate control signals for the musculoskeletal system (right figure). ([69]).

The short route model described by Warren, 1998 and Schöner, 1994 (as cited in [69]) does not address how the dynamical properties of interceptive behaviours are instantiated by human action. This was the objective of long-route models, which consists of dynamic formulations of the subsystems (i.e. sensory, neural, and biomechanical) and their interactions.

The long route has not been fully pursued until their current work. A full dynamical neuro-musculoskeletal model had not been formulated. Models of the neural (Dessing, 2002 as cited in [69]) and the musculoskeletal systems (Van Soest, 1996 & Beek, 1991 as cited in [69]) address aspects of the control of interceptive actions.

Limitations and gaps in the study: This is a descriptive study based on literature and no results from experiment or mathematical manipulation were included.

Possible endeavours ahead: Some of the hypothesis stated in the model could be

checked by experiments using tiny sensors.

**Ahmadi et al. [44]**

Topic: Investigation of monitoring the Kinematic Chain of the first serve swing in tennis and the level of proficiency of four male tennis players with different levels of skill using accelerometers.

Methodology: Three MEMS accelerometers were mounted on the knee, leg, and wrist of the tennis players. The serve during the backswing preparation as well as the forward swing motions were investigated. Each player performed approximately 10 first serves to ensure the system was not limiting their movements. Each player was then asked to serve and return to his original position after each serve. The player was then asked to delay for approximately 5 seconds before starting the next serve. The signals from other movements were identified and removed, and the players could focus on the next serve. The movements were captured by two digital video cameras (30 frames per second), and the accelerometer nodes were synchronized with the recorded images so that specific events could be identified. A model was developed from the acceleration data.

Outcomes: To maximize the ball velocity at impact, the Kinematic Chain pattern and correct angular and translational movements of the knee, waist and wrist of the player were discussed. The correct sequential order of the kinematic model of the tennis serve was observed as stated in the literature (Brian et al., 2006 as cited in [44]). The most obvious differences between the sub-elite athlete's serves and the developmental athlete's serves were detected in the hand side-forward motion and the waist forward motions. These differences were most apparent around the impact. Since the amateur player did not employ his waist to generate power to the serve, his side motion pattern was completely different from that of the sub-elite player. A significant difference in acceleration magnitude between the amateurs and sub-elite players around the time of impact time was found. The forward waist motion also exhibited a difference between the sub-elite and the amateur. The forward motion of the waist

was linked to the rotation of the waist in the service motion. The rotation pattern varied from the sub-elite players to the developmental players as there was either no rotation or some rotation at the wrong time observed in the developmental players. The full rotation occurred around the impact time for the sub-elite players. The repeatability of the swing was also examined. The sub-elite players had less variability through the complete swing compared to the developmental players. The sub-elite players were more consistent in their service and their action was more controlled.

Limitations and gaps in the study: In this study, video cameras were used as a reference to formulate the kinematic chain. The validation process was not outlined. The acceleration profiles were not matched to the video data.

Possible endeavours ahead: The sensor data could be validated by comparing the acceleration data with video estimated acceleration data using the mathematics of rigid body dynamics.

## 2.2   Ecology & Assessment

### Mann et al. [28]

Topic: Investigation of the quality of bat-ball contact, forcefulness of bat swing, and likelihood of dismissal on ten skilled cricket batters to examine two tasks on refractive blur. Two tasks were the resilience to refractive blur for batters facing a projection-machine, and the same for a situation when the batters faced live bowlers.

Methodology: All the subjects were wearing contact lenses of four refractive blur levels (habitual, +1.00, +2.00 and +3.00 D) while batting against bowling machine and a live bowler. The video footage of all testing was recorded by Sony HDR-FX1E digital video camera from an elevated position behind the bowler's release position. A Stalker ATS Sport Radar (Stalker Radar, USA) was used to measure the ball-velocity.

Outcomes: A significant level of blur (+3.0 D as stated in this study) was required for any significant decreases in performance. This result replicated those reported previously by Mann et al., 2007 (as cited in [28]). The same result was observed in case of the bowling machine and a live bowler when pre ball-flight information is available, and when ball-speed is increased towards the upper limit of velocities experienced in sport. However, temporal demands of faster ball-velocity resulted in an earlier blur that lead to a decrease in interceptive performance even at +2.0 D blur level.

Limitations and gaps in the study: The use of video cameras in this study could be replaced by the tiny sensors. The measurements parameters: quality of bat-ball contact, forcefulness of bat swing, and likelihood of dismissal could be documented quantitatively using sensor data. In this study only a qualitative assessment of those parameters was reported.

Possible endeavours ahead: The authors suggested that sensors (accelerometers and gyroscopes) might be used to examine the torque with which the bat is swung, and vibration sensors may evaluate the quality of bat-ball contact quantitatively. High-speed cameras and force plates could be used to record the time-course of movements and validate the tools.

**Pinder et al. [18]**

Topic: Investigation of information-movement couplings of eight right-handed and four left-handed junior batters (classified as "less skilled") performed the forward defensive and forward drive strokes when facing a bowling machine and bowler.

Methodology: A video camera (Sony HVR-VIP) was used to capture the drives and a second synchronized camera to capture the point of ball release from the bowler and bowling machine. Markers ware placed on different body location of the batter, helmet and edges of the bat facing the camera and a sports radar gun was used to measure bowling speed. The ultimate aim was to compare the different phases of movement timing and coordination during a drive between the bowling machine and

live bowler conditions. The different phases of the batting strokes were stated as backswing initiation, initiation of front foot movement, initiation of downswing, front foot placement, ball impact with the bat.

Outcomes: The result in this study indicated that the batters showed delayed initiation of the backswing and front foot movements during the bowling machine condition compared to live bowlers. This study observed that these batters (assessed as less skilled) demonstrated a similar level of coupling between the two mentioned strokes under both the bowling machine and bowler conditions. These developing batters showed no differences between the ratios of the backswing-downswing across these two different tasks. However skilled batters were able to alter the ratios addressed by previous research (Renshaw et al., 2007 as cited in [18]). No significant difference in the position of the head over front foot was noticed between those practice task constraints. However, at impact, larger angles of the elbow and front knee indicated significant spatial changes in the movement pattern when facing a bowling machine due to added temporal constraints.

This work supported the previous suggestion about the use of bowling machine in practice at a developmental stage of batting. That is, using bowling machine in practice session and an over-reliance on it might delay the player development (Araújo et al., 2007 as cited in [18]).

Limitations and gaps in the study: This study used a video camera with markers placed different body locations of the batter. This methodology could be replaced with tiny sensor methodology that can provide precise, continuous and uniform data.

Possible endeavours ahead: Future research to discover the exact sources of information is critical to regulate actions at different stages of the skill pathway in cricket batting. Tiny sensors could find these information sources.

**Müller et al. [25]**

Topic: Examination of the abilities of highly skilled and less skilled batters to utilize

visual information prior to and during sections of ball flight.

Methodology: In this study six highly skilled (three left-handed and three right-handed) and six lesser-skilled batsmen were required to bat against three right-arm, male fast bowlers. The batsman's vision was controlled during the batting remotely via a laptop computer where each batman wore a pair of PLATO liquid crystal spectacles that could be opened (to provide vision) or closed (to occlude vision). The spectacles allowed the experimenter to control the duration of the batsman's vision of a delivered ball (or amount of visual information available) so that: (i) vision was occluded as close as possible to a point prior to ball release (providing vision of only advance information), (ii) vision was occluded as close as possible to a point prior to ball bounce (providing vision of advance information and early ball flight) or (iii) no occlusion, where vision of advance information, early ball flight as well as ball bounce and late ball flight were all visible. The batsman's task was to attempt to strike the delivered ball like they would in a match situation to score runs without being dismissed. Two cameras were used to record the action in each trial. A Peak high speed video camera sampling at 200 Hz was positioned behind and slightly to the off-side to capture the batters movements as well as the bowler's run-up and delivery stride, the ball bounce, and the moment of display occlusion (signaled by illumination of a LED in the camera's field of view and triggered by closure of the occluding spectacles). A standard VHS camera (sampling frequency 25 Hz) was positioned behind the stumps at the bowler's end (in the position usually occupied by the umpire) to capture vision of bat-ball contact from a front-on position.

Outcomes: This study reported the body positioning involving the lower limbs and quality of bat-ball interception of both groups on the basis of the advanced ball flight and ball bounce information pick up. The results were reported as follows:

  (a) Foot movement accuracy:  Highly skilled batters had superior judgement capability at the pre-bounce and no occlusion conditions for full length delivery. Highly skilled batters significantly improved their judgement from pre-release to pre-bounce. Less skilled batters were unable to improve their judgement across both

conditions. For short length deliveries, highly skilled batters were able to pick-up and utilise advance information to guide foot positioning in a manner significantly superior to low skilled batters at the pre-release occlusion.

(b) Bat-ball contact accuracy: In long length deliveries a higher percentage of 'all' contacts by highly skilled batters was observed over low skilled batters at the pre-bounce and no occlusion conditions but not at the pre-release occlusion. From pre-release to pre-bounce, highly skilled batters improved 'all' contacts significantly. No significant improvement in contacts was found for low skilled batters across either occlusion conditions in this delivery. A larger percentage of 'good' contacts was attained by highly skilled batters at the pre-bounce and no occlusion conditions, but not at the pre-release. Highly skilled batters improved their contacts significantly from pre-release to pre-bounce and from pre-bounce to no occlusion, whereas no significant improvement in contact was found for low skilled players across either occlusion conditions. In short length deliveries, at the pre-bounce occlusion, the percentage of contacts was larger in the case of highly skilled batters, but not at the pre-release or no occlusion conditions. In this delivery highly skilled batters improved their contact significantly from pre-release to pre-bounce, but not from pre-bounce to no occlusion conditions. Low skilled batters are unable to improve their contacts across either condition, but showed a trend for improvement from pre-bounce to no occlusion conditions in this short length delivery.  In relation to 'good' contacts neither skill group was able to significantly improve their contacts across pre-release to pre-bounce or pre-bounce to no occlusion conditions. At the pre-bounce and no-occlusion conditions, moderate effects were reported for superior attainment of 'good' contacts by highly skilled batters.

This work demonstrated that experts can successfully deal with task constraints in improving their interceptive performance using their ability to judge the ball bounce position by picking-up advance visual information.

Limitations and gaps in the study: This study used bulky video cameras. The accuracy of the captured data was sometimes prone to error due to the fixed position

of the cameras, and the foot movement and bat-ball contacts may change with each event.

Possible endeavours ahead: Using tiny sensors the foot position and ball-contact could be recorded precisely. These sensors are independent of the varying positions of the limbs and bat.

**Mann et al. [39]**

Topic: Determination of whether induced myopic blur and hence sub-optical visual function would affect the performance of an interceptive cricket task.

Methodology: Using video camera, the drives of eleven males (aged 19-30 years) junior state cricket batters were captured. The batters faced four types of deliveries (short at the off-side, full at the off-side, short at the on-side and full at the on-side) from a bowling machine and the drives from five refractive conditions (wearing no correction for visual problem, wearing contact lenses of the patient's prescription, wearing contact lenses of +1.0, +2.0, and +3.0 D over-refraction).

Outcomes: This study measured the performance of the batter through two means: (i) evaluating the nature of the contact between bat and the ball ('good', 'bad', 'no contact' using the protocol advocated by Muller and Abernethy, 2006 as cited in [39]), (ii) grading of the quality of the stroke measuring firstly the percentage of balls for which a contact had occurred and secondly the percentage of balls for which only 'good' contact was made. This study found significant changes in batting performance with the introduction of +1.00 and +2.00D of induced myopic blur. A +3.00D over-correction was required before any significant decrease in batting performance was detected, demonstrating that batters needed to be essentially legally blind (as simulated through the use of the +3.00D over-refraction) before there was any significant measurable decrement in batting performance. This study concluded that optimal vision might not actually be required for superior performance in a highly demanding interceptive task. The addition of blur might prove to be a useful training tool, enhancing concentration, and stressing the earliest possible decisions to be

made. Thus a batter is able to tolerate considerable amounts of myopic blur before there is any measurable decrease in batting performance.

Limitations and gaps in the study: This study has used a video camera that might be prone to error due to its fixed position. Measures of bat-ball contact were derived through categorical judgements made by a trained research assistant with cricket experience. This judgement is dependent on the ability of the human observer.

Possible endeavours ahead: Tiny sensor technology can be used to have precise bat-ball contact data as a numerical format rather than the qualitative assessment by the trained research assistant.

**Renshaw et al. [23]**

Topic: Examination of forward defensive strokes from four right handed batters who played in Premier League competition in the U.K. against right arm medium pace bowlers of equivalent performance standard to the batters and against a bowling machine.

Methodology: The strokes were captured using a video camera (Sony DCRTVR 900E as mentioned in [23]) placed 13.5 m from the batter with the plane of motion perpendicular to the batting crease and at right angles to the movement direction of the shot using the 3-4-5 triangle method. A split-image filming device was used to capture the point of ball release as well as the image of the batters. This study investigated whether the different ecological constraints of batting would result in differences in timing and coordination in cricket batting on the basis of the time of initiation of (i) backswing; (ii) front foot movement; (iii) downswing; (iv) planting of the front foot.

Outcomes: The results in this study were summarized as follows:

 (a) Temporal differences:

(i) Major differences occurred in relation to the two phases of the backswing. When

facing the bowling machine, batters began the backswing much earlier than when facing the bowler.

(ii) Similar differences were observed for the timing for the downswing phase which commenced earlier when facing the bowling machine compared to the bowler.

(iii) In comparison, front foot movements were both initiated and planted at similar times in the two conditions, with movements beginning slightly earlier when batting against the bowler.

(iv) The timing of the foot placement was later when facing the bowler.

(v) The length of the stride was shorter when facing the bowling machine compared with a bowler.

(vi) The peak height of the backswing was higher and a more consistent peak backswing was observed with the bowler.

(vii) Shorter bat swing time (measured from backswing initiation to impact) when facing the bowler. Interestingly despite the backswing starting earlier when facing the bowling machine, backswing duration was similar in the two conditions.

(viii) The downswing was faster against the bowler.

(ix) The time difference between backswing and front foot movement was always greater when facing the bowling machine compared with bowler.

(b) Coordination differences:

(i) Against the bowler, batters started the backswing and front foot movements at similar times, whereas against the machine, the backswing started closer to the time of ball release. This finding implies that, at front foot initiation, the bat was already moving back and up (reflected by elbow angle differences at ball release and front foot initiation, and front foot knee angle differences at backswing initiation). It is also worth noting the higher standard deviations for both elbow angles in the machine

condition at ball release. These differences in timing mean that batters were at different stages of their stride when the downswing started. However, differences were also apparent in elbow angles. These differences were due to batters swinging the bat back higher when facing the bowler.

(ii) At front foot placement, the elbow differences showed that the downswing was nearer to completion when facing the machine.

(iii) At impact, the elbow angles of greater magnitude were observed with the machine.

(iv) All batters took longer strides against the bowler.

Considering both temporal and coordination differences, the findings in this study suggested that practising under bowling machines can lead to the development of coordination patterns and timing that differ considerably when compared to batting against a real bowler. Further research was suggested to manipulate the ball speed and skill level in order to observe whether information-movement couplings are affected by different ball speed and skill levels of the batter.

Limitations and gaps in the study: This study used video technology to measure the temporal and coordination parameters in which errors are likely due to the fixed camera position.

Possible endeavours ahead: Tiny sensors can provide more accurate results.

### Müller et al. [24]

Topic: Examination of the differences in ability to pick-up easily ball flight information on six highly skilled batters (three left-handed and three right-handed) and six lower skilled cricket batters (all right-handed males) faced three different leg-spin bowlers.

Methodology: Same as in Müller et al., 2009 (as cited in [24]) stated above except

leg-spin bowlers were used.

<u>Outcomes</u>: The objective was to determine the relative importance of information from prior to ball flight, from pre-bounce ball flight, and from after the ball bounce, to players with different batting skill.

The result of this study showed that that pre-bounce ball flight information appeared to be most critical for both highly skilled and lower skilled batters for guiding correct foot movement against the bowlers. While early triggering of foot positioning movements from advanced information available from the pre-release movement pattern of the bowler would be theoretically advantageous, the execution of such movements would be time consuming, and a stable whole body position in advance of ball arrival might be important for facilitating successful bat-ball contact. No strong evidence of advance pick-up of length information was apparent. When occlusion occurred prior to the release of the ball, both skill groups appeared to adopt a default strategy/response bias of presuming the ball would be of full length. The foot movement for full-length deliveries was consequently systematically better than for short deliveries in the pre-release occlusion. The foot movement accuracy for shorter deliveries approached zero for the lower skilled group in the absence of ball flight cues, suggesting a complete absence of advance information pick-up by this group. The accuracy of the highly skilled group was superior but still at a level not significantly different to that which could have arisen simply through guessing.

(i) It was clear that the information needed for the judgement of overall delivery length that guides gross foot movement positioning was not identical to that which was critical for the bat-ball contact. While foot positioning appeared to be achieved entirely on the basis of information prior to the bounce of the ball (from pre-bounce ball flight in the case of batting against spin bowlers, probably supplemented by pre-release/advance information in the case of batting against fast bowlers), precise interception of the ball appeared dependent on the availability of both pre-and post-bounce ball flight information. The later ball flight information appeared to be especially important for fine-tuning of the interceptive action. This was most evident

in the increase in the proportion of bat-ball contacts that are 'good' under the no occlusion condition compared to either of the conditions occluding visual information.

(ii) The results of this study showed that skill-related differences in the use of ball flight information could be more readily demonstrated through this type of in situ investigation than through traditional laboratory-based studies. While mediated in part by the length of the bowled ball, and hence the respective lengths of the pre-bounce viewing period and the post-bounce prediction period, consistent skill-related differences were nevertheless evident in the ability to use early pre-bounce ball flight information to improve interception (only the highly skilled batters showed an ability to do this) and the performance improvement generated from vision of post-bounce ball flight (highly skilled batters showing greater performance improvements). This is remarkably similar to that previously documented in relation to advance information pick-up in other ball sports (Abernethy et al., 1984 as cited in [24])-the more skilled batters being attuned to early visual information that the less skilled cannot use. The highly skilled batters are able to judge essential characteristics such as the landing position and the direction of spin from the movement of the ball in flight as well as 'off the pitch' whereas the less skilled are dependent solely on the later source of information. Under such circumstances the more hurried, less effective batting actions characteristic of the lower skilled batters are not surprising.

(iii) As ball flight forms an essential part of the constraints to batting, and as expert performance appears to be intimately linked to the capability to pick-up early ball flight information, it follows that an attempt to design training to accelerate the acquisition of perceptual expertise in sports like cricket (Muller and Abernethy, 2006 as cited in [24])  needs to address the provision of natural ball flight information. Given this, there may be merit in considering the use of the occluding spectacles technology not simply as means of measuring anticipatory skill but also as an integral part of a systematic training intervention.

<u>Limitations and gaps in the study</u>: Same as in Müller et al. [25] stated previously.

<u>Possible endeavours ahead</u>: Same as in Müller et al. [25] stated previously.

**Weissensteiner et al. [63]**

<u>Topic</u>: Examination of the relationship between anticipatory skill in cricket batting and the developmental practice histories of a total of 102 cricket male batters, from six different skill levels and age groupings.

<u>Methodology</u>: In this study skilled and lesser skilled batters of U15, U20, and adult age completed two discrete sets of tasks—a laboratory-based task to measure anticipatory skill in cricket in which they were required to use prerelease kinematic information to predict the type and length of delivery being bowled, and a structured interview of the participant's practice and developmental histories. This study proceeded in three parts. First, different age and skill levels participants' ability to anticipate the type and length of delivery being bowled by a medium-fast bowler was assessed using an established laboratory-based temporal occlusion task (from Müller et al., 2006 as cited in [63]). Second, the total hours of developmental sporting investment were detailed across the different skill and age groups using their memory to determine what developmental/practice variables differentiated the various cohorts. Finally, an attempt was made to match the anticipatory and practice history data to find those aspects of the participant's practice histories that were most predictive of their anticipatory skills.

<u>Outcomes</u>: In relation to anticipatory skill, this study hypothesized that the skilled batters would be capable of earlier and more accurate prediction of delivery type and length. This is in line with the result by Müller et al., 2006 (as cited in [63]), in terms of a selective ability to pick up useful predictive information in the time period from front foot impact to release. In line with Abernethy, 1988 (as cited in [63]), it was further hypothesized that an adult would be able to establish the expert advantage but not the earlier age group.

In relation to practice histories, this study expected that skilled batters would invest more time than lesser skilled batters in organized cricket-specific activities as well as

in other sports which transfer anticipatory skill to cricket batting skill (i.e., other fast ball sports in which early "reading" of the opponent's intention is needed for successful responding). Based on the Côté et al. developmental model of sport participation (Côté, 1999; Côté & Hay, 2002 as cited in [63]), this study predicted that these differences would emerge at approximately 13 to 15 years of age. Considering the variation in age, this study expected that greater hours of involvement in cricket and cricket-related activities, organized or unorganized, would reveal superior anticipatory skill and account for substantial individual variance in anticipatory skill.

This study showed that systematic skill and age group differences were relevant in both the type and length predictions. Skilled batters outperformed the less skilled batters and the adult and U20 batters outperformed the U15 batters. In terms of the time course of advanced anticipation, skilled adult and U20 batters showed a capability to use information in the period of bowling from front foot impact (FFI) to release (R) to improve prediction accuracy of ball type, and to a level better than guessing. This capability was absent in both the younger (U15) skilled group and in the less skilled groups of any age. Adult skilled batters, plus the less skilled U20 batters also showed a capability to significantly improve their accuracy in predicting ball length from information available in the period from the bowler's front-foot impact through to release. The anticipation of ball type through information pick up in the FFIR (front foot impact to release) by highly skilled but not less skilled adult aged batters was consistent with the findings of Müller et al. ,2006 (as cited in [63]).

The accumulated hours spent in organized cricket emerged from the second part of the study as the main discriminator of both the skill groups and the age groups. Across all three age groups examined, the highly skilled batters self reported having accumulated 2–3 times more hours of organized cricket experience than their age-matched controls. The total number of hours accumulated in unorganized cricket activity was also greater for the highly skilled batters in the U15 age group, but not among the older age groups. Likewise, the number of hours of experience

accumulated in sports (both organized and unorganized) was greater for the skilled cricket batters at the U15 age but less than that for the less skilled batters for the U20 and adult ages, consistent with the transition of the older skilled batters into the investment stage of sports participation (Côté, 1999; Côté & Hay, 2002 as cited in [63]).

This study suggested that the anticipatory skill and the volume of sport-specific experience might be closely associated. This study found that highly skilled batters (of adult and U20 age) have anticipatory skills superior to those of less skilled batters and that highly skilled batters (of all ages) have accrued significantly greater amounts of cricket-specific experience than their less skilled counterparts.

Weissensteiner et al. [63] emphasized for future research should seek to further differentiate types of cricket-specific practice (e.g., solitary batting practice, net-based practice with a bowler, net-based practice with a ball machine, game-context practice, video-based practice) and make clear, in organized settings, a distinction between the hours of experience accumulated in and outside of actual matches.

Limitations and gaps in the study: Same as in Müller et al. [25] for the experimental part of this study.

Possible endeavours ahead: Same as in Müller et al. [25] for the experimental part of this study.

**Müller et al. [70]**

Topic: The transfer of motor skill learning.

Methodology: Literature review.

Outcomes: This study stated that the level of skill learning and the success of skill transfer can have a potent influence on competitive performance. For example, will batting against a bowling machine maximise skill learning and will this transfer to an enhancement of batting performance against a bowler? For coaches, sports scientists

and sport practitioners it is important to know the factors of enhancing motor skill learning. The investment of time and financial resources in the design of practice can be targeted. This study found that a considerable body of research exists on the transfer of learning in cognitive (thinking) skills, this includes analogical transfer (i.e., learning of skills in one context and application of the skills to different context(s), namely problem-solving), formal discipline (i.e., transfer of memory skills, reasoning and logic learned from studying mathematics or language to the completion of everyday tasks), teaching intelligence (i.e., analytical, creative and practical thinking) and the impact of schooling (i.e., influence on IQ and success in securing jobs) (Barnett & Ceci, 2002 as cited in [70]). However, in relation to sport, little or no scientific evidence exists concerning the transfer of motor skill learning or the mechanism(s) underpinning this transfer. This study reported that anecdotal evidence of transfer exists in cricket. Thus elite batters with a background in baseball may transfer perceptual-motor skills that are beneficial to expert performance in cricket batting (so called talent transfer). However, whether skills can be transferred between baseball and cricket has not been confirmed through scientific investigation.

This study provided a model to examine questions directly related to the structure of the learning and practice environment created by coaches, (see Fig. 2.3). In relation to the physical context of these questions includes, for example, does batting practice indoors against a bowler on a synthetic grass pitch transfer to a match situation resulting in an improvement in batting performance? Does indoor batting practice against a bowling machine transfer to a match?

This study suggested that it would be valuable to determine if practice immediately preceding (few hours) or several days before a match best facilitates transfer. This could determine how psychological/physical fatigue and rest may contribute positively or negatively. This study cited that experts from field hockey, netball and basketball (invasion sports) are superior to non-experts at 'reading' the position of defensive batters, with this capability of experts transferred across all of these sports (Abernethy et al., 2005 as cited in [70]). This capability of experts may be related to

their broader learning experiences that may allow them to transfer skill learning to a greater extent and with greater success (referred to Fig. 2.3). However, this study commented that further investigation is required to determine the extent of expertise transfer between and within sports to confirm this claim.
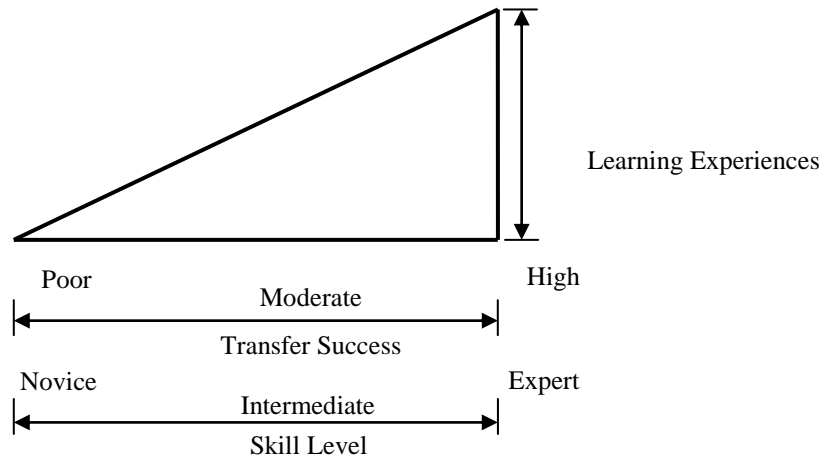


**Fig. 2.3**    Transfer of learning success relative to skill level and learning experiences (from [70]).

Limitations and gaps in the study: Not applicable because the publication was a literature review.

Possible endeavours ahead: The necessities of further investigations to determine the extent of expertise transfer between and within sports would be of value. Experimental investigations could be conducted using inertial sensors on cricket bat swing and bat swing in other sports (e.g. baseball and golf).

### Karliga et al. [71]

Topic: Proposed an innovative video analysis system for analyzing 3-D motion of golf swing based on a coarse-to-fine grain video object analysis framework similar to Luo et al., 2005 (as cited in Karliga et al., 2006 [71]).

Methodology: Video object segmentation technique.

Outcomes: As the first step, this study quantified the human body for analysis using a

object segmentation technique. This two dimensional information was utilized to obtain a three dimensional body model consisting of head, upper arms, lower arms, body trunk, upper legs, lower legs and feet using an iterative 3-D fitting algorithm and Dynamic Bayesian Networks (DBN). The system framework including the video object segmentation, the extraction of the lower arms of the batters, 3-D Human Body Model, the fitting of the human body to 3-D Model, as well as the Dynamic Bayesian Networks Model was explained.

Karliga et al., 2006, [71] proposed an automatic 3-D motion analysis system for golf which effectively integrates a video object segmentation technique based on mean shift region tracking, the locating of human body parts based on DBN modelling, and a 2-D to 3-D body fitting optimization algorithm.

Limitations and gaps in the study: This study used video footage data that might not have high level of accuracy due to the static position of the video. Moreover, the model was not validated by any other method.

Possible endeavours ahead: Tiny sensors could provide more accurate data as the sensor attached to a limb moves with the limb as a single body. As the sensor can provide direct 3-D data, so formulation of the model would be less cumbersome compared to the 2-D to 3-D body fitting algorithm.

## 2.3   Psychology

### Weissensteiner et al. [10]

Topic: Data from semi-structured interviews with fourteen male participants-three adult elite cricketers (EB1-EB3), two adult sub-elite cricketers (SEB1-SEB2), five elite cricket coaches (EC1-EC5), and four experienced cricket administrators (EA1-EA4) was used to generate a conceptual model of expertise.

Methodology: All interviews were transcribed verbatim and grammatical changes

were made to improve the flow of the text. Sentence-by-sentence open coding was then performed by the main researcher to draw out raw data themes in the form of quotations from each participant (Strauss & Corbin, 1998 as cited in [10]). Next, categories and sub-categories that captured the essence of the ideas or concepts being discussed by the participants were created using axial coding with each quotation being placed in the category (or sub-category) that it was deemed to best fit. Coding continued until theoretical saturation occurred, a point where no further properties, components, or relationships emerged from data collection and analysis (Strauss & Corbin, 1998 as cited in [10]). Following the completion of coding, conceptual models depicting the "hierarchical synthesis" of the emergent higher order categories (representing each major factor/skill component) and lower order categories (representing relevant sub-components), and the inter-relationships between them, were developed in the form of computer-generated mind maps. Finally, a global, multi-factorial model incorporating each of these critical factors and skill components, and depicting the inter-relationships between them in the form of a grounded theory, was generated from the analysis and compared with the relevant literature on expertise development.

Outcomes: The purpose of the study was to use multiple perspectives from credible sources to explore the development of expertise in cricket batting. The findings of this study supported the contemporary notion that expertise is inherently multi-factorial (Bailey & Morley, 2006 as cited in [10]). The data from this study provides a theory that encapsulated skill components and factors critical to the development of expertise and highlighted key factors that contribute to the development of expertise in cricket batting and influence the transition from "cricket scholar" (the aspiring batter eager to further his cricket education) to "expert" (the established international batter). Weissensteiner et al. [10] reported that successful progression along the pathway to expertise was seen to depend on the co-existence of five key factors, the developments that are inter-related and inter-dependent. Those factors were stated as Socio-Developmental (Contextual) Factors, Psychological (Cognitive) Factors, Visual Perceptual (Anticipation) Skill, Technical (Motor) Skill, and Intrinsic

Motivators.

In the model formulated by Weissensteiner et al. [10] it was concluded that a favourable socio-developmental environment (support, vast investment in creative and challenging play, sibling rivalry) provides the essential foundation for the development of positive psychological attributes (mental toughness, self-belief and confidence, ability to cope with adversity, adoption of individualized routines/rituals), technical skill mastery (optimal balance, speed of downswing, versatility of shot execution) and superior visual-perceptual skill. Intrinsic motivators (fun, enjoyment, challenge and achievement, desire to be the best, "love of the game", camaraderie) are regarded as essential to continuation and progression along developmental pathways. Facets of contemporary society and its constraints on free play emerged as one of the major limitations to the future development of expertise.

Limitations and gaps in the study: No experimental data is presented in this study. The model formulated from the interviewed data could be judged or validated by longitudinal studies.

Possible endeavours ahead: The authors suggested that further research is required to ascertain whether mental toughness can be fostered at an early age through psychological training. The transition from junior to adult competition was shown to be a critical step to expertise. To foster successful transition into adult competition, it is imperative that batters are technically, psychologically, and emotionally prepared, because a negative experience will have enduring effects on their confidence and belief.

**Müller et al. [72]**

Topic: Four experiments were used to identify the visual information used by cricket batters of different skill levels to anticipate the type and length of balls bowled by swing and spin bowlers. The objective was to determine whether expert performance was characterized by better use of the same sources of information as those used by novice and intermediate-level batters or rather by progression to the use of new and

additional sources of information to which the less skilled were not attuned.

Methodology: The four experiments in this study required batters to make advance predictions of ball flight (ball type) and landing position (ball length) by swing and spin bowlers from video simulations. In each experiment a different form of display manipulation was used to tease out the selective attunement of batsmen of different skill levels to potential sources of advanced information. In Experiment 1 a temporal occlusion was employed with the display occluded at different time periods during the medium-pace (swing) and slow (spin) bowler's delivery action. Each point of occlusion was linked to identifiable kinematic events within the bowling action. In Experiment 2 a common time course of information was provided but visibility to specific features of the bowling action was continuously masked using spatial occlusion (Abernethy & Russell, 1987 as cited by [72]). Experiments 3 and 4 also used forms of spatial occlusions—Experiment 3 only provided vision of the motion of isolated segments of the bowler's body whereas Experiment 4 provided for the progressive addition of vision of more proximal body segments to determine the additive value of motion of specific segments to the prediction of ball type and length.

A Sony DVCAM digital camera (model DSR300) was used to capture video images from a batsman's viewing perspective, of the bowling actions of one medium-pace swing bowler and one leg-spin bowler as they bowled a series of different deliveries on a conventional outdoor turf cricket pitch. Video images of the bowlers' actions were projected to a 1.78 × 1.38-m size using a SONY data projector (model VPL-CS5).

Outcomes: The experiments in this study demonstrated that advance information pick-up was not only dependent on the skill level of the batters but also to varying degrees, by the different task constraints imposed by swing and spin bowlers and the different requirements to predict either ball type or ball length. For the faster (swing) bowler, batters of all skill levels showed a reliance on ball flight information to judge the type of ball being bowled; however, the highly skilled batters demonstrated the

additional, unique capability to also extract advance information in the period from Front Foot Impact (FFI) to Release (R) (Experiment 1). Experiments 2–4 demonstrated that for this advanced pick-up of information to occur, the BA (Bowling Arm) and BH (Bowling Hand) must be simultaneously present, suggesting that it is the referential relationship between these two (that determines inter alia wrist angle) that is critical and to which only the highly skilled batters are attuned. The evidence in relation to the advance pick-up of information about the length of the ball being bowled by the faster bowler was more variable. Evidence for advanced identification of length information by the highly skilled group, and perhaps also the intermediate group, was obtained in Experiment 1 but no further evidence of this was forthcoming in subsequent experiments for any of the skill groups. For the slower (spin) bowler, only the highly skilled batters demonstrated an ability to pickup advance information to determine the ball trajectory. Experiment 1 revealed that this information pick-up occurred early in the bowling action (between Back Foot Impact (BFI) and Front Foot Impact (FFI)), with later experiments demonstrating that this information is derived primarily from the bowling hand (Experiments 2 and 3) although the simultaneous presence of the bowling arm enhances this information pick-up (Experiment 4). The evidence was mixed in relation to the prediction of length for the spin bowler. There was no evidence in Experiments 1 and 2 of any advanced pick-up by any skill group. In contrast, the highly skilled participants used in the later experiments showed an ability to make predictions of length on the basis of advance cues alone, and this appeared to be due to an interpretation of the information arising from the relative motion of the bowling hand and arm. No advanced pick-up of length information was possible when these cues were presented in isolation (in Experiment 3) but when they were simultaneously present (in Experiment 4) the prediction was statistically significant although again only for the highly skilled group. The prediction of both the length and the type of ball delivered by the spin bowler requires ball flight information to all skill groups to enhance prediction accuracy.

The findings of this study confirmed the previous observations of superior advance

75

prediction by skilled batters of the type and perhaps also length of ball bowled by swing bowlers (Abernethy & Russell, 1984; Penrose & Roach, 1995 as cited in [72]) and the type of ball bowled by spin bowlers (Renshaw & Fairweather, 2000 as cited in [72]).

Limitations and gaps in the study: No experimental batting action was used in this study. Also absent is how the batters of different skill level manipulated their motor tasks using the bowled ball information they identify.

Possible endeavours ahead: Batting experiments could be combined with the tasks performed in this study. The initiation of motor action of each participant could be categorized from the level of bowled ball information pick up.

## 2.4    Morphology & physiology

### Christie et al. [11]

Topic: Measured selected physiological responses during batting in a simulated high-scoring 1-day cricket game.

Methodology: Ten male university cricketers performed a batting work bout consisting of four sprints per over (six balls) for a seven over period. Testing was conducted outdoors with batters wearing full batting gear. All experimentation was conducted under temperate (range of 17-24º C) environmental conditions. During the simulated work-out, a portable on-line metabolic system (the $k4b^2$) was attached to the subjects for the continuous assessment of selected physiological variables including heart rate (HR), ventilation ($F_B$, $V_T$ and $V_E$), oxygen uptake ($V_{O2}$) and metabolic carbon dioxide ($V_{CO2}$) production. Energy expenditure was calculated from the oxygen consumption responses and substrate use was calculated from the $V_{O2}/V_{CO2}$ responses.

Outcomes: The result from this study indicated that all of the physiological responses

increased significantly from the first to the second over, while the heart rate continued to increase significantly until the end of the third over after which it stabilized. This is likely due to the many factors which can affect heart rate including emotional state and food intake. During the last four overs, the heart rate ranged between 149 ($\pm$19) and 155 ($\pm$18) bt min$^{-1}$ with a mean heart rate of 152 bt min$^{-1}$ (75% of age predicted maximum heart rate for the group). The mean oxygen uptake during the work-out was 26.7 ($\pm$1) mlO$_2$ kg$^{-1}$ min$^{-1}$. Breathing frequency increased more (26% from the first to the last over) than tidal volume (10% increases) indicative of maximal effort. Increased breathing frequency therefore had a greater impact on the minute ventilation response which increased by 32% from the first to the last over. As a result of the heavy anaerobic work performed during the sprinting of one pitch length, the respiratory exchange ratio (RER) was above 1.00 from the second over onwards. This shows that there was additional production of $CO_2$ from the buffering of hydrogen ions and also that there was a predominance of carbohydrates as the preferred energy source. The mean energy cost during the work bout was 2536 kJ h$^{-1}$ (302 kcalm$^2$ h$^{-1}$).

This study demonstrated that although technical skills are predominant factors in sports like cricket, the training status of the cricketers also plays an important role. Despite the acknowledgement for the need for adequate physical training for cricketers, the physiological demands of the game are not well defined.

Limitations and gaps in the study: The instrument and devices attached to the batter's limbs in this study might have provided certain degree of unusual circumstances. This study did not mention anything about these encumbrances.

Possible endeavours ahead: This study concluded that as no research has specifically compared the physiological profile of different cricket matches, and because the demands placed on cricketers are highly dependent on the type and nature of the game, it is recommended that future studies consider more in-depth analyses of the physiological profile of different types of cricket matches and batter responses (batting, bowling and fielding). This study further suggested that in order to enhance

the research design, these investigations would need to be compared to a control condition.

## 2.5   Injuries and implements of batting

**Koenig et al. [31]**

Topic: Two distinct sets of experiments measured the swing speed of college baseball and fast-pitch softball batters using weighted rods and modified bats. Experimental and analytical studies of bat swing speed were conducted with particular emphasis on the influence of the bat moment of inertia.

Methodology: Studies 1 and 2 involved speed measurements of bats swung by experienced players in controlled hitting situations. In study 1 male collegiate baseball players used production bats and weighted rods. Female collegiate fast-pitch softball players as well as male collegiate baseball players participated in study 2 and used production and modified production bats. In this work the basic measurement in both investigations was the time of flight of the bat between vertically oriented light beams and light sensors. Bat speeds reported in this work were calculated by dividing the distance between sensors by this time of flight.

In the first study, data were obtained from three arrays units of upward-looking light sensors illuminated by overhead sources.

Seven 4.2 mW lasers provided the light for the second experiment. The lasers were positioned so that each illuminated a corresponding sensor mounted in a regulation-size home plate. The lasers were 2.4 m above the plate. Uncertainty in beam spacing was estimated to be +0.2 mm about a nominal value of 50 mm. Semiconductor-based photo detectors like the ones used in the first study were set in the home plate so that each receiving lens was approximately 6 mm below the plate surface and aligned with the corresponding laser. Sensor outputs were sampled at 50 kHz by a PC-based digital oscilloscope and data acquisition system. Uncertainties in sampling and

switching times were the same as those in study 1.

<u>Outcomes</u>: This work revealed that as the bat inertia increases the swing speed decreases. For both women and men, speeds were slower for swings at pitched balls than for swings at balls on the tee. There was more deviation from the general trend for swings at pitched balls for both groups of batters. These slower and more variable bat speeds would appear to be largely a consequence of the greater amount of decision-making and adjustment required in order to hit a moving ball. The rather large variations in speed for swings at the pitched balls also suggest that bat properties in addition to the moment of inertia of the bat play a role in swing speed.

This study illustrated the complexity of the bat swing process. It demonstrated that in determining bat speed, multiple bat inertial properties, the moment of inertia about a body axis and the mass principal played important roles. However, there was not sufficient data available to accurately quantify these roles. The authors reported that their results along with others cited in their work provided general measures of those roles.

The analysis in this work predicted relatively well the decrease in swing speed that occurred for moderately large increases in bat moment of inertia about a body axis. The inclusion of body translation and rotation about a wrist axis were important.

The analytical model in this work assumed pure rotation of the batter/bat system about a vertical axis through the batter's body. Aerodynamic drag of the batter's arms and the bat was included in the model. The independent variable was bat moment of inertia about the rotation axis. There was reasonable agreement between the model and the measured speeds. Detailed differences between the two suggest the importance of additional degrees of freedom in determining swing speed.

<u>Limitations and gaps in the study</u>: The data predicted by the model were compared to the light sensor array data but the validation of these two systems was not carried out. Video or motion capture system could be used for the validation procedure.

Possible endeavours ahead: The authors suggested more accurate representations of batter inertial properties and strength capabilities should be pursued; and proposed that the model based on pure rotation about a body axis, provides a useful framework for estimating bat swing speed.

**Fleisig et al. [73]**

Topic: Investigation of the relationship between bat mass properties (mass and moment of inertia) and bat velocity (linear and angular) for baseball and softball.

Methodology: Seventeen male collegiate baseball batters and 17 female collegiate softball batters were asked to swing aluminum alloy bats with various mass and moments of inertia. The moment of inertia (MOI) about the handle was calculated by measuring the period of each bat's pendulum motion when the bat was suspended about the knob at the end of the bat. The moment of inertia about the bat's C.G. (centre of gravity) was calculated using the parallel axis theorem. Five bat with different mass of a Louisville Slugger TPS softball bat and five of an Easton B5 baseball bat were used. Nine male participants were randomly selected to test two lighter unmodified bats – an Easton BE40W and a Louisville Slugger TPX. For each bat, the rubber knob at the end of the barrel was covered with reflective tape (3M, St Paul, MN, USA). In addition, a 0.6-cm wide band of reflective tape was wrapped around each bat 56 cm from the marker at the end of the barrel. All testing was captured by a four-camera 200 Hz automatic digitizing motion analysis system (Motion Analysis Corporation, Santa Rosa, CA, USA). A pitching machine was set to pitch balls at a typical practice velocity ($26m.s^{-1}$) from a distance of 13 m from the home plate, as recommended by the coaches. After taking one or two warm-up swings, the batter took three swings for data collection.

Outcomes: The linear velocity varied significantly among bats, and these variations were significantly related to bat MOI, not the bat mass. Variations in the bat angular velocity were not significant for both the baseball bats and softball bats. The relationship between the linear and angular parameters was not intuitively obvious in

this study. It was observed that the bat motion could be described as either a rotation about a moving instantaneous centre of rotation or a combination of linear and angular motion of a fixed point on the bat, such as the butt end of the handle.

Limitations and gaps in the study: Although the current study allowed calculations of the bat velocity it did not investigate the effects on the batted ball velocity. This is because the weighting and machining of the bats grossly affected the bats' flexural properties and momentum transfer, so the result on batted ball velocity was thought not be practically relevant.

Possible endeavours ahead: This study proposed for measuring the batted ball velocity. This would allow bat manufacturers to circumvent the minimum bat weight rule by modifying the design of a low mass/low MOI bat with extra mass placed within the handle.

## 2.6   Literature using sensors methodology for other sports

### Ahmadi et al. [43]

Topic: Comparison of the results of the developed inertial sensor techniques, and marker-based inertial sensor techniques with accepted videographic techniques when applied to the upper arm rotational velocity measurement in tennis serve.

Methodology: To measure upper arm rotation angle during the tennis serve by a subject, a network of two inertial sensors on the upper arm and the chest was used. A marker-based virtual gyroscope (MBVG) was derived using a vector-based method of marker trajectories and a series of geometric transformations from Vicon marker positions in the standard Plug-in-Gait model. The three different methods were compared from selected three of ten serve performed by a subject. The average value for the inertial gyroscope as well as the MBVG was calculated. The normalized average outcomes from the inertial gyroscopes and the MBVGs are presented along with the published videography results.

<u>Outcomes</u>: Between 0 and 0.4 normalized time, which corresponds to the preparation phase of the serve, the results in this study showed a close agreement in normalized angular velocity between the marker-based virtual gyroscope and videography between normalized time 0–0.2 ($r = 0.9698$, $p<0.0001$). Between the marker-based gyroscope and videography results the agreement continue from normalized time 0.2–1 ($r = 0.9470$, $p<0.0001$). The same trend is seen between the results from the gyroscope and the videography ($r = 0.9762$, $p<0.0001$) only between normalized time 0.2–1. The videography data used in this study were obtained from the literature (Elliot et al., 2003 as cited in [43]) which means that the athlete used in the MBVG and gyroscope methods were different to the athletes used in the videography method. Then, the difference between the videography, the MBVG, and the gyroscope methods can be partially due to differences in skill level and style of the participants in the two methods, this study stated.

<u>Limitations and gaps in the study</u>: This study has used different subject's videography data from the literature to compare the marker-based gyroscope and virtual gyroscope. The duration of agreement in angular velocity between two methods is within 0.2 but the preparation phase of the serve is 0.4 normalized time.

<u>Possible endeavours ahead</u>: The limitations in using different subject's data from literature could be overcome by capturing the serve using video camera or optitrack system. Then it would be more authentic to compare the same subject's data in different method. Also the same skill level and style of the same subject in two methods could enlarge the duration of agreement in whole preparation phase of the serve.

**Wixted et al. [74]**

<u>Topic</u>: Measurement energy expenditure using MEMS-based triaxial accelerometers identifying anthropometric and kinematic sources of inter-athlete variability in accelerometer output during running and walking of elite athletes in treadmill.

Methodology: In the first of two separate treadmill studies, ten male Australian football players walked and ran using their natural cadence at ten speeds on a motorized treadmill. A triaxial accelerometer system fixed into a semi-elastic belt was fastened around the subject's waist ensuring that the sensor was pressed into the L4–L5 medial lumbar vertebra region of the runner. The accelerometer placement was approximately the subject's center of mass and its axes were aligned with the vertical, mediolateral, and anterior–posterior axes of the subject. The second study was conducted in a similar way as the first one but ten mixed gender recreational athletes were the subjects. In this study, oxygen consumption ($VO_2$) during the exercise of the athletes was also monitored continuously using respiratory gas analysis from an open-circuit calometric system. Uniaxial energy estimators were generated for all three axes using the integral of the square of the acceleration signals. That was the summation of the square of the analog-to-digital converter output after removing the device offset and gravity. The triaxial energy estimator used the integral of the sum of the squares of the signals from the three accelerometers. This energy estimator was referred to as "Accelerometer Counts" when it was taken as a 10-s average from a period of steady-state walking or running at each speed.

Outcomes: This study reported that speed against energy estimates from $VO_2$ (corrected for the subject's mass) gave a correlation coefficient $R^2=0.96$ by the regression analysis. Walking speed was correlated with triaxial and vertical-uniaxial accelerometer counts ($R^2=0.83$, $R^2=0.62$). Uniaxial accelerometer counts at running speeds varied widely between individuals and gave no useful correlation with speed. A range of individual correlations with substantial inter-subject variation was obtained from triaxial accelerometer counts at running speeds. Triaxial counts were tended to give a more linear individual running response than the corresponding uniaxial counts. Across both trials, step frequency had strong correlation with speed, with walking having a stronger step-frequency to speed correlation ($R^2=0.89$) than running (0.69). Step-frequency correlated highly with mass adjusted $VO^2$ energy estimates ($R^2=0.80 -0.99$) for individuals. In contrast, however, the group results

were far weaker ($R^2$=0.29).

Limitations and gaps in the study: The study itself stated some limitations within the developed system as also the solution for it. For instance, Step-frequency resolution decreased significantly as sample rate decreased. This limitation could be partly resolved by averaging the frequency estimate of successive steps, this study suggested, but did not provide evidence or explanation. The results from this study have been assessed using comparisons to video data, physiological and biomechanical data from treadmill and track running, as well as comparison to manually categorized football data. This study reported that generated step-frequencies from different activities matched those calculated manually. Discrepancies existed between the system output and the manually categorized data, this study confessed. This is because the two types of data came from two different systems, even from different activities, say, football as mentioned. Moreover, this study stated that the system was designed for open field sports and not suitable for monitoring court-based sports such as basketball and tennis. Because in those sports run lengths are short and there is high lateral acceleration and strenuous upper body activity.

Possible endeavours ahead: The same system could be used in cricket batting for energy expenditure measurement, particularly, to know the relation between two key parameters, for instance, how the energy expended in stride is related to bat velocity during a drive by measuring the accelerometer counts.

**Fallon et al. [51]**

Topic: Evaluation of different types of sensors, such as accelerometers, strain gages and microphones to monitor the collision of a baseball and bat.

Methodology: A wood baseball bat was instrumented with several different types of sensors, including four strain gages, four microphones, four piezoelectric accelerometers, a variable capacitance accelerometer and a gyro assembly. The series of tests included stationary bat impacts, noncontact swings and finally swings

impacting a ball off a tee were performed. To avoid the exceed range of the sensor due to swinging the bat at batter's maximum potential, a effort was made to swing it at approximately half-speed. The bat was supported by a single hand grip approximately 15 cm (6 in.) from the knob for the stationary impact tests. A Liberty (part no. 269-945083, manufactured by LDS Test and Measurement LCC, Wisconsin, USA) ruggedized DAQ (Data Acquisition) System was used to acquire all accelerometer, gyro, strain-gage and microphone responses. To evaluate the measurement accuracy relating to location and velocity, high-speed motion analysis was used. Data were collected and were statistically quantified to compare the effectiveness of each technology. Time values were extracted which corresponded to each sensors first response to the impact of the ball on the bat. Additionally, the time values associated with the peaks of the first microphone responses were also extracted. The time values were plotted against the sensor's location along the bat. A line was curve-fit through the data and the location in which the slope of the line was zero was recorded as the predicted impact location by that type of sensor. This predicted impact location was compared against the actual as measured by the chalk mark and the motion analysis system.

Outcomes: For the stationary bat tests, the accelerometers resulted in the best predictor of impact location—being able to predict the impact location within 5 cm (2 in.) and within 2.5 cm (1 in.) 63% and 38% of the time, respectively. The microphones were slightly less accurate with the start time analysis providing better results than the peak-time analysis. The strain gages were the least accurate in estimating impact location partly due to the difficulty in identifying a signal near the end of the barrel. For the swing and tee-hitting tests, also the accelerometers and microphones were the best at determining impact location with the most consistent and most promising method of data interpolation. However, data from the accelerometer response were slightly less accurate than the stationary bat results.

Limitations and gaps in the study: Issues of voltage saturation in some cases were reported in this study as limitations. Also the strain gages and gyro had considerable

noise. This study just compared the technology but did not provide the idea to classify the hits location, for instance, the sweet-spot hit region etc.

Possible endeavours ahead: Using inertial sensors the hit location around the sweet-spots could be identified from the bat and wrist recorded acceleration in batting. The idea could be how the bat transfers the maximum energy to the impacted ball recording minimum value of acceleration and minimum jarring of the wrists from the sweet-spot hits.

### Sabatini et al. [75]

Topic: Assessment of the walking speed and the incline by conducting treadmill walking trials at several controlled combinations of speed and incline values by the foot inertial sensing approach.

Methodology: The system, built around a simple Inertial Measurement Unit (IMU, composed of one biaxial accelerometer (Analog Devices ADXL210E) and one rate gyroscope (Murata ENC-03J)) placed on the instep of the (right) foot and attached snugly to the shoe with a Velcro strap. Two footswitches (one was placed underneath the heel and one underneath the big toe (right foot), and taped to the foot with some tape) were also used as a reference standard to detect the gait events and to confirm the validity of the gait phase segmentation procedure. The system gathered information about the occurrences of different gait events (heel-off, toe-off, heelstrike, foot-flat) and reconstructs the sagittal trajectory of the sensed anatomical point—the instep of the foot—, yielding information about walking speed and incline. To compute the mean velocity ($V_m$), mean incline ($I_m$), mean relative stance ($RS_m$) and standard deviation of velocity, incline and relative stance, data from the gait cycles inside the interval [50, 110] s of each trial were used. Using standard regression tools, the relationship connecting $RS_m$ to $V_t$ (velocity measured from the treadmill) and $I_t$ (incline measured from the treadmill) was analyzed. A comparison was made between $V_m$ and $V_t$, and $I_m$ with $I_t$ to assess the accuracy of the proposed measuring method, in terms of root mean square errors (RMSEs).

Outcomes: 300 gait cycles at varying speeds and inclines from two subjects were averaged and the results indicated that the foot gyroscope measuring method tends to detect the toe-off earlier (on average: 35 ms), whilst the heelstrike is detected without any systematic difference (on average: 2 ms, confidence interval at 95%: [ 16, 12] ms), as compared with the footswitch measuring method. The $RS$ values are not significantly influenced by the incline. The relationship between $RS_m$ (averaged across subjects and inclines) and $V_t$ was reported and found $r^2 > 0.99$. The foot angular velocity and the offset-corrected sagittal orientation of the foot were shown, for three consecutive gait cycles from a walking trial carried at $V_t = 4$km/h, $I_t = 0\%$. The relationship between estimated speed $\hat{U}_m$ (averaged across subjects and inclines with corrected drift) and $V_t$ was constructed and found $r^2 > 0.99$. The relationship between estimated incline $\hat{I}_m$ (averaged across subjects and speeds with corrected drift) and $I_t$ was constructed and found $r^2 > 0.99$. The overall uncertainty in the speed and incline estimates were RSME=0.18 km/h (0.05 m/s) and RSME=1.52%, respectively.

Limitations and gaps in the study: This study itself reported that the main error sources affecting the response of inertial sensors are related to the effects of sensor uncertainty, namely offset, and sensitivity. In the data in this study, it was observed that performance degradation occurred at the steepest incline; also, the regression analysis indicated that both walking speed and incline turn out to be slightly underestimated. The limitation in sensor range was explained as the sign of that fact.

Possible endeavours ahead: The system, built around a simple IMU in this study could be used to measure the commencement of stride and its length during a batting stroke played by different skills level players to judge their foot works.

**Helten et al. [76]**

Topic: A motion classification system for automatically classifying trampoline routines based on inertial sensor input.

Methodology: The trampoline performances of four female, non-professional athletes with intermediate skills were recorded by an inertial sensor-based mocap (motion

capture) system. The system was consisting of seven Xsens MTx3 sensor units. In these sensor units, inertial sensors are combined with other sensor types, earth magnetic field sensors and gyroscopes as used in Kemp et al., 1998 and Luinge et al., 2005 as cited in [76]]. In this contribution, the 3D accelerations, 3D rate of turn data and three degrees of freedom orientation data were available by the sensor units.

The sensors were placed inside a suit together with a wireless transmission system which sends the measured data directly to a computer. In total, 109 routines with difficulty scores ranging from 0.4 to 3.1 comprising a total of 750 jumps were recorded. Out of these 109 routines 13 routines were chosen to form a routine database $D_R$: From the remaining 96 routines, for each of the 13 jump classes 16 instances—four instances for each of the four actors—were manually assembled. The resulting dataset, containing 208 jumps, was denoted as cut database $D_C$: $D_C$ was then partitioned into two databases $D'_C$ (learning database) and $D''_C$ (evaluation database) each containing two jumps per actor from all 13 jump classes, amounting to 104 jumps. As for the predefined motion categories, this study used suitable training data to learn class representations that described the characteristics of a specific trampoline jump.

Outcomes: This study classified the jumps by reporting three attempts with revealed outputs and comparing them with the templates learned from the training data. Those attempts were feature representation, class representations, and classification and experiments.

In the feature representation, three different feature types were introduced. The first feature type $\varphi_s$ measures the angle between the X axis of a sensor s and the horizontal plane, the second type ($\theta_{s,t}$ or $\psi_{s,t}$ differed by the way the feature is computed) measures the enclosed angle between two limbs and the third type ($\omega_s$) captures the angular velocity of the sensors X axis. In other words, third type feature type measures the velocity as a limb rotates around its longitudinal axis. Total nine features ($F_1$~$F_9$) were defined based on these three feature types. The result was

represented by a feature matrix (F (D)) of which each row represents one feature, while each column represents the feature values obtained from sensor data stream D.

In the class representations, the characteristic properties of an entire motion class were represented based on feature matrices by adopting the concept of motion template (MT).

In the classification and experiments part, an unknown jump was locally compared with all class MTs and then labelled according to the class MT having the smallest distance to the jump. This part was divided into two sub-parts of which the first one was titled as 'Influence of feature types'. This sub-part reported an experiment on that was used for how the quality of the classification depends on the used feature types. Confusion matrices were used here, which gave a qualitative impression which jump classes were classified correctly, and which jump classes were confused among each other. Such confusion matrices displayed the ratio of how many motions from a given class (abscissa) were classified as a certain class (ordinate), where dark entries represented a high percentage of motions. If the used feature types discriminated jump classes well, this would result in a dark diagonal leading from the top left of the matrix to the bottom right. The second sub-part was titles as 'Routine classification' where the overall system performance was evaluated in a realistic trampolining scenario. For this evaluation, the thirteen routines from the database $D_R$ were used for evaluation, while the motion templates are again learned from the databases $D'_C$.

Among the feature sets, this study could identify if there was lack of any one of the feature types, which feature set performed worst, which feature set were too sparse for distinguishing different jump categories, which feature sets could classify the jumps correctly and which could indicated the jumps that were mixed up among each other. The examples were provided in this study where 14 out of 18 jumps were classified correctly.

To measure the classification accuracy for each jump class, a quantitative analysis

was done in this study in addition to the qualitative analysis. An automatically segmented jump was considered as classified correctly if its segment boundaries lied in the neighbourhood of an annotated jump (using a tolerance of 0.15 s) and if the computed class label coincides with the annotated label. To handle significant performance variations, a masking scheme based on variance templates was introduced.

Limitations and gaps in the study: The parameters to classify a jump extracted from the sensor-based mocap system were not validated using the conventional videography or optitrack system.

Possible endeavours ahead: Using the same system and analysis a batting template for a specific drive by an elite batter could be formulated for training purposes. The data could be validated using the conventional tools. Though different styles involved based on the anthropological data for each elite player but the key strategies for a successful drive would be similar and benefited to the skill development program.

**Schulze et al. [77]**

Topic: Evaluation of the performance of the developed wearable joint kinematics measurement system (KINEMATICWEAR) for assessing maximum knee joint angles during extended periods of normal walking by comparing it to objective measurements.

Methodology: The developed wearable joint kinematics measurement system (KINEMATICWEAR) consisted of a combination of wearable sensor nodes containing a triaxial accelerometer, a 3D gyroscope and a 3D magnetometer, were attached with kinesiotape to the thigh and shank of a subject while walking at different speeds on a treadmill. The algorithm used to estimate the angles from the system worked in the following way. Primarily gyroscope raw data were filtered and then transformed into angles based on the angular velocities. Subsequently, the cumulated sum of the gyro data for each point in time was calculated in order to gain

the angles, from which then the initial 'zero position' angle (determined while the subject stands still) was subtracted. Finally, for each of the two sensors (thigh and shank) the absolute angles were computed, and the knee angle was calculated from these two. The computed maximum knee joint angles were compared with reference measurements performed by a physician on video frames captured during walking, as was the correlation between both value sets. Therefore this study performed the walking experiment on a treadmill using a video camera to record leg movement. The subject was asked to walk at speeds of 1, 2 and 3 km/h (0.28m/s, 0.56 m/s and 0.83 m/s) in order to simulate 'normal' walking speeds of persons affected with symptomatic osteoarthrosis. The angles were measured by overlaying two lines meeting at the knee joint's transversal rotation axis, originating from the rotation axis of the ankle joint and the major trochanter of the femur.

Outcomes: The results of this study showed a correlation of 0.96 between clinical reference measurements and the computed angles. The accuracy was reported good for slow walking speeds of 0.28 m/s (l km/h, mean error: 2.6 deg±1.5) and 0.56 m/s (2km/h, mean error: 2.0 deg±1.6), but the algorithm over-estimated the angles by 6.3±3.6 degrees at 0.83 m/s (3 km/h), and the over-estimation was guessed to be induced by soft tissue motion during heel-strike.

Limitations and gaps in the study: It is confessed in this study that the relative error at higher speeds is inacceptable, and the algorithm needs to be corrected. It was suspected that the deviations are caused by the influence of the treadmill, i.e. by additional oscillations triggered by its suspension. The other reason for the over-estimation of angles was reported as the artifact generated by a multi-axis rotation movement of the soft tissue during heel-strike that leaded to excessive gyroscope recordings. A third reason was noted as the inability of the gyroscope to settle to a rest position during more vigorous continuous leg motion, which leaded to the build-up of the measurement error. These issues need further investigation, this study suggested.

The reference measurements using the video images are error-prone, this study reported. Because the determination of the reference points - in particular the moving rotation axis of the knee -is difficult. Additionally, the measurements in this study had been performed with a healthy subject (a PhD student), albeit with slow walking speeds expected in arthritis patients. Therefore this study has to be repeated with more healthy subjects and especially with arthritis patients in order to claim generalizability.

Possible endeavours ahead: Using the same systems developed by the sensors could be used to measure the angles of the limbs and bat at the point of ball contact during a stroke play. That measurement could provide the spatial position of the bat and limbs of an elite batter to have the kinematics data for training purposes.

**Kavanagh et. al. [78]**

Topic: Determination of inter- and intra-examiner reliability, and stride-to-stride reliability, of acceleration data collected from multiple locations on the body during self-selected slow, preferred and fast walking speeds.

Methodology: Eight subjects attended two testing sessions. Four custom designed lightweight accelerometer nodes (consisted of two biaxial accelerometers, analog devices ADXL202, range $\pm 2$ g, mounted perpendicular to each other on a $1.5 \times 2.6$ cm printed circuit board) were attached to each subject to measure 3D accelerations during walking. Accelerometer nodes were attached over (1) the occipital pole of the head with a firm fitting elastic headband, as well as (2) the neck (C7 spinous process), (3) the trunk (L3 spinous process), and (4) the right shank (3 cm proximal to the lateral malleolus) with rigid sports tape. Each accelerometer node was connected via shielded cable to a custom designed lightweight processor box fixed to the subject's waist.

During two testing sessions subjects performed 5 five straight-line walking trials along a 30m level walkway at self-selected slow, normal and fast walking speed conditions. In the initial session, the accelerometers were attached to the subject who

subsequently performed the walking protocol. For inter-examiner comparisons, the walking protocol was repeated after the accelerometers were reattached by a different examiner. For intra-examiner comparisons, one examiner from the initial testing session repeated the test in another session conducted within 24 h. To prevent order effect on the results, the order in which walking speed trials were performed was counterbalanced. All acceleration data were low-pass filtered using a dual pass zero lag Butterworth filter with a cut-off frequency set at 20 Hz. Gait velocity was monitored using 3 pairs of Omron (E3JK-R4M2) photoelectric light gates spaced at 5m intervals in the middle of the walkway.

Outcomes: Using the coefficient of multiple determination (CMD, a waveform similarity statistic), reliability for each testing condition (4 locations, 3 directions, 3 speeds) was quantified. CMD's estimated from the results ranged from 0.60 to 0.98 across all test conditions and were not significantly different for inter-examiner (0.86), intra-examiner (0.87), and stride-to-stride reliability (0.86). The highest repeatability for the effect of location, direction and walking speed were for the shank segment (0.94), the vertical direction (0.91) and the fast walking speed (0.91), respectively. This study reported that no significant differences in gait velocity were detected between gait analysis sessions. ICC's calculated for within subject repeatability of gait velocity data ranged between 0.84 and 0.93, and increased from slow to preferred, and preferred to fast walking speed conditions. Furthermore, in this study, inter- and intra-examiner CMD's and systematic errors were not significantly different. It indicated that the patterns of accelerations were not influenced by whether the accelerometers were attached by the same or different examiners in the retest. Overall, the experienced examiners were equally able to replicate the location and orientation the accelerometers from the initial test to the retest. This study demanded these findings as important from a practical perspective, stating that so long as the examiner is relatively skilled, the same person need not conduct all testing sessions.

Limitations and gaps in the study: The study itself reported some its limitations. The

recorded signal could be contaminated by skin motion artifact due to impact loading and muscle activation. The output signal might be influenced substantially by the anatomical location and orientation of the attached accelerometers. However, this study demanded that this issue is particularly relevant if the examiner attaching the devices has limited experience or if different examiners attach the devices under retest conditions.

Possible endeavours ahead: Inter- and intra-examiner reliability, and stroke-to-stroke reliability, of acceleration data collected from a specific stroke at different performance environment and time could be conducted as done in this study. The results could be used to judge the robustness and reliability of sensor data.

**Ohgi [79]**

Topic: Discrimination of the stroke phases and estimation of fatigue by the wrist acceleration using a tri-axial acceleration data logger and a tri-axial acceleration/angular velocity data logger attached on the wrist joint of the swimmers.

Methodology: The data loggers (named as 'prototype I' for tri-axial acceleration and 'prototype II' for tri-axial acceleration/angular velocity) developed by the authors were tightly attached on the distal of the swimmer's forearm by taping and bandage. For discrimination of stroke phase, the experiments on crawl and breast stroke were covered in the water flume. Both top level crawl stroke and breaststroke college swimmers were used as subjects and same acceleration pattern was measured repeatedly in swimming trial. Therefore, only single stroke acceleration was examined. Four video cameras were equipped from the side and beneath the water flume for the observation of underwater swimmer's stroke motion; synchronization between the data logger and the videography was achieved by a trigger start function of the data logger which enabled the video timer to start simultaneously.

For fatigue estimation, four male and one female triathlon athletes were involved in the experiment. In order to determine each subject's swimming speed, a three speed test (300m×3) was taken before the main experiment. Then onset of blood lactate

accumulation (OBLA) speed of each subject was estimated and 50m target time (OBLAT) was defined at 1st set of the experiment. At the OBLA speed intensity, the blood lactate begins to increase exponentially and so the swimmer's fatigue also begins to accumulate. The heart rate was measured immediately after each set and blood lactate was sampled 3 minutes after each set. A LactatePro (Model LT-1710, Arkray Inc., as stated in this study) was used for blood lactate sampling test.

Outcomes: Four stroke phases, the entry and stretch (I), downsweep (II), insweep (III) and upsweep and recovery (IV) phase were discriminated by the typical local maximums and local minimums in the swimmer's wrist acceleration during a single stroke. Because of some of these local maximums and minimums of the tri-axial acceleration were corresponded with the transition timing of the underwater stroke phase. The prototype II gave the acceleration and angular velocity during swimming. Thus the status of the underwater stroke phase's movement was estimated.

Average swimming velocities and blood lactates of the subjects were shown for fatigue estimation, where all subjects swam almost same time as their target time in each set. This study reported that when the swimmers finished final set, they were almost exhausted. Because their blood lactates were between 6.8~14.9mmol/l. For a particular subject (for instance, subject C), the tri-axial acceleration and the angle and angular velocity of the elbow joint for the first and last trial on the final set were shown in this study. From those data, when the subject was completely exhausted was identified, for instance, after last trial of 50m subject C was completely exhausted. The change of elbow angle ($\theta_e$) and its angular velocity ($\omega_e$) were plotted and from these angular parameters, the local maximum (after the global maximum) almost corresponded to the maximum elbow flexion timing. The exhaustion of the swimmer was noted from this elbow flexion timing. Before the exhaustion, it occurred at about 0.93sec, then it shortened to 0.83sec at the fatigue situation on $8^{th}$ trial for subject C. So the tri-axial acceleration indicated the evidence of the swimmer's fatigue and change of the stroke motion.

Limitations and gaps in the study: The acceleration/velocity profiles obtained from

the data loggers in this study was not validated using the video data whether the same profile could be resulted. The validation could buttress the timing references taken from the video for phase discrimination.

Possible endeavour ahead: Using the wrists attached sensors recorded acceleration in a cricket stroke the quality of bat-ball contact could be assessed by how the impact was made in the bat. While the maximum energy was transferred to the ball in a sweet-spot hit, the less amount of jarring of the wrists could be observed from the less acceleration transferred from the bat.

### Ghasemzadeh et al. [80]

Topic: A system which uses body sensor networks for developing a quantitative model which can provide feedback on quality of movements for the purpose of golf swing training. The system architecture, signal processing methods and experimental results of the system to quantify a golf swing with respect to wrist rotation were presented.

Methodology: Two sensor nodes were placed on the golf club (one near the club head and another near the grip), one on the right wrist, one on the left arm, and one on the back at waist level of the subjects to monitor the acceleration and angular velocities during the swing. The subjects must grip the club aligned with the nodes on the club. They were asked to keep their wrist fixed throughout the movements to allow the system to control the swing plane and all of the swings were performed in the absence of a golf ball. The sensor nodes had collected data for the sequence of actions in a swing and the quality of each segment (fine-grain manual segmentation was performed with the help of the video recorded during the data collection) was expressed as the amount of deviation from the target line after the analysis of the data at the base station. Before processing at the base station the sensor nodes collected data was pre-processed locally to facilitate subsequent in-network operations.

The quality of each segment (four major segments consisting of takeaway, backswing, downswing and follow-through) of a golf swing was measured with respect to different criteria. Examples of such criteria include the amount of wrist rotation and how out of plane a swing is. Several signal processing techniques including PCA (Principal Component Analysis) and LDA (Local Discriminant Analysis) were used to obtain significant information with respect to each criterion. A linear projection of feature space that monotonically changes while the angle of rotation varies was found by LDA and was fed to a regression model to quantify the degree of improperness of movement. The system required a dataset with trials obtained from several variations of the wrist rotation in consistent physical movements in an in-plane swing. This implied the need for a highly controlled experimental environment. Therefore, a home swing trainer was used in this study.

Outcomes: The subjects performed swings after first addressing the ball with 20º, 40º, 60º and 80º clockwise and counter-clockwise rotations of the wrists. A perfect golf swing that has no wrist rotation or out-of-plane movements was also performed by each subject. LDA had created eight discriminant functions in the form of linear combinations of the input for nine different groups of wrist rotation. The projections obtained by applying LDA were used to build a linear regression. The validation set was used to measure the degree of wrist rotation based on the model acquired. The values of error in terms of RMSE (Root Mean Squared Error) and MAE (Mean Absolute Error) were shown in this study to evaluate the overall quality of the regression model. In overall, the amount of root mean squared error reported in this study was 15.5, 10.7, 8.9 and 9.1 for takeaway (TA), backswing (BS), downswing (DS) and follow-through (FT) respectively. The overall value of absolute mean error was found as 9.2, 7.7, 6.6 and 6.5 degrees for TA, BS, DS and FT respectively which introduced an average error of less than 10 degrees for all segments.

Limitations and gaps in the study: This study itself reported several limitations. The optimal sensor configuration, including the best senor placement and smallest set of sensors required the system was not investigated. The experimental setup for this

study was supposed to maintain an in-plane swing ensuring that different trials can differ only in the amount of the wrist rotation. The resulting model then ensures to be able to quantify incorrect swings in terms of angular rotation. But several types of mistakes could be made independently by the golfer, each of which must be quantified using individual models. Integrating evaluation of mistakes other than wrist rotation into the developed model is a problem, this study has confessed.

Possible endeavour ahead: This study focused on building their quantitative model for non-ideal movements due to wrist rotation. To evaluate this model for other types of incorrect swings requires controlling experiments for those types of errors. That could be a scope of further investigation, this study suggested. However, using the experimental set up and model used in this study, in cricket batting a planer straight drive could be investigated to measure the wrist rotations from the out-of-plane movement of the bat for imperfect swing.

## Lapinski et al. [81]

Topic: A compact, wireless, wearable system composed of a combination of low and high range sensors, a compass, an RF link to extract biomechanically descriptive parameters for evaluating professional baseball pitchers and batters.

Methodology: Several professional pitchers and batters were instrumented with the system and data was gathered over many pitches and swings. Each of the wearable battery-powered nodes consists of three single-axis ±120G ADXL193 accelerometers, three single-axis ADRX300 gyroscopes, a 3-axis ±8G LIS302DL accelerometer and a HMC6343 digital compass. To evaluate the system, the IMU (Inertial Measurement Unit) array was compared to an optical tracking system. The optical system employing "high-speed" cameras operating at 180 Hz, allowed positional tracking of each pitch. A series of 10 motion analysis cameras were set-up on a regulation-sized pitching mound. Utilizing the camera-based motion tracking system and IMU array (newly-developed in this study), a series of 4 professional baseball pitchers underwent simultaneous biomechanical testing. Subjects were fit

with both passive reflecting targets for the camera-based motion analysis and a 5 segment wireless IMU array. IMUs were carefully affixed to the chest, upper arm, forearm, wrist and waist with standard body tape. In order to synchronize and align the data taken by the optical and wearable systems, strobe signals from the optical tracker were also sampled.

Each pitcher threw ten recorded fastballs using a regulation baseball off a regulation pitcher's mound. The acceleration phase of the pitching cycle was isolated, and kinematic parameters of the shoulder were calculated from simultaneous recordings of position, acceleration, and velocity by the two systems. Maximum acceleration and velocities were compared at the wrist, shoulder, and hand. The speed of each pitch was monitored by a commercial radar gun which was logged manually.

Then to evaluate a series of five professional baseball batters, the players were fit with a 5-segment wireless IMU array. IMUs were affixed to the chest, upper arm, forearm, and to the bat itself. Players were then asked to perform 5 free swings. After the IMU node was removed from the bat and affixed to the waist, players then hit a ball off a tee for five additional swings. Relative speeds of the bat, hands, forearm, and chest were calculated. Ball/bat Impact times were calculated and hand speed at impact determined.

Outcomes: The pitching test results showed a rapid rise in elbow extension velocity and humeral internal rotation recorded in both the optical system and with the wearable IMUs. This study reported that the acceleration phase of the pitching cycle lasts from peak external rotation of the shoulder to the time of ball release and was identified as a sudden peak in the acceleration forces in the hand and upper extremity. Resultant g-forces were calculated from the IMUs. Peak hand forces averaged 90 g's in the acceleration phase of the pitch. The g-forces at the chest and waist were considerably slower at 10 and 8 respectively. Shoulder internal rotation values were estimated from the IMU measurements. Peak shoulder internal rotation velocity was identified for each pitch. No statistical difference was found in average shoulder internal rotation velocity measured by the optical system and the IMU array.

However, the average standard deviation of the IMU array was about 6% whereas the average standard deviation of the optical system was 15%.

The batting test results showed a similar rapid rise in g-forces and angular velocities during bat swings. This study demonstrated that impact could be detected from the hand node, as seen by a disruption of the bat speed curve. Relative body segment velocities & timing differences were determined for each swing. Average bat speed during a free swing was reported as 227.5 MPH (Mile Per Hour) with average standard deviation of 9.7 MPH. At impact average hand speed was found 74.5 MPH. Approximate bat speed predicted from hand speed by knowing the length of the bat and its angular velocity, was used to predict bat speed at the time of impact when a node was removed from the bat itself (nodes cannot withstand the force of impact if left on the bat). For each of the 5 players, this study verified this calculation using the free swing data (where a node was left on the bat for each swing). Average error in this calculation was $4.8 \pm 0.5$ %, the study reported.

This study demanded that its system was seen to sample 7-8 times more quickly than the optical tracker used in the tests, and provided much more granularity in the measurements.

Limitations and gaps in the study: This study itself listed some of the limitations and remedies for the upcoming tests. It reported that the error in the pre-sampling analog filters prevented the system from measuring high frequency data in the tests.

Persistent difficulties with the embedded software before the spring training deadline prevented the dataset presented in this study from also including information from the magnetometer (compass) and low-G accelerometer – also, although the high-rate gyro measurements produced good data, lower rate phenomena (such as during pitch windup, etc.) had insufficient signal-to-noise to enable a useful integration across a pitch.

This study stated the limitations about its RF datalink also. Although the RF datalink worked well in the lab, when moving to an outdoor location without nearby

walls to reflect the nodes' signals, substantial problems in signal absorption by the body was encountered–when the player was facing away from the base station, the bit error rate could become very high.

Possible endeavour ahead: Work on shrinking the nodes, improving the user-interface software, and making it much easier to apply and remove in the field was suggested in this study as the further development of system. The systems like this study developed would have wide-ranging practical and clinical applications for athletes, including injury prevention (youth pitching), aiding in conditioning/training, and improving post-operative rehabilitation, this study guessed. However, using the same system developed in this study, the batting stroke could be analysed to have a wide range of kinetic and kinematic parameters (forces, torques and other descriptive and evaluative features etc.) integrating the accelerometer, gyroscope, magnetometer, RF datalink together.

## 2.7  An overview of the literature reporting sensors signal analysis

The application of accelerometer sensors signal is emerging as a popular method of biomechanical quantification of health and sportive activity [82]. As written in section 2.6, Fallon et al. [51] assessed the applicability of five different types of sensor to identify impact location of baseball and bat and the swing speed of the bat. They found accelerometer and microphone sensors were the most promising, however, relative levels of the signals were used for comparison among the sensors. This study did not consider sensor errors but compared the sensor results. This means that although accelerometers have some errors in some motion measurements, the value of errors in many cases can be neglected if a gross relationship with movement parameters is sought or comparison is made among movements and sensor recorded signals. Several works have reported methods to minimize sensor error. Sipos et al. [83] proposed a calibration procedure for a triaxial accelerometer relying on optimal position and sensor number for minimizing cost and process time. They also compared three calibration algorithms applicable to tri-axial accelerometers to

determine a mathematical error model. In 2008, Tan et al. [84] proposed a solution for the estimation of drift free displacement of periodic motion from inertial sensors. This method is limited to periodic motion. Suh [85] proposed a new smoother method to estimate attitude and position of movement to be less sensitive to the uncalibrated sensor parameters and sensor noise. In that work using two boundary information (zero velocity interval), the attitude was estimated using a smoother as a combination of forward and backward filter. The velocity was estimated by a velocity smoother using the smoothed attitude. That study computed the position by integrating the estimated velocity. The proposed method is suitable for analysis of movement for short time intervals only.

## 2.8 An overview of the literature reporting swing modelling and ball contact location in the bat in other sports

In cricket literature the inclusion of mechanics in batting stroke parameterization is still not well established. Tennis bat and golf club swing literature contain descriptions of the bat swing mechanics using pendulum theory. For instance, Cross [86] investigated a tennis racket swing by modeling the forearm and the racquet as a double pendulum. The difference between the bat and a golf club swing was documented on the basis of the difference between a forehand and a serve. The moment of inertia was determined to be more important than the mass of a bat or a golf club on the swing speed. The findings were based on experimental data taken by filming an elite player at 300 frames/s when serving a ball at 45 m/s. The same researcher (Cross [29]) presented the experimental results from the large-amplitude motion of a double pendulum. Constructing a double pendulum from two 0.30 m long aluminum bars, each 20 mm wide Cross [29] showed that experimental results from the swing of a simple mechanical double pendulum agreed well with theoretical predictions. The findings demonstrated the significance of the masses of the two segments for mutual coupling between segments and the effects of the wrist torque used to start the swing. This study stated that positive wrist torque was needed early

in the swing to stop the arm rotating too far ahead of the implement. But the maximum possible swing speed was reduced for this torque. This study analyzed the forces and torques acting on each pendulum segment to explain its motion. The author demanded that the results showed the possibility of designing ''perfect'' bat to transfer all of the kinetic energy from the player's arm to the ball so that none is retained in the arms or bat after the impact. About the swing, the study reported that during the first half cycle the motion was reproducible and after that the behaviour was chaotic at large amplitudes. The first half cycle serves as an excellent model for examining upper and lower segments motion of the body and the swing of implements.

There is an optimum location on the cricket bat blade where batters feel little force and the ball receives maximum acceleration when they strike the ball. The impact point at that location is termed the sweet spot [87]. Cross [88] defined the sweet spot of a tennis racquet as the impact point for which the impulsive forces transmitted to the hand is the minimum. From the measurements and calculation, Cross [87] mentioned the sweet spot for a tennis racquet is the narrow impact zone where the total (translation+rotation+vibration) energy in the handle was minimal and that was likely to coincide with the location indicated by the players. Adair [89] pointed out that the "sweet spot" of a baseball bat is not a physics term, and is determined by the batter and not by physicists. In this work two experiments for cricket bat/ball contact were undertaken to determine the impact location and sweet spot hits using triaxial accelerometers. Fallon [51] found accelerometers and microphones can be used to determine the impact location from the collision of a baseball and bat. The centre of sweet spot region was defined in [90] at about 15 cm from the toe of the bat, the region is bat-dependent and extends for a significant distance range along the vertical axis of the blade. Bower [27] determined "sweet regions" in cricket using ACOR – apparent coefficient of restitution & ball rebound velocity. The locations were significantly different.

## 2.9    An overview of the literature reporting the cricket batting stroke that is known as the basis of all strokes

Attacking and defensive strokes are differentiated by the intention of the batter whether to score runs or save the wicket. The attacking nature of a drive compared to a forward defensive stroke is evident from the parameters involved in the two strokes. Those parameters are, for instance, back-lift, commencement of stride, downswing of bat, front foot placement, peak bat horizontal velocity, bat-ball closing velocity etc. [22]. It is said that the forward defensive strokes forms the basis of all of the drives [22].

The selection of shot, defensive or attaching depends on the ball bowled and recognition of ball's line, length and flight by the batter. An attacking shot is aimed to short or over pitched ball (in each case completely different shot) and defensive to a good length ball [91]. The batters natural ability and anticipation of ball flight are the main deciders.

Several researchers have conducted their works on defensive stroke in cricket batting considering it as a suitable task vehicle, because of the single plane of movement of bat and batters in this stroke allowing two-dimensional analysis (e.g. [92], [22] etc.). As written earlier in this chapter, using different ball delivery methods (ball machine and real bowler) Renshaw et al. [23] documented the movement coordination and timing of four standard batters during forward defensive stroke. They reported different ratios of backswing–downswing, peak bat height, mean length of front foot stride, the correlation between initiation of backswing and front foot movement under the two constraints. The differences between batting under a real bowler and a ball machine lead the authors to summarize that, practicing batting against bowlers will help batters to be attuned to information from bowlers' actions and acquisition of appropriate information-couplings for batting in competitive performance but batting against bowling machines might result in a lack of this ability. As included earlier in this chapter, Pinder et al. [18] examined information–movement coupling in developing batters by assessing the timing and

kinematic responses under two practice task constraints (facing a real bowler and a ball machine), when performing a forward drive and a forward defensive stroke. The authors found significant differences between the practice task constraints, initiation of the backswing, front foot movement, downswing, and front foot placement were earlier when facing the bowler compared to ball machine. Higher peak height of the back-lift and larger step length was observed when facing the bowler. The authors stated that the temporal and kinematic differences between drive and defensive shots suggested some differences about the perceptual abilities of non-expert batters. For instance, the different back-lift heights for the two shots revealed that batters were able to distinguish between a ball of good length and a half volley very early in the delivery which afforded them a defensive shot in the former case and a drive for the later. Picking up more ball flight information batters adjusted their movements appropriate for those shots.

## 2.10  Literature Review Summary

A review of literature in cricket batting and other implement swing like baseball bat, hockey stick, sword, hammer throwing, tennis bat, golf club, metal rod is provided in this chapter. The review is categorized into five sub sections as: (i) Biomechanics and motor control, (ii) Ecology & Assessment, (iii) Psychology, (iv) Morphology & Physiology and (v) Injuries and implements of batting. The topics, methodology, outcomes, limitations and possible future endeavor in each study are stated. The attention was on the methodology used and limitations reviewed and in some cases cited in the studies. Most of these studies used bulky equipment includes video cameras, opto-graphic system, involvement of humans like a coach, assessor etc. These tools suffered from a variety of drawbacks like high cost, match obtrusiveness, placement of instrument (marker) on/near head of the implement, not portable, time consuming data analysis, blurring effect in the video data (for a low sample rate, for instance, 25 Hz), inaccuracy in a dynamic event tracking due to fixed height of the cameras unable to move with the dynamic section of interest.

Newer technological tools were introduced several years back for extraction of cricket strokes, sword swing (Busch et al. [55], James [52]). The new tools are inertial sensors containing accelerometers and gyroscope. These sensors have advantages over the bulky equipment. Because of their small size with low weight, higher sampling rate (up to 500 Hz), instant data providing facilities, digital data logging and live data streaming opportunities, onboard data processing and low cost. In this chapter, after discussing five literature categories as mentioned above, the studies that have already used sensors methodology other than cricket is also included. However, using the sensors Busch et al. [55] showed only the possibility of cricket batting feature extraction. The study did not develop a mathematical representation of the cricket bat swing to explain the data. No researchers have used sensors in cricket bat swing analysis to identify the bat position in different phases of bat swing, how to maximize the swing velocity, bat-ball contact assessment, bat-hand coupling, effect of a parameter on swing profiles indicated the applied force level and validating the results using video confirmation as used by many researchers. This dissertation has addressed these issues using accelerometer sensors upon introducing a novel methodology which includes sensor platforms, data collection-calibration-conversion, and data interpretation for key feature extraction and error handling, signal processing, data validation and analysis method. Chapter 4 discusses the methodology and the subsequent chapter includes the description of batting strokes, base strokes and coaching points, and several key attributes of base strokes. The studies are outlined in the results section in Chapter 5.

# 3 **CRICKET BATTING STROKES: PARAMETERS, ISSUES FOR BAT SWING RESEARCH**

The goal of a batter is to hit the bowled ball to score runs and not to be dismissed. The batting stroke can be described in terms of the dynamics of the bat and limbs in space and time. The strategy behind choosing a stroke to play depends on the trajectory of ball bowled. The dynamics in the stroke is determined by the intention of the batter either to score runs or to prevent the ball from hitting the wicket. The important tasks for a successful stroke are the right batting grip, stance, and swing [93] and requires the limbs and bat to be in the right place at the right time. Although several factors are involved in a successful stroke and these vary stroke to stroke, there are several general guidelines documented for all stroke categories. Those guidelines state that the batter needs to get the right footwork (includes feet separation, stance and stride during the swing, body weight placement) work on the grip (includes softness and tightness of grip, top and bottom hand placement in bat's handle), watching the ball trajectory, swing bat with precision (includes placement of bat handle according to batter's limbs, head and eye orientation of the batter, forcefulness of the swing) and continue to practice [93]. These guidelines ensure that batter's body is ready to transfer power to the ball, regardless of what type of stroke is to be played.

## 3.2 **Batting strokes**

The common strokes played in cricket are the block, drive and cut, and there are many different styles of these strokes. The characteristics and batter's action to play these strokes are outlined in Table 3.1.

**Table 3.1** Basic strokes and theirs characteristics and how batters play those.

| Stroke | Characteristics | Batter's action and goal | Comments |
|--------|-----------------|--------------------------|----------|
| Block | It is defensive stance | Batter swings the bat at a | |

| | stroke to protect the wicket without scoring runs. | lower speed with minimal follow-through. The goal is to stop the ball touching the stumps by reducing the ball velocity off the bat. | |
|---|---|---|---|
| Drive | In the drive, the aim is to hit the ball with maximum force. | The batter aims to hit the ball with more power by swinging the bat in the vertical plane with significant follow-through along the path of the travelled ball. | Skilled batters can direct a drive toward specific areas of the playing field. According to the areas of the directed ball, each drive takes different names, such as, cover, on or off drives, referring to the part of the playing field where the ball is directed. |
| Cut | This shot is to direct more forward thrust on a ball, delivering faster ground speed than a drive. | In the cut shot, batters step into the swing and make the ball contact while bat is horizontal instead of vertical as in drive. | |

There are some advanced strokes known as strategic and aggressive strokes, these are hook shot, leg glance, sweep shots. Table 3.2 outlines the characteristics of those strokes including the situation when to play, and batters action to play.

**Table 3.2** Advanced strokes and theirs characteristics and how batters play those.

| Stroke | Characteristics | Batter's action | Comments |
|---|---|---|---|
| Hook shot | This shot is attempted when the bowled ball bounces on the pitch and | The batter steps inside the line of the ball's path and use a hook shot by swinging | When this stroke is executed correctly it often makes a full six |

| | | | |
|---|---|---|---|
| | comes up to the batter's head level. | the bat in an arc horizontal to the ground. | run. |
| Leg glance | In the leg glance the bat is swung vertically like a drive but less power and with a follow-through as small as block. | To execute this stroke batter steps through the ball's path and the flat paddle of the bat is used to deflect the ball behind the batter to the fine leg area. | |
| Sweep shots | Like leg glance the sweep is a similar stroke in which the ball is directed toward the batsman's onside. | The batter directs ball toward his/her onside by sweeping the bat toward the ball by dropping the back knee and pointing front foot toward the incoming ball. | A reverse sweep is executed similarly with dropping the knee, pointing the foot and making contact with the ball, and directing the ball toward the offside of the field by pulling the bat across the body before the ball comes in. This stroke often confuses the fielders and allows the batters to score more runs. |

The decision about choosing a stroke is dependent on the type of ball delivered by the bowler. The perception and its flight and length are important for determining the appropriate stroke type. The most common strokes are the block, drive, cut. In this work only the block and drive are investigated.

### 3.1.1 The basic strokes and coaching points

The batting shots when the bat is vertically orientated, the drive and defensive shots are said to be basis of all other strokes. Other batting strokes like horizontal batting

shots including the advanced shots are formed on the basis of these vertical batting shots. The root level coaching starts from these basic shots. For instance, a young player who is first introduced to cricket is usually taught the common strokes of defensive and straight drives. The initial focus will be on ensuring the player adopts a correct grip and stance. When the player has mastered those fundamental skills, the focus then shifts to the execution of the back-lift, foot placement to *intercept the ball at the right time and making ball contact with the optimal zone of the bat face*.

To play a straight drive efficiently, a coaching manual includes the following instructions to the trainee [56]:

-'Lean towards the ball with head and shoulder forward of the body.'
-'Good step forward towards the pitch of the ball, head directly above the front foot.'
-'Back-lift remains raised.'
-'Weight on bent leg, back leg straight with heel raised and inside of toe touching the floor, thus ensuring sideways body position.'
-'Diamond shape maintained by arms throughout the shot.'
-'Bat swings through the line of the ball.'
-'Toe of the bat follows direction in which the ball has been hit.'
-'Leading elbow high, close to head.'
-'Bottom hand, fingers and thumb grip (to allow flow of arms and bat through the line of the ball.'
-'High hands above eye level after the ball has been struck, forearms in line with the bat.'

However, the above coaching points instructs how to play this shot efficiently and safely but not when to play the stroke. This shot is usually played to an overpitched delivery on or outside off stump. *Research to determine how well a batter executed a swung can be of value. Preliminary work could be directed at checking of the trainee's ability to swing the bat straight in a plane, keeping aside the ball flight. A ball-free planar straight drive could be used to check the competency of a novice.*

Different performance levels can be compared to quantify how fast and effective, a particular trainee learns to bat.

The instructions for a straight drive in a coaching manual provide instructions for a front foot defensive stroke. The coaching instructions are as follows [94]:

-'Lean towards ball with head and shoulder forward of body.'

-'Good step forward to pitch of ball with weight on bent front leg.'

-'Diamond shape maintained by arms throughout shot.'

-'Hands forward of bat face on impact, below eye level.'

-'Complete shot looking over the top of the bat handle with elbow close to head.'

-'Fingers and thumb bottom hand gripped maintained on impact-acting as shock absorber.'

*The preliminary work for this stroke could be an assessment of the ball-contact position on the bat*. The coaching instructions are documented in the coaching literature. If compliance to these instructions can be readily measured then player development can be quantified.

The instruction on how to play a sweep shot are documented as follows [95]:

-'Stretch front-foot outside the line of the ball and bent with lowering back-foot parallel onto the ground.'

-'Lean head and front shoulder forward towards the ball.'

-'Counter the ball in front of the pads by the bat coming down from a high back swing.'

-'Roll the wrists to keep the ball on the ground if not playing in the air.'

-'Finish the follow-through over the leading shoulder.'

Technology based strategies for measuring and validating stroke play appear to be a useful coaching and skill assessment tool. Several key parameters which describe the gross features of a bat swing are discussed in the next section.

## 3.2    Key parameters in the basic strokes

For the straight drive, the position of the head and shoulder of the batter could be measured at the top of the back-lift where the downswing starts. It is likely that novice batters will move their head back from the sudden forward movement of hand and bat but the head and shoulder should not lean back at this stage. This is the transition from the back-lift to the downswing, where the bat and the batter's body come to a halt. Attaching sensors to batters limbs, the recorded acceleration profiles at this sudden halt situation could identify the head and shoulder movement to check batter's competency.

The commencement of the stride and its length is one of the key parameter because it indicates the ball-delivery and flight judgement capability. The position of the head during the stride is another parameter to consider. These two parameters are addressed in the coaching points relating to stepping towards the pitch of the ball, head position with respect to front foot. The limbs attached sensors recorded acceleration profiles could determine the temporal and spatial parameters on stride and head position.

Peak height of the back-lift is another parameter addressed by coaches. The ratio of the back-lift to the downswing speed is one parameter that has been used to judge the skill levels of the batters on the basis of oncoming ball delivery and flight assessment. Sensor recorded acceleration profiles can provide these two parameters (peak back-lift height and ratio mentioned).

Weight distribution is another parameter to measure how batter lean body forwards distributing the weight on the front leg and the back leg. The acceleration profiles recorded in the sensors attached to the appropriate limbs can provide the information about it.

The bat swing plane throughout the drive and hand position after the ball is struck are the parameters used to address competency. Bat and hand attached sensors recording three dimensional data could provide the information on how the bat is swung through the line of the ball and the hand position with respect to eye level and bat line after the fruitful ball-contact.

The follow-through is another parameter used to characterize the ball-contact on the basis of its complete or incomplete situation. A completer follow-through where the toe of the bat follows the direction in which the ball has been hit indicates the successful hit of the ball in straight drive. In the literature, the quality of ball-contact has also been addressed by assessing the follow-through and in the coaching points shown above has stated about the direction of bat's toe movement too. Sensor recorded acceleration profiles can judge the nature of follow-through from its continuation and consistency.

Grip pattern adopted by the batters is another parameter to work on to check its effect on the flow of arms and bat during the stroke, and dominancy and coupling differences between the top and bottom hands. Acceleration profiles from the hand-attached sensors can differentiate the actions from top and bottom hands during a stroke play.

Similarly, for the front foot defensive stroke, the position of the head and shoulder, stride commencement and its length, the weight on front leg, position of hands and eye level on impact are parameters to address about this stroke. These parameters are to ensure the well balance of the bat and batter body system during the contact and its effectiveness, and can be measured by sensors attached to the appropriate limbs of the batter.

The grip patterns of the top and bottom is another important parameter to measure the batter competency to control the incoming ball pace and direct it to the desired direction. How grip is maintained to neutralize the incoming ball pace can be measured using the sensors data on how the two hands are coupled at bat-ball contact.

The position of bat and elbow at the completion of the stroke are also two parameters to comment on the batters stroke how well the basics were followed. The top of the bat handle with the elbow should be close to the head. The relative distance between the top of the bat's handle and head could be measured by the sensors data converting the acceleration data in distances with appropriate procedure (i.e. eliminating the error hazards originated from the mathematical operation, say, integration for velocity, distance calculation).

In the existing literature, many of the parameters stated above have been addressed in a descriptive way by using the bulky, expensive and labor intensive measurement equipment. This dissertation assessed how these parameters could be addressed in a precise mathematical way using tiny, inexpensive sensors. However, video analysis is also based on mathematical representation and can provide quantitative feedback to an athlete but in a controlled environment and unable produce real-time feedback.

## 3.3 Existing data collection methods in cricket batting research

### 3.3.1 Data collection methods in cricket batting research

To capture the motion of the bat and limbs in cricket, the predominant data collection method is visual pattern recognition systems. Several of these systems are composed of a network of video cameras and high performance computers; several include wired sensors systems and microwave radar techniques. The prime requirement of any motion capture system is to capture the maximum displacement of the batter from the crease in all directions during the execution of the stroke (i.e. range and

accuracy should be ascertained by the system). The system should allow the batter to move freely (i.e. not be hindered by its components). It should include adequate lighting as the ball travels at speeds of up to 140 km/h. In certain applications it should be portable. It must be able to capture the required type of information (i.e. 3D motion of an object under observation) and be cost effective. Existing visual recognition systems (for instance, video based systems) satisfy many of the constraints, but the costs are high for instrumentation, the collection of data and analysis. In addition, human involvement (as assessors/observers) is necessary for kinetic and kinematic feature extraction from the data recorded by visual pattern recognition systems. The accuracy of the data is dependent on the visual acuity of human beings. Such systems are generally ineffective in performance conditions. Electromagnetic positional sensors like those found in the Polhemus Fastrak System [96] suffer from the problems from the wire links used. These wires links also are cumbersome to the batter and the freedom of movement might be compromised.

### 3.3.2 Overcoming the limitations in existing data collection methods

The existing data collection methods used in cricket batting research (the technology used and human involvement) have two significant issues. They are generally costly, bulky, non-flexible, performance obtrusive and sometimes prone to error or are unreliable. The high speed video cameras, networks of video cameras and computers, opto-reflective motion capture systems require significant financial investment. Most of the cases these systems are complex to set up, difficult to transport and use in the game or match environment. Every experiment requires calibration and synchronization is needed to repeat experiments at other places and at other times. These procedures require cost in time and persons. Sometimes the cables and the devices on limbs hinder movement. The cameras introduce obstacles to broadcasting for other observers in real match environment. The space required for setting of those bulky systems even in laboratory environment is also a concern. The collected data sometimes suffers due to an inability to record three dimensional data uniformly in each dimension. For instance, if a camera is capturing a vertical cricket shot (in the

plane normal to ground) by positioning it at a distance ninety degrees to the plane of the bat swing, the captured bat length will appear to vary because the images are not linearly scaled. As the real bat length is constant, then the calculation of the instantaneous radius of rotation from the video footage data is likely to be contaminated. The reason for the variations in bat length according to the camera height was explained in baseball bat swings by Cross [65]. Similarly Portus [60] commented about the inclusion of possible error in the measurements conducted by Pinder et al. [18]. They reported a shorter stride length and increased elbow angles for ball machine studies using a video camera in sagital plane. Portus [60] stated that shorter stride length and larger elbow angle could be erroneous because of ball machine bias, or a curved ball trajectory, which resulted the batter striding further out of the sagittal plane (i.e. the front foot more proximal to the camera), or a backswing moving out of plane (more distal to the camera). The more proximal position of front foot and more distal position backswing movement to the camera could have contributed to the shorter stride length and an increased elbow angle respectively [60].

The advent of micro-electronic devices which are miniature in size, cheap, portable, user- and match-friendly, and capable of recording digital data in three dimensional spaces uniformly has provided opportunities for researchers to solve the limitations in video. One class of devices are inertial sensors which have the size of a match box and are operated with low power and allow the user to modify the hardware and software according to the application requirements. These wireless sensors can measure inertial changes hundreds of times a second and are light enough to be placed on any part or segment of the performers body without hindering performance. Other than cricket bat swing, a variety of researchers have started using these sensors to extract the kinematics and kinetic features of bat swing in other sports. For instance, Ahmadi et al. [44] investigated translational and rotational motion of the first serve swing in tennis, James [52] reported the basic swing of Japanese swordsmanship and multi-limb motion monitoring, Kavanagh et al. [78] reported the assessment of limb segment acceleration in gait analysis, Ohgi [97]

detected the kinematic chain in golf lateral swing, very recently King et el. [50] documented the method of using the miniature, wireless MEMS inertial measurement unit (IMU) and the measurement theory for analyzing three-dimensional baseball bat dynamics. In cricket research Busch et al. [55] outlined the possibility of using inertial sensor to extract the features of a batting shot. That work did not address features extractions and only explained the sensor revealed acceleration profiles to show how a stroke's features might be extracted. The use of tiny sensors has opened a novel methodology for research in many sports but in cricket bat swing no such publications are available in the literature. Bat swing research in other sports has proved that the tiny sensors can overcome the limitations of using research/measurement methods requiring expensive, non-portable, hard-wired equipment.

# 4   METHODOLOGY AND ANALYSIS

## 4.1   Research methodology

The research methods commonly used include experimental research, survey research, and case studies etc. [98]. Consistent with other fields, in cricket batting research the variations in methodology comes from the variations in data collection systems and analysis routine. In this work the main objective was to make measurements relevant to batting performance. Studies using a wooden pendulum and human batting studies were performed with and without ball contact.

Three categories of human subjects were used in these investigations:

1) Novice batters: These participants had no previous experience playing cricket but had engaged in other sports.

2) Amateur batters: These participants had played grade level cricket for two years or more.

3) Sub-elite batters: These participants had played at national level.

Ethics approval was granted by Griffith University Ethics Committee (approval number ENG/16/10/HREC)

### 4.1.1 Architecture of the inertial sensor platform

An inertial sensor is a module or platform used as a motion sensing device. Accelerometers and gyroscopes are two types of such devices of which the first one is used for linear and the second is used for angular acceleration measurements along three axes of the three dimensional spaces. The motion related data are converted to electrical signals. One of the basic mechanisms of measuring the acceleration is by converting the motion to a change in the electrical parameters within these sensors. The small sensors commonly use some form of Micro-Electro-Mechanical Systems (MEMS). These systems work by detecting the change in position of a suspended mass relative to the body as a change in capacitance. The sensors are commonly

manufactured in silicon, and its body, proof-mass, the suspended systems are silicon, with the components etched in the silicon using similar techniques to semiconductor manufacture. Each sensor platform is composed of a readily available low cost microprocessor and features on-board memory, inertial sensors, and USB (Universal Serial Bus) communications. The accelerometer sensor platform contains two embedded inertial sensors; each is capable of measuring accelerations in two perpendicular directions. This facilitates collection of data in three dimensional spaces. The important feature of this platform is that it is user friendly and easily customized by someone having limited programming experience. While both types of sensors (accelerometer and gyroscope sensors) are integrated into a single chip both linear and angular data become available as six degrees of freedom. The integrated system together with other peripheral electronics devices and chips embedded as single system is known as an inertial measurement unit (IMU). A number of different accelerometer sensor units with different characteristic were used for different experiments in this research. The architecture and operating system of a typical accelerometer sensor platform (devised by Davey et al. [99]) are outlined.

### 4.1.1.1 Sensor platform and operating system

An RISC (Reduced Instruction Set Computer) based Atmel ATmega324P microprocessor is at the heart of the sensor platform. It has 8 channels for analogue input (for sensors) and 32 Kbytes Flash memory for programming together with 1 KByte EEPROM (Electrically Erasable Programmable Read Only Memory) and 32 digital I/O (Input/output) lines and SPI (Serial Peripheral Interface) bus for communicating with peripheral devices ([99]). Additionally the processor features with variable clock frequency operation in the range from several KHz up to 20 MHz allowing for extremely low power operation or high performance operation (up to 10 MIPS (Million Instruction Per Second) processing throughput). The platform contains 2 Mbytes of on board memory for data storage, associated with a storage mode that assists tri-axial acceleration data collection for over an hour at a rate of 100 samples per second or more if compression techniques are applied. The tri-axial accelerometer in the platform has features of programmable gain for specific

activities of interest to be investigated with good resolution. There is also an on-board USB chip and connection socket in the platform for easy communications with a PC (Personal Computer), and features for including RF (Radio Frequency) communications. External analogue and digital connection sockets for additional sensors and peripherals allow the platform to be more easily customizable for specific applications.
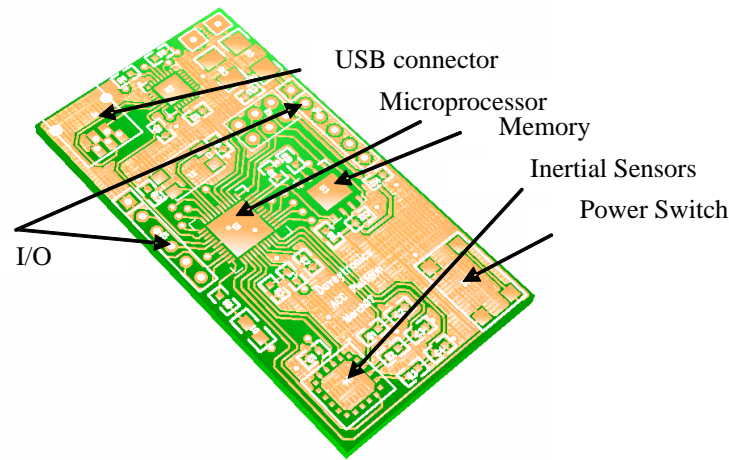


**Fig. 4.1**    Sensor platform board layout showing key components ([99]).

The platform can be powered by 2 AAA battery cells and also higher density solutions such as Lithium-ion replacements could be used. Fig. 4.1 shows the board layout for the platform. It consumes about 5 mA in record mode and able to record up to 44 hours.

The operating system and configuration for the sensor platform is capable of performing sensing, data acquisition, signal processing, communications and wireless network management on a limited power budget. A loosely-coupled, low-power, embedded, Real Time Operating System (RTOS) is implemented on the data acquisition platform, and the RTOS was developed within the CWMA (Centre for Wireless Monitoring and Analysis) at Griffith University by Wixted et al. [100]. The RTOS can minimize power consumption and assists application developers in

minimizing application power use at the same time. The RTOS have real-time components and processes for data acquisition platform to monitor real-time events and is able to operate within a data network. A synopsis of the architecture of the RTOS is shown in Fig. 4.2.
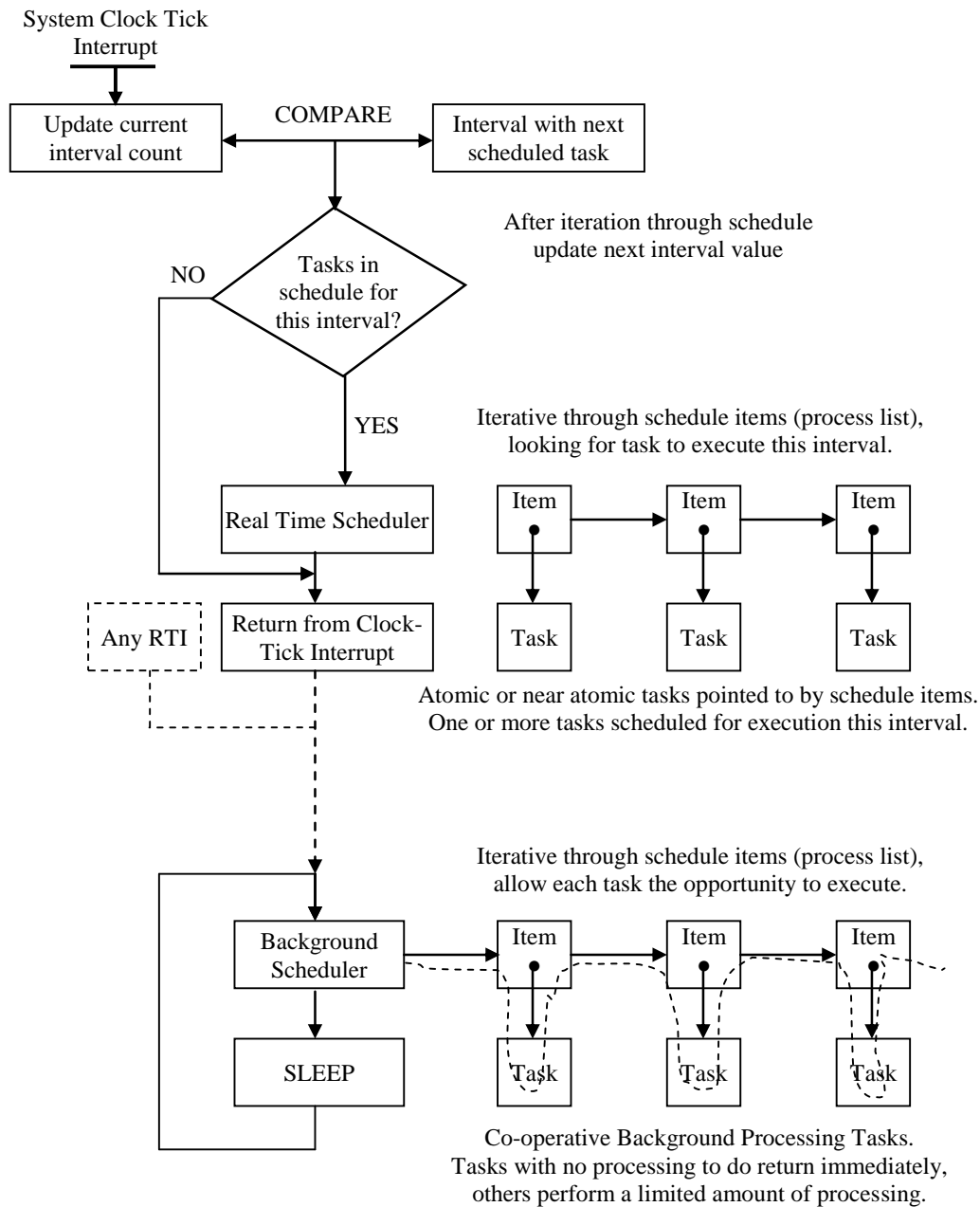


**Fig. 4.2**    Architecture of RTOS for the sensor platform [100].

The RTOS uses two background schedulers and some independent threads managing specific tasks. Two lists of tasks are provided by the operating system, the RTS (Real-Time Scheduler) and BGS (Background Schedule). RTS are normally atomic or near atomic tasks but can start an independent thread of control for non atomic real time where needed. It can also add tasks to the BGS. The RTS runs independently from the BGS and is designed for either simple tasks or routines that are going to use a separate interrupt routine. Whereas BGS is used for long running tasks or the tasks those are not time critical. Usually long running tasks are run by the BGS or on an independent thread. High priority tasks, such as data sampling, are placed in the RTS. An example of a typical independent thread is a full data log buffer which needs the data to be transferred via the serial bus to the flash memory.

### 4.1.1.2 Data collection and calibration

These accelerometer sensors are true DC accelerometer devices and report a static 1g acceleration when any of the three axes is aligned to the gravity vector. Sensor data once collected by the platform can be stored on flash memory. The recorded data is formatted into three streams corresponding to the three axes. When stationary (static position) the sensor data shows only the orientation of each axis with respect to gravity. The wireless features of the sensors can send the data directly to the computer via a Bluetooth network. For the sensors that don't contain any wireless facility; the recorded data stored in memory can be downloaded to the computer via USB. Before starting to collect data each sensor needs to be calibrated for converting the recorded data to a gravity scale. The calibration is done by orienting each axis separately exactly along and opposite to the gravity direction. Fig. 4.3(a) shows a typical recorded profile resulting from the calibration for each of sensor's X-, Y- and Z-axis followed by a straight drive bat swing.

The rectangular portion of the acceleration profiles is the result of the calibration process and this is followed by the straight drive. As seen in Fig. 4.3(a) the difference between the steady peak levels (upward and downward steady level) of the rectangular signals between vertically down (align to gravity) and up (opposite to

gravity) position of an axis of a sensor indicates the scale of twice the gravitational acceleration (2g) for that particular axis. For example, the upward signal level (let's say $\Psi$) during the Z-axis calibration is 600.20 units while the downward level (let's say $\Phi$) is 418.30 units as shown in Fig. 4.3(a) (labelled Zcal), then 90.95 units is equivalent to 1g acceleration for the Z-axis.
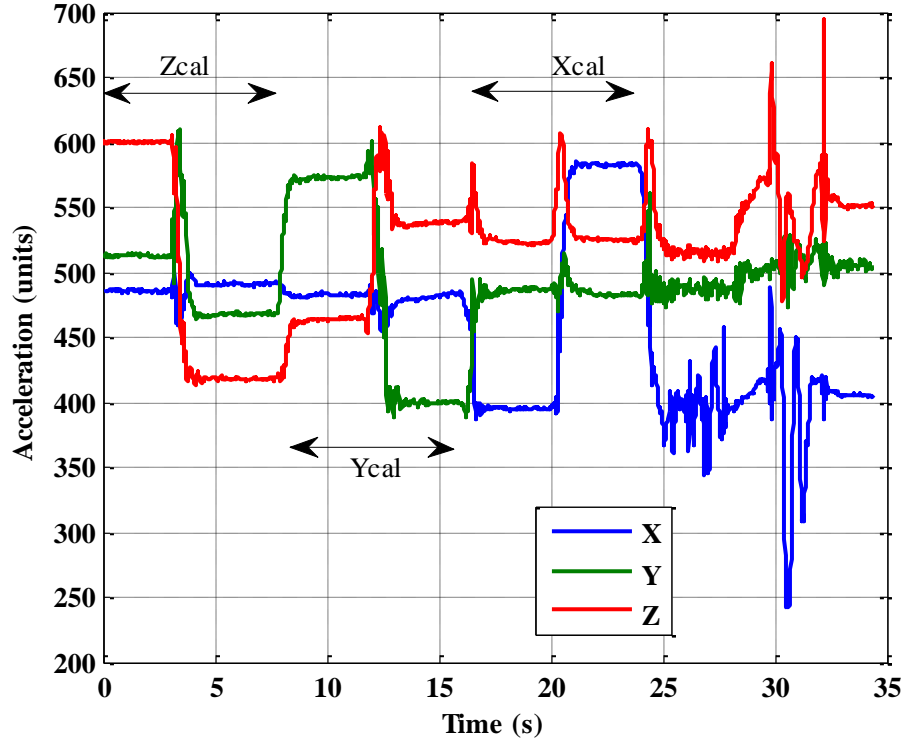


**Fig. 4.3(a)**     Typical acceleration profile recorded in an accelerometer sensor from calibration (b levels) and a straight drive bat swing (t = 25 to 33s).

Likewise, the 1g equivalent units for the Y-and X-axes are 86.89 and 93.68 respectively considering the signal peak levels along the duration of Ycal and Xcal. The acceleration in Fig. 4.3(a) can be converted in gravity scale (say *A(t)*) using following procedure:

$$A(t) = \frac{a_r(t) - \delta}{\kappa}$$
(4.1).

where, $a_r(t)$ is the raw acceleration recorded in sensors as plotted in Fig. 4.3(a); $\delta$ is the

offset calculated as $(\Psi+\Phi)/2$; and $\kappa$ is the linear scaling factor. Fig. 4.3(b) shows the converted g-scaled acceleration profiles. From the X-axis, Y-axis and Z-axis accelerations (say $A_X$, $A_Y$, $A_Z$ respectively) the total acceleration ($A_T$) is calculated as:

$$A_T = \sqrt{(A_X)^2 + (A_Y)^2 + (A_Z)^2} \qquad\qquad (4.2).$$
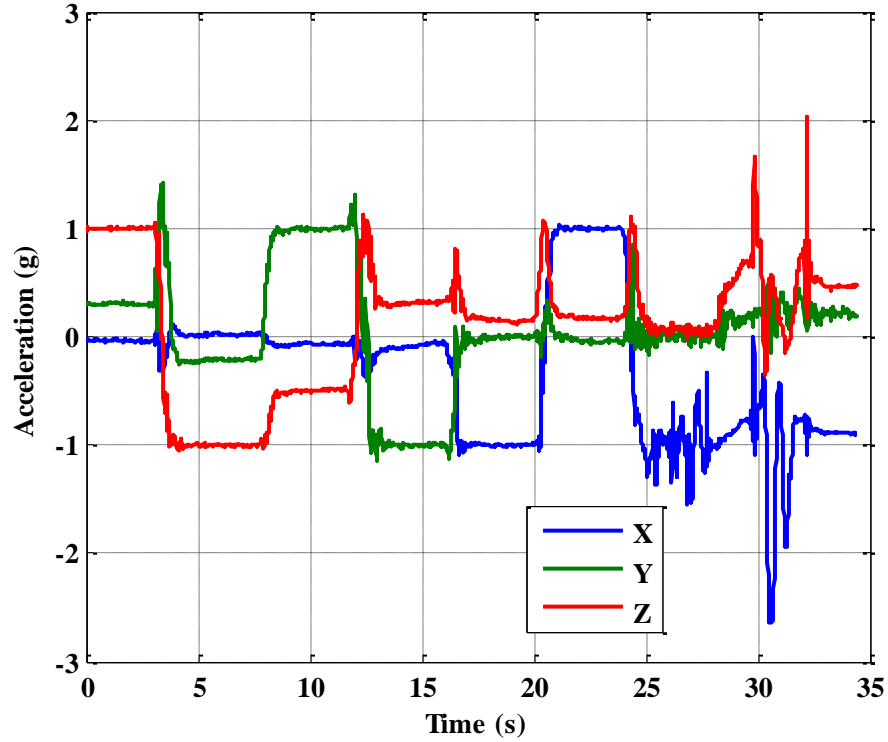


**Fig. 4.3(b)**      Gravity scaled typical acceleration profile of Fig. 4.3(a).

This calibration process is a manual calibration and is prone to errors if each axis of accelerometer sensor is not aligned perfectly to the direction of gravity. The error can be minimized by the 6-point Newton-Raphson iterative based calibration techniques of Lai et al. [101], that does not require the device to be aligned exactly with gravity but only requires six distinct stationary orientations. This technique assumes that 3 axes are exactly orthogonal in order to have minimal error, which is practically not possible. However, with the tolerance of current generation of MEMS sensors, the error is small enough that it can be neglected. Additionally, in the

manual calibration it is noticed from Fig. 4.3(a) that Y-axis acceleration during Zcal and Z-axis acceleration during Ycal is not zero, rather varied by 50 and 100 acceleration units respectively. This resulted from the fact that sensor's Y-and Z-axis are not perfectly aligned to those axes of cricket bat. Because the back of the bat where the sensor was placed is not flat, the details about it and necessary corrections are stated later.

### 4.1.1.3 Conversion of collected data to the desired frame of reference

The data recorded along sensor's X-, Y- and Z-axis due to movement is the result of the changes in the orientation of the axes in three dimension space. To convert those data to a known reference frame (say the world coordinate frame, i.e. inertial frame of reference), the signal recorded in the sensors must be rotated along the axes of the desired reference coordinate system (say world coordinate axes, x-, y- and z-axis). This rotation can be performed when the angles between the sensors axes and the desired reference axes are known. This is performed mathematically by taking the projection of the sensor recorded signals from each axis on any one of the desired reference axis. Then the total signal projected from sensor's each axis along that reference axis is the converted signals along that axis. Thus the converted signal along each desired reference axis is the resultant signals projected on that axis from all three axes. The most convenient way to do this conversion directly is to use the rotation matrix based on Euler Angles (named for Leonhard Euler, 1707-1783.) By identifying the current orientation of the sensor's axes according to the desired reference axes, three angles representing rotations about three axes are identified. Then the rotational tensor (3x3 matrix) is applied to the measurements. This is described in more detail in the following section.

Fig. 4.4 describes the position of the sensor on the bat and the orientation of sensor relative to the bat. While the sensors (two sensors S1 and S2) are attached to the back of the bat as shown in the Fig. 4.4(a), there is a difference in the bat axes ($X^B$, $Y^B$, $Z^B$) and sensor axes ($X^{S1}$, $Y^{S1}$, $Z^{S1}$ of S1 and $X^{S2}$, $Y^{S2}$, $Z^{S2}$ of S2) shown in Fig. 4.4(b) because the back of the bat is not flat. The difference in the axes orientation between

125

the bat and the sensor is in the transverse plane ($Y^B Z^B$-plane, parallel to ground as shown in the Fig. 4.4(a)). The magnitude of sensor recorded y-axis acceleration and z-axis acceleration ($a_y$ and $a_z$ hereafter recorded in either sensor S1 or S2) is different to the original acceleration (from the bat's movement) along the bat's $Y^B$- and $Z^B$- axis acceleration ($A_Y$ and $A_Z$) by the cosine of angle between the bat's face and sensor's y- or z-axis as follows:

$$a_y = A_Y \cos \delta, \quad a_z = A_Z \cos \delta \tag{4.3}.$$

There is no difference between bat's $X^B$-axis acceleration ($A_X$) and sensor's x-axis acceleration ($a_x$ recorded in either sensor S1 or S2).
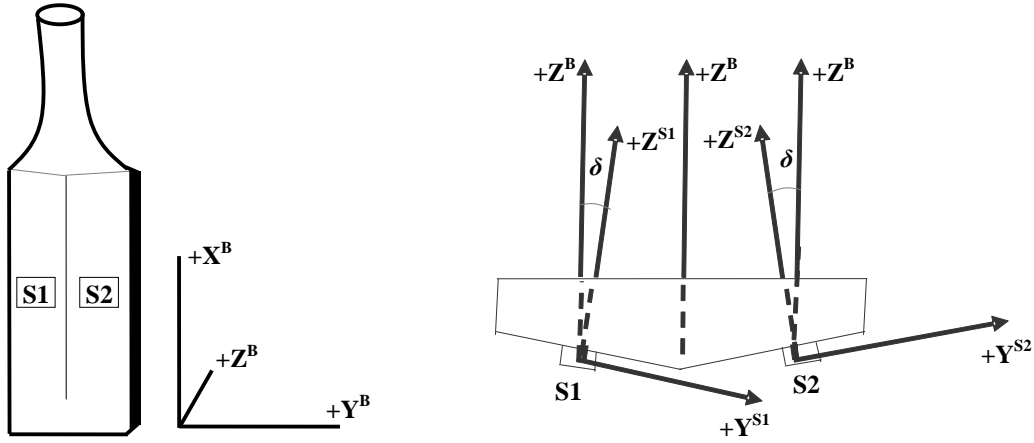


**Fig. 4.4**    Accelerometer sensor placement in the bat and difference in orientation of bat's and sensor's axes. (a) Sensor orientation in the bat and $X^B$, $Y^B$ and $Z^B$ bat axis definitions, (b) The difference in orientation between sensors' y($Y^{S1}$, $Y^{S2}$ for S1 and S2 respectively) and z($Z^{S1}$, $Z^{S2}$ for S1 and S2 respectively)-axis and bat's $Y^B$- and $Z^B$-axis by an angle ($\delta$).

Fig. 4.5 shows the world coordinate system (defined by the vectors *I, J, K*) and the coordinate system of the bat face (defined by the vectors $i_f$, $j_f$, $k_f$) in the position of the bat in the stance phase of a drive. For convenience the bat coordinate system is used to describe how the sensor acceleration components can be converted into the acceleration according to the world coordinate reference. The differences in the

conversion arising from the differences in the sensor's transverse plane coordinates and those of the world system coordinates can be compensated using equation 4.3. As seen in Fig. 4.5 the *IJ*-plane is the ground plane (shown by the dotted mat) and the *JK*-plane is the vertical plane in which the bat is swung for a vertical drive (for example a straight drive) along *J* direction. In Fig. 4.5(a) the angle between $j_f$ and *J* is $\theta$ (actually it is angle between $j_f$ and its projection on the ground *IJ*-plane as $j_{proj}$ shown in the figure), and between $k_f$ and *K* is $\varphi$. In this figure the bat's coronal axis vector ($i_f$) is aligned (or parallel) with *I*. Then the angles $\theta$ and $\varphi$ have the same value. In this case the position of the bat is the rotated in the world's coordinates by an angle $\theta$ about *I*. The bat position can be expressed using the rotation matrix as follows:

$$\begin{bmatrix} i_f \\ j_f \\ k_f \end{bmatrix} = \begin{bmatrix} 1 & 0 & 0 \\ 0 & \cos\theta & \sin\theta \\ 0 & -\sin\theta & \cos\theta \end{bmatrix} \begin{bmatrix} I \\ J \\ K \end{bmatrix}$$

(4.4).

The position of the bat in the stance phase of the drive shown in Fig. 4.5(b) is different only about the coronal axis orientation of the bat. Unlike Fig. 4.5(a) here the $i_f$ vector is not aligned to the *I* vector rather it is tilted by an angle $\beta$, the angle between $i_f$ and its projection on ground plane as $i_{proj}$ as shown in Fig. 4.5(b) and it is formed by the rotation of the bat about $j_f$. In this case $j_{proj}$ is not parallel to *J* as in Fig. 4.5(a); rather there is an angle between them (not shown in the figure to avoid complexity). If the position of the bat in Fig. 4.5(b) is considered as a rotation sequence of the bat from Fig. 4.5(a), then the bat is rotated first about *I* and then about $j_f$, then the bat position can be expressed using the rotation matrix as follows:

$$\begin{bmatrix} i_f \\ j_f \\ k_f \end{bmatrix} = \begin{bmatrix} \cos\beta & \sin\beta & 0 \\ -\sin\beta & \cos\beta & 0 \\ 0 & 0 & 1 \end{bmatrix} \begin{bmatrix} 1 & 0 & 0 \\ 0 & \cos\theta & \sin\theta \\ 0 & -\sin\theta & \cos\theta \end{bmatrix} \begin{bmatrix} I \\ J \\ K \end{bmatrix}$$

(4.5).

Using equation 4.4 for the case in Fig. 4.5(a) and 4.5 for Fig. 4.5(b), the accelerations recorded in the sensor (along $i_f$, $j_f$, $k_f$ as $a_y/\cos\delta$, $a_z/\cos\delta$ and $a_x$ respectively) can be converted to world coordinates system vectors ($I$, $J$, $K$).

If the bat is initially rotated about $K$ by an angle $\alpha$ during its vertical position before being tilted as shown in Fig. 4.5(a), then according to the sequence of rotation by angles $\alpha$, $\theta$ and $\beta$ then equation 4.5 takes the form:

$$
\begin{bmatrix} i_f \\ j_f \\ k_f \end{bmatrix} = \begin{bmatrix} \cos\beta & \sin\beta & 0 \\ -\sin\beta & \cos\beta & 0 \\ 0 & 0 & 1 \end{bmatrix} \begin{bmatrix} 1 & 0 & 0 \\ 0 & \cos\theta & \sin\theta \\ 0 & -\sin\theta & \cos\theta \end{bmatrix} \begin{bmatrix} \cos\alpha & \sin\alpha & 0 \\ -\sin\alpha & \cos\alpha & 0 \\ 0 & 0 & 1 \end{bmatrix} \begin{bmatrix} I \\ J \\ K \end{bmatrix} \quad (4.6).
$$



(a)  (b)
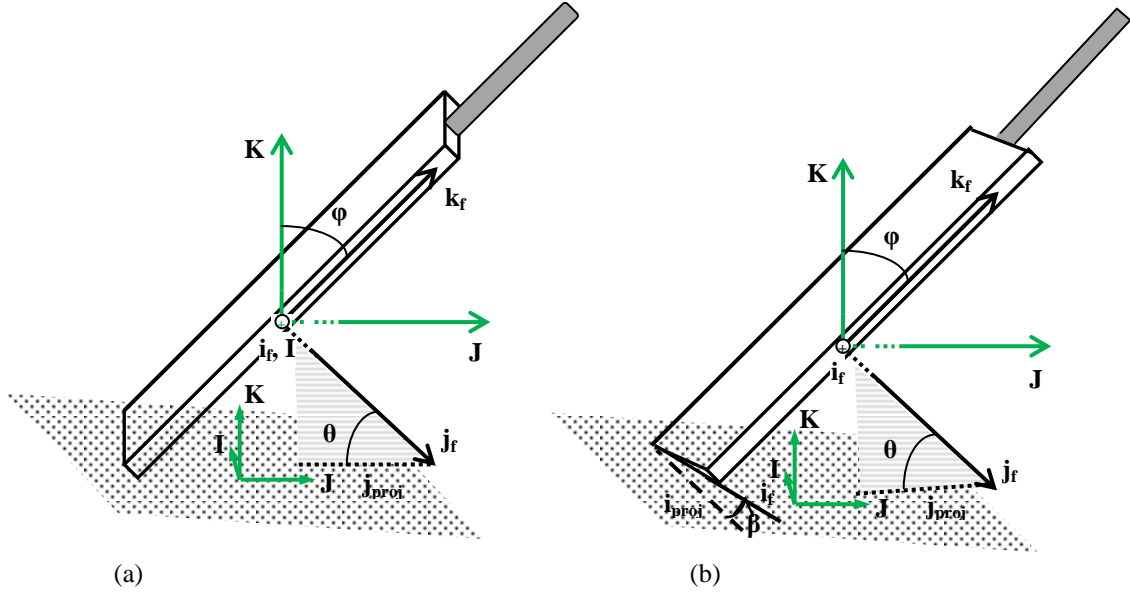
**Fig. 4.5**    The world coordinate system (defined by the vectors $I$, $J$ and $K$) and coordinate system of bat's face (defined by $i_f$, $j_f$ and $k_f$) in the stance phase of a drive in the vertical plane ($JK$-plane, where vector $K$ is normal to ground). (a) Orientation of world coordinate system axes and bat's axes while coronal axis of each system are parallel ($I$ for world system, $i_f$ for bat system) and other two pairs of $J$, $j_f$ and $K$, $k_f$ are of each differed from their corresponding counterpart by angles of $\theta$ and $\varphi$ respectively. (b) Orientation of the two systems same as stated for figure (a) but the bat's coronal axis ($i_f$) is now tilted by an angle $\beta$ with that of world's axis ($I$), i mean, bat's $i_f$ axis is not aligned to ground plane ($IJ$-plane) rather tilted by $\beta$.

The accelerometer measures only gravity for a stationary bat. Then from the measured acceleration the angles $\alpha$, $\theta$, and $\beta$ can be calculated. Using the relation shown in equation 4.6, the measured acceleration values at any instant of the bat swing can be converted from the device coordinate system to the world coordinate system according to the work by Fong et al. [102] for planar motion. For instance, due to planar motion, say there is no rotation about vertical $K$-axis, then $\alpha$ can be set to zero and equation 4.6 takes the same form as equation 4.5. For the initial pure vertical position of the bat we can have the values of $[I\ J\ K]^\mathrm{T}$ vector in equation 4.5 as $[0\ 0\ -1]^\mathrm{T}$ and the values of $[i_f\ j_f\ k_f]^\mathrm{T}$ recorded in the sensors. Then putting these values in equation 4.5, the values of $\cos\theta$, $\sin\theta$, $\cos\beta$, $\sin\beta$ can be evaluated as follows:

$$
\begin{aligned}
\cos\theta &= -k_f \\
\sin\theta &= \sqrt{1-k_f^2} \\
\cos\beta &= \frac{-j_f}{\sqrt{1-k_f^2}} \\
\sin\beta &= \frac{-i_f}{\sqrt{1-k_f^2}}
\end{aligned}
\tag{4.7}.
$$

Putting the values of $\cos\theta$, $\sin\theta$, $\cos\beta$, $\sin\beta$, and sensor recorded $i'_f$, $j'_f$, $k'_f$ acceleration at any instant of the bat movement in equation 4.5, the recorded acceleration can be converted in world coordinate system as $I'$, $J'$, $K'$ by using equation 4.8 as follows:

$$
\begin{bmatrix} I' \\ J' \\ K' \end{bmatrix} =
\begin{bmatrix}
\dfrac{-j_f}{\sqrt{1-k_f^2}} & \dfrac{i_f k_f}{\sqrt{1-k_f^2}} & -i_f \\[3mm]
\dfrac{i_f}{\sqrt{1-k_f^2}} & \dfrac{j_f k_f}{\sqrt{1-k_f^2}} & -j_f \\[3mm]
0 & -\sqrt{1-k_f^2} & -k_f
\end{bmatrix}^{-1}
\begin{bmatrix} i'_f \\ j'_f \\ k'_f \end{bmatrix}
\tag{4.8}.
$$

*4.1.1.4 Errors associated with sensor and recorded data*

Errors associated with the accelerometer sensors will limit the accuracy of calculating the applied force. These errors are dependent on the fabrication technology chosen for the sensor and the measurement precision. The dominant error sources in inertial sensors are fixed bias, scale factor and cross-axis coupling error. These nine parameters relate to the errors in three-axis accelerometer sensors.

A fixed bias error is the displacement from zero of the measured force which is present when the applied acceleration is zero. The amount of the error depends on the motion to which the accelerometer is subjected. The value of this error is expressed in units of milli-g or micro-g.

Scale factor errors exhibit in the ratio of a change in the output signal to a change in the acceleration to be measured. It is expressed as a percentage of the measured full scale quantity or simply as a ratio; parts per million (ppm) is commonly used. The non-linearity in the scale factor describes the deviation from the theoretical straight line, or the fitted function that governs the relation between output signal and acceleration.

Cross-coupling errors occur due to the non-orthogonality of the sensor axes and are the result of manufacturing imperfections. This is because MEMS based accelerometer sensors were available in single and dual axis packages at the time of development. To create the triaxial accelerometer assembly, a dual axis accelerometer mounted on a flat circuit board was combined with a single or dual axis accelerometer oriented vertically. The vertically mounted device was either mounted directly on the circuit board or on a small vertically mounted daughter board. In both cases the manufacturing imperfection is unknown and subjected to the degree of control over the orientation of the vertical component. The cross-coupling error can create large acceleration errors from accelerometer sensitivity to accelerations that are applied to the normal to the input axis.

Some other types of errors in the sensors are well known as vibro-pendulous errors

and random errors. The vibro-pendulous errors are the dynamic cross-coupling errors in pendulous accelerometers that arise owing to the angular displacement of the pendulum which gives rise to a rectified output when subjected to vibratory motion. This type of error depends on the phasing between the vibration and the pendulum displacement. The maximum error occurs when the vibration acts in a plane normal to the pivot axis, at 45° to the sensitive axis, and when the pendulum displacement is in phase with the vibration. Other types of errors are well documented for gyroscopic sensors. These include repeatability errors, temperature dependent errors, switch-on to switch-on variations and in-run errors.

Error in the sensor recorded data increase with increasing bandwidth. The input signal to the sensors is affected by the orientation of the device with respect to gravity and the direction of travel. The calibration errors directly affect the accelerometer output signal and consequently the recorded data. Clothing mounted sensors on the athlete's limbs results in loose coupling between sensor and athlete which can generate inertia related movement artifacts. Accelerometers sometimes may be subjected to overload and recovery related errors due to high over-range acceleration. The accelerometer data is subjected to serious cumulative errors when the device is used as a technique for dead reckoning of position.

### 4.1.1.5 Accelerometer data interpretation

Both the kinetic and kinematic features of motion can be extracted from the sensor data. While a gross movement signatures or kinetic parameters are sought to be interpreted by the sensor recorded data, the errors discussed in the previous section can, in many of the cases, be disregarded. As an example of extracting the bat movement during a forward straight drive, Fig. 4.6 shows the sensors data according to the position of the sensor in the bat as in Fig. 4.4. The acceleration profile in Fig. 4.6(a) is the data recorded in one sensor on the bat. The rectangular wave portion shows the calibration signal and the bat swing for the straight drive is expanded in the Fig. 4.6(b). The duration of the forward swing in this figure is shown by the shaded bar. The first three peaks in the Z-axis acceleration comes from the three bat

taps before the drive. The forward swing duration shown in Fig. 4.6(b) was confirmed by the video and the validation is described in the results.
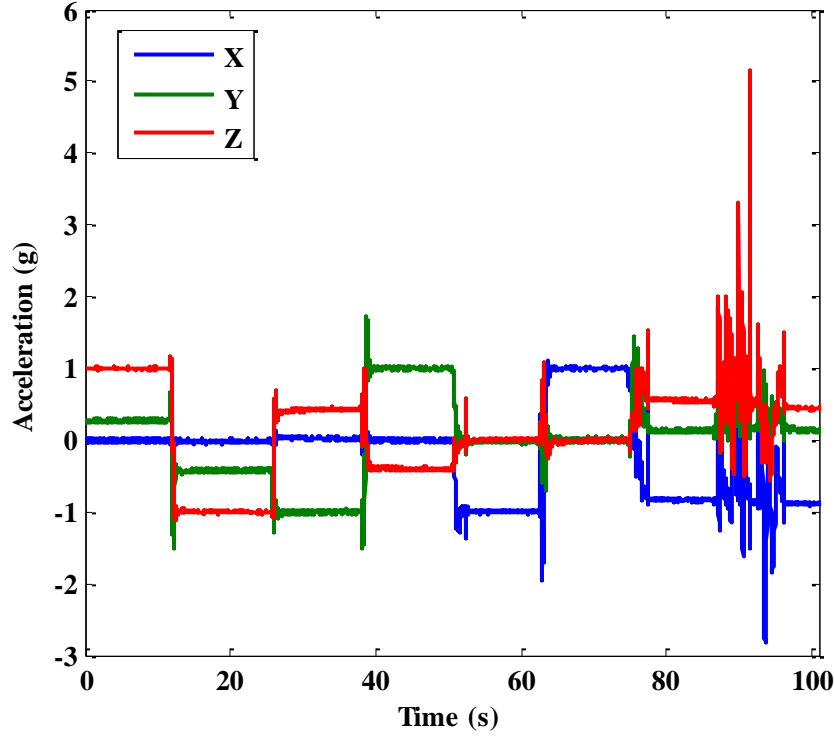


**Fig. 4.6(a)**      Accelerometer profiles from a typical straight drive including calibration, bat taps and bat swing signals. The rectangular signals are from the calibration part and other are in the dense signal portion of the figure after 80 second, and the zoom in version of those signals are shown in Fig. 4.6(b).

The sharp spikes in Fig. 4.6(b) resulted from sensor errors (interpreted later) confirmed by the fact that these peaks (at 88.29, 88.36, 89.99, 90.07, 91.58, 96.07s etc., for example, in Z-axis acceleration) happen by the sharp jump of the signal at one data point.

The accelerations shown in Fig. 4.6(b) are referenced to the sensor coordinate system. These accelerations can be converted to the world coordinate system using equation 4.6. The novice batter was instructed to perform the straight drive without twisting the bat (rotation of bat about bat's vertical $k_f$-axis according to Fig. 4.5) during a swing in the vertical plane. Assuming that the batter followed the instruction
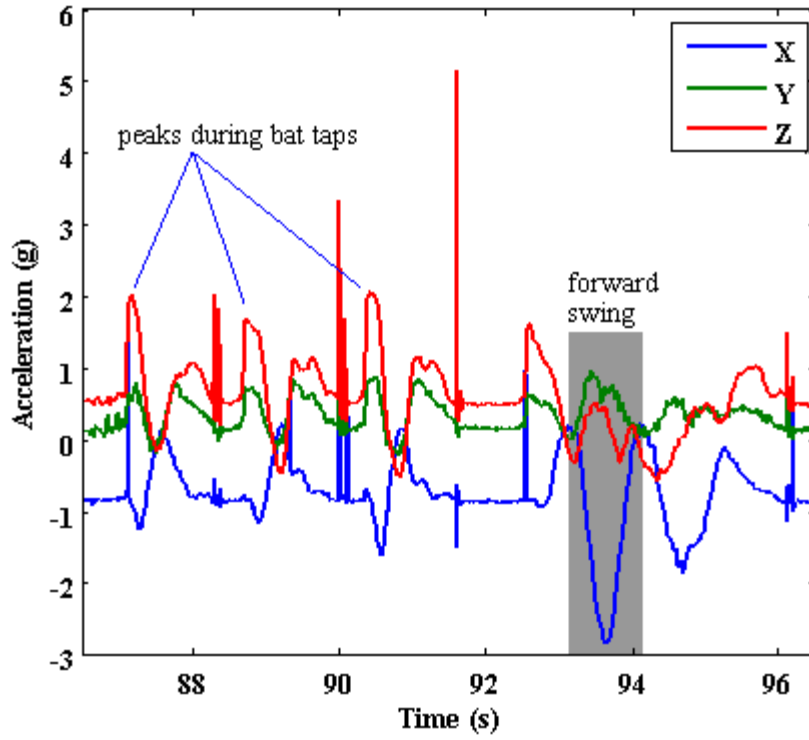
**Fig. 4.6(b)**       Accelerometer profiles for bat tap and bat swing from the typical straight drive corresponding to the zoom in version of the dense signal shown in Fig. 4.6(a).

at least at the start of swing, then the angle $\alpha$ is chosen to be zero. The angles $\beta$ and $\theta$ were calculated from the start point accelerations of Y- and X-axis (or Z-axis) in Fig. 4.5(b) while the bat was stationary and used in equation 4.6 following the procedure by Fong et al. [102] done for a planar motion. Fig. 4.7(a), 4.7(b) and 4.7(c) show the profiles for X-, Y- and Z-axis accelerations respectively both referenced to sensor and the world coordinate systems.

A significant difference is obtained in X-axis acceleration magnitudes between the two coordinate systems as seen in Fig. 4.7(a). However, the overall shape of the acceleration profile is preserved. This confirms the conversion procedure. In the case of the Y-axis acceleration, there is no significant difference between the two profiles shown in Fig. 4.7(b) referenced with respect to the two coordinate systems. This is due to the fact that at the start of the drive, the sensor's out of swing plane axis
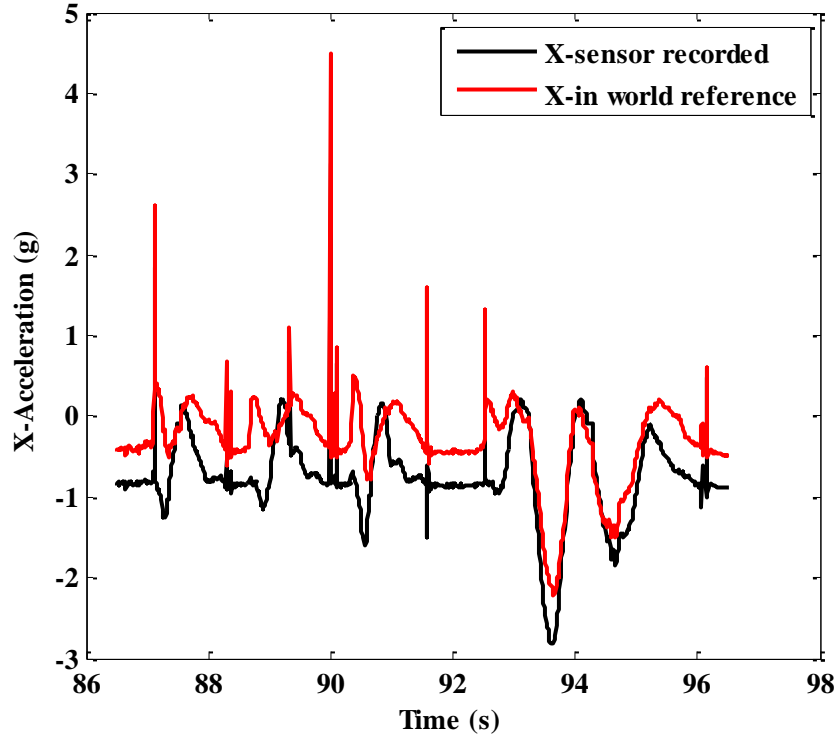
**Fig. 4.7(a)**     X-axis acceleration from the drive in Fig. 4.6(b) as recorded by the sensor with reference to its body attached coordinates system and as converted for reference to world's coordinate system.

(normal to swing plane, $i_f$-axis as shown in Fig. 4.5) was in line with the world coordinate $I$-axis (or parallel to the $I$-axis). Then $\alpha$ was chosen zero for the conversion. However, the difference (though not significant) between these two profiles has come from the effect of the other two axis acceleration on the sensor's $i_f$-axis resulting from the sensor's error if the three axes are not perfectly orthogonal in fabrication. This error is discussed in detail later.

There is also a noticeable difference in the magnitude of the Z-axis acceleration between the two coordinate systems but the overall profile shape is preserved (Fig. 4.7(c)). This is also true in the X-axis case. The maximum difference happens during the forward swing at the instant that the out of swing plane acceleration (accountable

134

for bat twisting) is maximum (Fig. 4.6(b)). This effect is not observable in sensor acceleration but becomes discernible while converting it to the world's coordinate system. This is discussed in detail later.
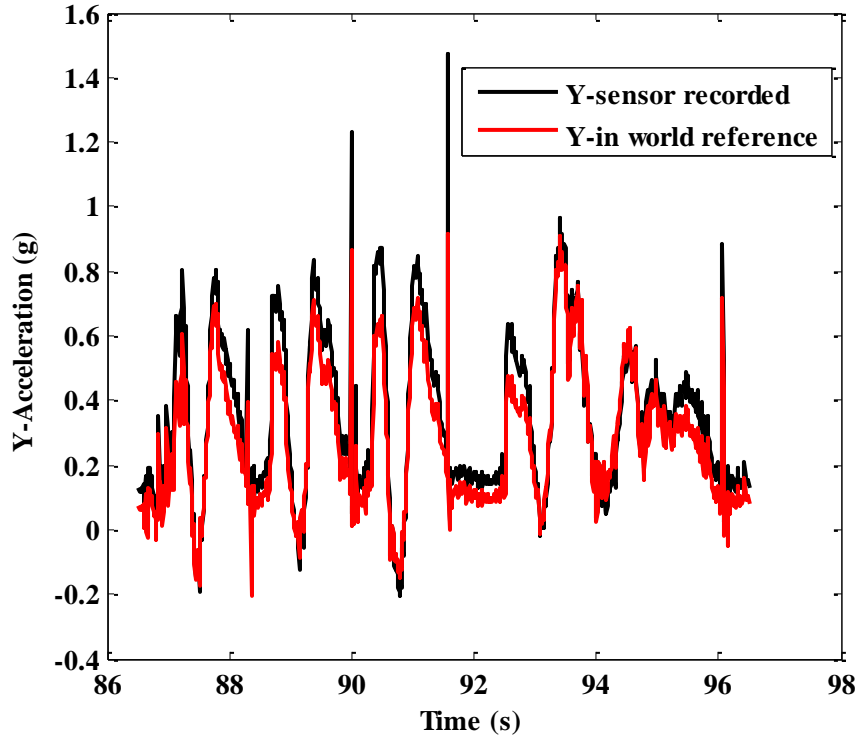


**Fig. 4.7(b)**       Y-axis acceleration from the drive in Fig. 4.6(b) as recorded by the sensor with reference to its body attached coordinates system and as converted for reference to world's coordinates system.

This section discusses the errors in the sensor data. Fig. 4.8(a) is the zoom in version of part of Fig. 4.6(a) during one half of the Z-axis calibration procedure (Z-axis was put straight downward along gravity direction). The mean values of the X-, Y-and Z- accelerations are -0.0030g, 0.2714g and 0.9988g respectively. The X-axis is approximately zero and the Z-axis is aligned to gravity.

The Y-axis is not exactly orthogonal to gravity vector, rather 74.25° with it. If it is assumed that the calibration was within one percent, then the deviation of the Y-axis from the perfect normal to gravity is 15.75° resulting in an angle ($\delta$) between sensor

y-axis and bat Y-axis (see Fig. 4.5). This was the fixed misalignment in the z-axis, but as the batter swings the bat there are additional misalignment variations. Within the value of 15.75º there is a chance of a cross-coupling error due to the non-orthogonality of the sensor axis due to imperfect fabrication of the sensor.
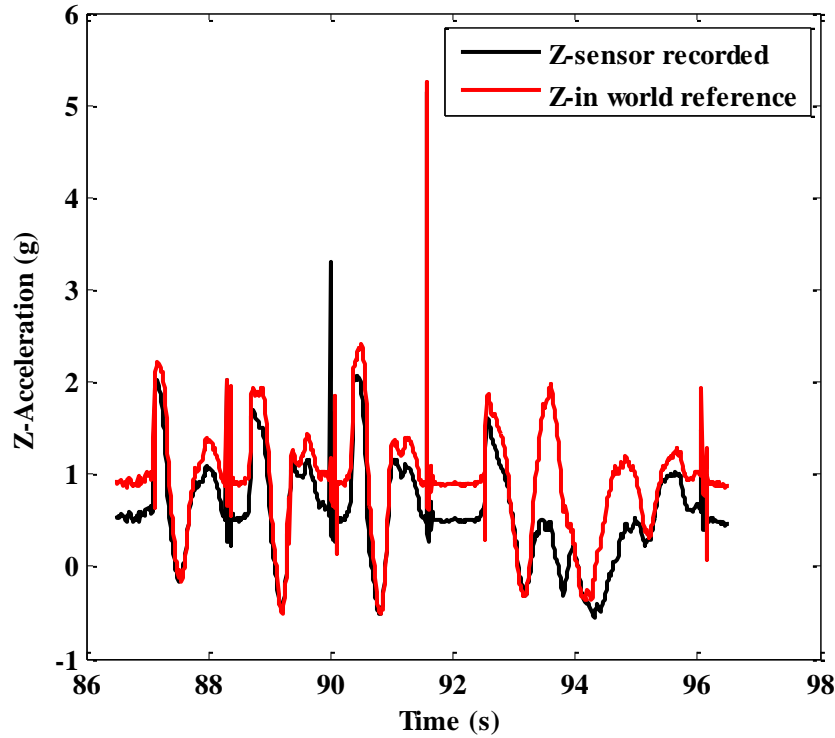


**Fig. 4.7(c)**    Z-axis acceleration from the drive in Fig. 4.6(b) as recorded by the sensor with reference to its body attached coordinates system and as converted for reference to world's coordinate system.

A more detailed zoom of Fig. 4.8(a) for Z-axis acceleration is shown in Fig. 4.8(b). The Z-axis acceleration is not a constant 1g value but has fluctuation of $\pm0.011g$. This is known as dither. The dither is a digitization uncertainty due to comparing the analogue output of the sensor to the digital signal from the decoder. The value depends upon the resolution of the decoder used in the accelerometer sensor. The dither during the forward swing of the drive is also seen in Fig. 4.8(c). The profile in Fig. 4.8(c) is not smooth but the overall trend of the signal is obvious. The dither can

be removed using a smoothing filter. The filtering techniques are discussed in Section 4.1.2.
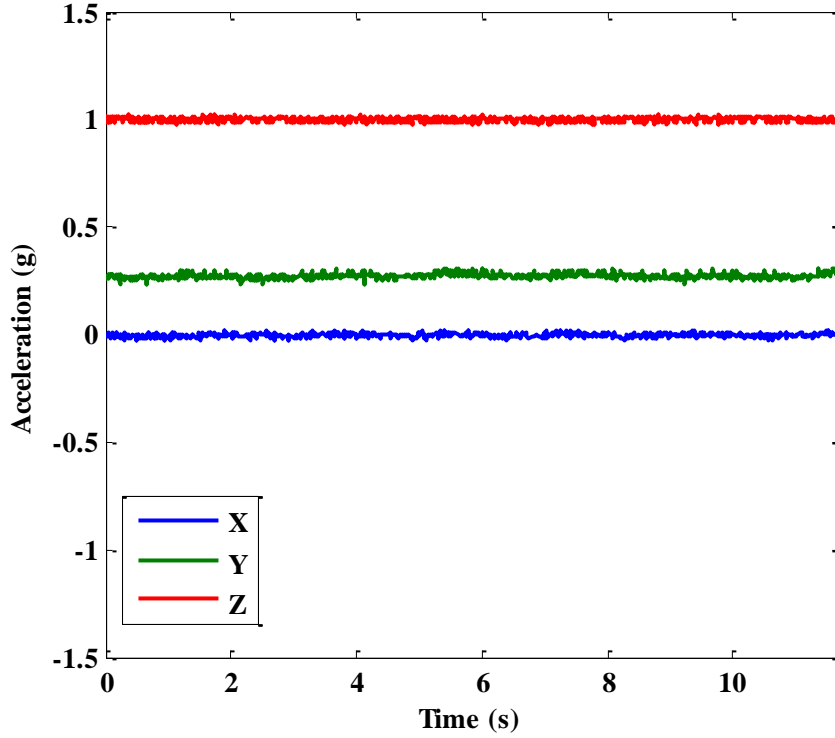


**Fig. 4.8(a)**     Acceleration profiles during Z-axis calibration (part of Fig. 4.6(a)) as recorded by the sensor with reference to its body attached coordinates system.

The fixed bias error is visible in Fig. 4.8(d) in X-axis acceleration during the Z-calibration procedure. If the calibration is perfect, then the value of the X-acceleration should be zero. The dither in Fig. 4.8(d) is not centered on zero; rather it is about -0.01g. This means that the expected value of X-acceleration is shifted by a bias of -0.01g and this error is called the fixed bias error.

High sensitivity is required for a sensor to have the highest resolution. The scale factor is the measure of how the changes in output signal is related to the changes in acceleration. As an inertial accelerometer is sensitive to gravity, the changes in angle along any sensor axis with respect to gravity direction should change the output signal.
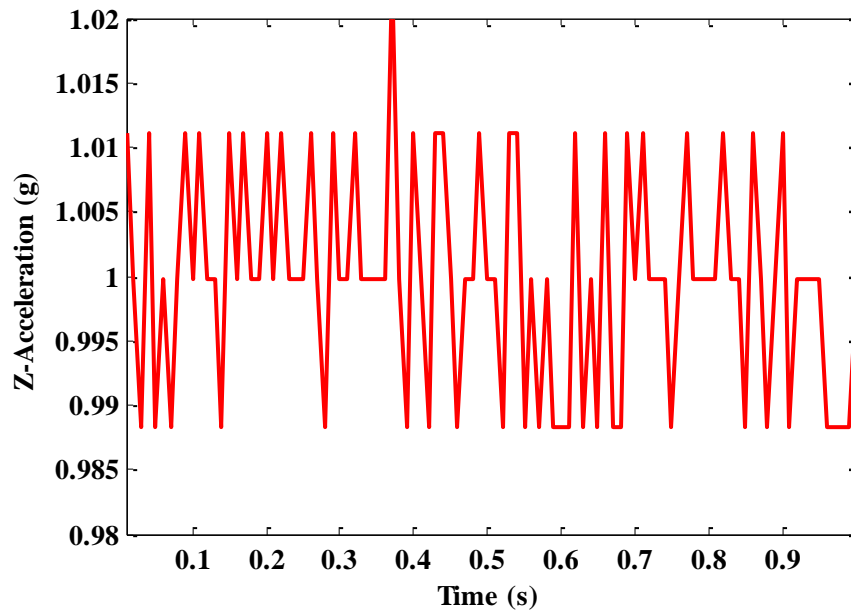
**Fig. 4.8(b)**　　　Error for dither in Z-axis acceleration profile during calibration as in 4.8(a) dependent on the resolution of the decoder used in accelerometer sensor.
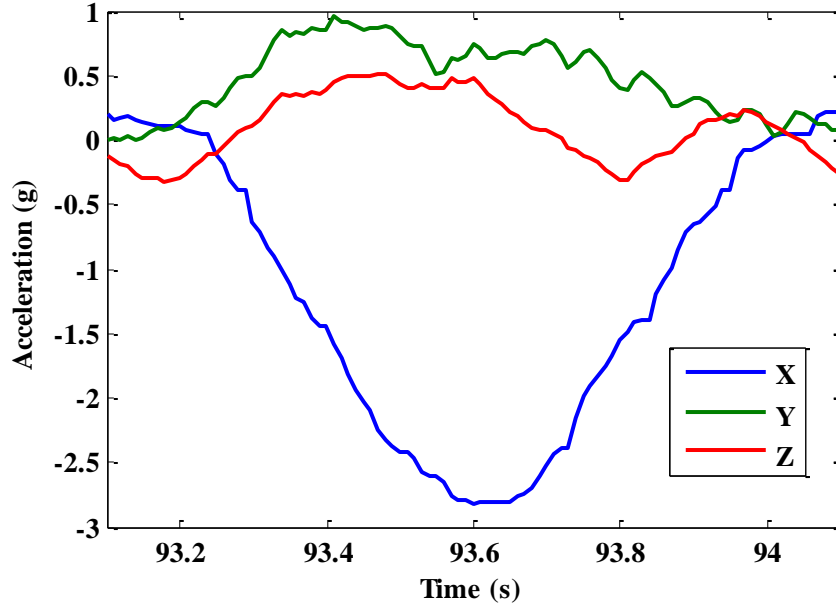


**Fig. 4.8(c)**　　　Dither in the acceleration profiles during the forward swing for the typical drive as in Fig. 4.6(a).
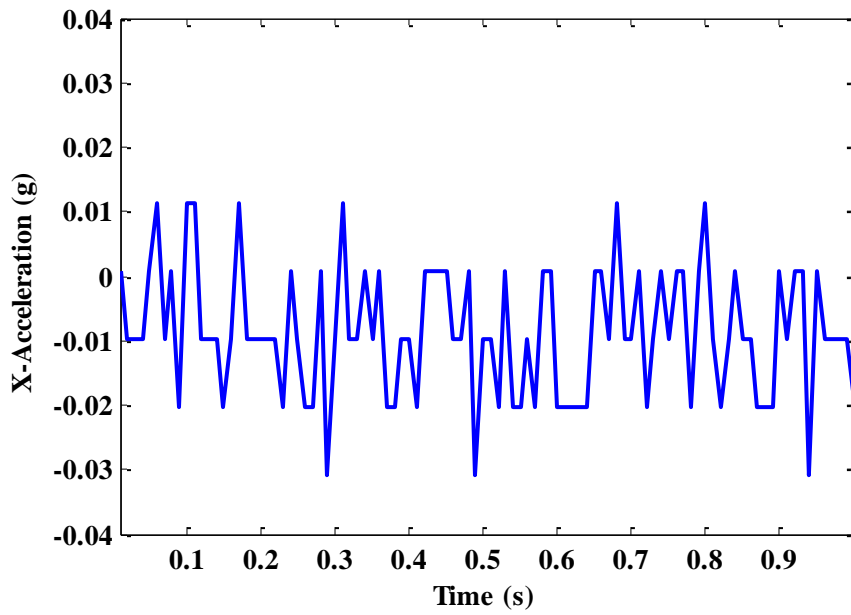
**Fig. 4.8(d)**    Dither in the X-acceleration profiles is about the base of -0.01g during the Z-axis calibration as in Fig. 4.8(a), showing the fixed bias error of around -0.01g in X-acceleration.
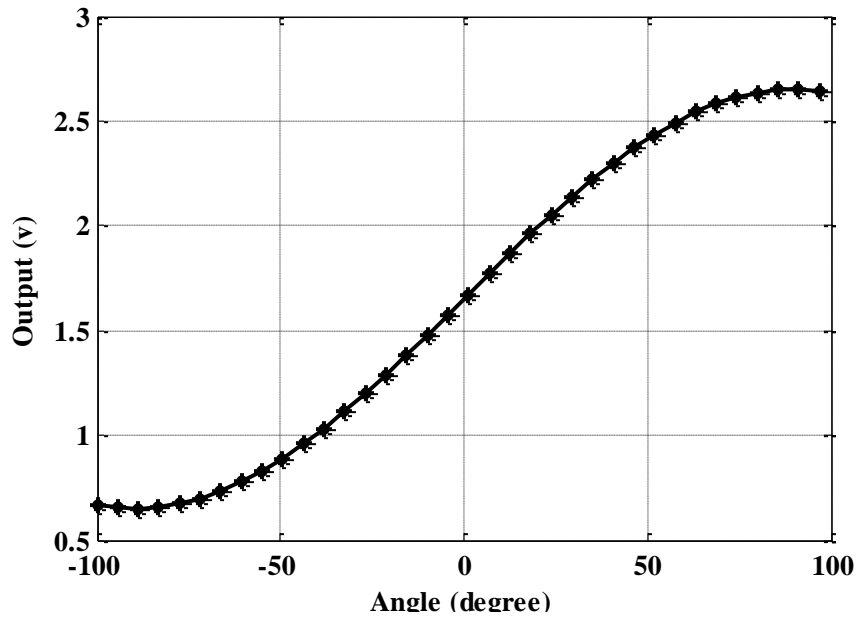


**Fig. 4.8(e)**    Typical nonlinear output in voltage of the X-axis of a typical accelerometer with respect to its alignment to gravity (Freescale semiconduct inc. [103]).

For a capacitive MEMS accelerometer, the output is more like a sine wave (Freescale Semiconduct inc. [103]). Fig. 4.8(e) shows the typical output of the X-axis sensor plotted against the angle measured to gravity (Freescale Semiconduct inc. [103]). For angles in the range -40º to +20º the accelerometer output voltage is proportional to the input angles. Outside this range the relationship is no longer linear. This nonlinear region will introduce a systematic error called scale factor error.

### 4.1.2 Signal processing of accelerometer data

The triaxial accelerometer data are in the form of three streams of numerical values (for each of three axes) and reflect both static and movement information. Numerical signal processing techniques can be applied to extract the key features of movement. While the static position of a sensor reports only gravitational acceleration, during movement the gravity components add to the movement components. To extract the movement signature the effect of gravity must be removed. In addition minor displacement of the sensors (even though attached tightly to the limbs and bat) must be considered. A filter can be used to separate the static and dynamic effects. The error signals might also be included in the recorded data and can be removed by filtering. The vertical orientation of the sensor when there is no movement can be extracted from the acceleration components. During movement, the gravity component from the recorded signal can be deduced by filtering. As the sensors are attached to the batter's limbs and bat, (assuming they are attached firmly), extracting the sensor orientation gives an approximate orientation of the sensor and so the batter's limbs and bat. A comparison between long-term and short-term orientation facilitates various aspects of batter activity. The time periods that describe long-term and those that describe short-term events are activity specific. The orientation of a batter's limbs and bat can be calibrated by conducting static measurements and comparing the result with a known reference. However, the orientation signals from the sensor can also be highlighted by filtering. The frequencies of wanted and unwanted signals are important parameters in the numerical analysis. The Fast Fourier Transform (FFT) is one of the signal processing tools for sensor data. Other

signal processing tools like auto-correlation and cross-correlation are also useful for specific movement activities of interest. The signal processing tools are discussed in the following section with examples of interpreting the movement signature and overcoming or minimizing the errors associated with the static gravitational acceleration.

### 4.1.2.1 Filtering

A filter removes the unwanted frequency components. To provide the filtering during data recording is limited or hampered by the low processing power and small system memory. The most convenient and best way to filter is during the post processing of data utilizing a desktop computer. The common filtering techniques used include moving average filter, Hamming Windowed Finite Impulse Response (FIR) filter, and Rectangular Windowed FIR filter. The difference between the two windowed filters depends upon the characteristics of the smoothing windows. The frequency response of the smoothing window is a continuous spectrum with a main lobe and several side lobes. The Hamming Window function has a wider main lobe than the rectangular window function, so a bigger attenuation between the main and the highest side lobe compared to rectangular window function.
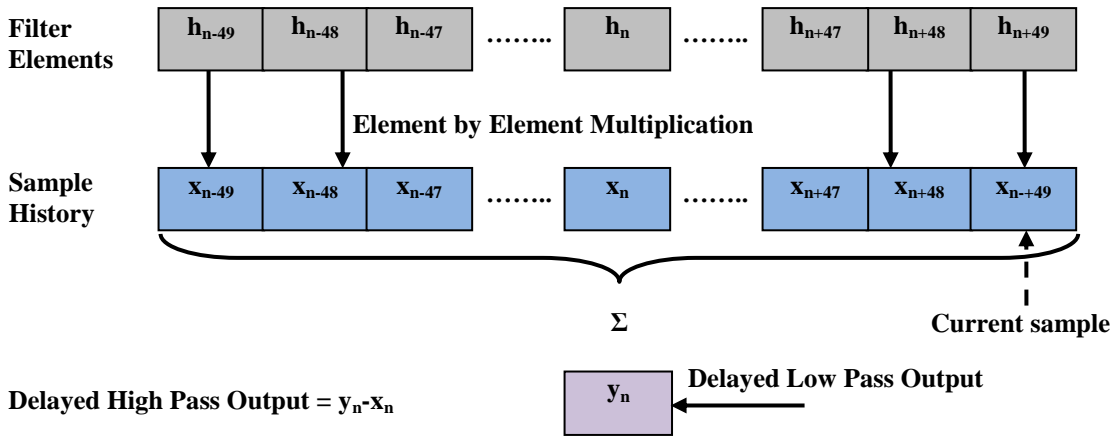


**Fig. 4.9(a)** The 99 sample Hamming Windowed FIR Filter. Each element of the sample history must be multiplied by the corresponding element of the filter and the multiplication results summed to give the filter output. Multiple filters could be applied concurrently and the outputs combined to generate high-pass, low-pass or band-pass signals as desired.

Fig. 4.9(a) shows a 99 sample Hamming Windowed FIR filter blocks. The 'filter element' in the figure is the filter coefficients calculated by using Hamming Windowed FIR techniques [104]. The sample history and current samples are the data streams of previous and after the desired sample of whose value is being changed by filtering ($x_n$ as shown in Fig. 4.9(a) for a typical filter). Each element of the sample history is multiplied by the corresponding element of the filter and the results summed to give the filter output.
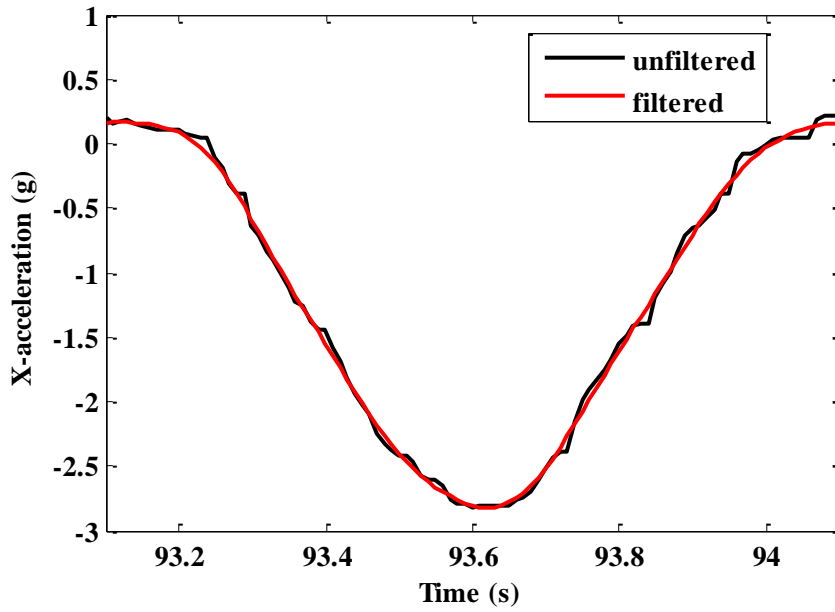


**Fig. 4.9(b)**      X-acceleration signals filtered (using Hamming Windowed FIR filter) and unfiltered as recorded in the sensor shown in Fig. 4.8(c).

Fig. 4.9(b) shows the filtered output of the X-acceleration signal as shown in Fig. 4.8(c) using a Hamming Windowed FIR low pass filter with a filter length 40 and cut off frequency 5 Hz. The algorithm used for the filter was developed in a signal processing tool box titled as 'ADAT' by the work by Wixted et al. [100]. The cut off frequency was chosen from the FFT analysis (discussed later) where 5 Hz is the dominant frequency component in the drive. It was suggested in ADAT that for an efficient filter (with minimal distortion of the wanted signal) the filter length should be at least three times of the ratio of the sample to cut off frequency. For Fig. 4.9(b)

four times of ratio of the signal to cut off frequency was chosen. As the signal recording frequency of the sensor is 100 Hz, the filter length was 40.

A comparison of the two signals in Fig. 4.9(b) reveals that after filtering the dither is removed and smoother signal resulted. However, as the low pass filter was used to remove the dither, the gravity signals and low frequency noise signals that are below 5 Hz remains. Researchers in sports monitoring of limb movement and implement suggested that sports movement and gravity are within 0 to 0.9 Hz (Wixted et al. [53]). Thus using a band pass filter of frequency range 0.9 to 5 Hz allows only the movement signal in the cricket ball-free bat swing to be extracted. The ball-contact signal has a much higher frequency (more than 5 Hz). This is discussed later.

A moving average is a simple digital filter that smoothes data by replacing each data point with the average of the neighbouring data points defined within the span. This process is equivalent to low pass filtering with the response of the smoothing given by equation (4.9):

$$y_i = \frac{1}{n} \sum_{j=-m}^{m} x(i+j)$$
$$i = m+1, m+2,............N-m$$

(4.9),

where $y_i$ is the smoothed value for the $i^{th}$ data point, $m$ and $n$ are the order of the filter and number of data within the span respectively, $N$ is total number of data points recorded in the experiment. For example, a second order ($m=2$) five point ($n=5$) moving average filter requires only two pre and post data points to produce smoothed acceleration ($y_i$). This filter works well for the statistical analysis, however, careful consideration about its frequency is required so that important information is not lost. To preserving and enhance the quality of the experimental data, the optimum cut off frequency selection is crucial. Equation (4.10) shows the relationship between sampling rate ($f_s$), cut off frequency ($f_c$) and order of the moving average ($m$) according to [99]:

$$m = 0.443 \frac{f_s}{f_c} \qquad\qquad (4.10).$$

According to the experimental requirements, the order, sampling frequency and cutoff frequency can be optimized by manipulating these variables. A weighted moving average method is an improved version of the simple moving average method defined as:

$$y_i = \frac{1}{W} \sum_{j=-m}^{m} w(j)x(i+j)$$
$$i = m+1, m+2, m+3, ..............N-m \qquad\qquad (4.11),$$
$$W = \sum_{j=-m}^{m} w(j)$$

$w(j)$ is called the coefficient of normalization and contains the time-weighted values for each element of the filter. The filter coefficients can be derived by performing an unweighted linear least-square fit using a polynomial of a given degree. The coefficient of weight vectors and the normalization are presented in Table 4.1 from second to sixth ordered weighed average smoothing method based on a polynomial approximation. This approximation is named the Savitzky-Golay (Savitzky et al. [105]) method and it follows these rules:

-The span must be odd.

-The polynomial degree must be less than the span.

-The data points are not required to have uniform spacing.

**Table 4.1** Coefficients ($w$ $(j)$) of Savitzky-Golay moving average smoothing for different filter orders ($m$):

| $m \backslash w(j)$ | -6 | -5 | -4 | -3 | -2 | -1 | 0 | 1 | 2 | 3 | 4 | 5 | 6 |
|---|---|---|---|---|---|---|---|---|---|---|---|---|---|
| 2 | | | | | -3 | 12 | 17 | 12 | -3 | | | | |

| | | | | | | | | | | | | |
|---|---|---|---|---|---|---|---|---|---|---|---|---|
| **3** | | | | -2 | 3 | 6 | 7 | 6 | 3 | -2 | | |
| **4** | | | -21 | 14 | 39 | 54 | 59 | 54 | 39 | 14 | -21 | |
| **5** | | -36 | 9 | 44 | 69 | 84 | 89 | 84 | 69 | 44 | 9 | -36 |
| **6** | -11 | 0 | 9 | 16 | 21 | 24 | 25 | 24 | 21 | 16 | 9 | 0 | -11 |

Fig. 4.9(c) shows the unfiltered and filtered signal using a sixth order weighted moving average filter as shown in Fig. 4.9(b) where a hamming windowed FIR filter was used. Comparing the root mean square error of the two filters (Fig. 4.9(b) & (c)) in relation to the raw data, it was found that the 6th order moving average filter was a closer representation to the raw data.
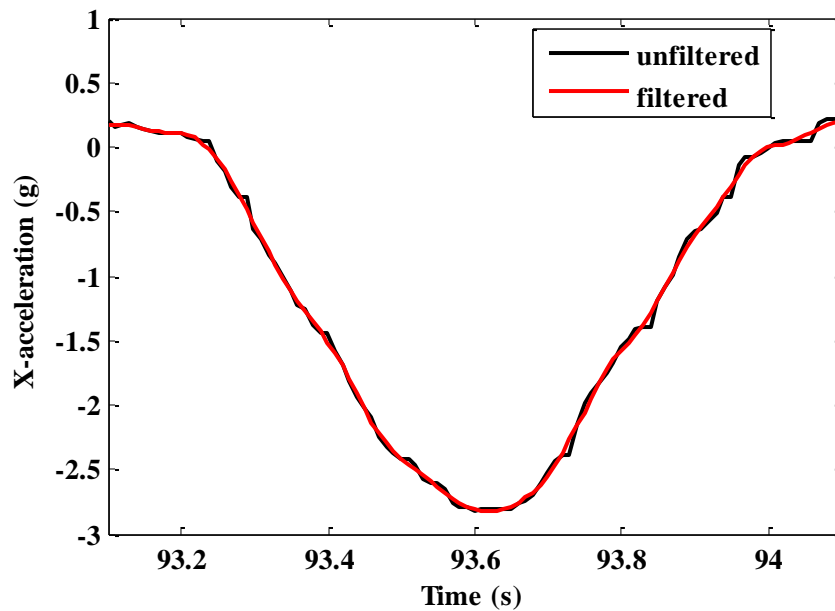


**Fig. 4.9(c)**     X-acceleration signals filtered (using Weighted Moving Average filter) and unfiltered as recorded in the sensor shown in Fig. 4.8(c).

### 4.1.2.2 Estimating orientation

As the inertial sensors respond to gravity, the orientation of these sensors in sports science is always estimated by the gravitational acceleration. It is desirable that the sensor is firmly attached to the athlete; otherwise there might be difference between

the actual orientation of the athlete and orientation of the sensors due to movements of bone and skin. Even though the sensors are firmly attached to the athlete limbs, the sensor orientation is an estimation of athlete's orientation with respect to gravity. In case of firmly attached sensors to the athlete's limbs and/or implement, an approximate orientation can be derived using the sensor data in a sport event where a slow orientation change happens.

*Reference Orientation*, *Stationary Orientation* and *Average Orientation* are three common types of orientation available in sport activities measurement. Depending upon the interest of the orientation of a limb and/or an implement, sometimes only one type or combination of these types of orientation is required.

*Stationary Orientation* can be estimated from the stationary or motionless period of an athlete using trigonometry. In the case of sensors attached to the back of the cricket bat's hitting surface (Fig. 4.4), the sensor vertical axis ($X^S$-axis) is aligned to bat's vertical axis but other two axes, mediolateral ($Y^S$-axis) and anterior-posterior ($Z^S$-axis, direction of bat movement) axes, differ from those of bat's axes as shown in Fig. 4.4. Correcting the alignment difference for these two axes by using equation 4.3, the acceleration signal referenced to bat axes can be obtained. In case of a stationary, purely vertical bat, the vertical acceleration vector will show approximately -1g. An example of the other stationary position of the bat attached sensor orientation vector is shown in Fig. 4.10. In the figure, the sensor (red circle) recorded accelerations are -0.8865g, 0.2136g and 0.4592g along vertical (V), mediolateral (ML) and anterior-posterior (AP) axis respectively. The resultant of these acceleration components is 1g shown by red colored vector in figure, which confirms the stationary orientation of the sensor. The resultant vector is tilted 27.56 degree out of vertical (black colored vector in the figure), 65 degrees forward (or back) of the mediolateral axis.

*Reference Orientation* is estimated by performing the calibration of the athlete/sensor combination from two or more stationary positions. In cricket a batter might be asked to stand upright and motionless to calibrate his/her forward leaning while in the

stance and initiation phase.
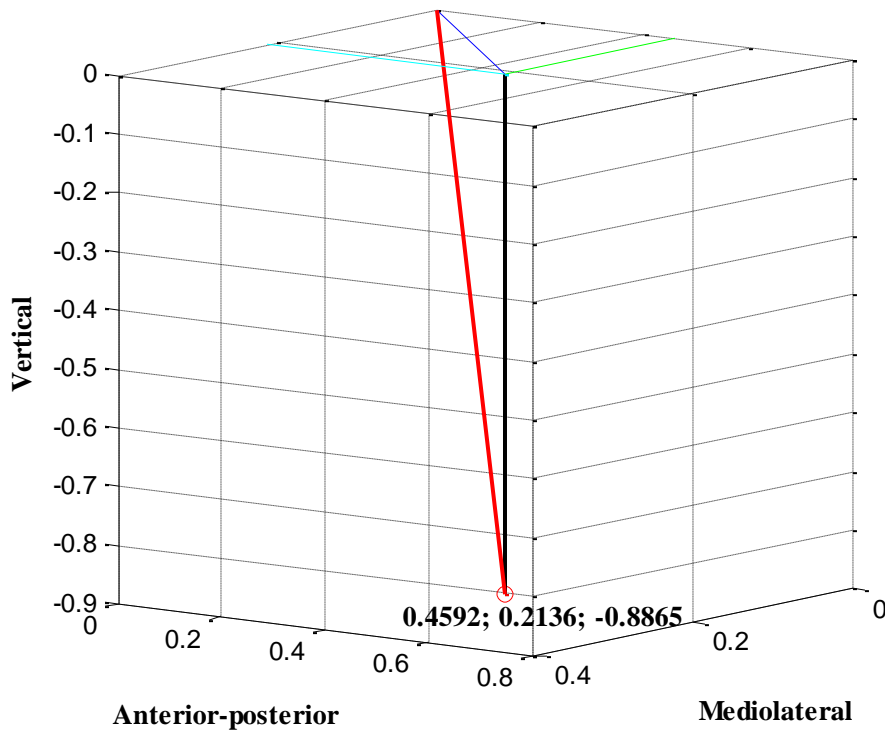


**Fig. 4.10** Extracting orientation of a stationary bat using an acceleration sensor attached to it.

The *Average Orientation* is the athlete's averaged position in relation to gravity during an activity. The average orientation will change according to the athlete activities and thus with the orientation of the athlete over time. During an athlete's activity the sensor signal will contain both the dynamic and static components of acceleration. The static component contains the gravity information that can be used to determine the average orientation. Using a low-pass filter with appropriate cut-off frequency, the gravity component of the sensor signal resulted can be extracted. The dominant activity and related frequency component will provide an idea about the frequency needed for the low-pass filter. The dominant frequency can be determined from the Fourier Transform (FT) of the sensor data (discussed in the next section). According to the literature, a low-pass filter with a 0.9 Hz cut-off frequency is typically used to extract the average orientation from the sensor signal during an

activity of an athlete ([74], [53]). In cricket where the straight drive bat swings out of plane (mediolateral axis-Y) the dominant frequency is about 4 Hz (shown in the next section by using FT). Therefore according to [100] and using an approximation that mediolateral axis acceleration contains only gravity at half of its dominant frequency, then 2 Hz cut-off frequency is enough to extract the average sensor orientation during a drive. However, it is important to note that changing the filter frequency will affect the orientation signal and lead to a different orientation result. For instance, an increased filter cut-off frequency will result a leakage of activity signal into the orientation signal. On the other hand, reduced filter frequency will results in a signal that does not contain the information about fast orientation changes [100].
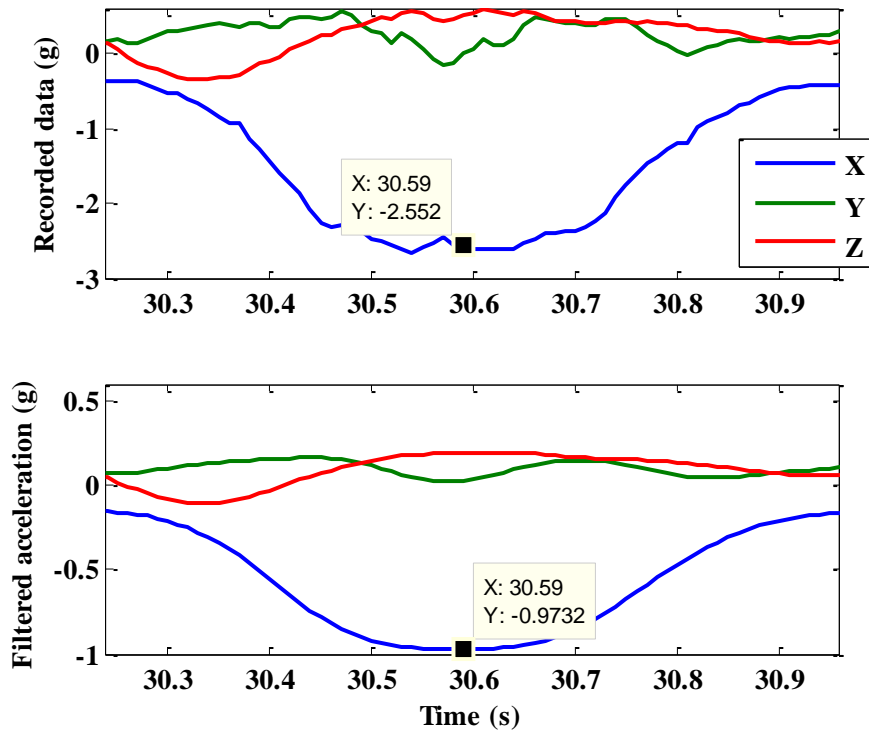


**Fig. 4.11(a)**    Average orientation of the bat during straight drive from filtered acceleration data. The upper figure shows the acceleration during the swing and lower shows the low pass filtered signal ( Hamming window filter of window length 18 with a cut-off frequency of 2 Hz) to extract the gravity component. The order of the filter was estimated using equation 4.10.

Fig. 4.11(a) shows the sensor recorded acceleration signals during a ball-free straight drive by a novice together with the low-pass filtered signal (Hamming windowed filter of window length 18 with a cut-off frequency of 2 Hz). From the figure it is observed that the filtered vertical axis signal (X-axis acceleration) has a maximum amplitude when the recorded signal is maximum. As the filtered signal shows the gravity component in the recorded signal, it is noted that the recorded signal has maximum amplitude while the vertical axis (X-axis) is almost aligned to gravity at time 30.59s. This orientation of the vertical axis was confirmed from the video footage of the bat posture (see Chapter 5). This is also evident from Fig. 4.11(b) that the magnitude of filtered acceleration is equal to gravity (acceleration=1g) at the vertical orientation of the bat.
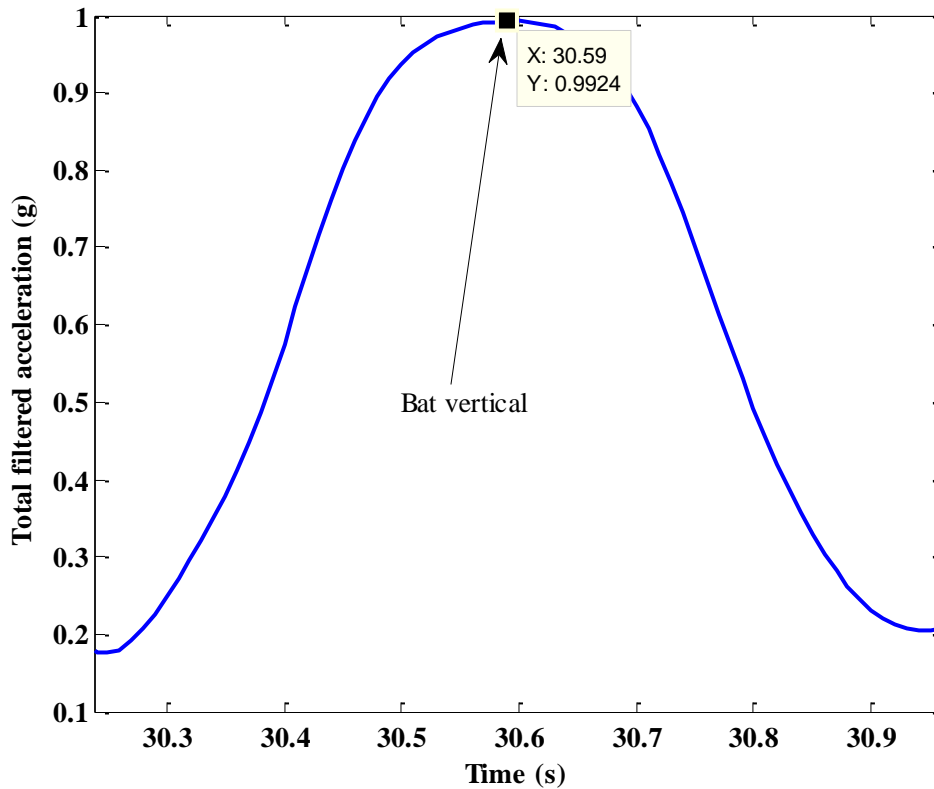


**Fig. 4.11(b)**  Magnitude of total acceleration of the filtered signal shown in Fig. 4.11(a). The average orientation of the magnitude vector with respect to gravity direction can be extracted by using the values in the profile of this figure together with those of the lower part of Fig. 4.11(a) using geometry referring to Fig. 4.10.

FT is a useful tool to determine the frequency components of an activity of athletes. Determining the FT can provide the power spectral density about a particular key signature of a sports activity. For instance, the sensor recorded data can be used to estimate the energy expenditure of an athlete generating a signal power vs. time function similar to the signal power vs. frequency generated by the FT [100]. These techniques have shown a high correlation with human energy expenditure [74]. When the square of the magnitude of the FT of sensor data (in magnitude) is used, the resultant graph is a Power Spectral Density. This is analogous to the time-domain power spectral density and could be referred to as the Power Temporal Density [100].
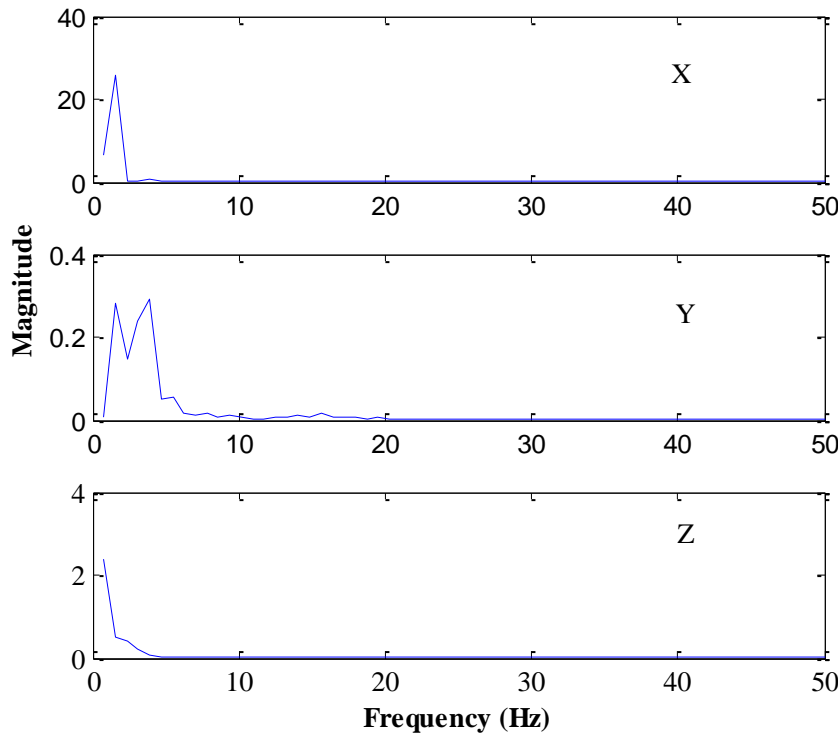


**Fig. 4.12(a)**     FT of the sensor recorded swing data shown in Fig. 4.11(a).  ADAT tool box devised by James et al., 2011 in [106] was used to calculated FT having a data length window 128 starting at the first data in Fig. 4.11(a).

However, the Power Temporal Density estimated in this technique is not scaled. The magnitude commonly referred to as 'counts' is sufficient to provide the gross

information about the energy expenditure during a movement..Fig. 4.12(a) shows the FT of the sensor recorded swing data as shown in Fig. 4.11(a). By using ADAT tool box [106] the FT was calculated using 128 data length window starting at first data shown in Fig. 4.11(a). It is observed from Fig. 4.12(a) that the mediolateral axis (Y) dominant frequency is about 4 Hz, where the vertical axis frequency is 1.56 Hz that is double of the anterior-posterior axis (Z) dominant frequency (0.78 Hz).
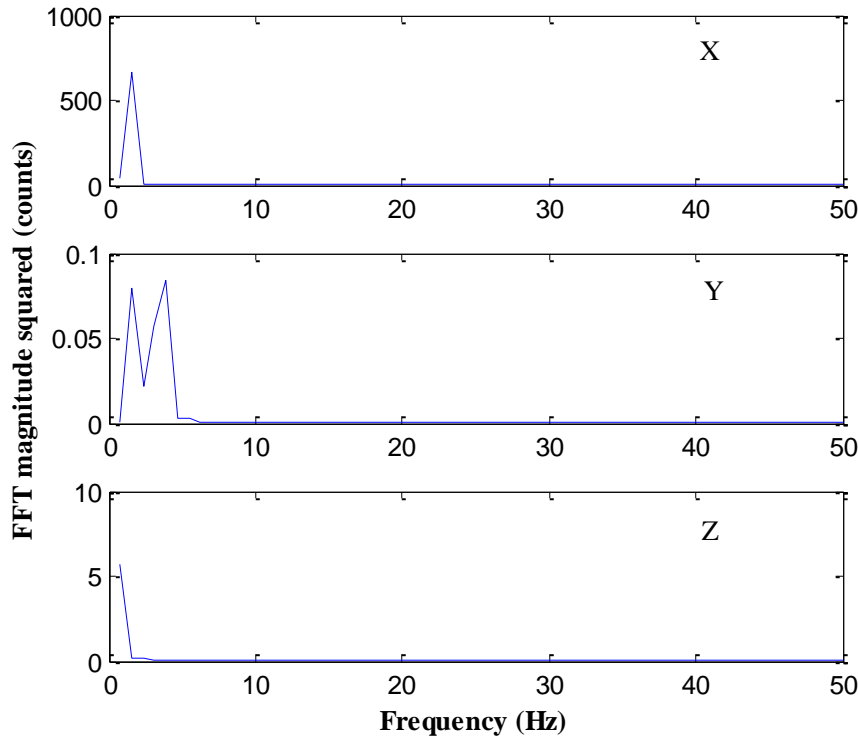


**Fig. 4.12(b)**    Power Spectral Density of the signal shown in Fig. 4.11(a) using the square of the magnitude of the FFT data shown in Fig. 4.12(a).

The Power Spectral Density of the signal shown in Fig. 4.11(a) for each axis is shown in Fig. 4.12(b). The Power Spectral Density was estimated taking square of the magnitude of the signal shown in Fig. 4.12(a) for each axis and is plotted against frequency. These signals are analogous to the Power Temporal Density of each axis in time-domain. The energy expenditure during an athletic event can be obtained by taking FT of the magnitude of sensor recorded X-, Y- and Z-axis acceleration with

removed gravity (1g) and then calculating the Power Temporal Density [100].

It is observed from Fig. 4.12 that using only the FT of the signal could provide the power spectral density shape. Although FT is a useful tool for producing power spectral, there are some limitations that must be considered. For instance, in short bursts of activity or longer-term variable frequency activity, the FT is not an accurate frequency estimator [100].

### *4.1.2.4 Numerical integration for velocity and displacement*

Accelerometer outputs can be numerically integrated to obtain the velocity. Likewise, the velocity can be further integrated to determine displacement. But the calculated velocity and displacement data might be very erroneous if precautions are not taken.
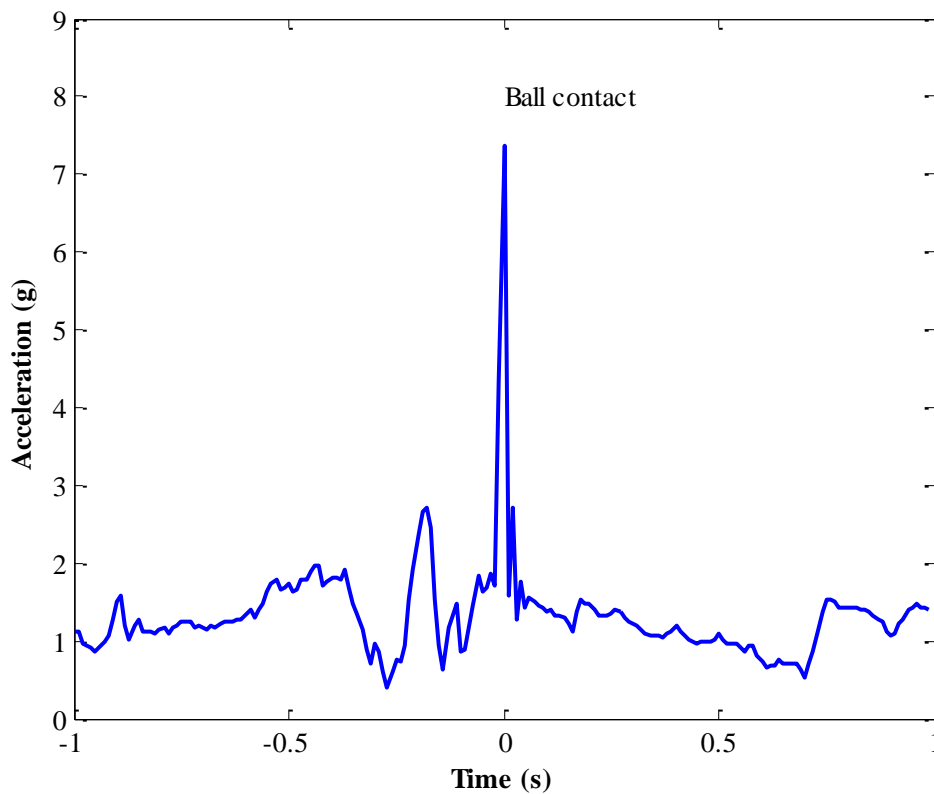


**Fig. 4.13(a)** A typical acceleration profile of a defensive stroke recorded using a wrist attached sensor The zero time is showing the ball-contact moment and also evident from the large spike in the acceleration data.

The errors originate from several of sources, first of all, from low frequency signal components. While in the recorded data the low frequency signal (for instance, the gravity and/or little movement of the sensors itself while not attached firmly) components are present in the athletic activity related dominant frequency, the output of the numerical integration of the whole signal will be encountered with a cumulative error from the low frequency components through the integration of a constant. This can be identified as an accumulation in velocity with time.
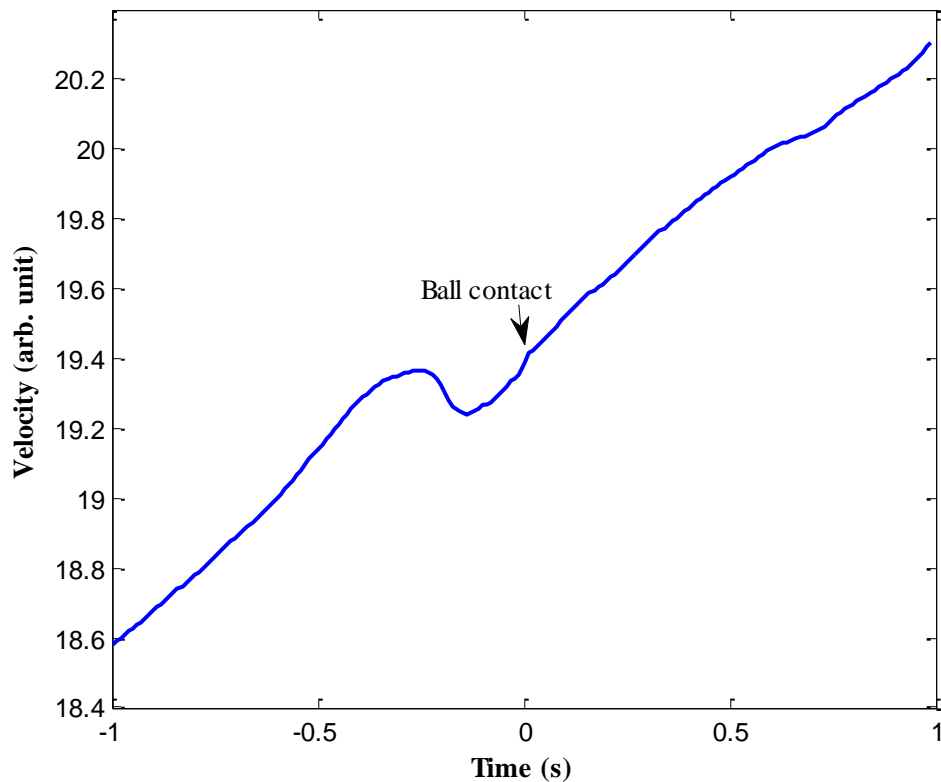


**Fig. 4.13(b)**     Velocity profile obtained by directly integrating the profile shown in Fig. 4.13(a) without separating out the low frequency signal components. The profile suffers from a cumulative error so that it increases with time over the entire time duration.

It is essential to separate the low frequency signal from the dynamic signal by filtering. Even though the low frequency components can be removed before integrating the acceleration data, the velocity signal is still subject to cumulative error with the magnitude of the offset changing over time [100]. Then it is necessary to

high-pass filter the velocity data again. After integrating the velocity data to extract the displacement, the integrated data again needs to be high-pass filtered. In fact, high-pass filtering the signal is necessary at each stage. Without filtering integration using trapezoidal formulae gives Fig. 4.13(b). The erroneous signal results in the velocity increasing continuously. By filtering out the low-frequency signal using a high-pass filter of cut off frequency 1 Hz before integration, (the filter frequency was chosen from the FT of the profile shown in Fig. 4.13(a)) gives Fig. 4.13(c). The velocity profile shows a peak at time zero corresponding to ball-contact, which reflects the dynamics of the stroke.
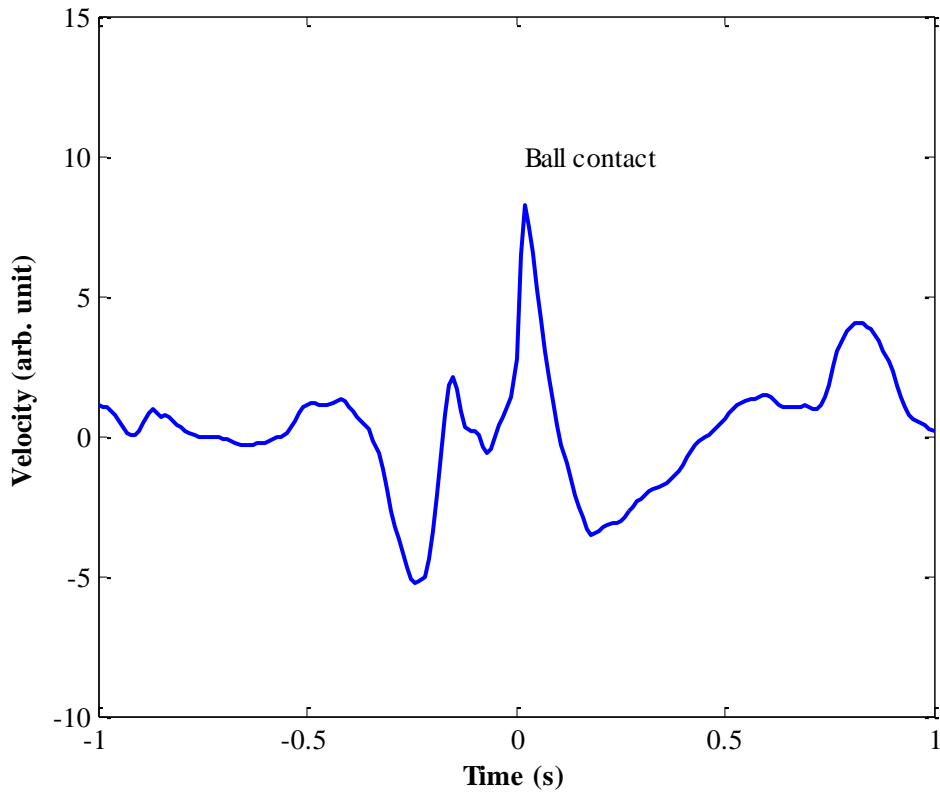


**Fig. 4.13(c)**    Velocity profile obtained by integrating the high-pass filtered signal from the profile shown in Fig. 4.13(a). A high pass-filter of cut off frequency 1 Hz was chosen to minimize the low frequency signal components. Trapezoidal integration function was used from matlab software.

The bat-ball contact corresponds to the peak in the velocity profile is clearly noticeable. The velocity units shown in the Fig. 4.13(c) are arbitrary because the

integration constant is chosen as zero so the profile does not show the true value but the shape only. To overcome the error in the velocity profile the profile needs to be passed through a high-pass filter. Similarly, in estimating the distance profile from the velocity data, after the integration of the data high-pass filtering is needed.

### *4.1.2.5 Auto-correlation of sensor recorded data*

Auto-correlation is a useful mathematical tool for extracting repeated patterns of a signal obscured by noise or detecting relationships in apparently random signals. It is a useful technique for identifying the missing fundamental frequency in a signal implied by its harmonic frequencies. In sports where an athlete engaged in a regular repetitive activity, the accelerometer recorded signal sometimes appears as a regular signal with considerable noise. Then the use of auto-correlation might be helpful to identify some key parameters from the noise. It is primarily used for people with injuries as a method of comparing data from various step frequencies and speeds. Auto-correlation describes the correlation of the values of the process at different times as a function of the time difference. In cricket batting, a measure of bat swing consistency can be assessed at template and auto-correlation. Whether same swing profile is produced by that batter at different times within the same batting environment (same type of bowl, bowling speed, length etc.) could be judged using auto-correlation on acceleration data.

### 4.1.3 Validation processes

Acceleration data can be validated using the existing video and opto-reflective based methodology. After capturing any motion, the video footage sometimes needs to be converted into two-dimensional or sometimes three-dimensional coordinate planes by software. Those calculations output the coordinate's values as measure of distance in terms of unit pixel size. Sometimes the conversion is not needed, for instance, in case of opto-reflective marker based system the data can be available in terms of distance directly in six degree of freedom (3 streams of data presenting the rotation about each of the Euler axes, and another 3 streams representing the translation about the Euler axis). The video extracted points can be used to calculate the acceleration

using the mathematics and movement dynamics of the body (say rigid body rotation dynamics). The method of extracting the movement signature using the video extracted points is detailed in the 'Analysis' section of this chapter. Not only is validation but also a solid reference for the time sequence of a movement event for the sensor data becomes available. First, the video based validation tools are discussed. The video calibration is achieved in three steps.

### 4.1.3.1 Video calibration and event captured

The first of three steps is to synchronize the sensor data and video record. This procedure includes the calculation of the video frame rate and identifying a start point which is clearly visible and simultaneously detectable in the sensor data. The average frame rate is calculated by dividing the total frames in a clip by the total time of that clip as follows:



**Fig. 4.14**    Vertical bat tapping to synchronize the time between sensor profile and video footage event. Left part of the figure shows the lifting bat from ground and right shows the impact on ground that produced a large spike as shown in right part of Fig. 4.15 at 56.73 second.

$$\text{Frame rate} = (\frac{\text{frame}}{\text{sec}}) = \frac{\text{Total frames}}{\text{Total clip time}} (\frac{F}{s}) \qquad (4.12).$$

To identify a starting event of the video footage in the sensor data, say recorded in bat attached sensor, the bat is first impacted vertically to the ground. This is illustrated in the right part of Fig. 4.14 (the left part of Fig. 4.14 shows the lift of bat

156

from ground). This is called vertical bat tapping and it causes high frequency vibration of the bat which is easily identified by the large spike in the sensor's gravity aligned axis data (X-axis acceleration for the typical sensor used in this research) as shown in the right part of Fig. 4.15 at 56.73 seconds. From this bat tapping the impact frame in the video footage and impact time in the sensor are determined. This information and frame rate facilitates the synchronization of events between the video and sensor data per

$$\text{Event Frame} = \text{Impact frame} + (t_e - t_{impact})\text{Frame rate} \qquad (4.13).$$

Here the time when an event occurs in the sensor data are denoted as $t_e$ and $t_{impact}$ is the time at which the large spike occurs.

Fig. 4.15 shows an example of synchronization of an event in the video footage with the sensor data as a sequence from Fig. 4.14. The data for this example were recorded in the bat mounted sensor from a ball-free defensive stroke bat swing. The objective
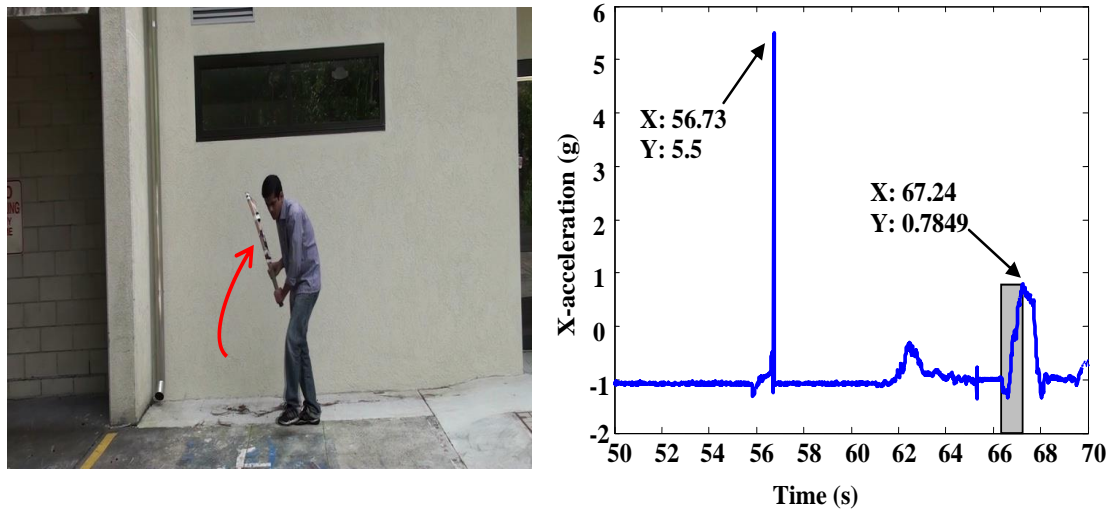


**Fig. 4.15**    Video footage (left) of the end of back-lift in a typical defensive stroke bat swing and part of the corresponding acceleration profiles of the stroke (right) showing the back-lifting event (shown by gray bar) and large spike (at 56.73 second) from bat tapping as right part of Fig. 4.14.

was to identify the position of the bat at the end of back-lift using sensor data. In the

sensor data (right part of the Fig. 4.15) the large spike at 56.73s denotes the bat tapping that happened at frame 138 in the video. From the video, the end of back-lift occurred at frame 664. Then the value of $t_{impact}$, Impact frame, and Event Frame are 56.73s, 138, and 664 respectively. A total of 16322 frames were recorded in 326s (only three frames and part of the acceleration data are shown in Fig. 4.14 and 4.15), so using equation 4.12 the Frame rate of the video was 50.0675 F/s (originally the camera frequency was 25 Hz, and each frame was separated into two interlaced frames using software to operate the camera at high frequency for reducing blurring effect). The time at which back-lift occurred was found to be 67.23s calculated using equation 4.13. So the peak at 67.24s (as shown in Fig. 4.15) in the sensor data occurred at the position of the bat at end of the back-lift with considering a tolerance of 0.01s. In the similar way, the start of the back-lift was at 66.39s as shown in Fig. 4.15 corresponding to video frame 622. The time duration and associated sensor profiles for the back-lift are shown in Fig. 4.15 by the vertical gray bar.

To get the distance in two-dimension or three-dimension coordinates from the video footage, it is necessary to convert pixels to the dimensions of length. This can be done by viewing an object of known length in the video. In this research, the reference length used was the edges of the cricket bat. The calibration was done in both the horizontal and vertical directions to account for any differences caused by the camera lens. In the two dimensional video footage (converted from three dimensional to two by software), for instance, the total number of pixels forming the image bat length along one dimension (horizontal or vertical) were counted, then the scale factors ($SF_V$ for vertical and $SF_H$ for horizontal) for pixel-to-millimeter were calculated using the linear scaling factor:

$$SF_V = \frac{Bat\ length\ (mm)}{Pixels_V}, SF_H = \frac{Bat\ length\ (mm)}{Pixels_H} \tag{4.14}.$$

Here $Pixels_V$ and $Pixels_H$ are total number of pixels forming the bat length in vertical and horizontal direction in the two dimensional video footage. In this

research the real bat length was 850 mm and the bat length in pixels in vertical and horizontal direction of a typical video footage shown in left of Fig. 4.15 were 283 and 298 respectively. The values of $SF_V$ and $SF_H$ were 3.00 mm and 2.85 mm respectively. Once the coordinates of two points in the video footage are known in terms of pixels, the length between those two points or the slope with respect to the vertical reference in the video was calculated by converting the pixels to millimeters using the scale factors.

The third step in calibration is needed to measure the misalignment of the camera's vertical axis from the true vertical. The stationary sensor accurately measures its orientation with respect to gravity, for instance, as in Fig. 4.5(a) the angle between sensor's $k_f$ and world's coordinate axis $K$ as $\varphi$ could be measured from the acceleration data recorded along sensor's $k_f$ axis. If the camera's vertical axis were aligned correctly with true vertical then the same angles should result from the measurement of the slope of the two points (say P1 and P2) along the bat image in the video using the following relationship:

$$P1 = \begin{bmatrix} h_1 \\ v_1 \end{bmatrix} pixels, \quad P2 = \begin{bmatrix} h_2 \\ v_2 \end{bmatrix} pixels$$
$$\Delta h = (h_2 - h_1)SF_H, \quad \Delta v = (v_2 - v_1)SF_V \qquad (4.15).$$
$$\varphi_{video} = \tan^{-1}(\frac{\Delta v}{\Delta h})$$

However, the misalignment of the camera vertical axis (if any) is known from the difference between the $\varphi$ and $\varphi_{video}$.

The video camera used to conduct the studies in this thesis was placed at a height of 1.4 m from the ground and 5 m lateral from the batting arc to make full trajectory of the bat swing visible.

**Fig. 4.16**   Still image showing the drive capture set up for opto-reflective method by optitrack motion capture system. Two of the four camera stands are visible in the picture; other two are placed in other two corners of the square space. The system composed of eight cameras in which each stand holds two.

The Opto-reflective method is one of the motion capture systems allowing the recording of motion by tracking a number of marker points in space. Those points are translated into a 3 dimensional digital representation. Each captured point represents the instant location of a point on a moving rigid body with six degrees of freedom, that is, each point has 6 streams of numerical data representing the position of the point in free space at any instant. These data consists of three translational and three rotational components from the 3 dimensional axes. The subject must be located in the detection volume, with the key points positioned on the object such that they best represent the orientations of the moving parts. For example the joints or pivot points might be tagged. In order to accurately triangulate the marker positions at least 4 cameras are used, however generally no more than 32 are used. Fig. 4.16 shows the

camera opto-reflective system used to capture a batter's cricket shot. The system comprised of 4 camera stands with 2 cameras attached to each stand. Note that only 2 camera stands are shown in Fig. 4.16. In the figure the batter is in the stance phase of the shot. The reflective markers are placed on the bat and the participant's limbs. For instance, in Fig. 4.16, three markers (formed as triangle) are placed on each wrist of the batter, and three markers in the back of the bat (two at center of mass in two edges and one at the end in the center line of the bat). To describe the process involved in reading and processing motion capture data, some **terminology** and **notational style** are used in Motion Capture (**MOCAP**) system [107]. The details of these terms and reading and processing of MOCAP data are documented in appendix A.

## 4.2   Analysis method

Considering the similarity with other swing sports like golf swing and baseball bat swing, the method of analysing cricket bat swing can be developed from the literature in those sports. The relevant analysis of the pendulum with moving pivot, inverted pendulum and double pendulum with their modified versions applicable to cricket are stated in the results section. The pendulum parameters were linked with the sensor recorded data to parameterize the bat swing to extract key features. Considering the cricket bat as a perfectly rigid body (neglecting the elasticity) the bat swing dynamics is derived using rigid body dynamics to compare the results from sensor recorded data. Using rigid body rotational dynamics the total acceleration $\bar{a}$ for gravity, rotation and translation is calculated from the following equation:

$$\bar{a} = \frac{d^2\bar{r}}{dt^2} - \bar{g} + \frac{d\bar{\omega}}{dt} \times \bar{l} + \bar{\omega} \times (\bar{\omega} \times \bar{l}) \tag{4.16},$$

(Ohta et al. [54]) where $\bar{r}$ is the position of the origin of the segment coordinate system from the reference coordinate system, $\bar{g}$ is the gravitational acceleration vector and $\bar{l}$ is the length of the body.

In different phases of the bat swing for different cricket strokes, the analysis and the derivation of associated dynamics depends on the style of the batters. So, to derive the equations of batting dynamics, the constraints associated in each phase of real batting are applied in the general theory of pendulums. Those constraints originate from the general movement of the composite system of bat and limbs.

Statistical analyses were conducted on the results obtained from the sensor data to measure the strength of a relationship. The Chi square test, ANOVA (analysis of variance), MANOVA (multivariate analysis of variance), ANCOVA (analysis of covariance), MANCOVA (multivariate analysis of covariance) test, Tukey pairwise mean comparison, Post-hoc Tukey, Tukey HSD, Greenhouse-Geisser adjustment/correction analysis, Pearson product-moment correlation coefficient tests, Bonferroni correlation, are the popular statistical analyses used in cricket research. In this thesis the correlation method, least square fitting and Bland Altman ANCOVA method were used in the statistical analysis.

# 5 <u>RESULTS AND DISCUSSIONS</u>

This chapter includes several studies conducted for this thesis. Each study is presented with several sections named as background (originated from and referred to the 'literature review' chapter), experimental procedure (referred to 'methodology and analysis' chapter), results and discussion (the sole findings from the study), and conclusions. First of all, the study on a pendulum swing using the sensors is presented. Attaching the sensor to a wooden pendulum, its static and dynamic position during the swing was analysed. The angular position of both static and dynamic sensor was compared with those from inclinometer readings and pendulum equation. For matching the dynamic profiles with those from pendulum equation, the constants associated in the equation were estimated by the Fast Fourier Transform (FFT) of the sensor recorded profile and the initial conditions. In second part of this pendulum study, hits on the pivot arm were distinguished using acceleration values. The investigation was to get an idea about the optimal contact location for maximum the energy transfer to the ball. In next study, using state vector equation approach, the nonlinear equation of a pendulum with moving pivot was solved and then the bat angle during a straight drive was modeled. The equation derived angle profile and those estimated from the sensor recorded data was compared. The effects of various parameters (the initial angular velocity, the radius of rotation, and the pivot phase angle) on bat length aligned acceleration profiles during the bat swing were investigated for quantification of the level of maximum force applied by the batter.

In next study, the results from consecutive and repetitive bat swing in straight drive were included to identify the temporal and spatial posture of bat. The results were validated by theory and video. This study was conducted to assess the competency and consistency of a batter by using sensor data. Next, 61 bat-ball contacts in defensive strokes were assessed by bat and wrists mounted sensors recorded data. This study was conducted to categorize the sweet-spot hits by the sensors data. The next study was about the bat angle and the applied force in a straight drive by several batters. In this work, an approximate equation for the bat angle as a function of time during the straight derived was compared with the video derived angles. The bat

length aligned acceleration profile was derived from the equation and compared with sensor recorded profiles for matching. The angles at the end of a drive were also correlated with the acceleration peaks from 63 swings by seven amateur batters in this study. Bland Altman covariance correlation approach was used to find the correlation between the angles and acceleration peaks individually for each batter and among the batters. The term 'forcefulness' of batting in the literature is quite indistinct, and then the results from this study were attempted to define it clearly by measuring the level of force applied by the batter. The next study was conducted on the defensive stroke to investigate the effect of back-lift height on bat orientation during ball contact by sensor recorded data. On and off defensive strokes were also discriminated using total acceleration (the vector sum of the measurements from a tri-axial accelerometer) recorded in bat mounted sensor in this study. The following study was to validate the sensor recorded data with the video derived data in an orthodox straight drive using rigid body dynamics. A decision matrix was formulated from the bat posture to estimate the appropriate acceleration terms (static/translational/dynamic) for the video derived acceleration profiles. This matrix and rigid body dynamics were used to match the video revealed results with that recorded by the sensor. The key parameters for maximising the drive and the control force in the straight drive were derived while matching the results from the two systems. The last study reported in this chapter was on the defensive stroke to determine the relation between bat and wrists accelerations to judge the differences how two hands are coupled with the bat before and after ball-contact. Five batters' defensive strokes acceleration were recorded in bat and wrists mounted sensors. The difference between top and bottom hand in experienced batters were compared with the non-experienced. The correlation between bat and wrists velocities were outlined for all batters' data.

## 5.1 Pendulum swing results and insights for bat swing parameterizations

There are still challenges in using sensors in terms of measurement reference results, calibration error, skin artifacts when attached to human skin, and drifting or offset error when integrating the acceleration to derive velocity related parameters [108]. Attaching a triaxial accelerometer sensor to a rigid wooden pendulum the tilted and deflection angles during stationary and swing position of the pivot arm was investigated. The investigation was extended to identify the hit locations (upper part, middle and lower part) of the suspended wooden pendulum arm with the accelerometer attached at its centre. The idea for the first study was to observe the deviation of the sensor signals from the equation derived pendulum swing profile and comment on the possible sensor errors. The wooden pendulum is not friction less. The static position of the pendulum at different steps was measured using the sensor output and compared with inclinometer readings. The correlation between the sensors results and those from equation and inclinometer were calculated and the correction was attempted. The idea behind the second part of this study was to identify the middle, bottom and top hits on the pendulum arm from the sensor. The literature has described the sweet spot as the location where a hit results in minimum values of the acceleration of the hand and maximum energy transfer to the ball [88]. The hits on the wooden pendulum arm were used to explore ideas suggested in the literature. This study was conducted as ground work for seeking the swing parameters and impact locations. An attempt was made to minimize the bias error, however the non-uniformity in the out of plane movement was not considered.

### 5.1.1 Background

The background of this study stated in section 2.7 of the literature review chapter. As stated in that section that relative levels of sensors recorded signal could be useful to extract the key signatures of sporting activities, and also the errors accompanying with the signals could be minimized or bypassed by effective signal processing techniques (for instance, calibrating the sensors, filtering the signals etc.).

### 5.1.2 Experimental Procedure

One of the accelerometer sensors shown in Fig. 4.1 in Section 4.1.1.1 capable of measuring 6g was attached by tape to the swing arm of the wooden pendulum as shown in Fig. 5.1.
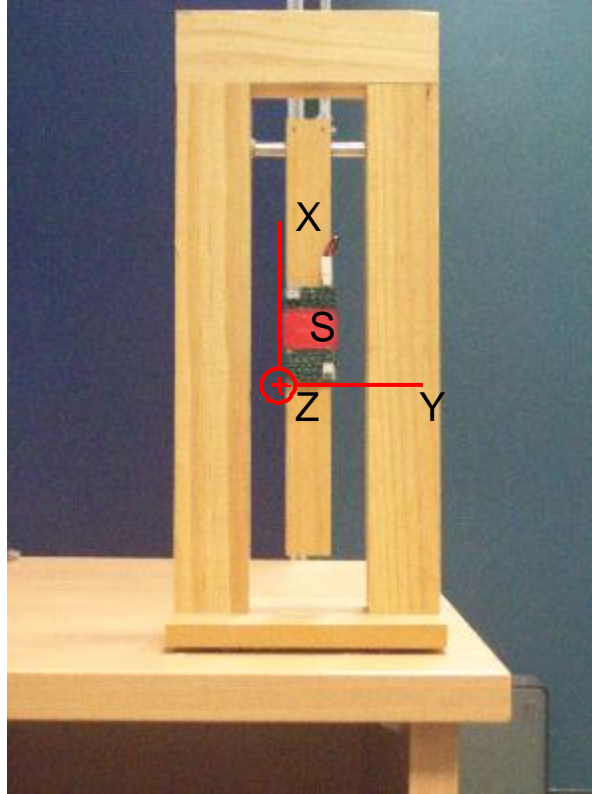


**Fig. 5.1**   Sensor (S) attached wooden pendulum and definition of sensor's axes. The centre wooden part is free to rotate about a horizontal axis (metal rod).

The sensors axes (X, Y, and Z) are shown in the Fig. 5.1 and the swing of the pendulum was along the Z-axis direction in the ZX plane (perpendicular to the ground YZ-plane). The pendulum was oriented at a fixed angle to the vertical and released. The subsequent oscillations were recorded using the accelerometer. The swing arm was initially stationary at different angle steps (-3º, 0º, 6º, 9º, 25º, 45º, 75º, 90º) measured by an inclinometer (vertical axis reference). The arm was oriented so that the sensor Z-axis was in the same direction as gravity (opposite to positive swing direction) before allowing the pendulum to swing freely. The negative angle for first

166

step was due to the fact that the swing arm was not precisely vertical at rest. At the last step (90º) with sensor Z-axis aligned with gravity, the swing arm was released for free swing. The X-, Y- and Z-axis acceleration data were recorded during the first part of the experiment. In the second part three hits were made on the stationary pivot arm at approximately the middle (where the sensor was placed), bottom and top on the back of the arm (opposite side of the sensor placement).

### 5.1.3 Results and discussion

Fig. 5.2 shows the X-, Y- and Z-axis acceleration profiles ($A_x$, $A_y$, and $A_z$) from the static experiment. The magnitude of the average acceleration of each of $A_x$ and $A_z$ during each step was used to calculate the tilted angles $\theta_x$ and $\theta_z$ using cosine and sine function respectively. The angles shown in Fig. 5.2 were measured by the inclinometer.
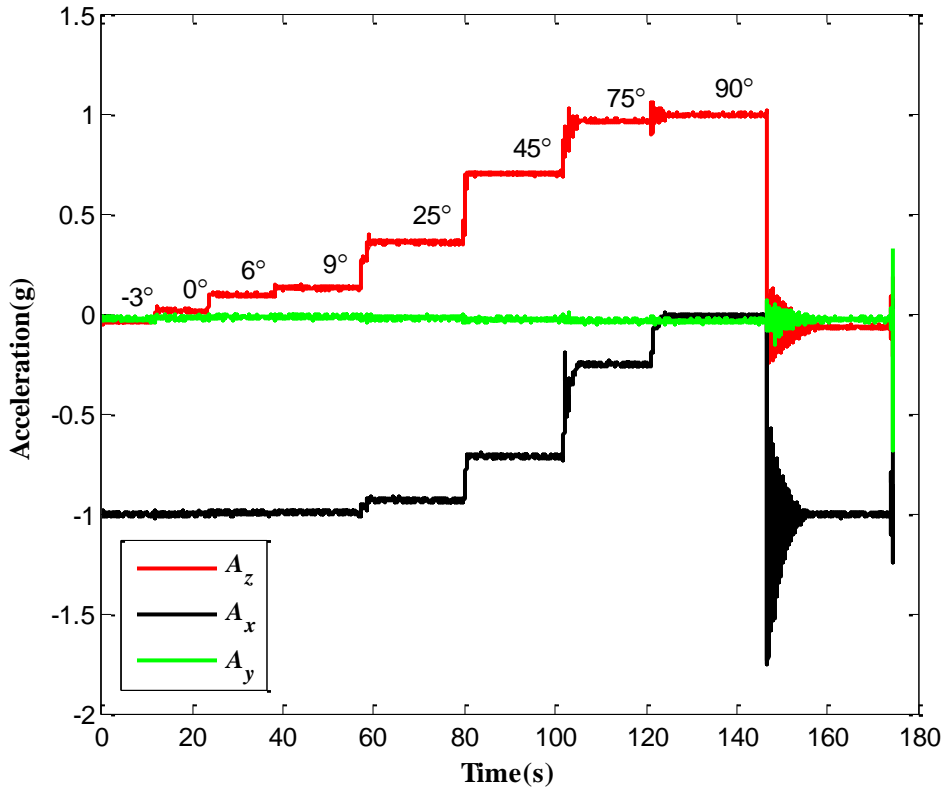


**Fig. 5.2**    Sensor recorded acceleration in tilted and swing position of the wooden pivot arm. The tilted angles in each step were measured by inclinometer.

167

The Table 5.1 shows the value of the angles measured by inclinometer ($\theta_I$) and accelerometer ($\theta_x$, $\theta_z$ using X-axis and Z-axis acceleration respectively) using the

**Table 5.1** Accelerometer and inclinometer measured angles during tilted positions of the pivot arm.

|  | Step-1 | Step-2 | Step-3 | Step-4 | Step-5 | Step-6 | Step-7 | Step-8 |
|---|---|---|---|---|---|---|---|---|
| $\theta_I$ (degree) | -3 | 0 | 6 | 9 | 25 | 45 | 75 | 90 |
| $\theta_X$ (degree) | 0 | 0 | 3.35 | 6.31 | 20.94 | 44.38 | 75.29 | 89.19 |
| $\theta_Z$ (degree) | 2.32 | 0.86 | 5.32 | 7.37 | 20.86 | 44.32 | 74.27 | 83.52 |

data shown in Fig. 5.2 in the tilted position of the pivot arm. To assess the strength of the relationship between inclinometer measured angles and those measured by accelerometer, $\theta_X$, and $\theta_Z$ were plotted against $\theta_I$ shown in Fig. 5.3.
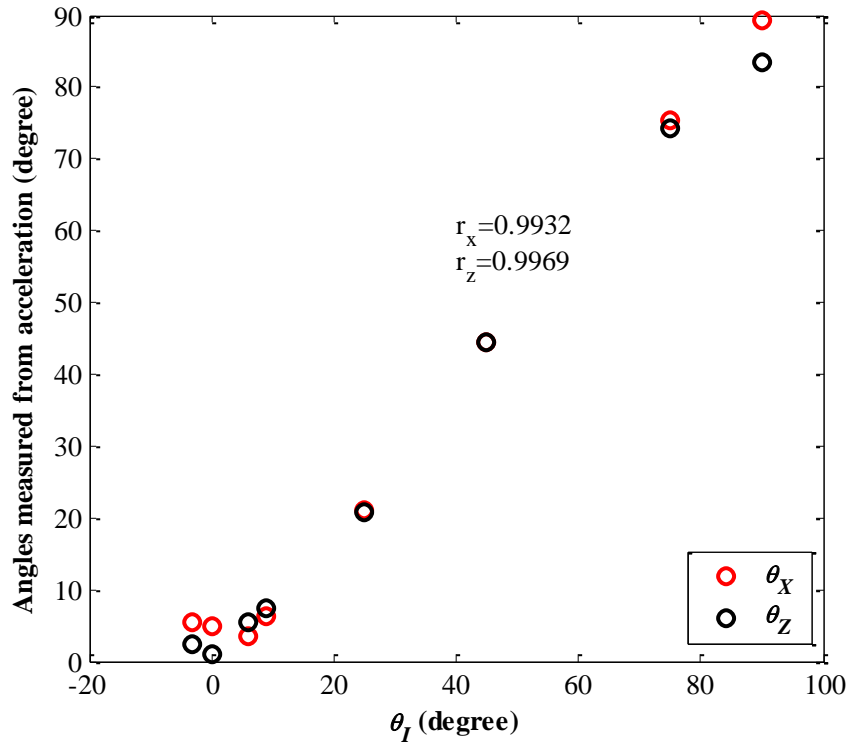


**Fig. 5.3** Inclinometer measured angles ($\theta_I$) versus those measured from acceleration data ($\theta_X$ from X-axis acceleration, $\theta_Z$ from Z-axis acceleration) for stationary tilted arm. The correlation coefficients shown in the figure as $r_x$ and $r_z$ are between $\theta_I$ and $\theta_X$ and between $\theta_I$ and $\theta_Z$ respectively.

A strong linear relationship between $\theta_I$ and $\theta_X$ ($r_x$=0.9932, $p$<0.0001) and between $\theta_I$ and $\theta_Z$ ($r_z$=0.9969, $p$<0.0001) was obtained. However, the relationship was checked within 0° to 90°, but it is noted that at the start (around 0°) and end (around 90°) of the plot in Fig. 5.3 the data diverts slightly from the linear relationship. This tendency indicates that if the measured range could be extended the profile would exhibit some degree of the nonlinearity resulting from the sensor sensitivity error as evident in Fig. 4.8(e).
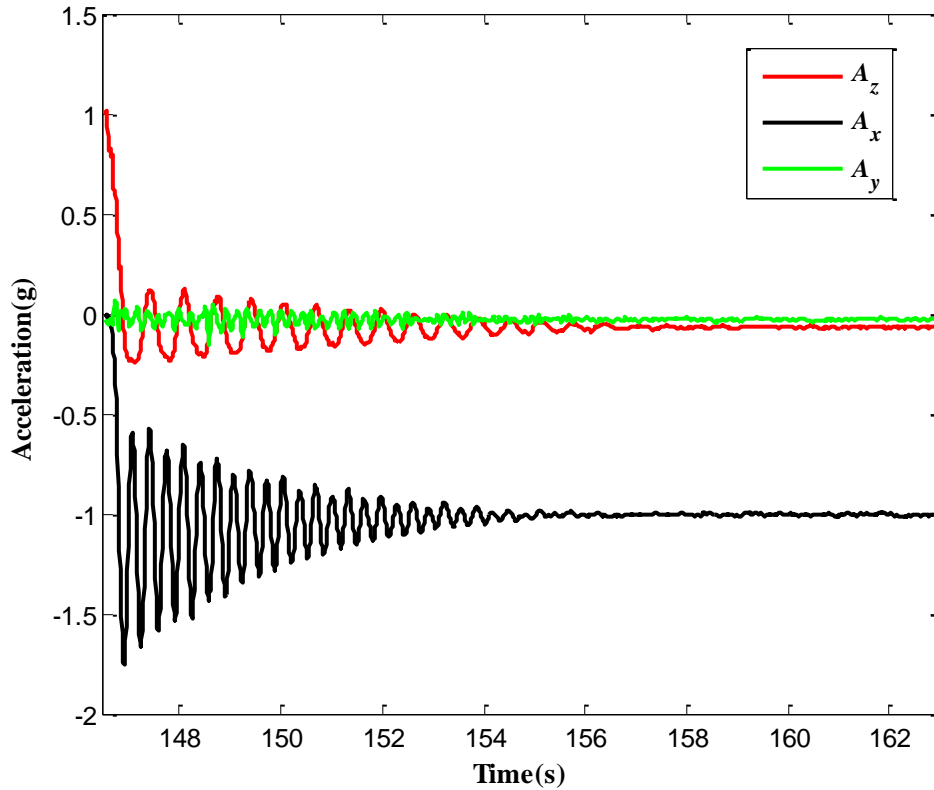


**Fig. 5.4(a)**     Expanded version of the acceleration of the wooden pivot arm during the swing shown in Fig. 5.2.

The acceleration during the swing position is shown in Fig. 5.4(a) as an expanded version of Fig. 5.2. The swing starts at 90° (the pendulum arm is parallel to ground and normal to gravity) with Z-axis aligned and X-axis normal to the gravity direction. $A_z$ and $A_x$ have the values 1g and 0g value as seen in Fig. 5.4(a). The $A_z$ profile indicates that the pendulum does not swing symmetrically about the 0g axis

169

and does not converge to 0g acceleration at the end of the swing. This is due to the -3° offset at rest.

As a first approximation the data was corrected by subtracting $\sin(-3^\circ)$ from $A_z$. However, any bias observed in $A_y$ is due to either imperfections of the pendulum structure (e.g. friction which is angle dependent) that leads to Y-axis having movement or cross-axis error within the sensor. Fig. 5.4(b) shows all the three profiles of Fig. 5.4(a) with the bias offset removed and from $A_y$ by subtracting its mean value.
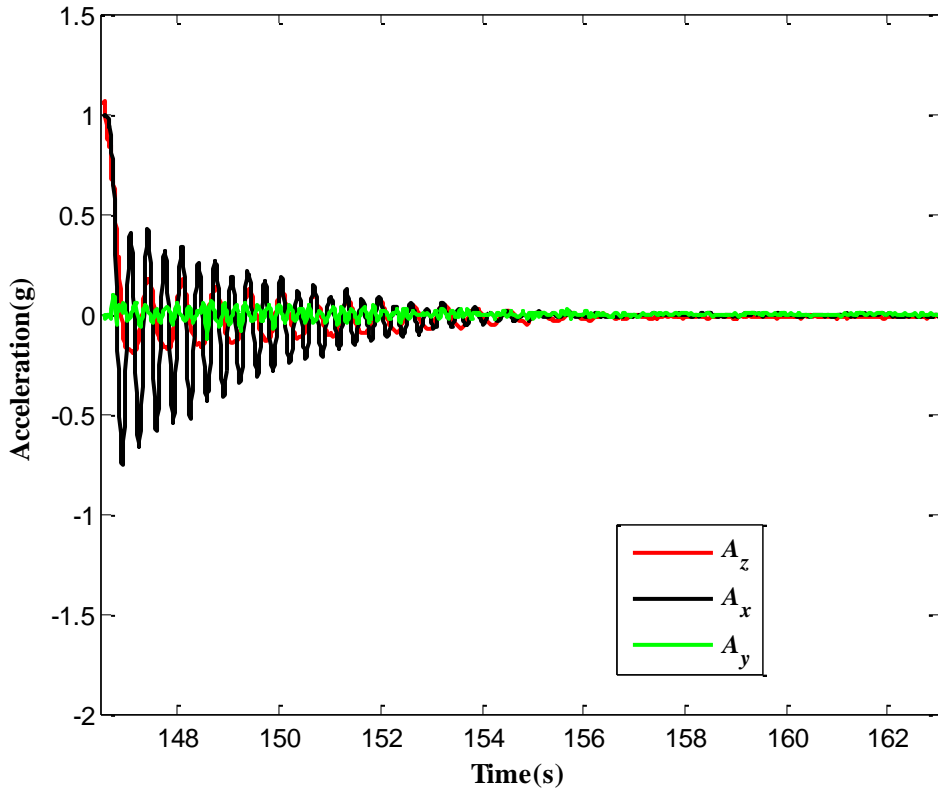


**Fig. 5.4(b)**     DC bias removed version of the acceleration shown in Fig. 5.4(a).

The mean value of $A_y$ shown in Fig. 5.4(a) is -0.0276g and when converted to angle using cosine function it gives 91.58°. So the sensor's Y-axis is not exactly 90° with the swing plane. As seen from Fig. 5.4(b) all the accelerations converge to 0g acceleration at the end of the swing. A close inspection of the first several cycles

from Fig. 5.4(b) reveals that $A_y$ has values (Fig. 5.4(c)) that arise from the wooden structure manufacturing error or cross-axis error. As seen in Fig. 5.4(c), at each peak value of $A_y$ (indicated by arrow), $A_x$ has a larger peak compared to the other peaks (positive) while $A_y$ has steady changes around zero. $A_x$ is not symmetric between the positive and negative peaks. Another observation in Fig. 5.4(c) indicates that the swing frequency of $A_x$ and $A_z$ are different. This difference is obvious as the centripetal acceleration, $A_x$ is proportional to the square of angular velocity, so its frequency differs from the value of the swing angle frequency, but the frequency of tangential acceleration, $A_z$ does not differ. Because $A_z$ is proportional to the angular acceleration, that is the second order derivative of the swing angle, and then the frequency of $A_z$ remains the same as in swing angle.
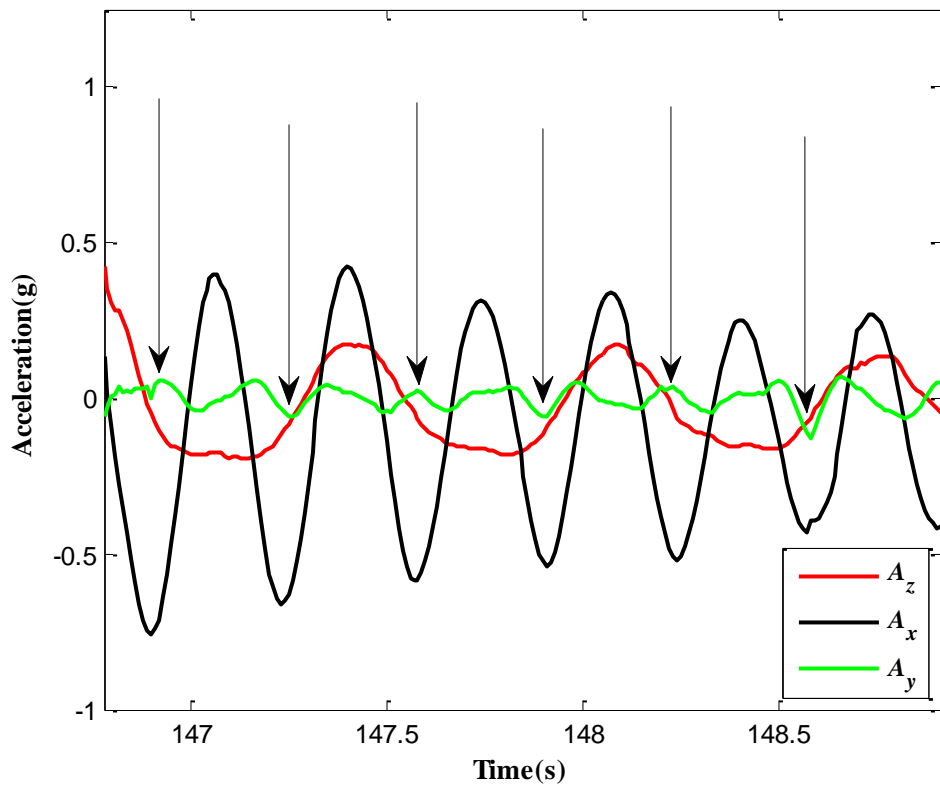


**Fig. 5.4(c)**     Expanded version of the acceleration during several cycles as shown in Fig. 5.4(b).

From [109] the general equation of the swing angles ($\theta$) as a solution of a damped pendulum equation is given as follows:

171

$$\theta = Be^{-kt} \cos(ht) + Ae^{-kt} \sin(ht) \qquad (5.1),$$

where *A* and *B* are the constants and *k*, *h*, *t* are the damping constant, angular swing frequency and time respectively. Differentiating Equation 5.1 gives an expression for the angular velocity:

$$\frac{d\theta}{dt} = (Bh - Ak)e^{-kt} \cos(ht) - (Ah + Bk)e^{-kt} \sin(ht) \qquad (5.2).$$
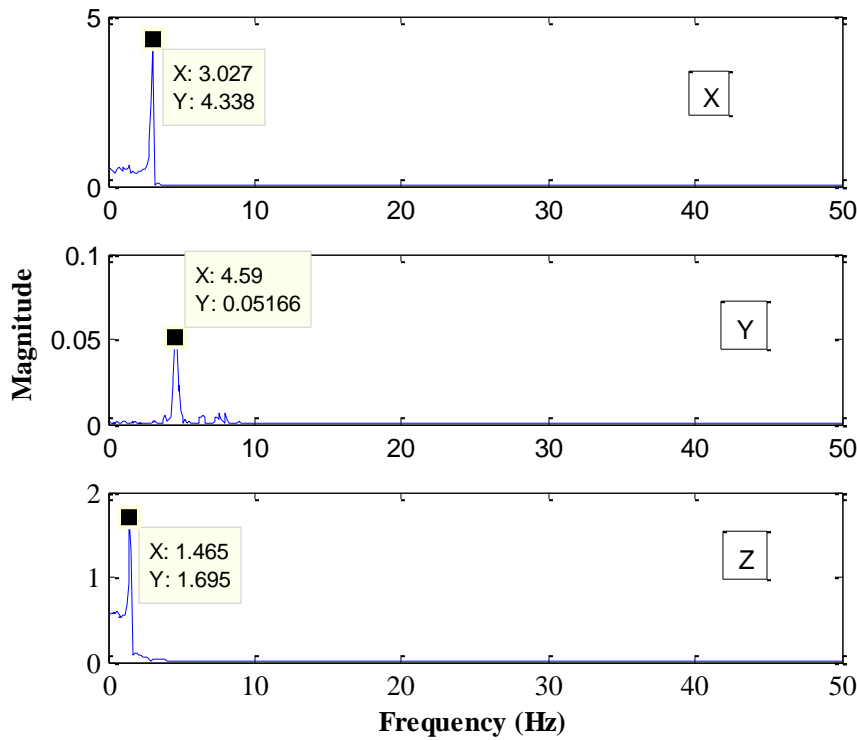


**Fig. 5.5** FT of the acceleration profile shown in Fig. 5.4(a). FFT was calculated using ADAT tool box developed by [106] taking 1024 data points window.

To calculate the swing angle from the profile shown Fig. 5.4(a), an FT of the acceleration profile was used to estimate the dominant frequency. This allows the gravity components to be removed. Fig. 5.5 shows the FT of a 1024 sample window calculated using the FFT in the ADAT tool box [106]. It is observed from Fig. 5.5 that 1.5 Hz, 2.3 Hz, 0.73 Hz frequency are low enough for the low pass filters to

extract the gravity components in X-, Y- and Z-axis respectively according to [100], assuming that artifact related low frequency signal is approximately zero. A Butterworth filter was used to extract the gravity components. The order of the filter and the Butterworth natural frequency for each axis was determined using the 'buttord' function in MATLAB software allowing less than 3 db losses in the pass-band and at least 60 db attenuation in the stop-band. Fig. 5.6 shows the angles during the swing ($\theta$) calculated using the gravity acceleration components ($A_{gx}$, $A_{gy}$ and $A_{gz}$) by pitch angles using the calculation method described by Bai et al. [110]:

$$\theta = \arctan(\frac{A_{gz}}{\sqrt{A_{gx}^2 + A_{gy}^2}}) \qquad (5.3).$$
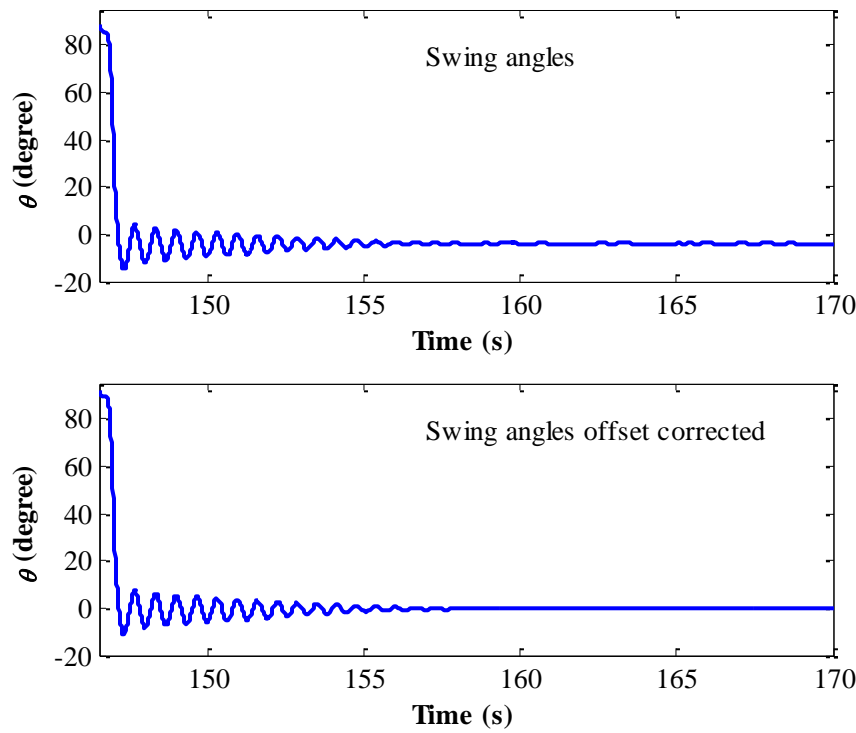


**Fig. 5.6**    Swing angles of the pendulum calculated from the gravity acceleration component in each axis by the pitch angle calculation method as stated by Bai et al., 2012, [110].

The upper part of Fig. 5.6 shows the calculated angles from the low-pass filtered data

using Equation 5.3 and the lower part the calculated angles with off-set removed. As mentioned above the off-set resulted from the fact the pivot arm was not perfectly aligned to the vertical at rest due to the weight of the sensor battery pack attached to the pivot arm.

To compare the sensor estimated angles with those from Equation 5.1, the constants $A$, $B$, $h$ and $k$ were calculated in the followings ways:

At $t=0$ (start of the swing), $\theta$ is the initial angles of the swing. In this case the first positive angle peak (7.87°) in the swing profile in the upper part of Fig. 5.6 was chosen instead of the beginning angle (90°). This choice was made because at the beginning the pendulum arm was released by human hand and the release is not well controlled. So at this first positive peak, the angle and angular acceleration are 7.87° and 0 respectively. Putting $t=0$ and these two values in Equation 5.1 and 5.2 we obtain:

$$B = 7.87, \ Ak = Bh \tag{5.4}.$$

The angular swing frequency $h$ can be estimated from the FFT of the swing angle profile in Fig. 5.6 starting from the first positive peak. The FFT analysis (using a 1024 data window) gives the frequency 1.56 Hz, and then the value of $h$ is 9.8. The damping constant $k$ was estimated from the values of positive peaks of $A_z$ profile in Fig. 5.4(a) using an logarithmic fit. As the profile follows a regular shape, looking for turning points the peak values were extracted using an algorithm written in matlab (see appendix B). Substituting the values of $h$, $B$, and $k$ in Equation 5.4 the value of $A$ was determined.

The equation derived and sensor calculated swing angle profiles are shown in Fig. 5.7. The angles showed good agreement (correlation coefficient, r=0.88). However the amplitude differed after first several cycles in both upward and downward peaks from 150.01s to 155.12s. Taking a variable damping constant of which the first 150 points is constant (from the logarithmic fit) and the rest as a increasing exponential

function of time, the differences between the profiles (150.01s~155.12s) were minimized (see Fig. 5.8).
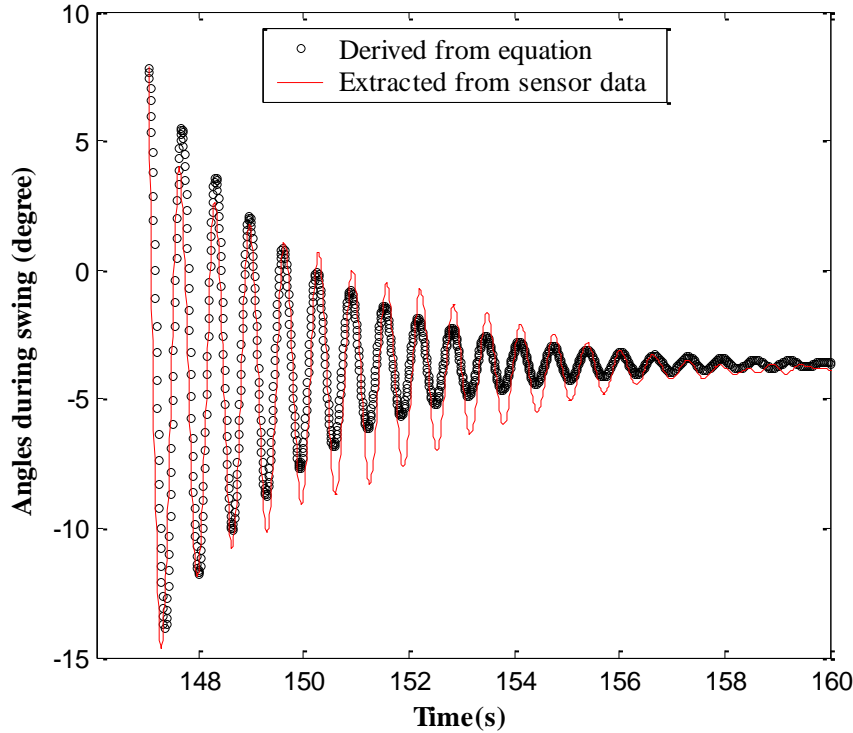


**Fig. 5.7** Swing angles of the pendulum calculated from sensor data and estimated from equation.

The exponential damping constant was chosen using trial and error around the value from logarithmic fit (Fig. 5.9). In this case the correlation coefficient between the equation and sensor angles improved (r=0.91) compared to the former case (r=0.88). Also the slope of the regression line improved to 0.97 compared to the previous slope 0.83.

The results from second part of the experiment on three hits are shown in Fig. 5.10. Fig. 5.10 shows the acceleration spikes due to the hits at middle, bottom and top part of the pivot arm. The arrows in the figure indicated the instant of hit and the profiles after each hit are due to free swing of the pivot arm. Fig. 5.10 reveals that middle hit acceleration spikes in the X- and Z-axis acceleration are smaller in value than the other two hits.
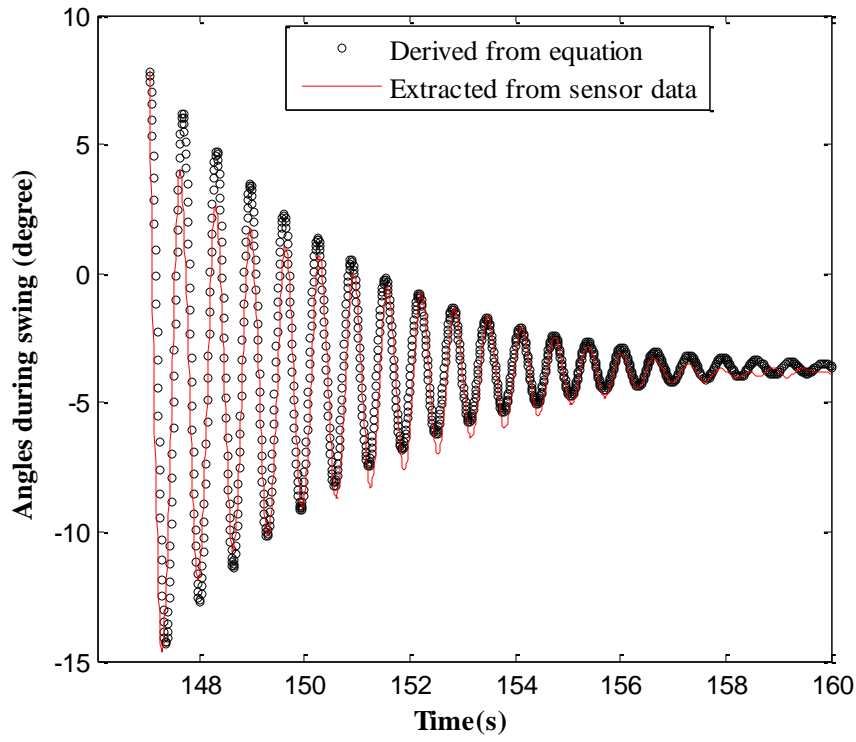
**Fig. 5.8**    Swing angles of the calculated from sensor data and estimated from equation with a variable damping constant shown in Fig. 5.9.
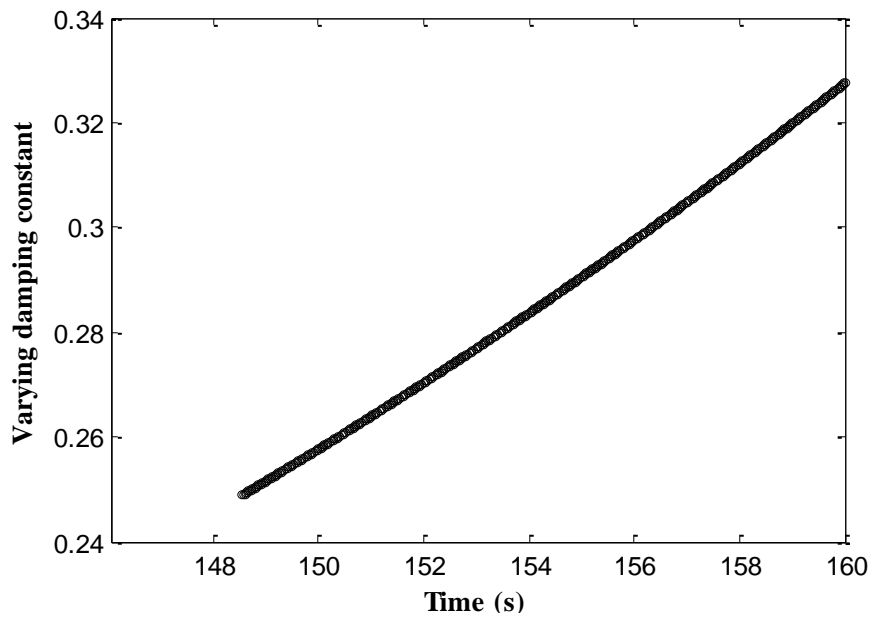


**Fig. 5.9**    A variable damping constant used in the equation for after 150 points to derived swing angle

176

profile as shown in Fig. 5.8. Variable constant were taken to minimize the magnitude difference between equation and sensor profiles observed in Fig. 5.7, however, a constant damping constant was used for first 150 points.
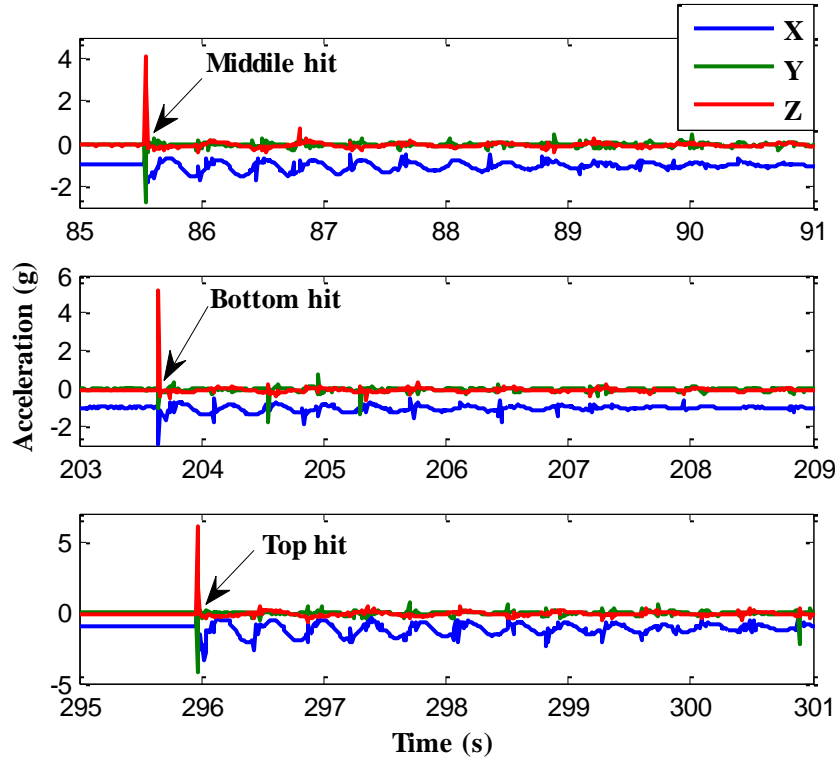


**Fig. 5.10**    Acceleration profiles from three hits (middle, bottom, top) on the wooden pendulum pivot arm (shown in Fig. 5.1) using attached sensor.

The values of the acceleration spikes for all the three hits are shown in Table 5.2. The comparatively smaller values of X- and Z-acceleration for middle hits (as seen from the table) is because these hits are closer to the region where the total energy (translation+rotation+vibration) was smaller in the pivot arm. The hit near the centre of mass (approximately the middle of the bat where the sensor was placed) maximizes the energy transferred. This finding indicated that if the pivot arm itself has kinetic energy (not stationary) then more energy could be transferred. In the cricket bat, the ball-contact region could be investigated for effective bat-ball contact to produce most ball recoil velocity.

**Table 5.2** Values of X- and Z-acceleration spikes for middle, bottom and top hit on the pivot arm for one trial.

|  | Middle hit | Bottom hit | Top hit |
|---|---|---|---|
| **X-acceleration** | -0.1641g | -2.8940g | 2.8650g |
| **Y-acceleration** | -2.7940g | -1.0100g | -4.1690g |
| **Z-acceleration** | 4.1140g | 5.1560g | 6.1050g |

## 5.1.4 Conclusions

The pendulum swing was used to investigate the angles from the static and swing positions of the sensor. Static angles from sensor data were compared with inclinometer angles and found good agreement (r=0.99). The swing angles were compared with angles estimated using the solution of a damped pendulum equation imposing the conditions for the constants. A good agreement between the two angle profiles from sensor data and equation were obtained (r=0.88). The matching of those two profiles was improved by taking a varying damping constant and obtained an enhanced correlation coefficient, r=0.91 and the slope of the regression line 0.97 instead of 0.83 in the former case. The selection of a variable damping constant was a trial. As the velocity of the swing decreases in time and the wooden pendulum was not ideal, the slowing process is not uniform. Thus the damping constant seems not to be same in all the swing time. The damping constant can be a criterion to measure of the applied force by the batter in the straight drive. How much swing inertia is overcome by the batters can be quantified by measuring this constant in matching the sensor and equation derived data. Repetitive swings profile could give a measure about how the damping constant is varying and that could be a measure of the consistency of a batter over a long period of time. In the second part of the study the location of hits on the stationary pivot arm could be distinguished using the sensor recorded acceleration spikes. This provides an insight about the optimum hitting location. Using sensors to identify the hit location of the ball-contact point could be an interesting topic to study further.

## 5.2 Pendulum theory and sensor results to quantify the force magnitude in bat swing

This study used pendulum mechanics to assess bat swing in a straight drive in cricket. A real batter executing a straight drive is not stationary, rather the batter moves with the bat. Thus a pendulum with a moving pivot was modeled to estimate the swing angles in a straight drive and compare with the video angles from the real drive. Using equation estimated angles, the centripetal acceleration profiles were matched with that recorded by the bat mounted sensor. The effect of initial angular velocity, radius of rotation and phase angle of the pivot motion were investigated on this acceleration profiles. The results were adopted to the sensor profile to judge the level of force applied by the batter. The different levels of the force were identified observing the changes in the swing profiles upon varying the parameters stated above. Comments were drawn for maximizing the force in the drive.

### 5.2.1 Background

The background of this study is included in section 2.8 in the literature review chapter. Other than cricket, the bat swing modeling was reported for tennis, golf, double pendulum made of metal bar in that section (2.8). In this study comparing the acceleration profile predicted by the mechanics of a pendulum with a moving pivot and that recorded in inertial sensors, the force applied by the batter in a straight drive bat swing was determined. The parameters required to maximize the force were investigated from pendulum mechanics and adopted to sensor profiles while matching the acceleration profiles from the equation and the sensor.

### 5.2.2 Theory: pendulum with moving pivot

Fig. 5.11(a) represents the position of a bat during swing in a planar drive as a pendulum with a moving pivot. [$X(t)$, $Y(t)$] are the coordinates of the pivot point 'P' with reference to the origin at 'O' of coordinates [0, 0], and $\theta$ is the angle between

the pendulum arm PB and the vertical line PR. According to Fig. 5.11(a) the



(a)                                                    (b)
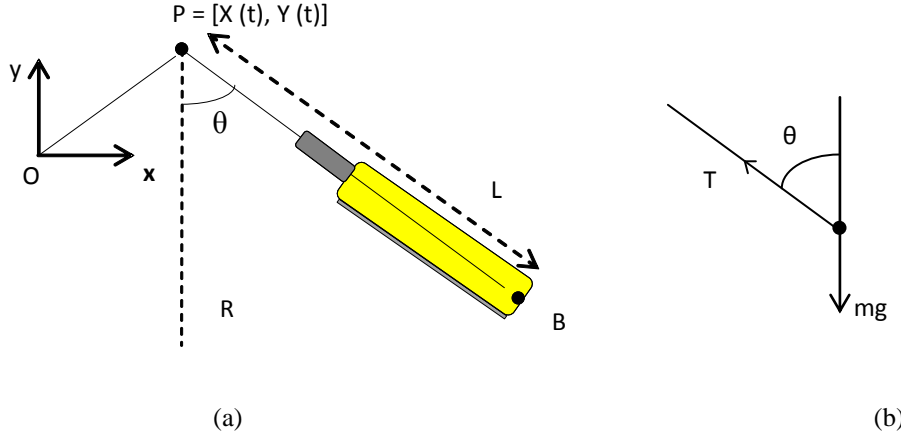
**Fig. 5.11**   (a) Bat as a pendulum arm during the swing in a planar drive with respect to point of reference point 'O' (taken as origin for the coordinates $x$, $y$). P and B are two end points of the pivot arm of length $L$ (resultant length of bat and hand) of a pendulum. PR is the gravity direction as a reference for the swing angles ($\theta$). The coordinates of the pivot is taken as [$X$ ($t$), $Y$ ($t$)] and its values changes with respect to time ($t$) during swing. (b) The vector representation of the Tension ($T$) along the pivot arm, weight ($mg$) of the pivot arm, and swing angle ($\theta$).

coordinates of the position, velocity and acceleration of point B can be expressed as follows:

$$\begin{aligned}
&\textit{Position of } B = [(X + L\sin\theta), (Y - L\cos\theta)], \\
&\textit{Velocity of } B = [(X' + L(\cos\theta)\theta'), (Y' + L(\sin\theta)\theta')], \\
&\textit{Acceleration of } B = [(X'' - L(\sin\theta)(\theta')^2 + L(\cos\theta)\theta''), \\
&\qquad\qquad\qquad (Y'' + L(\cos\theta)(\theta')^2 + L(\sin\theta)\theta'')]
\end{aligned} \tag{5.5}.$$

where $L$ is the length of the pendulum PB and dash and double dash marked parameters represent the first and second time derivatives of the parameter respectively. Fig. 5.11(b) represents the force related parameters. According to this figure the coordinates of the force vector ($F$) is given as:

$$F = [-T\sin\theta, (T\cos\theta - mg)] \tag{5.6},$$

where $T$ is the tension along the pivot arm (similar to the tension in the string of a pendulum) and $g$, $m$ are the gravity and mass of the pivot arm respectively, similar to

a typical pendulum but the mass is distributed unlike the swing mass at the end of the string of a general pendulum.

Setting *F=ma* and equating Equations 5.5 and 5.6 we have

$$-T\sin\theta = m(X'' - L(\sin\theta)(\theta')^2 + L(\cos\theta)\theta'' \tag{5.7},$$

$$T\cos\theta - mg = m(Y'' + L(\cos\theta)(\theta')^2 + L(\sin\theta)\theta'') \tag{5.8}.$$

Eliminating *T* and *m* from Equation 5.7 and 5.8 we have the equation of dynamics of a pendulum with moving pivot as follows:

$$L\theta'' + X''\cos\theta + (Y'' + g)\sin\theta = 0 \tag{5.9}.$$

Three types of motion for the pivot point P in Fig. 5.11(a) are considered:

$$(i) \ Horizontally: X = A\sin(\omega_p t), Y = 0,$$
$$(ii) \ Vertically: \quad X = 0, Y = A\sin(\omega_p t), \tag{5.10}.$$
$$(iii) \ Circular: \quad X = A\cos(\omega_p t), Y = A\sin(\omega_p t)$$

In Equation 5.10 the amplitude and angular frequency of the motion of the pivot point are denoted by A and $\omega_P$ respectively. Now for a planar straight drive, the pivot motion can be considered as a circular motion. The bat trajectory during an entire swing forms a circular arc. (a pictorial view is shown in Fig. 5.40 in Section 5.7 as revealed by video). Then using motion (iii) of Equation 5.10, Equation 5.9 becomes

$$L\frac{d^2\theta}{dt^2} + A\cos\theta[\frac{d^2}{dt^2}\cos(\omega_p t)] + [A\frac{d^2}{dt^2}\sin(\omega_p t) + g]\sin\theta = 0 \tag{5.11}.$$

Taking *A* and $\omega_P$ constant with respect to time for a planar bat swing, after manipulating the Equation 5.11 becomes:

$$L\frac{d^2\theta}{dt^2} = A\omega_p^2[\cos(\omega_p t - \theta)] - g\sin\theta \tag{5.12}.$$

This equation is a nonlinear second order differential equation and also time ($t$) appears explicitly in it, a numerical method is required to solve it. The state variables for the numerical method are introduced as follows:

$$u_1 = \theta,$$
$$u_2 = \theta',$$
$$u_3 = \phi' = \omega_P, \qquad\qquad\qquad (5.13).$$
$$u_4 = \frac{A}{L}\omega_P^2[\cos(\phi - \theta)] - \frac{g}{L}\sin\theta$$

The parameters superscripted by dashes in Equation 5.13 are the time derivatives of each parameter. $\phi$ is the phase of the motion term of the pivot.

Using the state variables in Equation 5.13 the solution of Equation 5.12 was estimated numerically using 'ode23s' solver from Matlab by a developed algorithm (see Appendix C). The initial condition of the state variable $u_1$, time span were chosen from video data during a typical drive by a novice. But the initial conditions for the angular velocity $u_2$, were chosen arbitrarily and close to the average angular velocity from video footage to match equation estimated and video revealed angle profile. The constants $A$ and $\omega_P$ were also chosen arbitrarily. The results from the solution are included in Section 5.2.4 while compared to the sensor data. Once the angular velocity ($\omega$) was determined from the solution of the Equation 5.12 using the state variables in Equation 5.13, the resultant acceleration ($a_l$) along the bat length ($l$) during the bat swing were calculated using:

$$a_l = R\omega^2 - g\cos\theta + a_{TR} \qquad\qquad\qquad (5.14),$$

here $R$, $g$ are the instantaneous radius of rotation and the value of gravity respectively, and $a_{TR}$ is the component of translational acceleration along the bat length. This translational component is due to the body motion of the batter and was included in Equation 5.14 to match the sensor profile to the equation. The first and second terms in Equation 5.14 are centripetal and gravity acceleration components acting along the bat length, respectively. The acceleration, $a_l$ shown in Equation 5.14

is analogous to that recorded in the bat mounted sensor's X-axis, because this axis is aligned to bat length.

Particular attention was paid to the effect of $R$, initial angular velocity ($\omega_0$) and initial phase angle ($\varphi_0$) of the pivot on the profile of $a_l$. The details are included in Section 5.2.4.

### 5.2.3 Experimental Procedure

A sensor platform [99] as shown in the Fig. 4.1 was attached to the middle part of the back of the bat's blade length to record acceleration data from a ball-free straight drive by a novice batter. The batter was instructed to swing the bat uniformly as planar (in the sagittal plane of bat during the straight drive) as possible without having any movement of the bat and batter's limbs in the mediolateral direction. The data in three dimensions (along sensor X-, Y-, Z-axis as $a_x$, $a_y$ and $a_z$ respectively) were recorded in the bat attached sensor where the planar drive was in ZX-plane along sensor's Z-axis. The details about the sensor and bat axes, sensor placement on the bat and drive direction are given in Section 4.1.1.3. The difference is that only one sensor was placed on the bat in this study instead of two. The drive was captured by a video camera and its placement and details is provided in Section 4.1.3.1. The video extracted angles ($\varphi$) were estimated from the video footage as described in Section 4.1.3 and using Equation 4.10 to 4.13.

### 5.2.4 Results and discussion

The sensor recorded acceleration profiles ($a_x$, $a_y$, $a_z$) during the straight drive by the novice are shown in Fig. 5.12. The profile in Fig. 5.12 is divided in three parts: the back-lift (*BL*), the forward swing (*FSW*), and the recovery (*REC*). The start of the profile is at the start of *BL* and this *BL* part ends by a peak (in $a_x$) shown by the arrow and text 'end of back-lift' in Fig. 5.12 where the *FSW* starts. The *FSW* ends where *REC* starts shown by the arrow and text 'end of forward swing'. The *REC* is the reverse swing of the bat after the end of *FSW* and it ends at the same side where *FSW* started. The profile for *REC* is shown as the rest of profile after the text 'end of

forward swing' in Fig. 5.12.
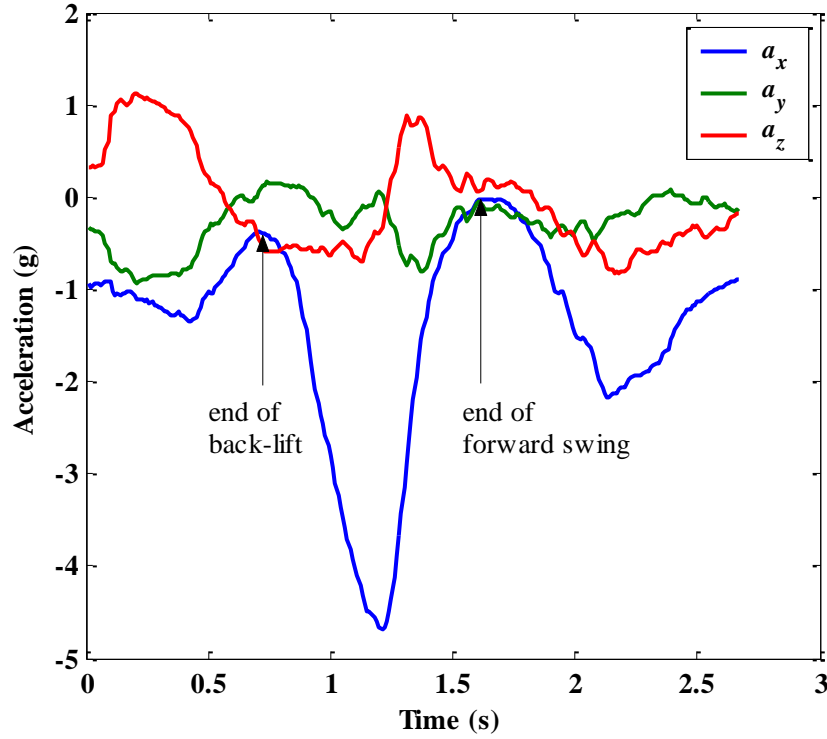


**Fig. 5.12** X-, Y-, and Z-axis acceleration ($a_x$, $a_y$, $a_z$ respectively) profiles recorded in the bat mounted sensor during a planar straight drive by a novice. The arrow indicated peaks in ax are at the end of back-lift, end of forward swing and vertical posture of bat were extracted from the video footage.

The timing of start and end of each part of swing in Fig. 5.12 were estimated from the video footage using the method in Section 4.1.3 and Equation 4.10, 4.11. The bat posture in different parts of the swing and corresponding acceleration profile were confirmed by the video footage.

To compare the video data with those calculated by equation as described in the section 5.2.2, both the equation estimated and video extracted bat swing angle (termed as 'bat angle' hereafter) during the swing were plotted against time as shown in Fig. 5.13. The vertically upward direction was chosen as reference for bat angle measurement. A noticeable similarity and consistency is observed in both the angle profiles from equation and video.
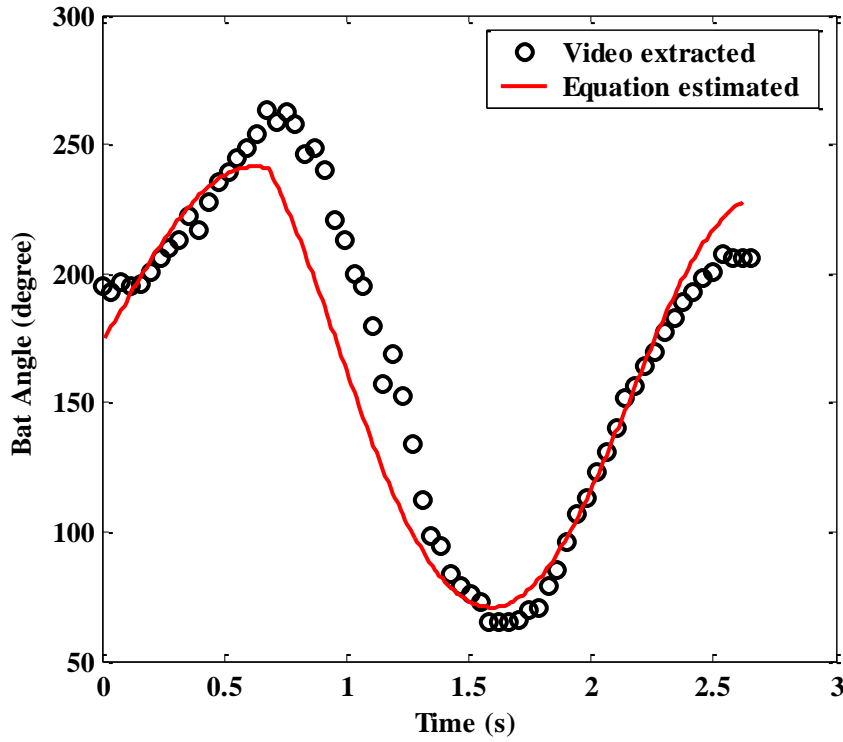
**Fig. 5.13**   Video extracted and equation estimated angle during the bat swing of acceleration profile shown in Fig. 5.12.

To observe the relation between them, the equation estimated angles were plotted against video extracted angles in each part of the bat swing as shown in Fig. 5.14. A strong correlation between video extracted and equation estimated bat angle is observed in each part of the swing. The correlation coefficients were calculated and found 0.96, 0.99 and 0.98 for *BL*, *FSW*, and *REC* respectively.

Using the equation estimated angular velocity from the analysis in the Section 5.2.2 the X-acceleration profile was calculated using Equation 5.14. The radius of rotation, *R* was approximated as an exponential function of bat angle ($\theta$) as shown in Equation 5.15:

$$R = R_0 \exp(b\theta) \tag{5.15},$$

this approximation is due to the fact that $R$ is not constant in the drive as the centre of swing is varying in time during the bat swing by the movement of batter's limb and bat together. Equation 5.15 was also used in [65].
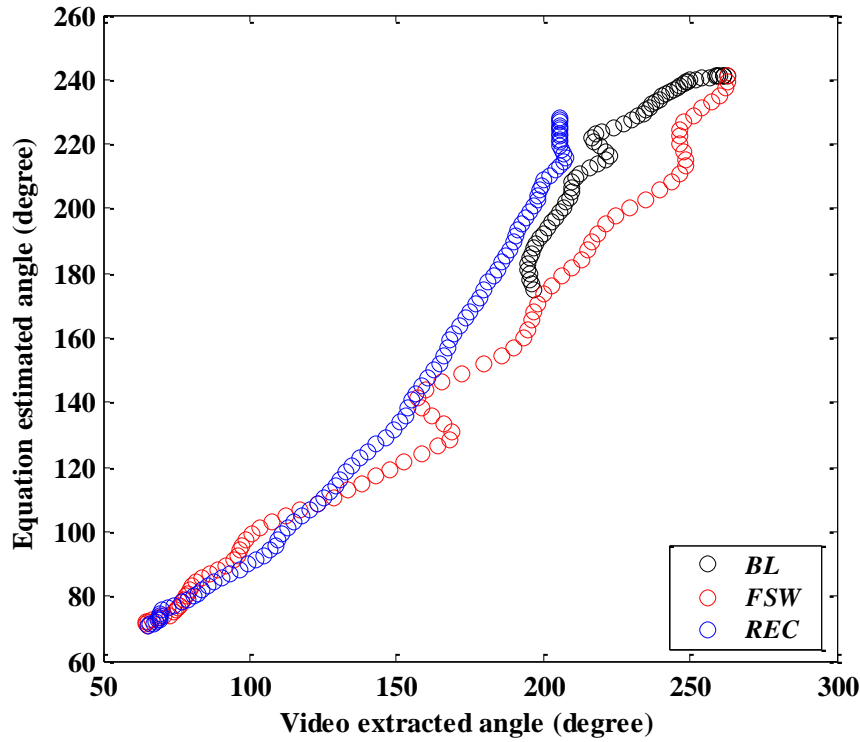


**Fig. 5.14** Equation estimated versus video extracted bat angles shown in Fig. 5.13 to predict the strength of relation between the two angles. The angles in different part of bat swing, back-lift (*BL*), forward swing (*FSW*) and recovery (*REC*) are distinguished by black, red and blue legend respectively.

The exponential function for $R$ was chosen to match the profile between equation predicted and sensor recorded judging the batting arc in the video, a typical example is shown in Fig. 5.41 in the study in Section 5.7. The equation estimated and sensor recorded X-axis acceleration (simply X-acceleration hereafter) profiles are shown in Fig. 5.15.
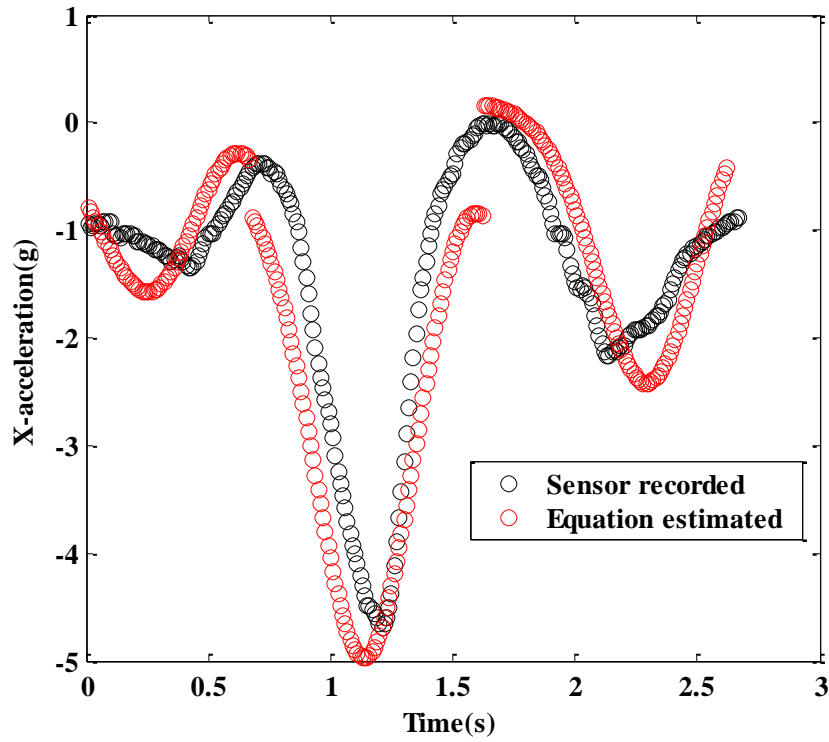
**Fig. 5.15** Equation estimated and sensor recorded X-acceleration profile matching at *BL*, *FSW* and *REC* part of bat swing. Equation revealed profile was predicted by using the angle data in Fig. 5.13 and Equation 5.14.

**Table 5.3** Curve fitting constants and parameters (in the upper part of the table) used to match the equation (Equation 5.14) profile shown in Fig. 5.15 and how those were chosen/estimated (in the lower part of the table).

|  | Optimized values in Equations 12-15 (the suffix zero represents initial value of the parameter) | | | Video derived parameters | | |
|---|---|---|---|---|---|---|
|  | *BL* | *FSW* | *REC* | *BL* | *FSW* | *REC* |
| $\theta_0$ | 175º | Angle at end of *BL* (240.89º) | Angle at end of *FSW* (66.23º) | 195.49º | Angle at end of *BL* (263.15º) | Angle at end of *FSW* (66.24º) |
| $\omega_0$ | 2.7 rad./s | 3.2 rad./s | 0.44 rad./s | 1.69 rad./s (average over time) | 3.62 rad./s (average over time) | 2.44 rad./s (average over time) |
| $\varphi_0$ | 0.067 rad. | 0.88 rad. | 0.067 rad. |  |  |  |
| *A* | 15 | 10 | 3.8 |  |  |  |
| $R_0$ | 1.5 m | 1.6 m | 1.5 m |  |  |  |
| *b* | 1.0 | 0.625 | 0.55 |  |  |  |
| $a_{TR}$ | 7.5 m/s$^2$ | 5.0 m/s$^2$ | 1.5 m/s$^2$ |  |  |  |

|  | How the parameter was chosen/estimated to maximise the matching between video estimated and sensor recorded profiles | | |
|---|---|---|---|
|  | **BL** | **FSW** | **REC** |
| $\theta_0$ | Chosen in trial and error method around the video derived value of 195.49º. | Chosen in trial and error method around the video derived value of 263.15º. | Chosen in trial and error method around the video derived value of 66.24º. |
| $\omega_0$ | Chosen in trial and error method around the video derived value of 1.69 rad./s. | Chosen in trial and error method around the video derived value of 3.62 rad./s. | Chosen arbitrarily because the value near the video (2.44 rad./s) failed to maximise the matching. |
| $\varphi_0$ | Chosen arbitrarily | Chosen arbitrarily | Chosen arbitrarily |
| $A$ | Chosen arbitrarily | Chosen arbitrarily | Chosen arbitrarily |
| $R_0$ | Chosen as the summation of the effective lengths of the bat and batter hand. | Chosen in trial and error method the summation of the effective lengths of the bat and batter hand. | Chosen as the summation of the effective lengths of the bat and batter hand. |
| $b$ | Chosen arbitrarily | Chosen arbitrarily | Chosen arbitrarily |
| $a_{TR}$ | Chosen arbitrarily | Chosen arbitrarily | Chosen arbitrarily |

The constants and parameters used for the equation estimated profiles for the solution of Equation 5.12 (using the method in Section 5.2.2) and for the Equation 5.14 are shown in upper part of the Table 5.3 together with a comparison with the video extracted values. The lower part of the Table 5.3 shows how those constants and parameters were chosen/estimated to maximise the matching between video estimated and sensor recorded profiles. The estimated $\omega$ (average over time) from the model/equations were 1.72 rad./s, 3.21 rad./s and 2.65 rad./s for *BL*, *FSW* and *REC* respectively.

A promising match is evident between the video estimated and sensor recorded X-acceleration (r=0.91) shown in Fig. 5.15. A close observation of Table 5.3 reveals that the initial angular velocity and phase of the pivot point is significantly larger in *FSW* than the other two swing parts. But the translational acceleration constant is larger in *BL* than the other two swing parts. The larger angular velocity in *FSW* is reasonable as it is accountable for negative maximum peak in the profile whose magnitude is larger than any peak of the other two parts of the swing. More translational acceleration constant in *BL* than other two is due to the upward translation of the body of the batter with the bat and hand together. In this part of swing the translational motion of the pivot was dominant compared to circular

motion with having smaller phase angle (0.067 radians) compared to *FSW* part of having phase angle of the pivot of 0.88 radians. Moreover, the larger value of radius constant (*b*=1.0) for *BL* part of swing than *FSW* part (*b*=0.625) also reflects the dominance of translational motion in *BL* where the radius of rotation is larger.
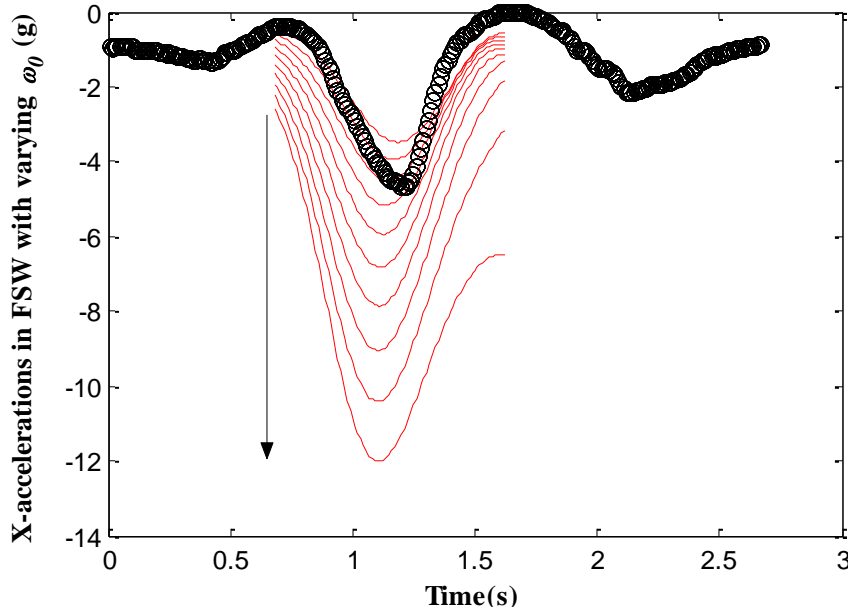


**Fig. 5.16** The Effect of initial angular velocity ($\omega_0$) on X-acceleration during *FSW* (the red colour plots). The direction of arrow in the figure indicates the increasing of negative maximum peak with increased value of $\omega_0$. The black colored plot represents the entire sensor recorded profile in all three parts of swing.

The effect of initial angular velocity, radius of rotation and phase angle of pivot on X-acceleration profile in *FSW* part are shown in Fig. 5.16, Fig. 5.17 and Fig. 5.18 respectively. The arrow in the figures indicates the trend of negative maximum peak of X-acceleration. As seen from Fig. 5.16, the magnitude of X-acceleration during *FSW* increases with increasing initial angular velocity. In Fig. 5.17(a) the same increasing trend is noticed with increasing the radius constant (*b*) for increased values of *R*. The profile of *R* in each value of *b* is shown in Fig. 5.17(b) to show the increased *R*. In contrast to *b* and $\omega_0$, a decrease of the X-acceleration magnitude during *FSW* was observed with increasing $\varphi_0$, as shown in Fig. 5.18. The relationships between the
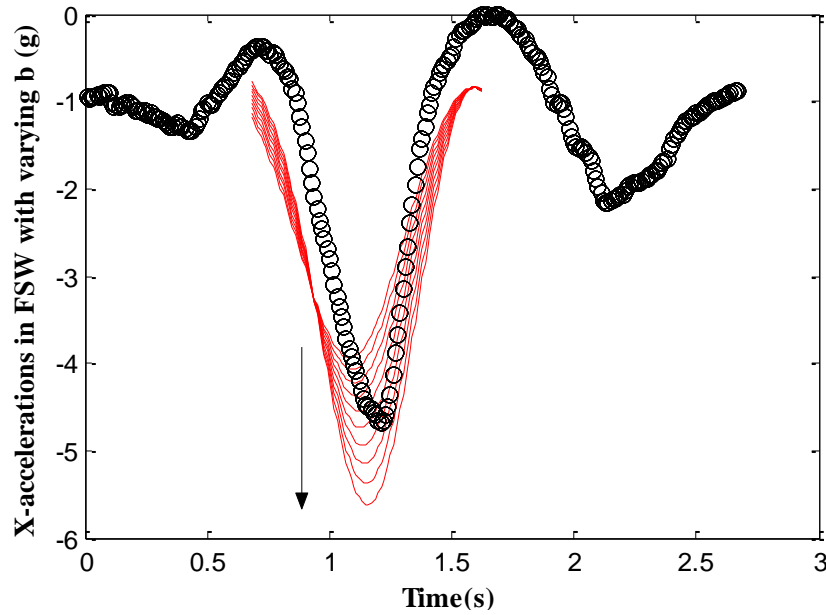
**Fig. 5.17(a)**    The Effect of radius of rotation ($R$) on X-acceleration during *FSW* (the red colour plots). The direction of arrow in the figure indicates the increasing of negative maximum peak with increased value of $R$ by increasing constant of exponent ($b$) in the exponential function of radius shown in Equation 5.15. The changes in $R$ profile with increased $b$ are shown in Fig. 5.17(b). The black colour plot represents the sensor recorded entire profile in all three parts of swing.
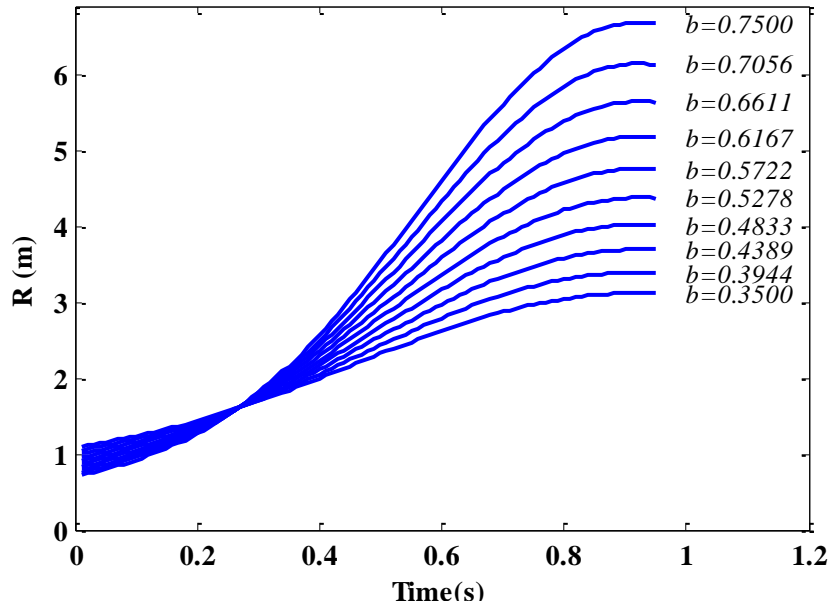


**Fig. 5.17(b)**    The changes in radius of rotation profile with increased $b$ used for the profiles shown in Fig. 5.17(a).

negative maximum peak and $\omega_0$, $b$, $\varphi_0$ are shown in Fig. 5.19. Strong correlation with coefficient of 0.98, 0.99, -0.99 for $\omega_0$, $b$, $\varphi_0$ respectively was observed, as shown in the figure.
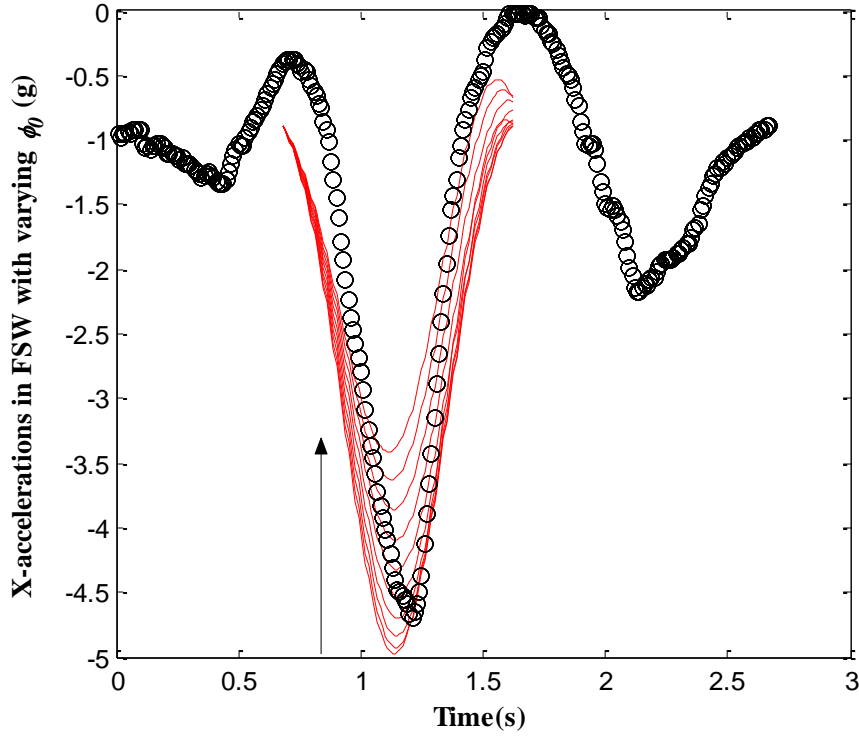


**Fig. 5.18**   The Effect of initial phase ($\Phi_0$) of the pivot on X-acceleration during *FSW* (the red colored plots). The direction of arrow in the figure indicates the decreasing of negative maximum peak with increased value of $\varphi_0$. The black colored plot represents the sensor recorded entire profile in all three parts of swing.

The results above indicate that in *FSW* more X-acceleration results with increased radius of rotation. A skilled batter can achieve this by moving the body forward in the straight drive to make the centre of rotation further away from the body. The centre of rotation is defined by the projection of the bat in two different angular positions. This means that when the batter moves forward the centre of rotation can be well beyond the shoulders of the batter. The smaller value of the pivot phase angle required for larger acceleration indicates the need for a translational motion in the drive rather than the pure circular motion of the pivot keeping body stationary. As

expected, a higher initial angular velocity results in a larger value of swing acceleration.
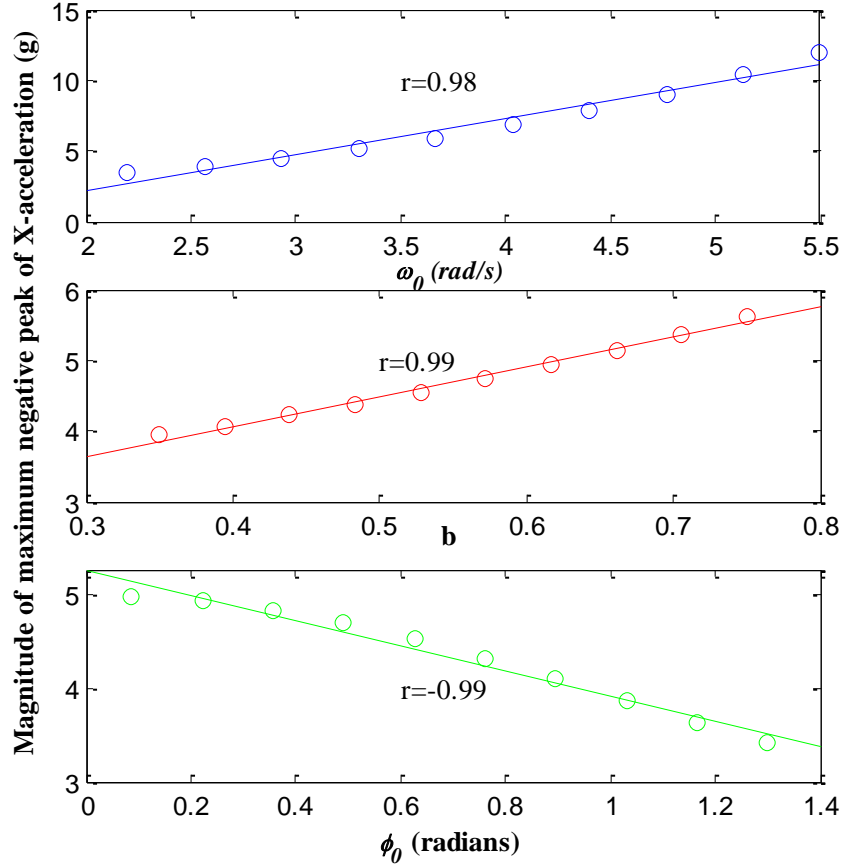


**Fig. 5.19**  The approximate linear relationship between the negative maximum peak X-acceleration during *FSW* and $\omega_0$, $R$ and $\Phi_0$ shown in Fig. 5.16, 5.17(a) and 5.18.

### 5.2.5 Conclusions

The mechanics of a pendulum with moving pivot was used to explain bat attached sensor recorded acceleration along bat length axis. The nonlinear equation of the pendulum with moving pivot was solved numerically using initial conditions from video swing angles and the equation were compared. A strong correlation with coefficient about 0.99 was obtained between the angles. Using the equation estimated angles the X-acceleration (along X-axis of the sensor aligned to bat length) were

calculated using initial conditions from the video and a radius of rotation as an exponential function of swing angles. The exponent of the radius function, the initial value of radius, translational acceleration, and phase angle of the pivot were chosen strategically (see Table 5.3) to match the equation estimated X-acceleration profile with those recorded in the sensor. A promising agreement was obtained between the two profiles. The effect on the profile with variations of the initial angular velocity, radius of rotation and phase angle of the pivot were investigated. The magnitude of the maximum peaks increases with increasing the value of radius of rotation and phase angle, but decreases with increasing phase angle of the pivot. These findings are reasonable in straight drives because in this drive batters can maximize force by moving the body forward to increase the radius of rotation or increasing the initial angular velocity. This indicates the translating of the pivot point rather than a pure circular motion. The decreased value of phase angle of pivot can increase the acceleration. The results from this study shows that sensor recorded profiles can be an estimator of quantifying force level in the straight drive measuring the value of the acceleration peaks. This might include information about how the batter executed the stroke in relation to the angular velocity, radius of rotation and phase.

## 5.3   Straight drive bat swing

Cricket batting is a dynamic interceptive task involves the batter perceiving relative motion of the bowled ball and formulating a response for a desired goal [111], [39]. A high degree of accuracy in spatial and temporal motion of the bat and batter before and at the instant of ball contact and the bat velocity are critical for achieving the goal [39]. Two experiments were conducted: a set of ball-free, straight drives by an amateur batter at nominal constant speed, and a set of straight drives at different speeds by the same batter accompanied by video tracking. In all cases the bat swing was in the x-z plane of the sensors placed on the reverse face of the bat. The bat face moves in the z direction of the accelerometer. The objective was to minimize accelerations perpendicular to the swing plane. Consistency of the drives, bat swing

intensities, bat position during the higher centrifugal force, acceleration difference between the on and off side of the bat, and the tilted position of the stationary bat at the start of each swing was determined from the acceleration profiles.

## 5.3.1 Experimental Procedure

The inertial sensor used is capable of measuring acceleration of $\pm 6g$ in three dimensional space. As shown in the Fig. 4.4(a) in Section 4.1.1.3, two PCBs [99] were attached to the middle part of the back of the bat's blade length. Fig. 4.4(a) also describes the orientation axes, where $+X^B$ axis refers to the acceleration along the length of the bat, while $+Y^B$ axis lies in the direction of the bat edges and $+Z^B$ axis is perpendicular to the face of the bat, that is, in the direction of a typical swing. As stated for Fig. 4.4 (b) in Section 4.1.1.3, the real bat acceleration along $+Z^B$ axis and $+Y^B$ axis differs from the sensors $+Z^S$ ($Z^{S1}$ and $Z^{S2}$) and $+Y^S$ ($Y^{S1}$ and $Y^{S2}$) axis accelerations by a factor of cosine of the angle $\delta$ (the angular displacement of sensors to the bat face). There was no difference between $+X^B$ and $X^S$ ($X^{S1}$ and $X^{S2}$) axes. Data recorded in S1 and S2 accelerometers are labeled as $a_{x1}$, $a_{y1}$, $a_{z1}$ along S1 axes ($X^{S1}$, $Y^{S1}$, $Z^{S1}$ respectively) and $a_{x2}$, $a_{y2}$, $a_{z2}$ along S2 axes ($X^{S2}$, $Y^{S2}$, $Z^{S2}$ respectively). The straight ball-free bat swings lie in $Z^B X^B$-plane (perpendicular to the ground $Y^B Z^B$-plane as stated in Fig. 4.4 (a)). The vertical bat tapping on the ground was used to synchronize the timing between the video and sensor data. A video camera was used to record the positions of both ends of the bat at all times. The position of the camera is provided in Section 4.1.3.1.

The camera was operated at frame rate of 100 f/s to minimize image blur. Each frame consisted of two interlaced images which were separated by software to a frame rate of 200 f/s in the swing footage.

## 5.3.2 Results and discussion

Fig. 5.20 shows the acceleration profiles obtained from a set of ten consecutive ball free drives along the X, Y and Z axes ($a_{x1}$, $a_{y1}$, $a_{z1}$ along $X^{S1}$, $Y^{S1}$, $Z^{S1}$ axis and $a_{x2}$, $a_{y2}$, $a_{z2}$ along $X^{S2}$, $Y^{S2}$, $Z^{S2}$). Each drive of Fig. 5.20 consists of two bat taps before

starting of the swing. The swing of the first drive started at 89.68s commencing with back-lift.
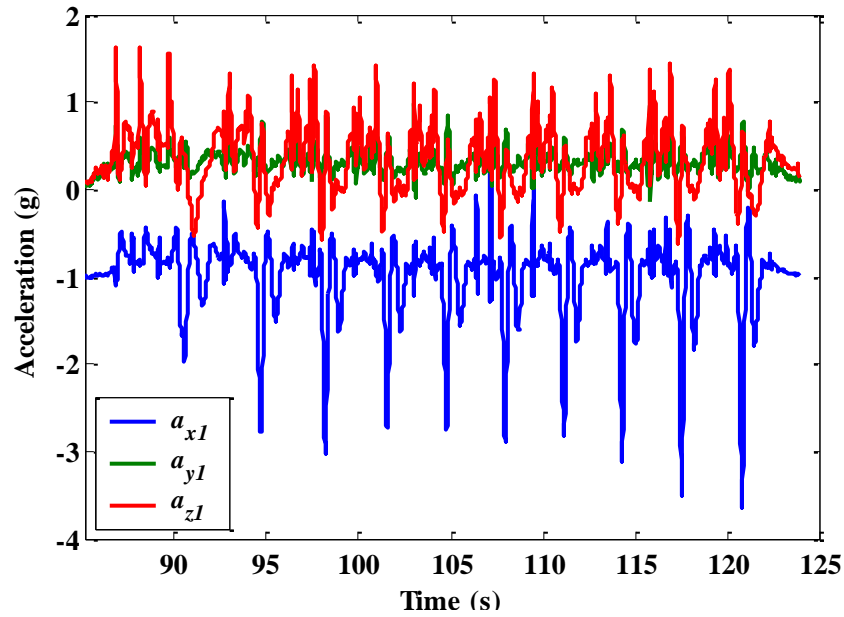


**Fig. 5.20(a)**     Acceleration profiles from S1 for 10 consecutive drives.
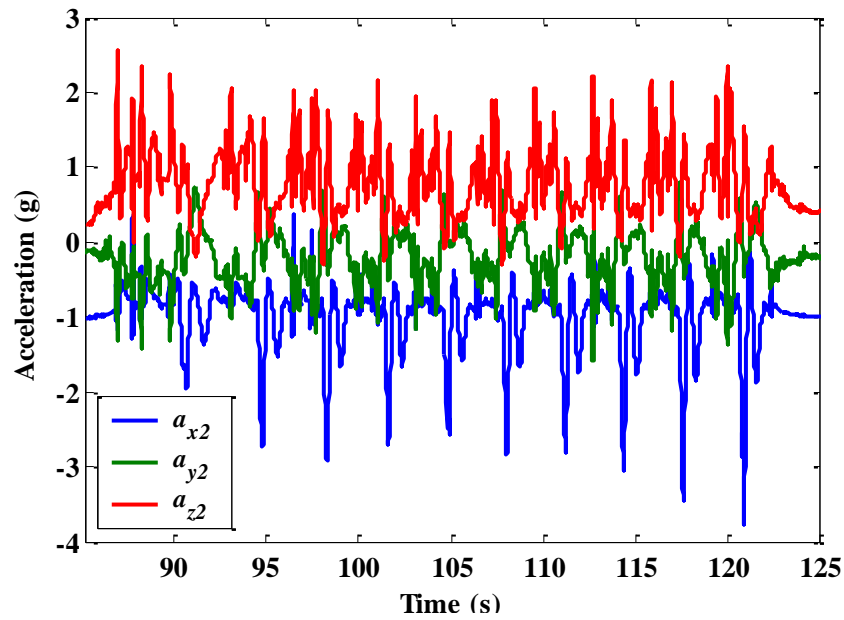


**Fig. 5.20(b)**     Acceleration profiles from S2 for ten consecutive drives.

Fig. 5.21 shows acceleration profiles along X- and Z-axis respectively for five repetitive drives (D1, D2, D3, D4, and D5) for S1. Similar profiles were obtained from S2. The large negative X-axis acceleration profiles, minimal variations in Y-axis acceleration in Fig. 5.20 and five similar profiles in Fig. 5.21a show good consistency. The peak prior to large negative peak in Fig. 5.20 comes from the back-lift and followed two bat tap peaks in drive 1 of $a_{x1}$ before 89.68s and confirmed by the video footage. The plots in Fig. 5.21(a) and also in Fig. 5.21(b) were aligned in time by the large negative peak and the large positive peak respectively. Because each of the five repetitive drives differed by their start time.

Strong linear variation ($R^2=0.999$) in both $T1_{Xmn}$ and $T2_{Xmn}$ and almost similar time differences between adjacent points of $P1_{Xmn}$ and $P2_{Xmn}$ of all the consecutive drives shows batter competency. $P1_{Xmn}$ and $P2_{Xmn}$ are the large negative maximum peaks of $a_{x1}$ and $a_{x2}$ respectively, and $T1_{Xmn}$ and $T2_{Xmn}$ are the time of happening of those peaks (Fig. 5.20(a) and Fig. 5.20(b)). However, there are time and magnitude differences between $P1_{Xmn}$ and $P2_{Xmn}$ peaks as observed from the Table 5.4 (a). For all the drives peak $P1_{Xmn}$ from sensor S1 had a greater magnitude (except drive 10) and occurred earlier than S2 peak, $P2_{Xmn}$. Similar results was obtained from five repetitive drives as shown in Table 5.4(b) except drive D2 in which $P2_{Xmn}$ is greater in magnitude than $P1_{Xmn}$. These differences came from the fact that the '*on-side*' edge of the bat is subjected to a greater velocity compared to the '*off-side*' and S1 was attached '*on-side*' of the batter. This fact is reinforced by the similar results obtained from peak to peak Z-axis acceleration ($PP1_Z$ from S1 and $PP2_Z$ from S2) differences in five repetitive drives as shown in Table 5.4(b). $PP1_Z$, $PP2_Z$ are the magnitude between the large positive peak (aligned in time as shown in Fig. 5.21(b) for S1) and next negative peak for each drive from S1 and S2 respectively.

In these drives shown in Fig. 5.20 the tilted position of the stationary bat at the start of each drive can be identified from the Z-and X-axis acceleration values. They differ from zero and minus one g respectively for the vertical stationary bat. For instance, drive D4 was tilted the most and D2 was tilted the least out of the 5 drives. Because

the drive D4 differs more from -1g and 0g in Fig. 5.21(a) and Fig. 5.21(b) respectively than other drives, but D2 is more close to these values in those figures accordingly compared to other drives.
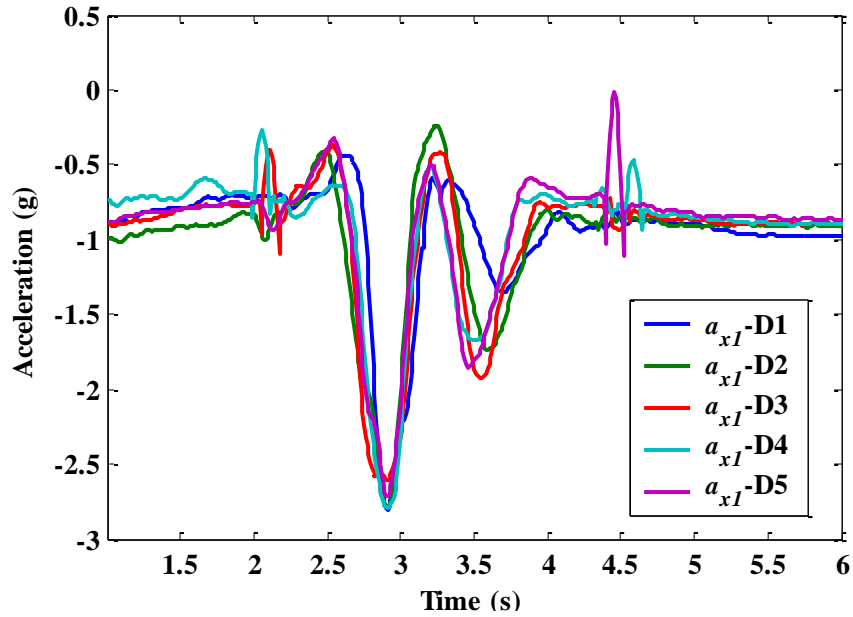


**Fig. 5.21(a)**     X-axis acceleration profiles from sensor S1 for five repetitive drives.
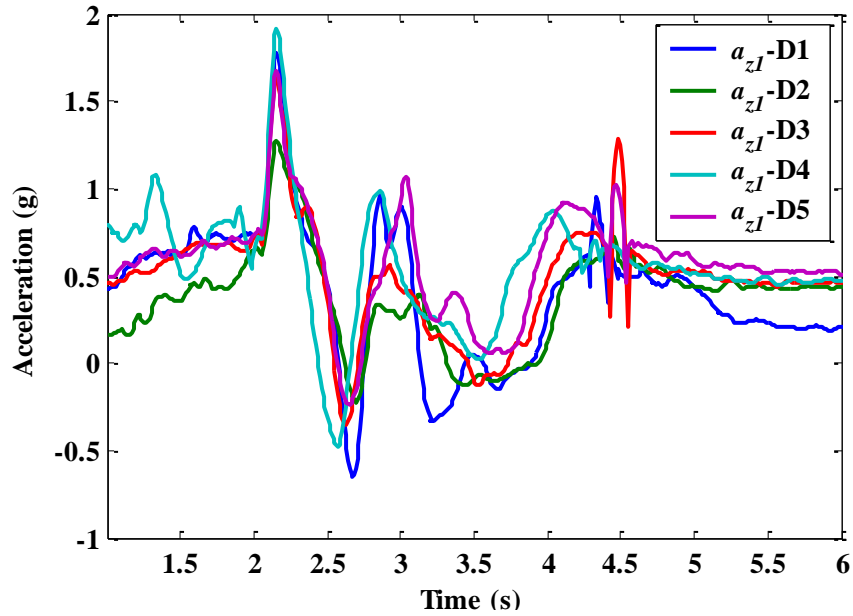


**Fig. 5.21(b)**     Z-axis acceleration profiles from sensor S1 for five repetitive drives.

The acceleration profiles from three different speeds straight drive ('*Slow*', '*Medium*', and '*Higher*') from S1 by the same amateur batter is shown in Fig. 5.22 (a similar trend of S2 profiles is not shown to avoid overcrowding of figures). Each drive commenced after three bat taps. Different speeds generated different maximum values in the acceleration profiles.

**Table 5.4** Temporal and magnitude data from the two sensors S1 and S2 for (a) ten consecutive drives, (b) five repetitive drives.

|  | 1 | 2 | 3 | 4 | 5 | 6 | 7 | 8 | 9 | 10 |
|---|---|---|---|---|---|---|---|---|---|---|
| $P1_{Xmn}$ (g) | -1.977 | -2.785 | -3.029 | -2.728 | -2.748 | -2.887 | -2.828 | -3.111 | -3.512 | -3.652 |
| $T1_{Xmn}$ (s) | 90.61 | 94.71 | 98.21 | 101.5 | 104.8 | 107.9 | 111.1 | 114.3 | 117.5 | 120.7 |
| $P2_{Xmn}$ (g) | -1.961 | -2.726 | -2.93 | -2.703 | -2.582 | -2.847 | -2.8 | -3.039 | -3.444 | -3.762 |
| $T2_{Xmn}$ (s) | 90.71 | 94.8 | 98.3 | 101.6 | 104.9 | 108 | 111.2 | 114.3 | 117.6 | 120.9 |
| $P1_{Xmn}$ - $P2_{Xmn}$ | -0.016 | -0.059 | -0.099 | -0.025 | -0.166 | -0.04 | -0.028 | -0.072 | -0.068 | 0.11 |
| $T2_{Xmn}$ - $T1_{Xmn}$ | 0.1 | 0.09 | 0.09 | 0.1 | 0.1 | 0.1 | 0.1 | 0 | 0.1 | 0.2 |

|  | $P1_{Xmn}$ (g) | $T1_{Xmn}$ (s) | $P2_{Xmn}$ (g) | $T2_{Xmn}$ (s) | $P1_{Xmn}$ - $P2_{Xmn}$ | $T2_{Xmn}$ - $T1_{Xmn}$ | $PP1_Z$ (g) | $PP2_Z$ (g) | $PP1_Z$ -$PP2_Z$ |
|---|---|---|---|---|---|---|---|---|---|
| D1 | -2.939 | 28.88 | -2.824 | 29.01 | -0.115 | 0.13 | 2.4287 | 2.1484 | 0.2803 |
| D2 | -2.781 | 36.82 | -2.792 | 37.2 | 0.011 | 0.38 | 1.4833 | 1.23832 | 0.24498 |
| D3 | -2.626 | 30.6 | -2.58 | 31.35 | -0.046 | 0.75 | 1.9685 | 1.6414 | 0.3271 |
| D4 | -2.816 | 29.36 | -2.75 | 30.29 | -0.066 | 0.93 | 2.4026 | 1.8561 | 0.5465 |
| D5 | -2.783 | 27.05 | -2.661 | 27.64 | -0.122 | 0.59 | 1.9215 | 1.40286 | 0.51864 |

Table 5.5 shows the maximum negative value of $a_{x1}$ and $a_{x2}$ ($P1_{Xmn}$ and $P2_{Xmn}$ respectively) and peak to peak value of $a_{z1}$ and $a_{z2}$ ($PP1_Z$ for S1 and $PP2_Z$ for S2 respectively) during stroke swing period at Slow, Medium and Higher speed. It is evident that the variation in the acceleration is larger in the Z-axis compared to the X both for S1 and S2 for all speeds. The reason for these differences in variability is related to the effect of the straight drive speed on the tangential and radial direction of the swing arc. As the Amateur accomplished the straight drives at almost the same
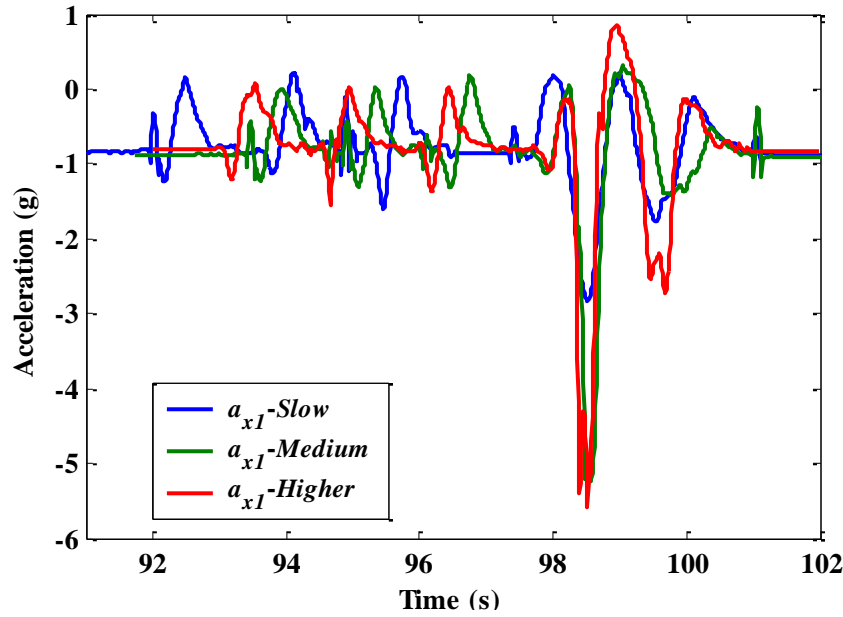
**Fig. 5.22(a)**   X-axis acceleration profiles from sensor S1 for straight drives at different speeds. The profiles are aligned based on the maximum negative peak of each drives started at different time.
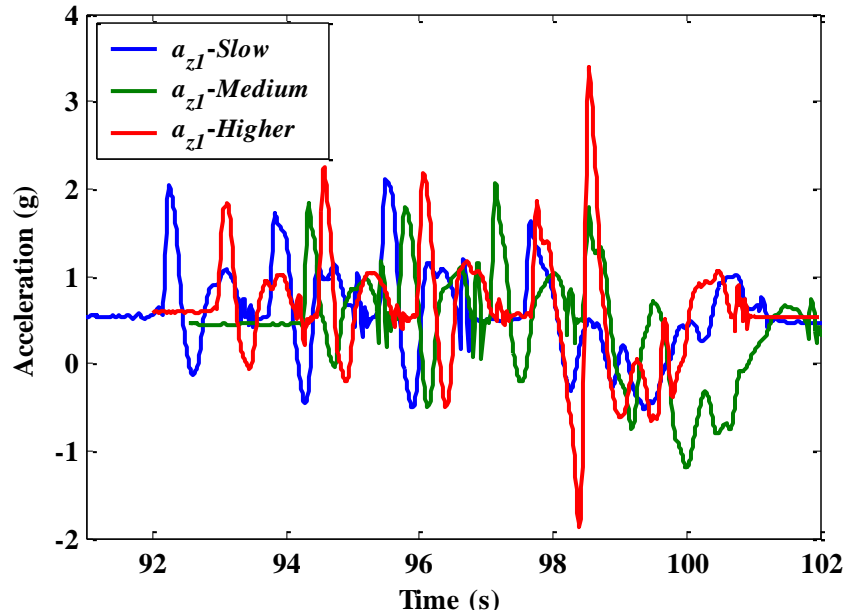


**Fig. 5.22(b)**   Z- axis acceleration profiles from sensor S1 for three straight drives at different speeds. The profiles are aligned based on the positive peaks during the forward swing in each drives.

radius of curvature during the swing by keeping his body in the same position for all three speed drives (confirmed by the video footage), the centripetal force in the radial

direction (X-axis direction) was affected less than compared to tangential direction force. The centripetal acceleration is shown in the last term of the right-hand side of Equation 4.16. This is because the straight drives and the speed variations were in tangential direction of the swing arc, then the centripetal force with similar radius of curvature in each drive was not affected significantly by different speed. However, in each of the three speed drives and also in the previous set of drives (ten consecutive, five repetitive), the X-axis profiles had a maximum acceleration when the bat was aligned to gravity (confirmed by the video). This is because of the higher centripetal force while the bat was close to the batter resulting in a minimum radius of gyration and maximum value of gravitational force. During the drive, the bat passes close and parallel to the legs of the batter. At this point, the radius of gyration is minimum.

**Table 5.5** Magnitude data of three speed drives. Note that the data are the maximum values in the X- and Z-axis profiles from sensor S1and S2.

|  | $P1_{Xmn}$ (g) | $P2_{Xmn}$ (g) | $PP1_Z$ (g) | $PP2_Z$ (g) |
|---|---|---|---|---|
| **Slow** | 2.82 | 2.81 | 0.83 | 1.28 |
| **Medium** | 5.23 | 4.95 | 1.55 | 1.80 |
| **Higher** | 5.60 | 5.72 | 5.28 | 6.45 |

### 5.3.3 Conclusions

Several sets of straight drives were recorded using triaxial accelerometer sensor together with video tracking to interpret bat swing. The acceleration profiles from the sensor data showed good consistency for all the drives. The time and magnitude difference between the '*on-side*' and '*off-side*' positioned sensors data for all the drives indicated a swing speed difference between the two sides of the bat. The highest magnitude of the acceleration along bat length direction was found when the bat was aligned to gravity. This was interpreted as the result of the highest centripetal force and maximum gravity at this time of swing. While the bat was very close to the batter the radius of gyration is smaller. Different speeds in the straight swing did not affect the acceleration (along bat length) but the speed variation was clearly realized from the acceleration in the straight swing direction. This resulted from the fact that the radius of rotation in the three speed drives was very similar, so this could not

have much effect on centripetal force. It affected the tangential acceleration much more. The tilted position of the stationary bat was determined from the acceleration values before commencing each drive. These results show that the accelerometer can replace other measurement technologies. These results need to be further investigated using more batters and the video data analysis system to finding out whether the same acceleration profiles result.

## 5.4    Sweet-spot impacts

Sweet spot impacts are accompanied by minimal jarring of the hands and forearms. Using 3 axis accelerometers mounted on the bat and the wrists, ball strikes were recorded for defensive drives along the ground. This work seeks to categorize the sweet spots hits from the cricket bat/ball contact using accelerometers.

### 5.4.1 Background

The background of this study was stated in section 2.8 in the literature review chapter. As included in that section, the literature is stating that sweet-spot hits should be categorized by the batters from the vibration transmitted from the bat to batter's hand. The motivation for this experiment was to identify the sweet spot hits on a cricket bat by judging the value of acceleration in the batters wrists attached sensors.

The first experiment used an accelerometer mounted on a stationary hand-held cricket bat in which three hits at the middle, upper and lower were conducted. The second experiment was designed to identify the sweet spot hits from defensive drives along the ground by five novice players. Accelerometers were attached to the wrists (left and right) and also the upper part of the back of the bat (opposite to hitting surface). The acceleration profiles from these experiments were used to identify the impact location on the bat, and the sweet spot hits.

### 5.4.2 Experimental Procedure

Accelerometer sensors capable of measuring acceleration of ±10g in three dimensional spaces were used in this work. Fig. 5.23(a) and Fig. 5.23(b) show the sensor (S) location in the bat for the first and second experiments respectively. The sensor and bat axis orientation is similar to Fig. 4.4.
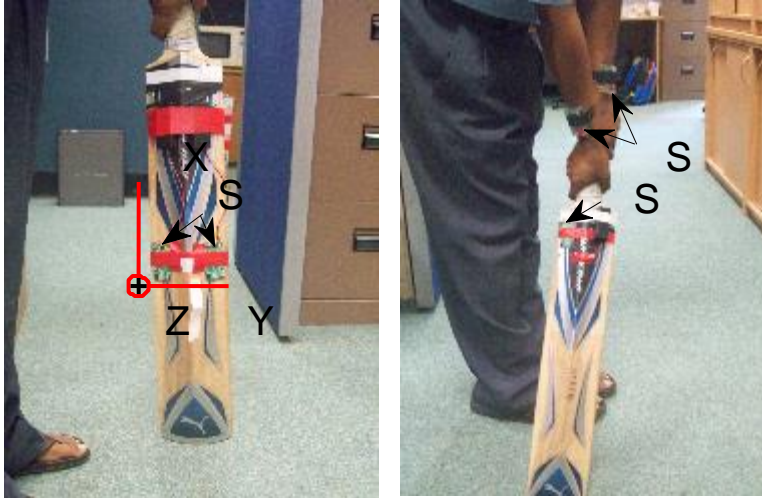


**Fig. 5.23**   Accelerometer placement in (a) hand-held bat for first experiment; (b) wrists and bat for second experiment.

The bat blade was notionally divided into three regions measured from the toe of the bat to categorize the hits. A low hit impacted that bat between 11-22 cm, a middle hit between 22-33 cm and the top between 33-44cm. The centre of mass of the bat was at 34.5 cm. The bat was swung in the ZX plane (perpendicular to the ground YZ-plane) in which X-axis was opposite to gravity direction (Fig. 5.23(a)). The wrists sensors were oriented in a similar direction. In the first experiment the bat was suspended just above the ground with hands placed in the normal batting position. The hits were performed at the bottom, middle and top position to a cricket ball thrown with constant speed at the stationary bat. In the second experiment, the novices were asked to hit the thrown ball in the middle of the bat using a defensive stroke. The bat was marked by tape in the three different zones. All ball-contacts were assessed and written down by an independent observer. The drives were also

captured by a video camera and its position detail is provided in Section 4.1.3.1. The video record was used to confirm the ball-contact location. The impact location (for sweet-spot impacts) was judged along the bat length (in 1D) in three regions. Only impacts close to the centre line of the bat were considered for analysis.

### 5.4.3 Results and discussion

A set of acceleration profiles from one ball contact in the first experiment is shown in Fig. 5.24. Fig. 5.24(a) shows the profiles from the sensor positioned on in the player side of the bat (left sensor in Fig. 5.23(a)) from ball hits on the stationary hand-held bat at bottom, middle and top positions on the blade. The acceleration before and after the hits was constant at -1g for X-axis and 0g for Z- and Y-axes. The spikes in the figure represent the hit. Fig. 5.24(b), (c) and (d) shows the expanded profiles during the hits. The contact points of the ball during the hits were measured manually (a reflective tape was used to locate the impact point): the middle hit was 29 cm from the toe of the bat, the bottom hit was 24 cm, and the top hit was 34.5 cm.
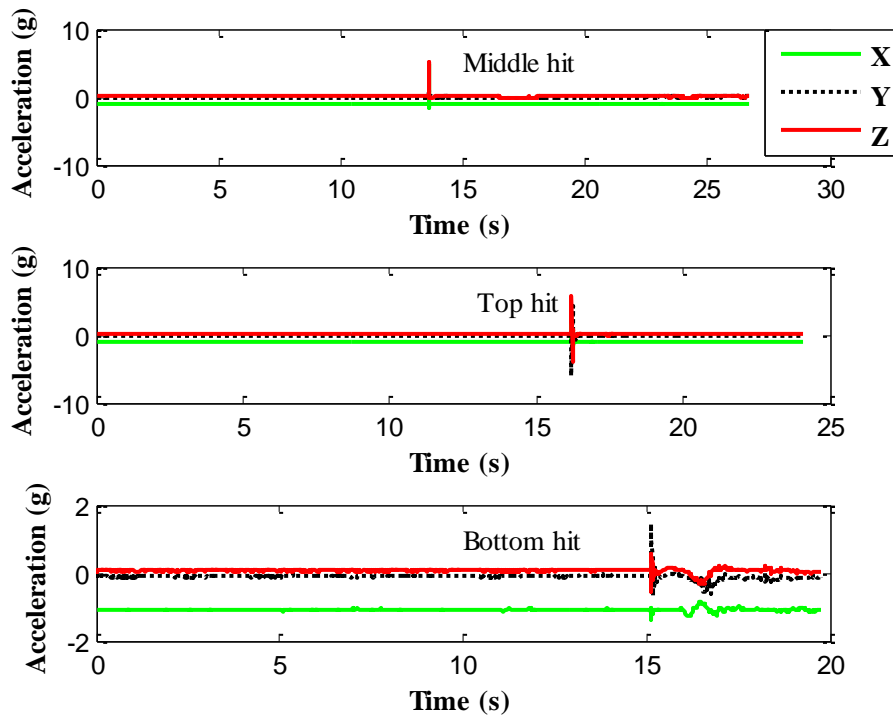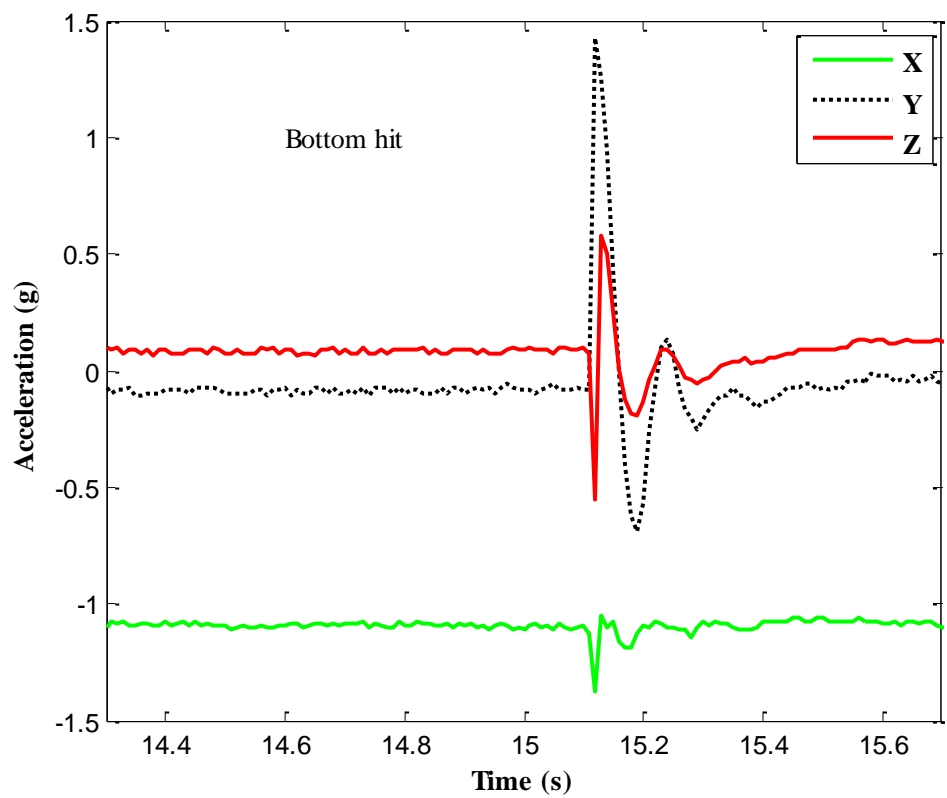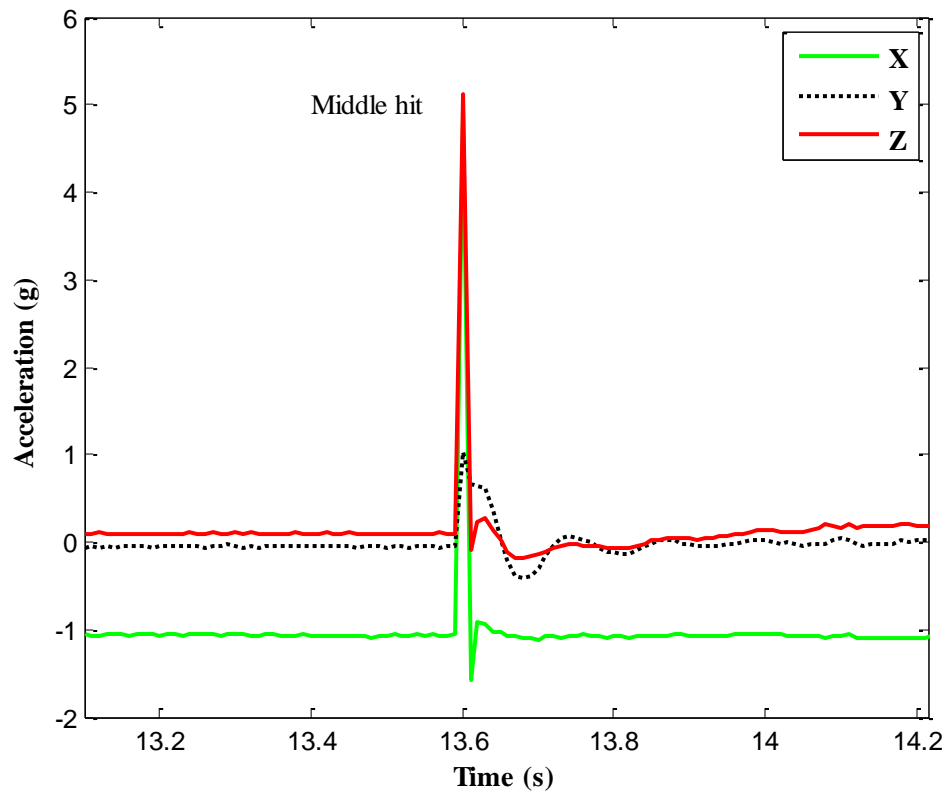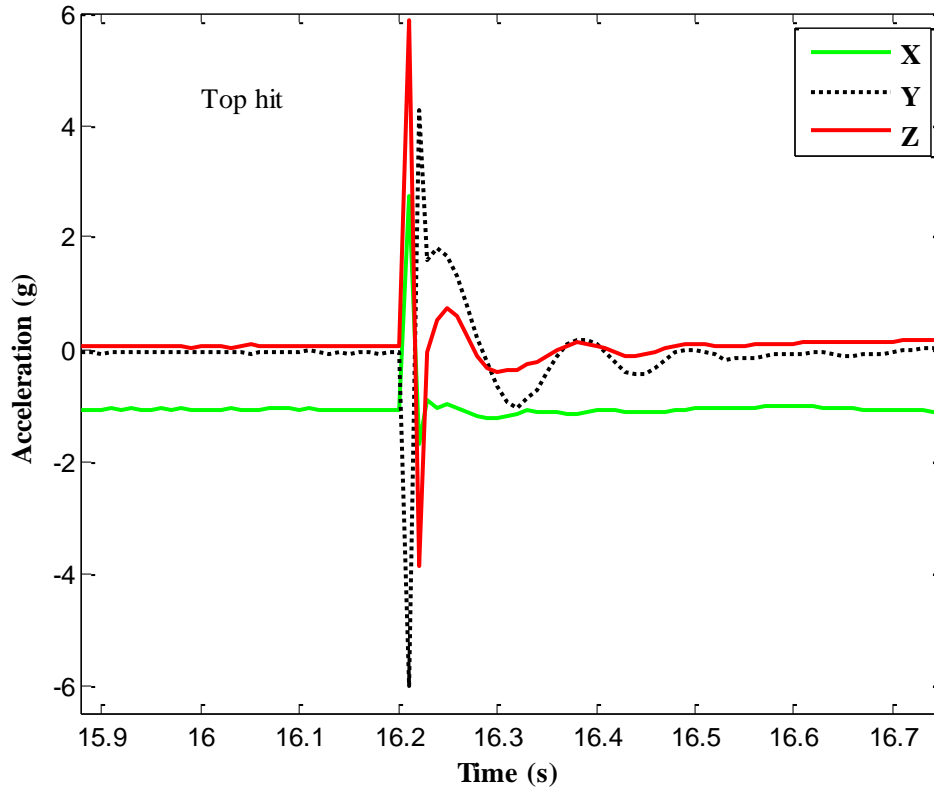
**Fig. 5.24** Acceleration profiles for all three hits on a stationary bat (a). The expanded view for a middle hit (b), bottom hit (c), and a top hit (d).

The X-, Y-and Z-axis acceleration values for the middle, bottom and top hits are shown in Table 5.6. For the top and middle hits, the X-axis acceleration has a positive value and for the bottom hit, it is negative according to the sensor X-axis orientation. The X-and Z-axis accelerations have small values for the bottom hits because that hit occurred close to the sweet spot (almost in agreement with [90] that stated the centre of sweet spot region was defined at about 15 cm from the toe of the bat, the region is bat-dependent and extends for a significant distance range along the vertical axis of the blade).

The results from the second experiments are shown in Fig. 5.25. Fig. 5.25(a) shows the spikes from the bat mounted sensor for 10 novice hits. Fig. 5.25(b) shows records from the wrists' (right wrist, left wrist) sensors. Total 61 hits were made by five novices (1st, 2nd and 3rd novice made 10 hits each in two sessions, and 4th, 5th novice

made 16 and 15 hits respectively three sessions each). Before each session the novices were instructed to tap the ground (see Fig. 4.14) for a timing reference with the video. Fig. 5.26(a) shows the total wrist accelerations normalized by the bat acceleration for all novice hits.

**Table 5.6** Magnitude of the acceleration spikes for three hits, one at the top of the bat, one in the middle of the bat and the other at the bottom of the bat (only one event was recorded for the three hits).

|  | Middle hit | Bottom hit | Top hit |
|---|---|---|---|
| **X-acceleration** | 4.884g | -1.380g | 2.748g |
| **Y-acceleration** | 1.026g | 1.431g | -6.031g |
| **Z-acceleration** | 5.123g | -0.557g | 5.874g |

The green dashed vertical lines indicate the points in the upper figure of Fig. 5.26(a) that show the good contacts assessed by the independent assessors and the red lines indicate points when no ball contact occurred.
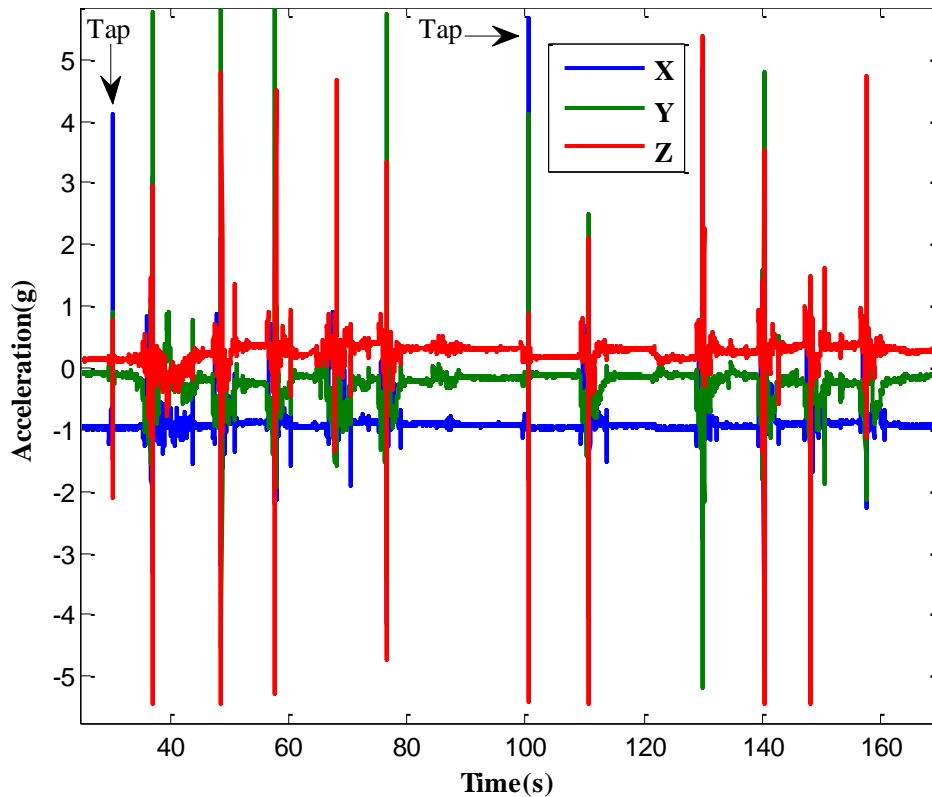


**Fig. 5.25(a)**     Acceleration profiles from ten hits using bat mounted sensors.
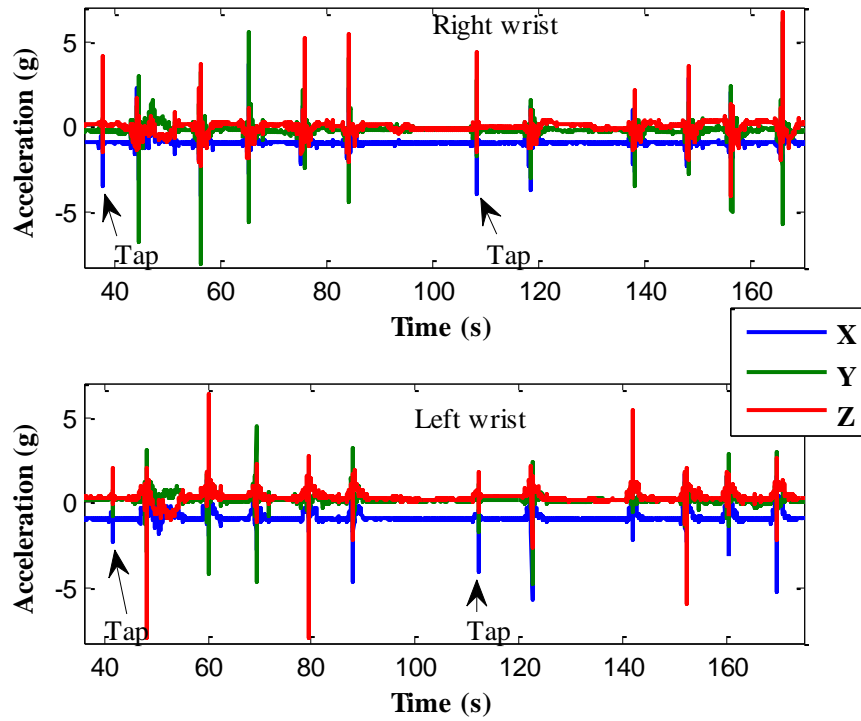
**Fig. 5.25(b)** Second experiment's acceleration profiles from 1st novice's ten hits in wrists' sensors.

The minimum values of the acceleration from the right wrist are observed for the good contacts (sweet spot hits in middle figure of Fig. 5.26(a)) with an exception the last two contacts. The average acceleration from both wrists are shown in the bottom figures of Fig. 5.26(a) and the lower values of acceleration are observed for sweet spot hits compared with poor contacts.

The Y-axis acceleration data from the right and left wrists ($Y_R$ and $Y_L$ respectively) and the resultant of X-,Y- and Z-axis acceleration from right and left wrists ($TOT_R$ and $TOT_L$) for all of the novices (N1~N5)' hits (C1~C16) are shown in Table 5.7. The red color figures in the tables represent very good contact around the middle (about 18~22 cm from the toe of the bat) assessed by the independent assessors and the video. The blue figures represent good contacts assessed visually. From the table, it is evident that for good contacts both the left and right wrists have a minimum Y-axis acceleration; that is, perpendicular to the swing plane accountable for the

dominant component of hand vibrations when the bat twists during the ball contact.
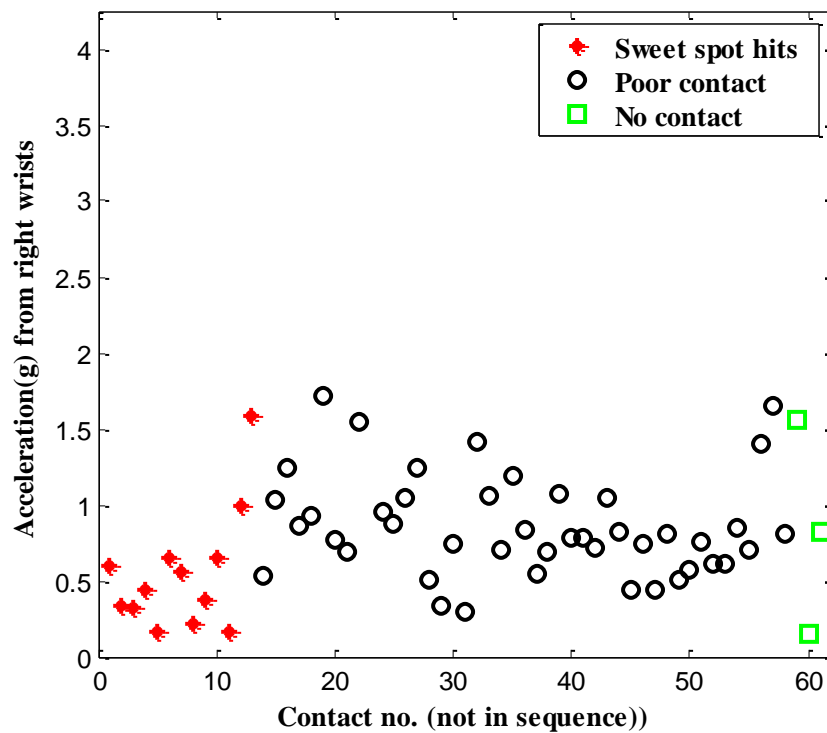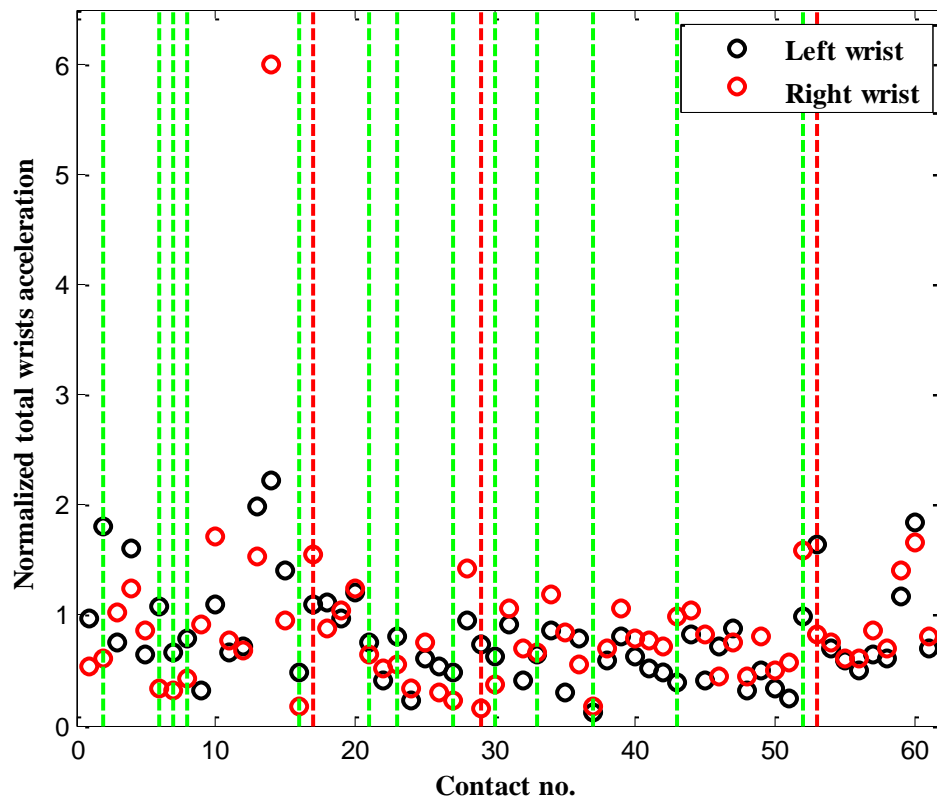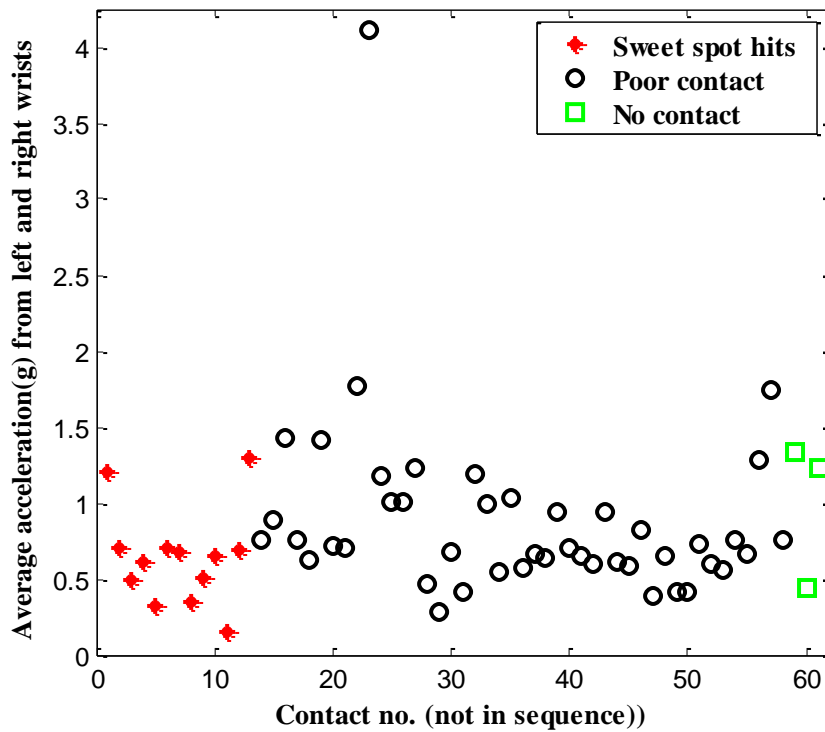
**Fig. 5.26(a)**     Wrists acceleration (normalized by bat's acceleration), the vertical green lines show the sweet spot hits, the three red lines indicates no contact (upper figure); write wrist acceleration grouped for sweet spot hits, poor contact and no contact (middle figure); average acceleration from both wrists in the groups as mentioned (bottom figure).

Fig. 5.26 (b) plots that Y-axis acceleration values averaged from right and left wrist data ($Y_R$, $Y_L$) shown in the upper part of Table 5.7. In the figure the red, blue, black legend represent very good (termed as 'excellent' in the figure to be consistent with the plot for lower part of the table), good and poor contact respectively. A minimum Y-axis average acceleration values is observed in the figure for 'excellent' and 'good' contact. In the table, the starred figures represent the swings with no ball contact. These events show a minimum Y-axis acceleration value because there is minimal jerking of hand due to no ball contact.

The acceleration from the right wrist (lower part of Table 5.7) also has a small value for both excellent and good contacts with an exception of contact C1, C3 by 3$^{rd}$ novice (N3) and C3, C13 by 4$^{th}$ novice (N4). The term 'excellent' was used to those

209

contacts characterized by the assessor and video, 'good' by visually and 'no contact' by the assessor only. In the table the 'poor' contacts are not marked but realized by the larger values of the acceleration. The plot for the 'excellent contact', 'good contact', 'no contact' and 'poor contact' marked in the table is shown in the Fig. 5.26 (c). In the coaching manuals for a defensive stroke it is stated that on impact the bottom hand should act as a shock absorber [94], so the total acceleration from the right hand (bottom hand) should also be small for excellent and good bat-ball contacts and it is observed in Fig. 5.26 (c) by the red and blue coloured legends.

**Table 5.7** Y-axis contact point and Total accelerations from right and left wrist sensors.

|  |  | C1 | C2 | C3 | C4 | C5 | C6 | C7 | C8 | C9 | C10 | C11 | C12 | C13 | C14 | C15 | C16 |
|---|---|---|---|---|---|---|---|---|---|---|---|---|---|---|---|---|---|
| N1 | $Y_R$ | 2.94 | 1.56 | 5.59 | -2.45 | -4.47 | 0.70 | 1.12 | 0.34 | 2.39 | -5.78 |  |  |  |  |  |  |
|  | $Y_L$ | 0.34 | -1.11 | 4.52 | -0.06 | -1.54 | 1.49 | 1.15 | 1.14 | 0.08 | -0.69 |  |  |  |  |  |  |
| N2 | $Y_R$ | -0.23 | -4.79 | -1.47 | -5.40 | 0.98 | 0.05 | -0.12* | -4.65 | 5.66 | 2.69 |  |  |  |  |  |  |
|  | $Y_L$ | 4.88 | 1.75 | 8.12 | -1.61 | 8.12 | -0.86 | -0.26* | 1.80 | -1.14 | 4.43 |  |  |  |  |  |  |
| N3 | $Y_R$ | 0.64 | 2.67 | -1.10 | 2.47 | -4.56 | -0.16 | 0.68 | -8.02 | 0.10* | -1.50 |  |  |  |  |  |  |
|  | $Y_L$ | -1.21 | -1.04 | -0.88 | 1.25 | 0.62 | 2.37 | 1.08 | -3.98 | 0.78* | 0.64 |  |  |  |  |  |  |
| N4 | $Y_R$ | 0.27 | 0.12 | 0.60 | -3.61 | -2.72 | 0.65 | -0.09 | 3.40 | 2.40 | 4.05 | 3.19 | -4.01 | 0.52 | -4.01 | -4.01 | 0.01 |
|  | $Y_L$ | 2.24 | -2.33 | -0.18 | -3.98 | 1.49 | 4.01 | 0.67 | 1.52 | -1.32 | -3.98 | -1.59 | 4.01 | 1.05 | -3.98 | -3.13 | -3.98 |
| N5 | $Y_R$ | -1.57 | -0.39 | 4.05 | 0.87 | -3.08 | -0.31 | 0.01* | -2.30 | -2.03 | -0.84 | 3.52 | 1.04 | -2.16 | 2.65 | -3.47 |  |
|  | $Y_L$ | -3.98 | -2.50 | 1.12 | 1.80 | -2.24 | 0.32 | 0.99* | -2.68 | -3.98 | -2.02 | -3.98 | -3.98 | 4.01 | 4.01 | 4.01 |  |

|  |  | C1 | C2 | C3 | C4 | C5 | C6 | C7 | C8 | C9 | C10 | C11 | C12 | C13 | C14 | C15 | C16 |
|---|---|---|---|---|---|---|---|---|---|---|---|---|---|---|---|---|---|
| N1 | $TOT_R$ | 4.35 | 2.16 | 6.66 | 6.14 | 7.24 | 2.04 | 2.82 | 3.55 | 5.09 | 8.91 |  |  |  |  |  |  |
|  | $TOT_L$ | 7.98 | 6.50 | 4.89 | 7.96 | 5.42 | 6.45 | 5.84 | 6.50 | 1.72 | 5.75 |  |  |  |  |  |  |
| N2 | $TOT_R$ | 6.50 | 4.83 | 8.79 | 10.39 | 5.78 | 1.40 | 2.45* | 6.63 | 7.39 | 9.75 |  |  |  |  |  |  |
|  | $TOT_L$ | 5.63 | 5.05 | 11.36 | 3.85 | 8.54 | 3.94 | 1.73* | 8.48 | 6.90 | 9.45 |  |  |  |  |  |  |
| N3 | $TOT_R$ | 4.52 | 2.99 | 4.95 | 2.71 | 5.32 | 2.22 | 0.90 | 8.69 | 0.46* | 2.17 |  |  |  |  |  |  |
|  | $TOT_L$ | 5.26 | 2.40 | 7.21 | 1.92 | 4.36 | 4.01 | 1.96 | 5.86 | 2.26* | 3.70 |  |  |  |  |  |  |
| N4 | $TOT_R$ | 5.60 | 4.96 | 5.72 | 6.51 | 6.22 | 4.69 | 1.48 | 5.31 | 5.37 | 6.99 | 6.52 | 6.88 | 5.72 | 6.88 | 6.88 | 4.13 |
|  | $TOT_L$ | 4.89 | 2.88 | 5.59 | 4.76 | 2.16 | 6.70 | 1.08 | 4.46 | 4.07 | 5.60 | 4.29 | 4.64 | 2.21 | 5.41 | 3.44 | 6.88 |
| N5 | $TOT_R$ | 5.79 | 4.05 | 6.87 | 4.12 | 5.42 | 3.31 | 1.04* | 5.05 | 4.57 | 5.66 | 6.69 | 5.68 | 6.00 | 6.19 | 6.58 |  |
|  | $TOT_L$ | 6.82 | 2.98 | 4.25 | 2.69 | 2.36 | 2.07 | 2.08* | 4.73 | 4.36 | 4.62 | 5.06 | 4.89 | 4.98 | 6.88 | 5.65 |  |
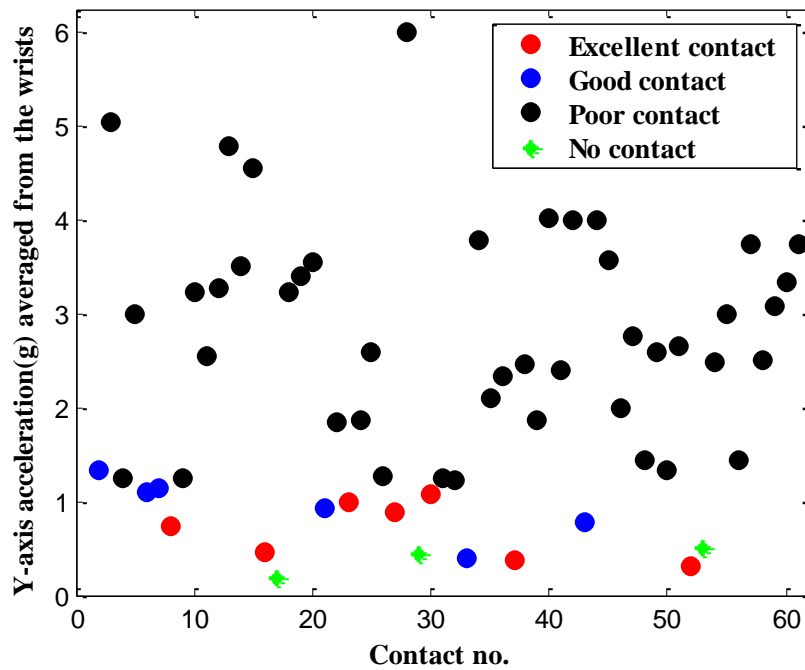
**Fig. 5.26(b)** Y-axis acceleration averaged from right wrist ($Y_R$) and left wrist ($Y_L$) data as shown in upper part of Table 5.7. The red, blue and black colour legends represent 'excellent', 'good' and 'poor' contact respectively, whereas, the green legend is for 'no contact'.
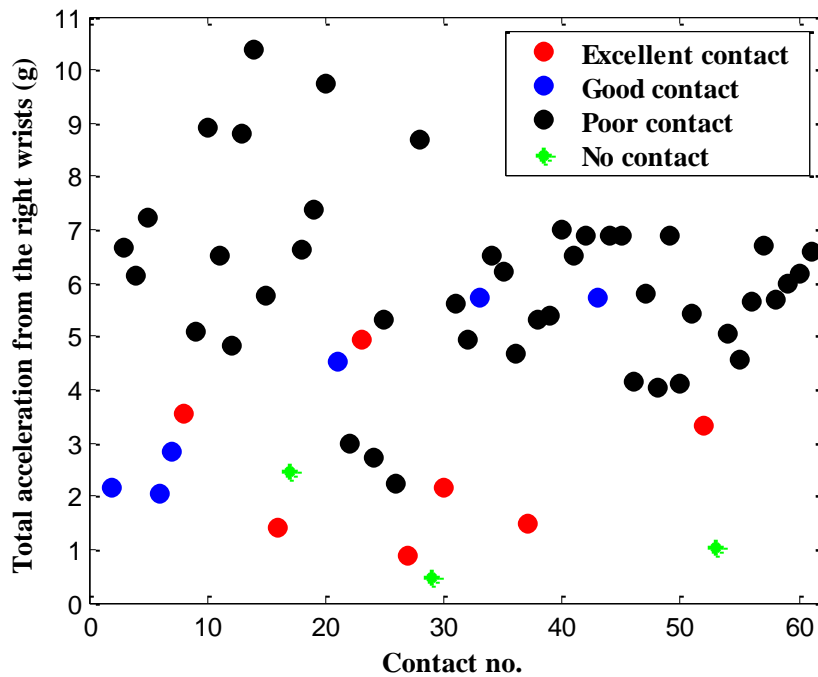


**Fig. 5.26(c)** Total acceleration from the right wrist ($TOT_R$) data as shown in lower part of Table

5.7. The red, blue and black colour legends represent 'excellent', 'good' and 'poor' contact respectively, whereas, the green legend is for 'no contact'.

Converting the acceleration into velocity by integration, Fig. 5.26 (d) shows the total wrist velocities ($V1_{LWR}$ ~ $V5_{LWR}$ for left and $V1_{RWR}$ ~ $V5_{RWR}$ for right wrists) plotted against bat velocity for all hits. The integration constants were taken to be similar for all the novices and the units of velocity are thus chosen arbitrary (arb.). A linear relationship was obtained between the wrists and bat velocity, meaning that wrist vibrations are the result of bat vibration for the ball contacts.
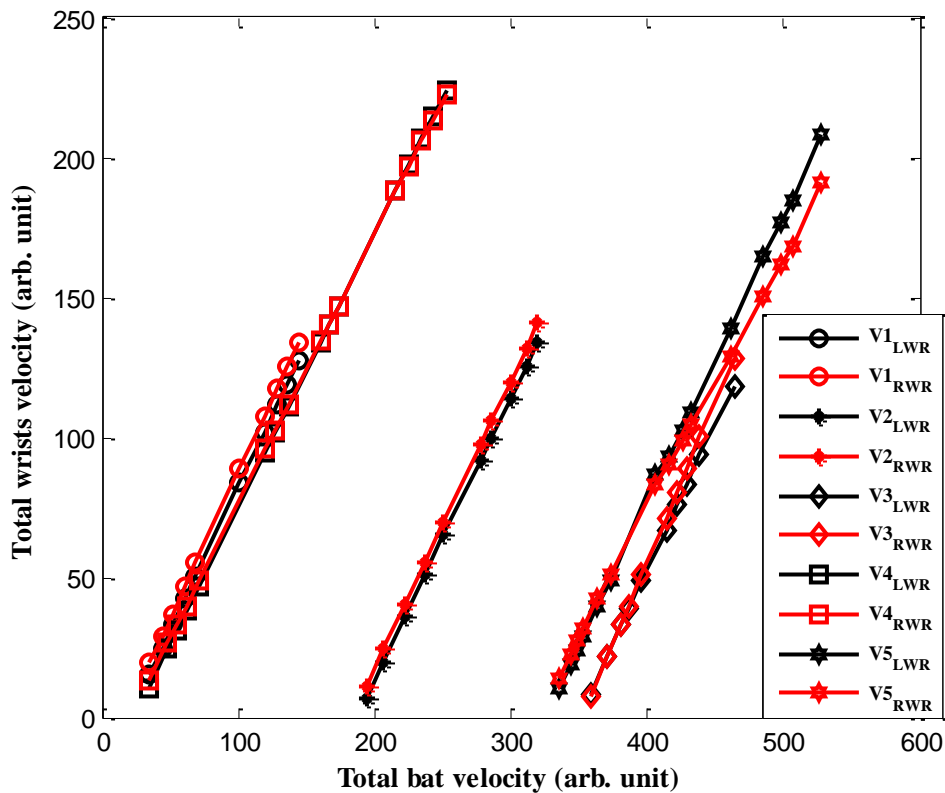


**Fig. 5.26(d)**  Wrist velocity versus bat velocity for all hits by all players.

### 5.4.4 Conclusions

Two experiments were undertaken to identify the accelerometer profiles for sweet spot hits on a cricket bat. The contact location of the ball along the length of the bat was identified using video and subject assessment. These experiments revealed that

sweet spot hits can be identified from minimum values of total wrist acceleration. Ball contacts at the bottom, middle, and top in the bat were distinguishable from the sign of the acceleration along the bat axis (X-axis acceleration). This is caused by rotations around the impact point of the bat. The Y acceleration of both the left and right wrists was comparatively small for sweet spot contacts. The minimum acceleration was observed for contacts made in the range of 18 to 22 cm from the toe of the bat. These experiments were limited by the visual contact assessment and inconsistent ball throw velocity. The identification of sweet spot hits from the wrists showed promise. Future work requires accurate sweet spot hit location in 2D and a larger pool of batters and a ball machine for consistent ball velocity and trajectory.

## 5.5    Bat angles in straight drives and force level quantification

The angular position of the bat at the completion of a stroke is a measure of the applied force on the ball. In-field acceleration measurements (match and practice nets) allow an assessment of batting skill.

### 5.5.1 Background

The aim was to study the bat angles during the drives. In this work, at first the angular position of the bat swing (back-lift, drive and return) was matched using a cosine squared function of time from which the force applied by the batter was calculated. While this function assumes symmetry between the angular acceleration and deceleration, the function could be used for other implement (like bat/racquet/stick) swing sports for extracting key features related to swing angles. The centripetal forces applied by the batters were calculated from accelerometer sensor data and correlated with those calculated from the equation, and good agreement was obtained. The acceleration profiles of the bat were correlated with video determined angular position from sixty three straight drive swings by seven novice batters. Bland Altman covariance correlation method (Bland and Altman [112]) was used to determine the strength of the correlations. This measurement

technique can be used in the field accurately with minimal interference to normal stroke play.

### 5.5.2 Theory

*Swing angles equations*

A straight drive bat swing was divided into three phases as 'back-lift', 'drive' and 'return'. Each phase is characterized by zero angular velocity at the start and end. For a typical swing these temporal phases in the accelerometer recorded accelerations ($a_x$, $a_y$, $a_z$) are shown in Fig. 5.27. The video footage revealed the bat angle profile shown in Fig. 5.28 and the angle was relative to the vertical direction (i.e. opposite to the gravity vector). The duration of each phase (denoted by background color in Fig. 5.27) was estimated from the video footage with the timing established using bat tapping (see 'experimental procedure' section).
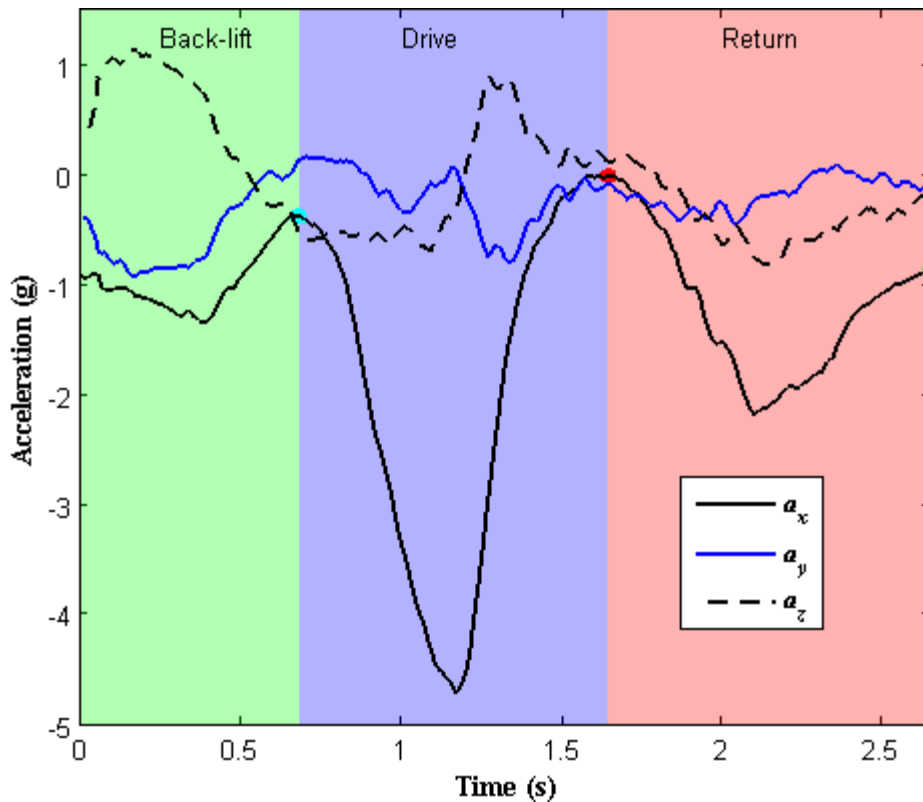


**Fig. 5.27**   Acceleration profiles from a typical swing showing the temporal phases: back-lift, drive, and return.

*Swing angle model*

As each bat phase starts with a stationary bat and ends with a stationary bat and the bat angle changes monotonically, video derived angles (Fig. 5.28) were fitted to a cosine squared time ($t$) dependence function. The bat angle $\theta$ measured from the vertical direction (relative to −g direction) is:

$$\theta(t) = K_1 \cos^2(At) + K_2 \tag{5.16}$$

where $K_1$, $A$, $K_2$ are the constants determined from the initial and final conditions in each phase of the swing.
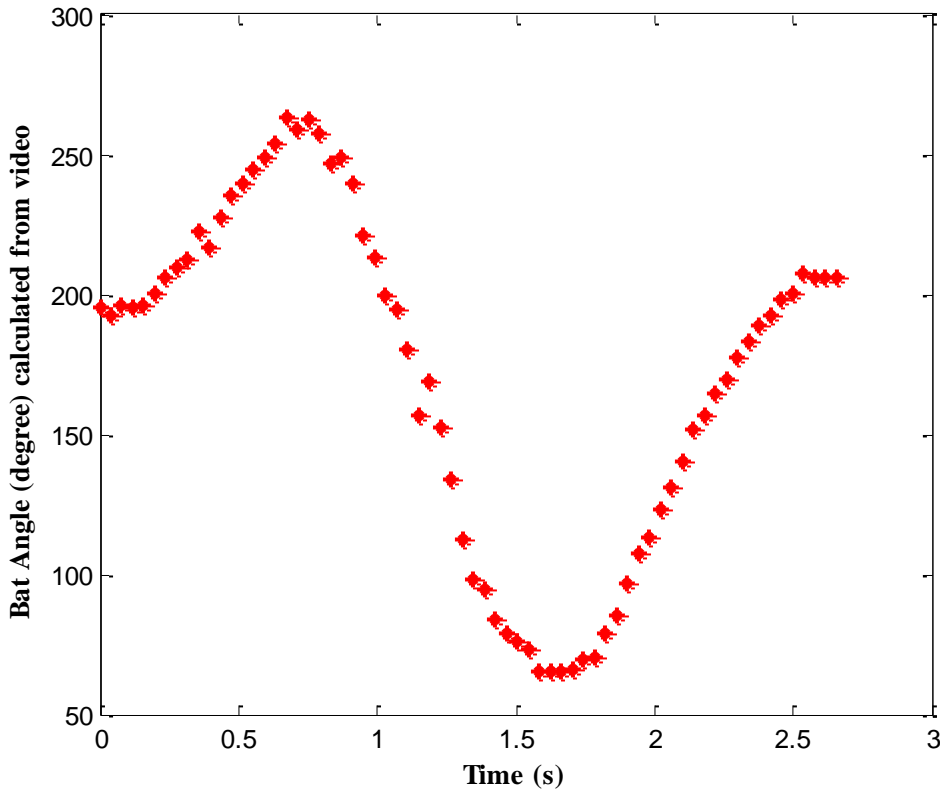


**Fig. 5.28** Bat angle variation for a typical swing (Fig. 5.27) determined from video analysis.

From equation 5.16, angular velocity $\omega$ is

$$\omega = \frac{d\theta}{dt} = -AK_1 \sin(2At) \tag{5.17}$$

The initial angular velocity at start of each phase (say at time= $t_1$) is zero, then we can write

$$\left.\frac{d\theta}{dt}\right|_{t_1} = 0 \qquad (5.18),$$

which satisfies equation 5.17.

The final angular velocity $\omega$ of each phase (say at time= $t_2$) is zero, then

$$\omega = \left.\frac{d\theta}{dt}\right|_{t_2} = 0 \qquad (5.19).$$

So from equation 5.17

$$AK_1 \sin(2At_2) = 0 \qquad (5.20),$$

and so $A = \dfrac{\pi}{2t_2}$ if the variation of $\theta$ is monotonic.

Substituting the initial angle of a phase (say $\theta_1$ at $t_1 =0$) in equation 5.16 gives:

$$K_1 + K_2 = \theta_1 \qquad (5.21).$$

Substituting the final angle of a phase (say $\theta_2$ at $t_2$) in equation 5.16 gives:

$$K_2 = \theta_2 \qquad (5.22).$$

Thus the equation of the swing angle can be written:

$$\theta(t) = (\theta_1 - \theta_2)\cos^2\left(\frac{\pi t}{2t_2}\right) + \theta_2 \qquad (5.23).$$

Using the video revealed initial ($\theta_1$) and final angles ($\theta_2$) of each phase of the bat swing (as shown in Fig. 5.28) and corresponding time duration, the swing angle

profile from equation 5.23 was estimated. Strong agreement (r=0.99) was obtained between the equation and the video swing angles in the drive. The same equation was applied to the other phases and r=0.97 and r=0.99 for back-lift and return phase respectively.

*Acceleration formulation*

## A.  Static Case:

The static case is when the bat is at rest. Then it is assumed that all first order and second order time differentials of the angle $\theta$ are equal to zero.
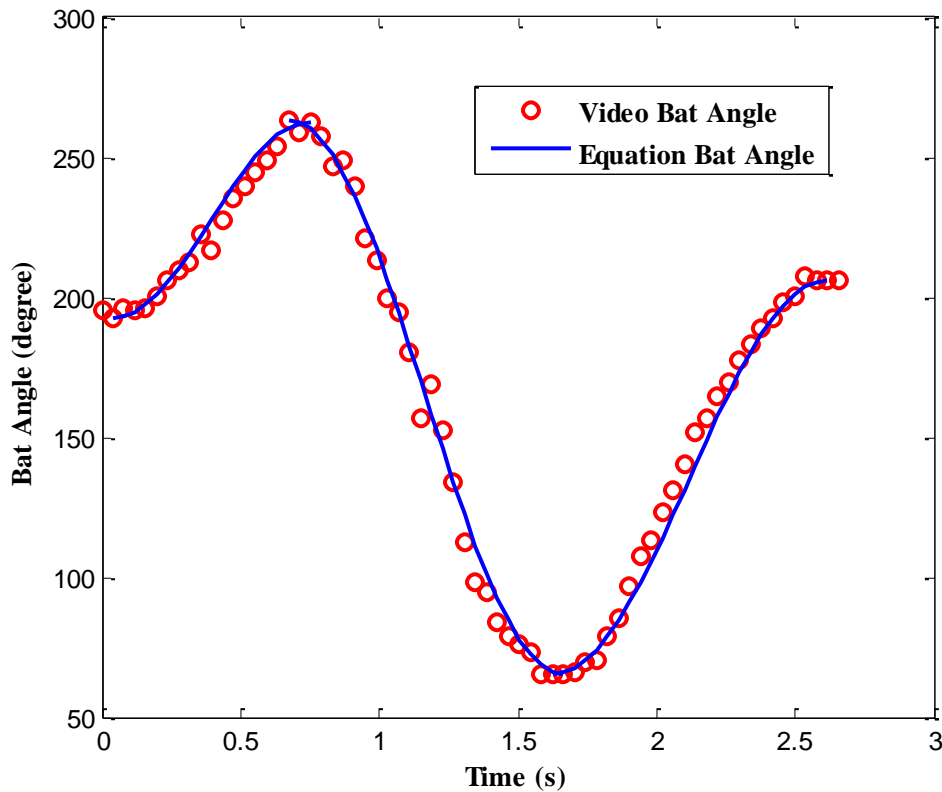


**Fig. 5.29(a)**       Video revealed and equation estimated swing angles for the typical swing in Fig. 5.27.

Thus the following two cases can be written:

$$\frac{d\theta}{dt} = 0$$

$$\frac{d^2\theta}{dt^2} = 0 \qquad\qquad (5.24).$$

Only the gravitational component contributes to the acceleration measured. Thus the three acceleration components on the sensor co-ordinate system can be converted to the gravitational co-ordinate system (using the traditional real world coordinates) as follows:
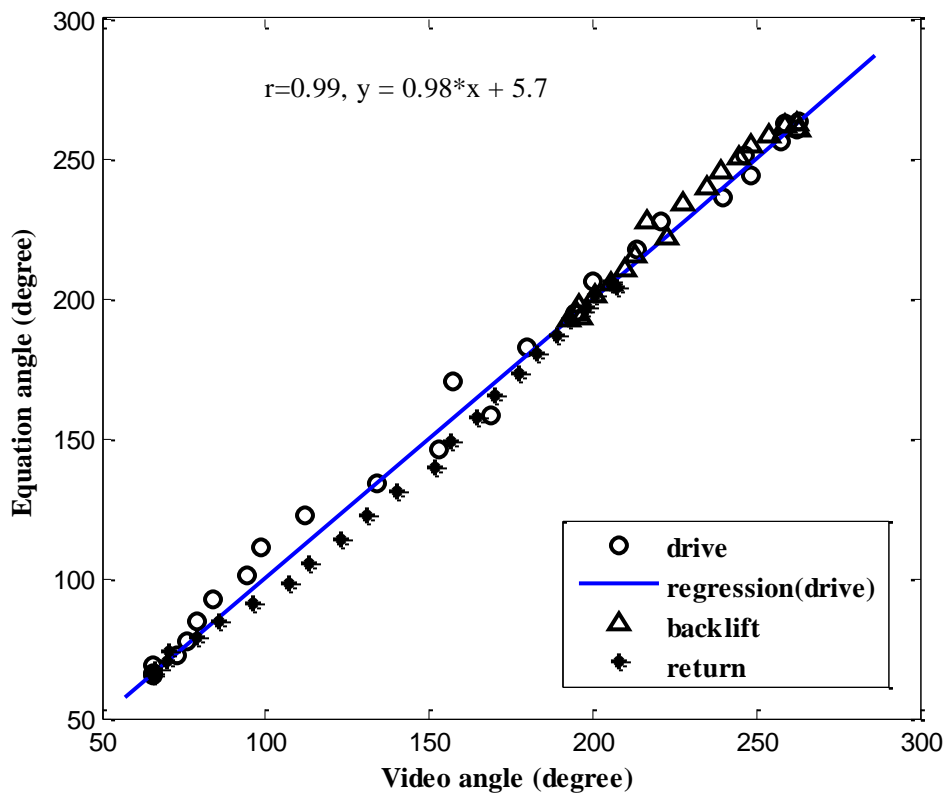


**Fig. 5.29(b)**    Video revealed versus equation estimated swing angles and the regression line (r=0.99) for the typical swing in Fig. 5.27.

$$a_x = g \cos\theta$$

$$a_y = g \sin\theta \sin\phi \qquad\qquad (5.25).$$

$$a_z = g \sin\theta \cos\phi$$

Then the total acceleration $a_{tot}$ is given by:

$$a_{tot}^2 = a_x^2 + a_y^2 + a_z^2 = g^2 \qquad (5.26).$$

Here $\phi$ is the angle between the sensor and bat z-axis. Because $\phi$ is approximately 15° (the back of the bat where the sensor was placed is not parallel to hitting face) then $a_y \cong 0$.

## B. Dynamic Case:

For simplicity an additional acceleration component $A_x$ in the x-axis direction is assumed only to contribute to $a_x$. This additional component accounts for the rotational and translational movements of the bat during swing.

Then the accelerations can be written as follows:

$$
\begin{aligned}
a_x &= g \cos \theta + A_x \\
a_y &\cong 0 \\
a_z &= g \sin \theta \cos \phi
\end{aligned}
\qquad (5.27).
$$

The total acceleration $a_{tot}$ is calculated using

$$
\begin{aligned}
a_{tot}^2 &= \left(g \cos \theta + A_x\right)^2 + \left(g \sin \theta \cos \phi\right)^2 \\
&= A_x^2 + 2A_x \left(g \cos \theta\right) + \left(g \cos \theta\right)^2 + \left(g \sin \theta \cos \phi\right)^2
\end{aligned}
\qquad (5.28).
$$

As $a^2{}_{tot}$ can be calculated from the measured acceleration data, then $A_x$ is calculated from the solution to the quadratic equation:

$$A_x^2 + 2A_x\left(g \cos \theta\right) - a_{tot}^2 + g^2 \cos^2 \phi + \left(g \cos \theta \sin \phi\right)^2 = 0 \qquad (5.29).$$

Then,

$$
\begin{aligned}
A_x &= \frac{-2\left(g \cos \theta\right) \pm \sqrt{4\left(g \cos \theta\right)^2 - 4\left(-a_{tot}^2 + g^2 \cos^2 \phi + g^2 \cos^2 \theta \sin^2 \phi\right)}}{2} \\
&= -\left(g \cos \theta\right) \pm \sqrt{a_{tot}^2 - g^2 \sin^2 \theta \cos^2 \phi}
\end{aligned}
\qquad (5.30).
$$

Thus the additional acceleration component $A_x$ can be calculated using equation 5.30, which might be due to translational acceleration and/or rotational acceleration.

For a planar straight drive, the bat swings in the two dimensional plane (say XOZ for the bat coordinate system). If $\phi = 15°$ throughout the swing then $\cos\phi = 0.97$ and $\cos^2\phi = 0.93$. If $a_{tot} \gg g$, (eg if $a_{tot} = \pm 4.7g$, arbitrarily chosen from the typical sensor data shown in Fig. 5.27 at the maximum negative acceleration of $a_x$) we can write an approximate formula as:

$$A_x \cong -(g\cos\theta) \pm a_{tot} \qquad\qquad (5.31).$$

Considering maximum value of $\cos\theta$ is unity, this represents 21% of the value of $A_x$ when $a_{tot} = \pm 4.7g$. We can write

$$A_x \cong a_{tot} \qquad\qquad (5.32)$$

at the time of maximum angular velocity which corresponds to the minimum x acceleration value (i.e. maximum negative value) during the drive. At this time we can calculate $a_{tot}$ using equation 5.26. Then we can write

$$R\omega^2 = a_{tot} \qquad\qquad (5.33),$$

where $R$ is the radius of rotation and $\omega$ is the angular velocity at this time.

So the maximum driving force $F$ is

$$F = ma_{tot} \qquad\qquad (5.34).$$

Thus equation 5.34 can be used to determine the level of force exerted by a batter in the typical straight drive bat swing. Using the data in Fig. 5.27, we have $a_x = -4.7g$, $a_y = 0.0266$ and $a_z = -0.3230g$, and the force $F$ for this swing is

$$F = 1.3 \times 4.7g\ N = 6.11g\ N.$$

where *m* is the mass of the bat (1.3kg in these experiments). The sensor was placed at the centre of mass of the bat so that any variation in bat characteristics has no effect on the force comparison.

## 5.5.3 Experimental Procedure

Acceleration data were recorded as $a_x$, $a_y$, $a_z$ along sensor's axes x, y, z respectively from 63 straight ball-free bat swings by seven novice batters of 9 swings by each. Novice batters were used as they are likely to have a greater variation between swings. Thus these results represent a worst case analysis. Elite batters should have far less variation in stroke formation. Each batter's 9 swings were divided in three groups of having almost similar bat elevation angle (lower, medium and higher) at the end of the swings. The timing between sensor and the video data were synchronized by bat tapping. To capture the full trajectory of the bat swings, a video camera was used and its placement detail is provided in Section 4.1.3.1. The frame rate of the camera and the method of increasing the rate by separating two interlace images of each frame was outlined in Section 5.3.1.

## 5.5.4 Results and discussion

*Accelerometer data peaks and bat angles*

The sensor's x-axis acceleration data ($a_x$) from each set of 9 swings are shown in Fig. 5.30. The red marked point at the end of drive duration indicated the end peak acceleration ($a_{end}$) of the drive. This peak showed an interesting relation with the bat elevation angles. The instant of occurrence of $a_{end}$ was noted from the video record. According to the video, the duration of drive part of a swing was between the first maximum (light blue dot) and the second maximum (red dot) value (see Fig. 5.27). The bat elevation angle ($\varphi$, the angle between *K* and $k_f$ in Fig. 4.5) at the end of swing was estimated from the video footage taking the vertical upward direction (opposite to gravity) as the reference axis.
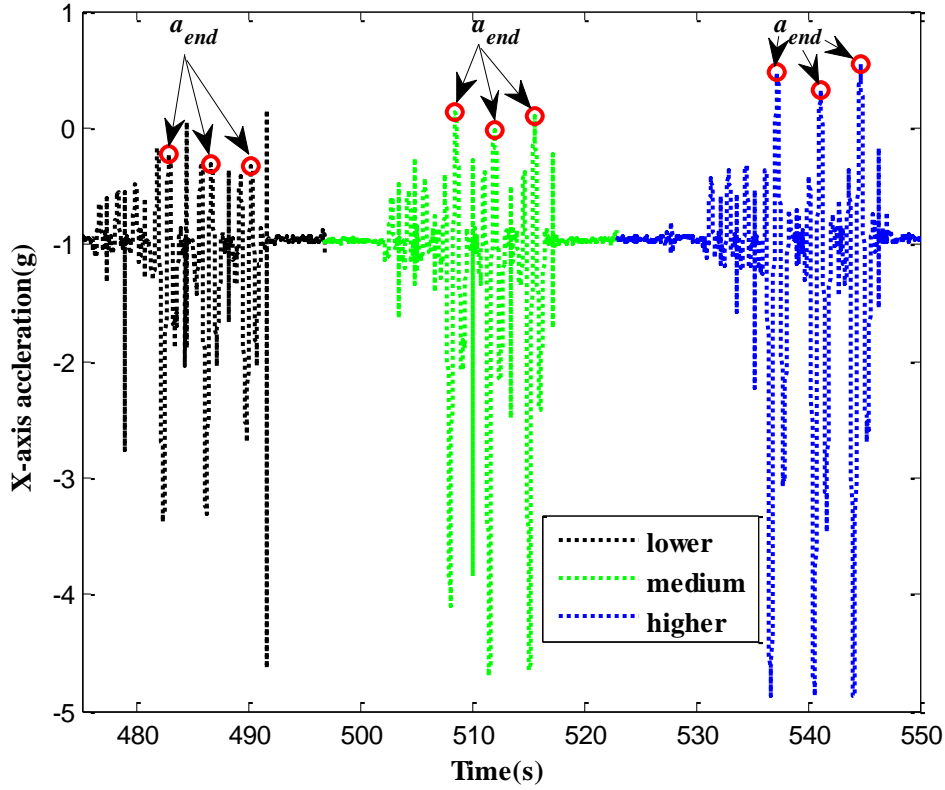
**Fig. 5.30** X-acceleration profiles versus time from 9 bat swings in three sessions of each having almost similar bat elevation angle (lower, medium and higher distinguished by three different colors) by a novice.

To determine the relation between $\varphi$ and $a_{end}$ for one batter, multiple regression analysis was conducted using the Bland and Altman approach [112]. The analysis of variance table (Table 5.8) was used to evaluate the changes in $a_{end}$ within the individual batter upon the changes in $\varphi$ irrespective of differences between the batters. This method is analysis of covariance and the relation between $\varphi$ and $a_{end}$ is shown in Fig. 5.31.

The correlation coefficient was calculated according to Bland and Altman [112] using the figures shown in Table 5.8 as follow:

$$r = \sqrt{\frac{Sum\,of\,squares\,for\,Bat\,angle}{Sum\,of\,squares\,for\,Bat\,angle + residual\,sum\,of\,squares}}$$
$$= \sqrt{\frac{7.79559}{7.79559 + 0.35502}} = 0.98$$

(5.35).

A strong linear correlation ($r$=0.98) between $\varphi$ and $a_{end}$ was determined, meaning that an increase in bat elevation angle within individual was associated with an increased in $a_{end}$ regardless of the differences between the batters.
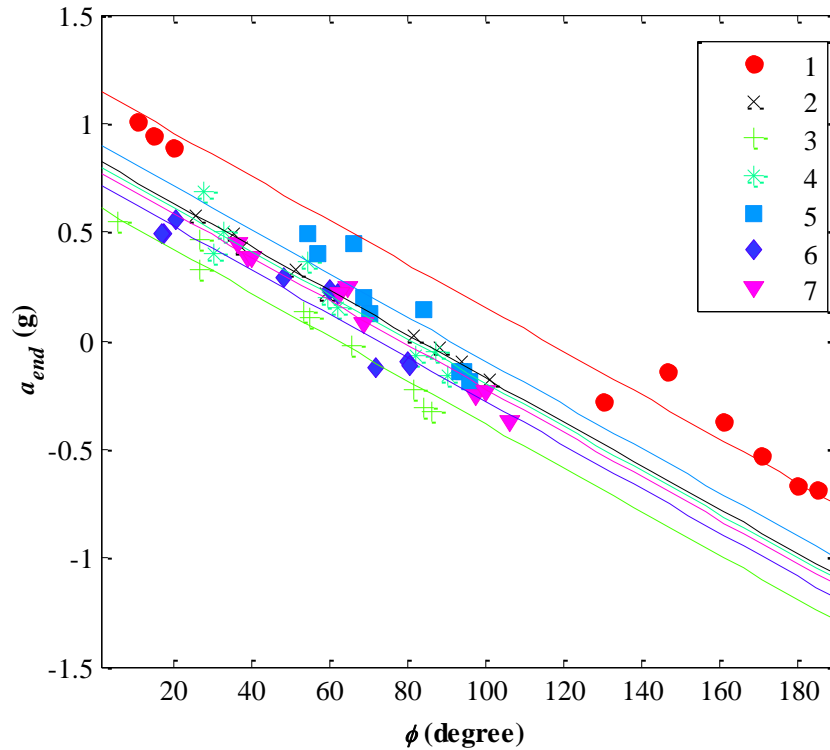


**Fig. 5.31** Bat elevation angle versus sensor recorded x-axis acceleration at the end of the drive and parallel regression lines for seven batters (nine swings each).

**Table 5.8** Analysis of variance for the data shown in Fig. 5.31.

| Source of Variation | Degree of freedom | Sum of squares | Mean square | Variance ratio (F) | Probability |
|---|---|---|---|---|---|
| Novices | 6 | 1.2054 | 0.2009 | 31.1 | <0.0001 |
| Bat angle | 1 | 7.7956 | 7.7956 | 1207.7 | <0.0001 |
| Residual | 55 | 0.3550 | 0.0065 | | |

Table 5.9 shows the correlation coefficients ($r'$) and probability ($p'$) (to get the correlation by chance when there is no true correlation) calculated for each batter

separately. Strong linear correlation ($r'=0.95\sim0.998$) with a very low $p'$ value (<0.0002) was obtained for each batter. The dynamic acceleration ($R\omega^2$ in equation 5.33) was added with the static acceleration ($g\cos\theta$, due to gravity in equation 5.25) to derive $a_x$. The derived $a_x$ was compared to that recorded by sensor to justify the relation between $\varphi$ and $a_{end}$. Imposing initial and final angular conditions ($\theta_1$ and $\theta_2$) and time duration from video, reasonable radius of rotation ($R$) was estimated for each phase of the swing. Again the value of $R$ was adjusted to match the equation derived acceleration profile with the sensor profile. The value of $R = 0.85$ m for back-lift and return $R = 1.2$ m for drive phase. The acceleration $a_x$ calculated by the equation was compared with sensor acceleration (see Fig. 5.32).
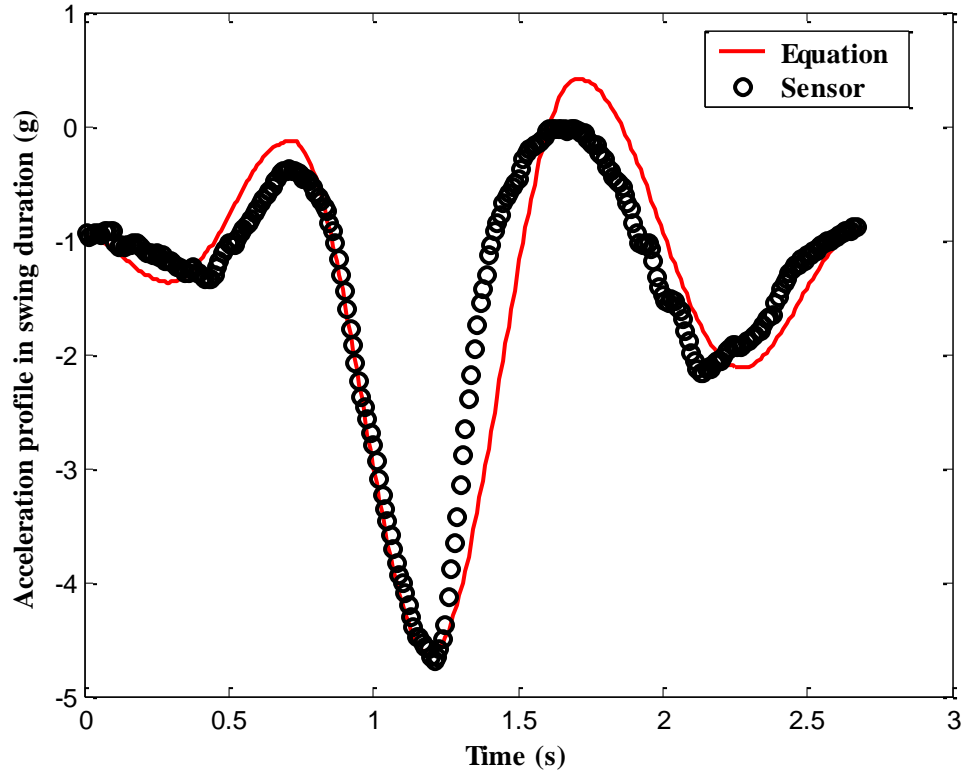


**Fig. 5.32**  Equation derived (using Equation 5.25 and 5.33) and sensor recorded typical x-axis acceleration profile.

To check the relation between the bat elevation angle and $a_x$ in the equation derived profile, the final angle ($\theta_2$) at the end of drive was varied sequentially until the minimum RMS error between the two data sets was obtained.

**Table 5.9** Correlation coefficients and probability for individual batters.

|        | 1      | 2      | 3      | 4      | 5      | 6      | 7      |
|--------|--------|--------|--------|--------|--------|--------|--------|
| $r'$   | 0.9940 | 0.9983 | 0.9862 | 0.9627 | 0.9480 | 0.9538 | 0.9857 |
| $p'$   | 0.0000 | 0.0000 | 0.0000 | 0.0000 | 0.0001 | 0.0001 | 0.0000 |

### 5.5.5 Conclusions

Bat elevation angles in straight drives and accelerometer sensor recorded acceleration peaks were recorded from 63 drives by 7 novice batters. A good correlation (r=0.98) was obtained between the sensor's gravity direction aligned acceleration peaks and bat elevation angles. Video recorded angle profiles in a typical swing was matched with the equation derived profile and a good match was obtained (r=0.99). The sensor recorded acceleration profile was matched to the equation estimated profile to justify the relation between bat elevation angle and acceleration peak at the end of drive. Good agreement was obtained by imposing initial and final angular and temporal conditions from video adjusting the radius of rotation in each phase of swing. The equation derived acceleration profile showed the same relation between the angle at the end of drive and acceleration peak mentioned above. So using that peak value the bat elevation after the drive could be judged. It will provide an estimation of the forcefulness in a usual straight drive for continuous swing. The radius of curvature ($R$) was adjusted (taken $R$=0.85 m during back-lift and return, and 1.2 m in drive phase) to match the equation derived acceleration profile with the sensor profile and the match is not perfect. It is speculated that future work could be done on the radius of curvature during bat swing and there might be some interesting outcomes regarding the force, and bat posture. The cosine square function may be applicable to other bat/racquet/stick sports. This work encourages the use of tiny, cheap, user friendly inertial sensors to identify the bat posture in a cricket drive. The

accelerometer technique can be used to establish the relationship between the elevation angle and time of impact and between the elevation angle and time of maximum angular acceleration, and the differences in these relationships for different batters. This should serve as a measure of batter competence. This could be validated through further investigations.

## 5.6 Back-lift height and bat alignment in defensive stroke and discrimination of on and off stroke by bat accelerations

Cricket batting strokes are named according to the bat and limb positions. Some are described in chapter 3. The most common strokes played are forward defensive strokes and drive off the front foot [113].

### 5.6.1 Background

The background of this study was documented in section 2.9 in the literature review chapter. In that section it's pointed out from the literature that defensive strokes forms the basis of all strokes and single plane movement of bat and batters in this stroke make it a suitable task vehicle by allowing two dimensional analysis. Using inertial sensors attached to the bat, this study was conducted to observe the effect of back-lift height on bat alignment during ball-contact in off and on defensive stroke played by three amateur batters. In the coaching literature it is said that the back-lift should be smaller in a defensive stroke (as stated in chapter 3) compared to drive. In this study the batters were not instructed about back-lift, but were asked to achieve good ball-contact by keeping bat vertical. The bat movement after contact (particularly changes from the vertical alignment) with back-lift was investigated. The total acceleration from the sensors was used to discriminate on and off defensive strokes.

### 5.6.2 Experimental Procedure

In this study the placement of sensor on the bat and the axes definition was same as

in Fig. 4.4. Each of three amateur batters faced a number of deliveries of similar speed (low) of which ten were chosen for analysis: five were directed to the on-side and five were directed to the off-side. The batters were asked to play defensive stroke using a planar drive (without movement in any lateral direction) having good ball-contact with the bat always vertical. However, no instruction was provided regarding the back-lift height. A video camera was placed lateral to the drive plane to capture the two dimensional footage of the full drive for good or bad or no contact and the timing reference. The placement detail of the camera is provided in Section 4.1.3.1. The quality of contacts was also assessed by an independent assessor together with the video footage.

### 5.6.3 Results and discussion

Fig. 5.33 shows the acceleration profiles for first, second and third amateur (*N1*, *N2*, and *N3* respectively*)* for off and on defensive drives.
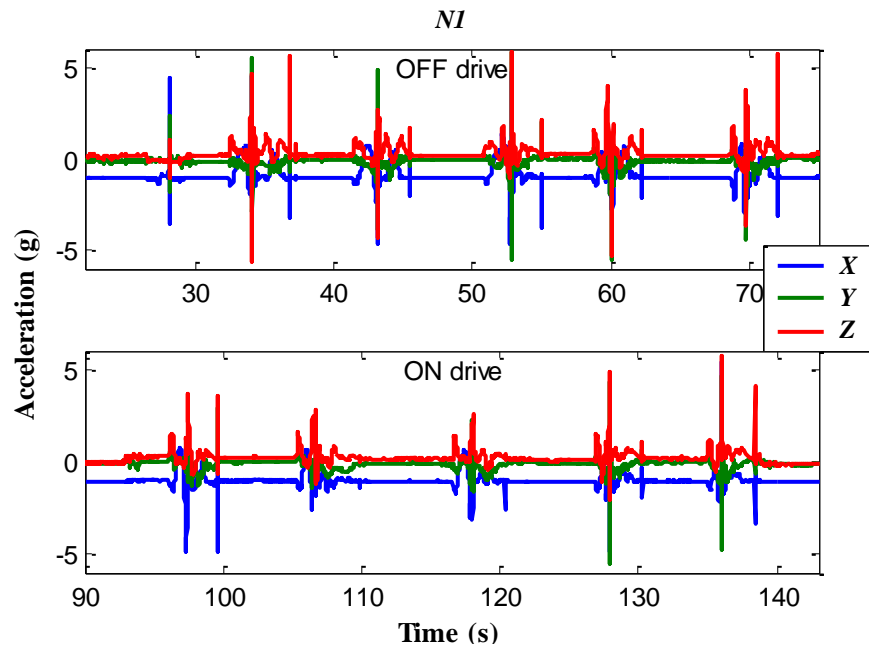


**Fig. 5.33(a)**    Acceleration profiles from off (upper) and on (lower) defensive drives by first amateur (*N1*). The first spike before 30s revealed from the straight bat tapping and next 10 from ten bat-ball contacts at 34.10s, 43.19s, 52.78s, 60.11s, 69.80s, 97.49s, 106.66s, 118.01s, 127.87s, and 135.99s.
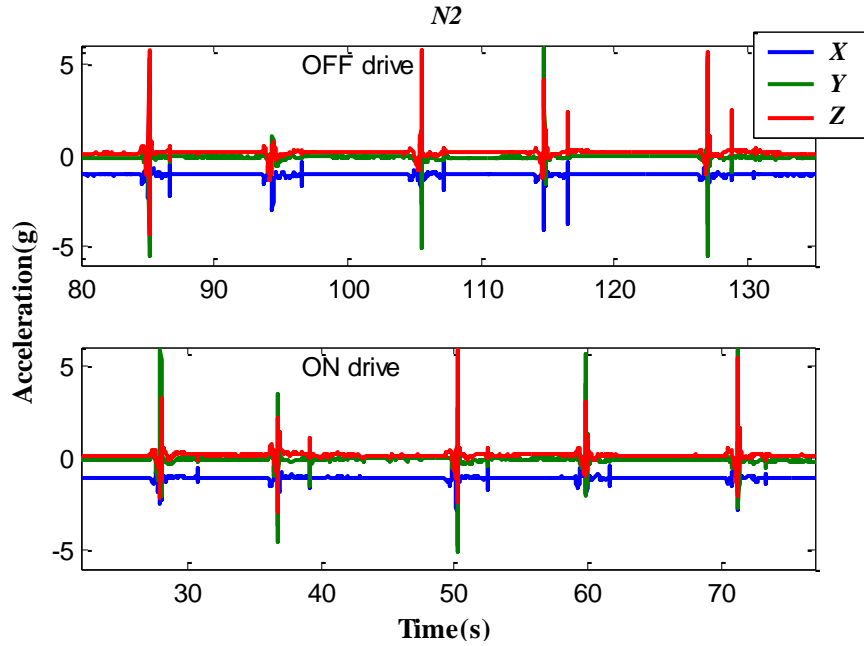
**Fig. 5.33(b)** Acceleration profiles from off (upper) and on (lower) defensive drives by second amateur (*N2*). Ten spikes are at 85.10s, 94.30s, 105.53s, 114.74s, 126.97s, 27.99s, 36.77s, 50.21s, 59.87s, and 71.25s, where nine from nine ball-contacts and second of the off drive (at 94.30s) from miss contact.
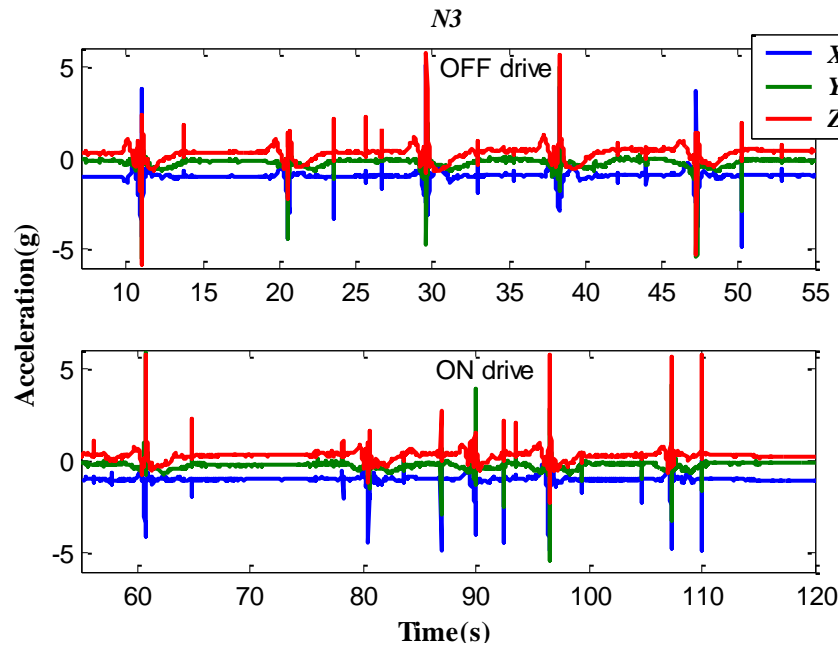


**Fig. 5.33(c)** Acceleration profiles from off (upper) and on (lower) defensive drives by third amateur (*N3*). Ten spikes from ten bat-ball contacts are at 10.94s, 20.59s, 29.62s, 38.33s, 47.28s, 60.77s, 80.52s, 89.93s, 96.50s, and 107.36s.

The first spike before 30s in the acceleration profiles in Fig. 5.33(a) for *N1* came from the straight bat tapping on the ground for video references as mentioned in chapter 4 and other ten spikes revealed the ten ball-contacts at 34.10s, 43.19s, 52.78s, 60.11s, 69.80s, 97.49s, 106.66s, 118.01s, 127.87s, 135.99s. The time of each ball-contact was confirmed by the video footage timing. However, other minor sharp spikes came from the sensor errors or tiny sharp movement of the bat by the batter. Fig. 5.33(b) show the ball-contact spikes for *N2* at 85.10s, 105.53s, 114.74s, 126.97s, 27.99s, 36.77s, 50.21s, 59.87s, 71.25s and miss contact at 94.30s. Ball-contact spikes for *N3* are shown Fig. 5.33(c) at 10.94s, 20.59s, 29.62s, 38.33s, 47.28s, 60.77s, 80.52s, 89.93s, 96.50s, and 107.36s. In Fig. 5.33(b) and 5.33(c) spike from straight bat tapping as seen in Fig. 5.33(a) were not included. The contacts time are listed according to the sequence of five off drive and then five on drives as shown in the figure.

Total accelerations were calculated from the acceleration profiles shown in Fig. 5.33 using the equation 4.2 to observe the difference between off and on drives. Fig. 5.34 shows the total acceleration for off and on drives within the 4.5s time span. The first ball-contact spike is located at 3.5s for all amateurs and next spikes are shifted in time by 0.2s from the contact time to make the plots distinguishable.

The total acceleration from the off and on drives at each contact point was plotted for each amateur (shown at upper, middle and lower part in Fig. 5.35 for *N1*, *N2* and *N3* respectively). Fig. 5.35 revealed that the acceleration in the off and on drive differed in values at the contact points for all three amateurs. Note that there was no contact at the second drive of *N2;* (the middle part of Fig. 5.35) and fifth drive of *N1* (upper part of Fig. 5.35).

It is seen from Fig. 5.35 that the contact acceleration is larger for the off drive compared to the on drive. The differences are 49.18%, 33.67%, and 26.84% for *N1*, *N2* and *N3* respectively, while summation of all contacts acceleration in the on drive and those in the off drive by each amateur better were compared. This result indicates
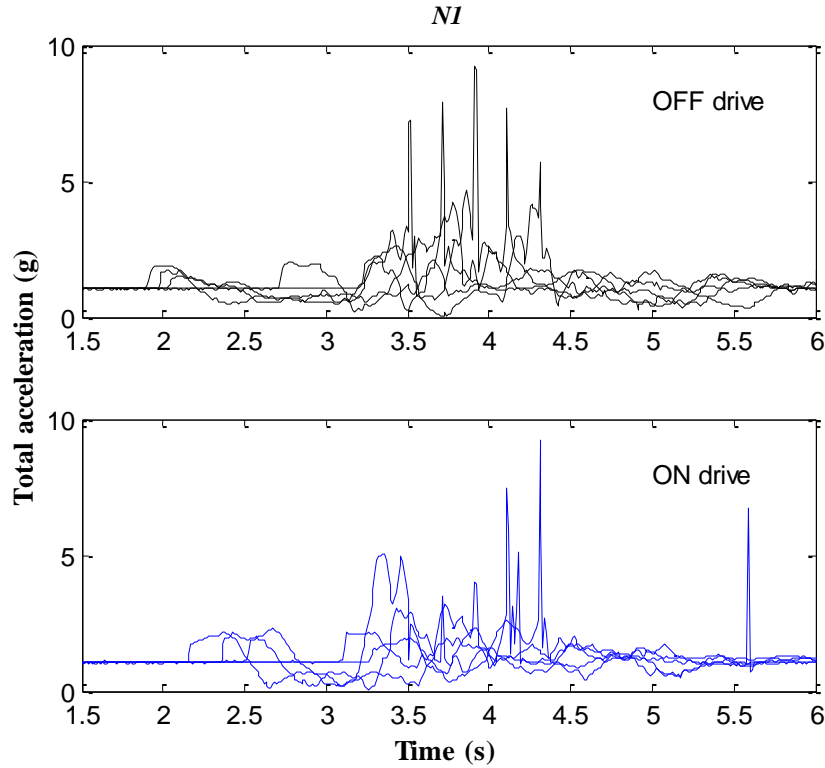
**Fig. 5.34(a)**     Total acceleration profiles from off (upper) and on (lower) defensive drives by first amateur (*N1*) using the data shown in Fig. 5.33(a). The first ball-contact spike is positioned at 3.5s where the next of each spikes are shifted by 0.2s from their immediate prior spike.

that more energy was imparted to the ball in the on drive than the off drive.

In Fig. 5.34 the acceleration before each contact of subject 1 was more than subject 2 and 3. The acceleration values at the top of the back-lift were chosen for a comparison among the amateurs to relate the back-lift acceleration peak values with the bat inclination angle at each contact. Fig. 5.36 shows the first off drive X-acceleration profiles are within 2s for all three amateurs for comparison of the back-lift peaks (indicated by arrow in the figure) where the ball-contact times were aligned at 3.5s. The higher values of the back-lift acceleration peaks are clearly observed in the first amateur's profile compared with the others.
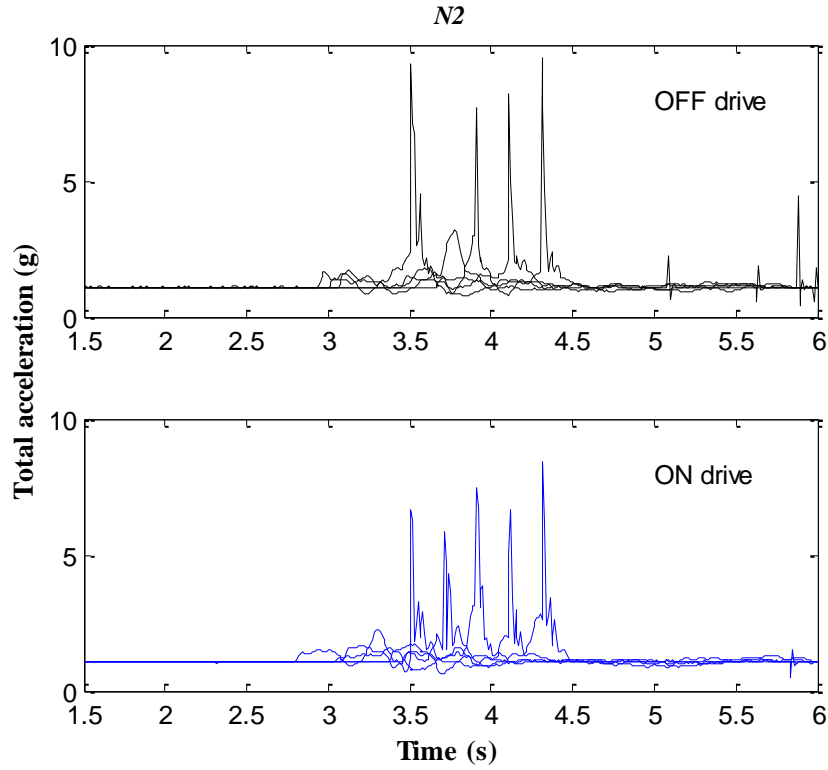
**Fig. 5.34(b)**     Total acceleration profiles from off (upper) and on (lower) defensive drives by second amateur (*N2*) using the data shown in Fig. 5.33(b). The first ball-contact spike is positioned at 3.5s where the next of each spikes are shifted by 0.2s from their immediate prior spike.

Fig. 5.37(a) and Fig. 5.37(b) shows the X-acceleration profiles for all off drive and on drive respectively for all amateurs, where the ball-contacts are aligned at 3.5s. The first amateur back-lift profiles clearly show higher acceleration values for the first three off and on drives. The X-acceleration values in the back-lift peaks (as shown in Fig. 5.36) in each of the drives were extracted by the time synchronization between sensor and video footage events using equation 4.4. Assuming that the bat is stationary at the top of the back-lift, the back-lift angles were calculated from the X-acceleration values (assuming only the gravity component) in the back-lift peaks using inverse cosine function. The angles were measured from the direction of gravity. The values are given in Table 5.10.
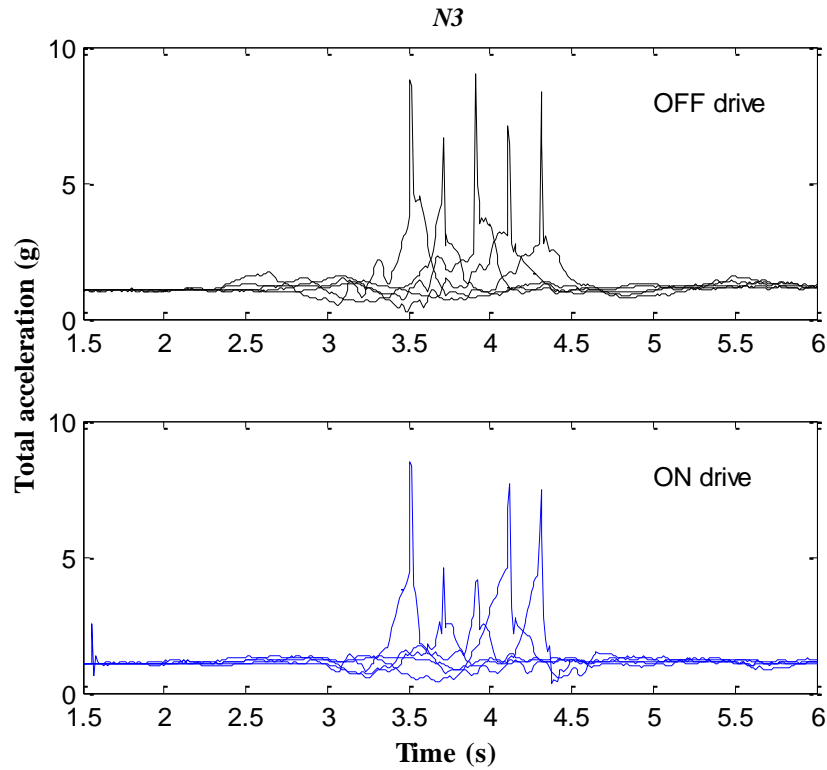
**Fig. 5.34(c)** Total acceleration profiles from off (upper) and on (lower) defensive drives by third amateur (*N3*) using the data shown in Fig. 5.33(c). The first ball-contact spike is positioned at 3.5s where the next of each spikes are shifted by 0.2s from their immediate prior spike.

**Table 5.10** Back-lift angles for all drives by all three amateurs (*N1*, *N2* and *N3*) of which first five off (D1~D5) and second five off (D6~D10). The angles are given in degrees where 0 degrees is vertically down.

|      | D1     | D2     | D3     | D4     | D5     | D6     | D7     | D8     | D9    | D10   |
|------|--------|--------|--------|--------|--------|--------|--------|--------|-------|-------|
| *N1* | 139.86 | 137.22 | 121.34 | 112.18 | 150.04 | 135.53 | 130.73 | 127.71 | 88.29 | 75.89 |
| *N2* | 60.78  | 53.11  | 66.64  | 23.66  | 52.38  | 42.03  | 64.07  | 58.75  | 58.75 | 44.58 |
| *N3* | 71.02  | 66.00  | 55.98  | 86.53  | 73.47  | 55.98  | 63.42  | 65.36  | 83.02 | 58.07 |

The inclination angles of the bat with the vertical in the swing plane (ZX-plane) and the mediolateral plane (XY-plane) during the ball-contacts were estimated using the *average orientation* method discussed in chapter 4. FT analysis shows that a filter cutoff frequency of 0.9 Hz is sufficient to separate the static component (gravity) from sensor recorded acceleration during the drives. Using a 0.9 Hz low pass filter

the gravity component along sensor's X-, Y- and Z-axis ($A_{gx}$, $A_{gy}$, $A_{gz}$) were determined.
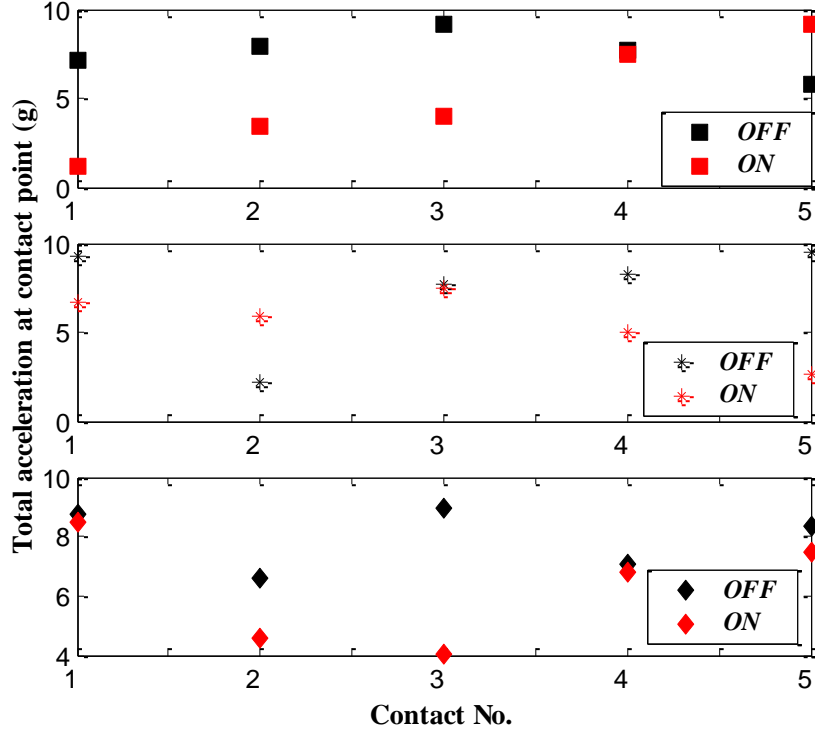


**Fig. 5.35** Ball-contact points total acceleration values from off drives (black legends) and on drives(red legends) by each amateur (upper: *N1*, middle: *N2*, lower: *N3*) using the data shown in Fig. 5.34. The second values of the middle part of the figure are from a missed contact. The off drive shows more accelerations than on drive, and the differences found were 49.18%, 33.67%, and 26.84% for N1, N2 and N3 respectively, while summation of all contacts acceleration in on drive and those in off drive by each amateur were compared.

As the defensive strokes played by the batter were along the sensor Z-axis in the ZX-plane, the pitch and roll angles were calculated using the method by Bai et al. [110]. The inclination of bat, i.e. sensor's X-axis, with vertical were calculated as follows:

$$Inclination\ of\ bat\ in\ ZX\ plane, \theta = \arctan(\frac{A_{gz}}{\sqrt{A_{gx}^2 + A_{gy}^2}}) \tag{5.35},$$

$$Inclination\ of\ bat\ in\ XY\ plane,\ \beta = \arctan(\frac{A_{gy}}{\sqrt{A_{gx}^2 + A_{gz}^2}})$$ (5.36).
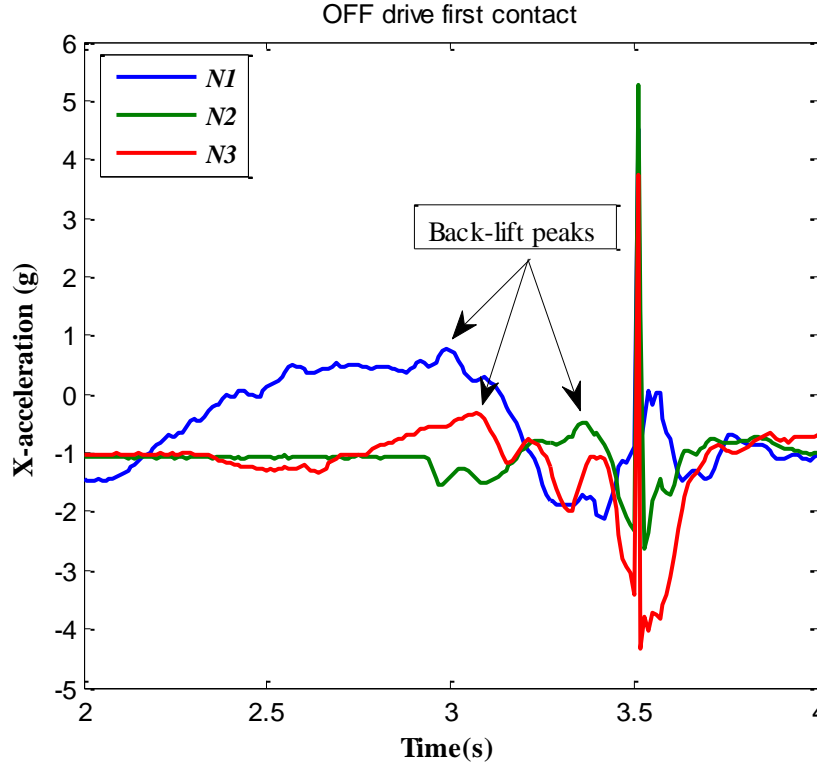


**Fig. 5.36**  All amateurs' first ball-contact in the off drive within 2s to observe the differences in the back-lift peaks among them. Ball-contacts are aligned at 3.5s and back-lift peaks are indicated by the arrows.

The bat inclination angles at the ball-contact for all drives were plotted against the corresponding back-lift heights (see Fig. 5.38 and 5.39). The first amateur had a larger deviation of the bat from vertical (more inclination angle) in most cases (3 exceptions) compared to the other two amateurs due to a higher back-lift as evident in Table 5.10. This means that this amateur had less control over the bat. The possible causes are the higher back-lift and a failure to follow the instruction to keep bat vertical.
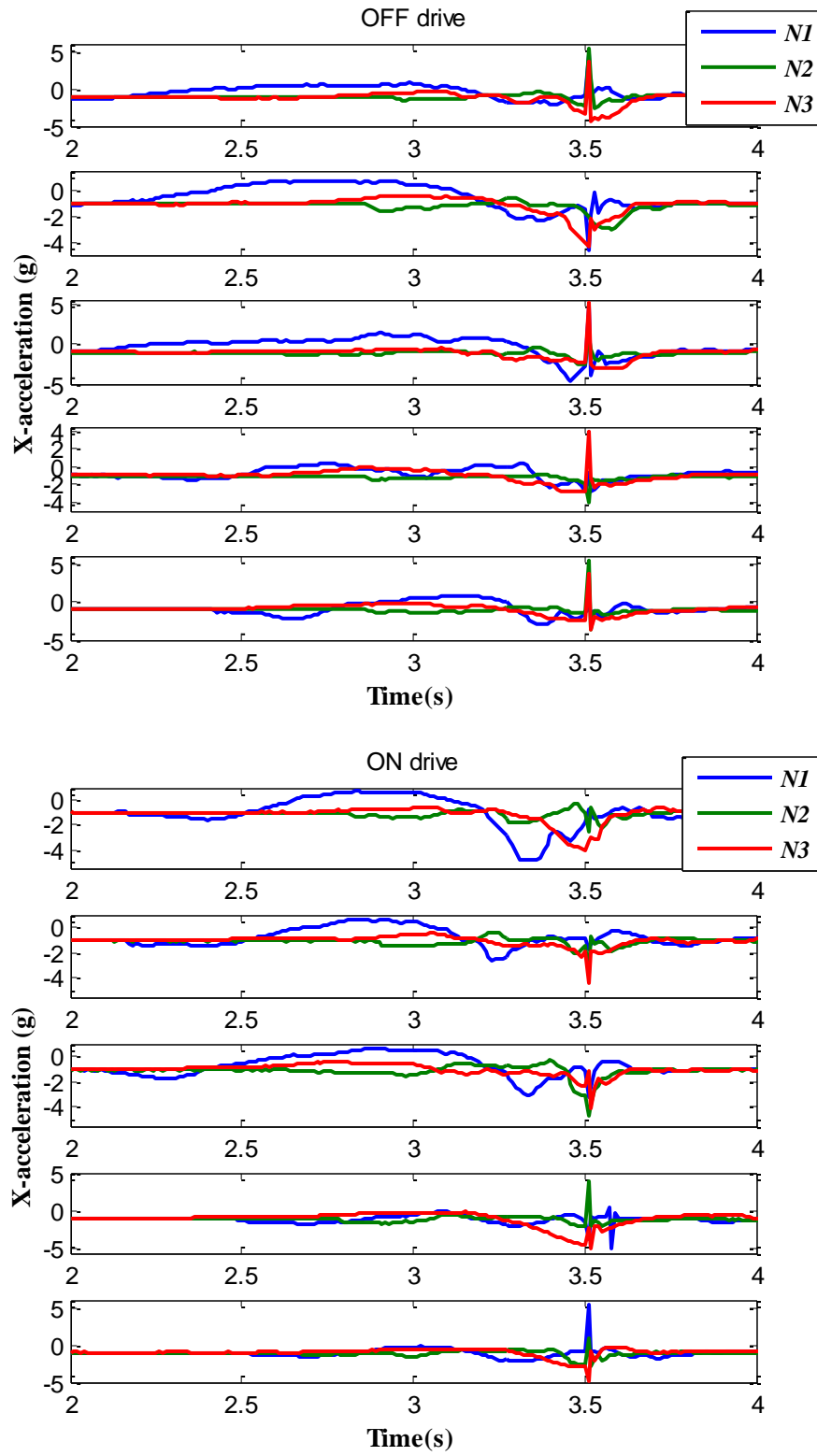
(a) Upper figure, (b) lower figure

**Fig. 5.37**   The acceleration profiles for all off drives (a) and on drives (b). The back-lift peaks are a measure of the back-lift angles. The ball-contacts are aligned at 3.5s.
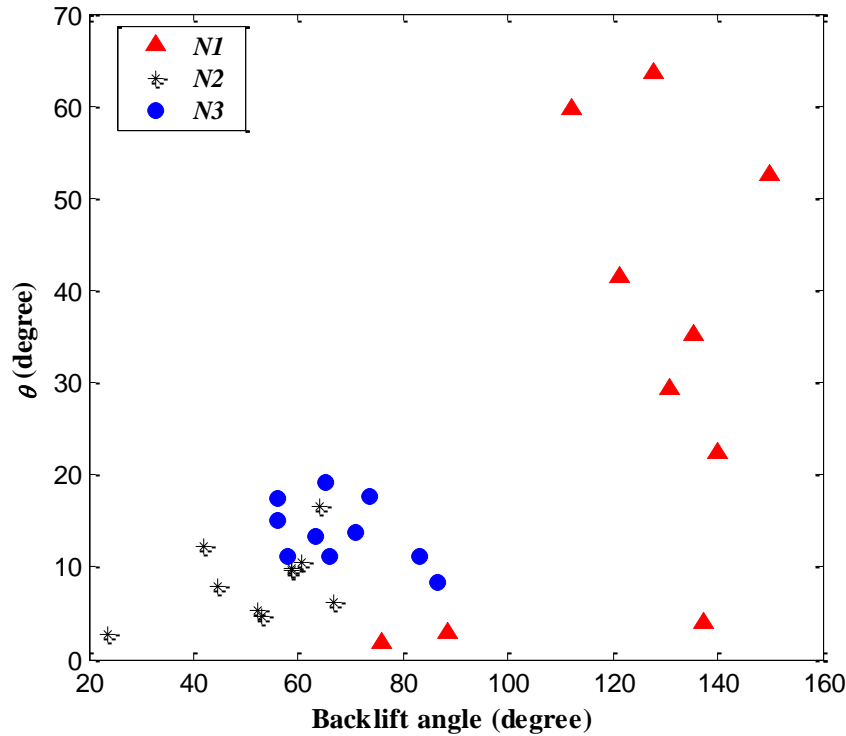


**Fig. 5.38**   Bat inclination angles in the swing plane: ball-contact angle versus the back-lift angle for all drives by all amateurs. The red, black and blue legends in the figure show data for the first, second and third amateur respectively.

An overall examination of data in Table 5.10 and Fig. 5.38 and 5.39 reveals that the second amateur had more vertical bat compared to others. This is possibly related to the lower back-lift angles. The mean back-lift angle of second amateur was 52.48°, whereas, those of first and third amateur were 121.88° and 67.89° respectively. The mean value of inclination angles of bat with vertical axis at the contact were 7.46° (in swing plane), 7.15° (in mediolateral plane) for second amateur compared to those of 31.54°, 31.48° for first and 29.45°, 29.80° for third amateur respectively.
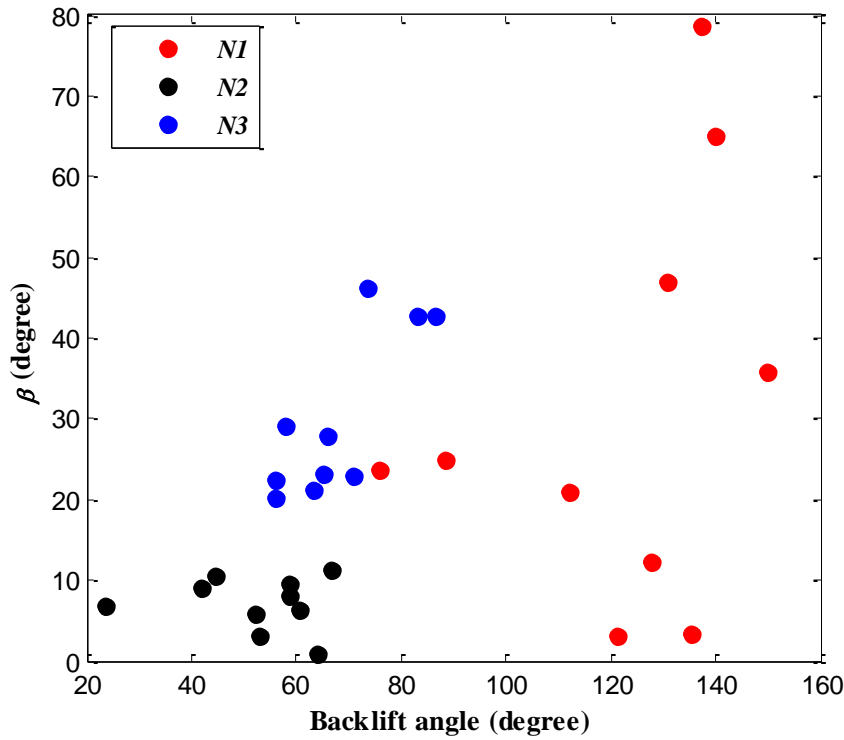
**Fig. 5.39** Bat inclination angles in the mediolateral plane: ball-contact angle versus the back-lift angle for all drives by all amateurs. The red, black and blue legends in the figure show data for first, second and third amateur respectively.

### 5.6.4 Conclusions

The effect of back-lift height on the bat alignment in on side and off side defensive strokes was analyzed using a bat mounted accelerometer. Three amateurs executed 30 defensive strokes. The higher back-lift was found to be detrimental to bat alignment. The batter with the highest back-lift showed least bat control (alignment). Inferior alignment means higher values of $\beta$ and $\theta$ in Fig. 5.38 and 5.39 respectively. On-side defensive strokes could be discriminated from the off side defensive strokes by observing a significantly lower magnitude acceleration at ball-contact (36.56% on an average of three amateurs differences). This suggests that more energy is imparted to the ball for on-side defensive strokes as the batters had more control over the bat.

In this study the deliveries were made by an amateur bowler being instructed to maintain a constant low ball speed. As the ball delivery speeds were not recorded, the total acceleration values might be biased by variations in the ball speed. However, this study showed that tiny can discriminate the two cricket strokes. The variations in bat swing can be quantified and used as a measure of batting effectiveness.

## 5.7 Comparison of straight drive profiles with video extracted profiles and key parameters extraction

Using accelerometer sensors, this work sought to extract the spatio-temporal parameters of a straight drive from acceleration profiles and key issues relating to swing motion. Two triaxial accelerometers were mounted on a bat and the data recorded during a straight drive was analyzed using high speed video. The spatiotemporal details from the video were used to match the accelerometer data using rigid body dynamics in the plane of the swing. Discriminating the drive from the back-lift and the return, the key issues of the swing motion and bat posture was investigated. The time between the start and the end of the drive can be readily determined from the accelerometer data, and from this, the maximum bat swing velocity and the time it occurs was determined. One parameter, the radius of rotation, to achieve maximum swing velocity in straight drive was determined by matching the sensor and video data. In each phase of the drive the acceleration components (rotational or translation) which dominate the acceleration profile was determined.

### 5.7.1 Background

So far existing batting literature has focused on the coordination and control, skill acquisition, the importance of vision and cue utilization under ecological and performance index constraints. Few papers on bat swing analysis discuss: (1) how to maximize the velocity of the bat, (2) whether the angular velocity of the bat or the linear velocity is important, (3) how swing kinetics influence shot power, shot direction, and the angle of elevation of the bat, (4) what are the key signatures in the

bat swing for a particular shot (i. e. Block, Drive, Pull, Cut, Hook etc.) that might be used as an ideal template. This work endeavored to fill some of those gaps beginning with the straight drive shot. Two issues addressed in this work were, firstly to judge whether tiny inertial sensors could identify the spatio-temporal parameters (validated by video). Secondly was to check the sensor's ability to document a straight drive shot. To do this a decision matrix was formulated according to the bat postures in the video footage to match the video data with the sensor data. An ideal movement template using an elite batter's straight drive might be formulated. At the start of an innings and often between strokes, batters commonly practice an ideal bat swing in the air (ball-free) for a particular stroke as imprinted in their subconscious.

### 5.7.2 Experimental Procedure

*Accelerometer procedure*

The sensor data in the form of $a_x$, $a_y$ and $a_z$ were collected during straight ball-free bat swings in the horizontal plane (referred as ZX-plane with respect to bat's axes in the world reference frame as shown in Fig. 4.4 in Section 4.1.1.3) by an amateur batter.

*Video procedure*

The drive was filmed using a video camera, the details about the placement of the camera is provided in Section 4.1.3.1 and its frame rate and how to increase it to minimize blurring is detailed in Section 5.3.1. Image pixels were converted into two dimensional distance co-ordinates using software. The top left most corner of the video footage window was taken as reference for measurement. A scale factor was used to convert the coordinates of the two ends of the bat image at its different positions during the swing. This scale factor was calculated from the physical length of bat and the number of pixels forming the image bat in that particular direction. The details of this scale factor are documented in Section 4.1.3. A LED (Light Emitting Diode) at the end of the bat and a point formed by reflective tape at the top

of the bat were connected in the same line of sight to indentify two points on the bat image. Before the start of the swing, the bat was tapped on the ground to provide timing synchronization between the sensor and video data.

Using the Equation 4.14 for a rigid body rotational dynamics the total acceleration $\bar{a}$ for rotation was calculated. In this study $\bar{r}$ was taken from the top of the handle of the bat from the reference point for the video image measurements. The magnitude of $\bar{l}$ was the length of the bat. In equation 4.14 the last two parts contributed to the tangential ($a_t$) and centripetal acceleration ($a_r$) of the bat due to rotation having magnitudes of $|\alpha l|$ and $|\omega^2 l|$ respectively, where $|\alpha|$ was the magnitude of angular acceleration and $|\omega|$ was the magnitude of angular velocity. To estimate the overall total acceleration $A_T$ ($A_{TX}$ for X-axis, $A_{TZ}$ for Z-axis), translational acceleration ($\tau_x$ for X-axis, $\tau_z$ for Z-axis) was taken into account along with the acceleration components stated in equation 4.14.

### 5.7.3 Results

*Video*
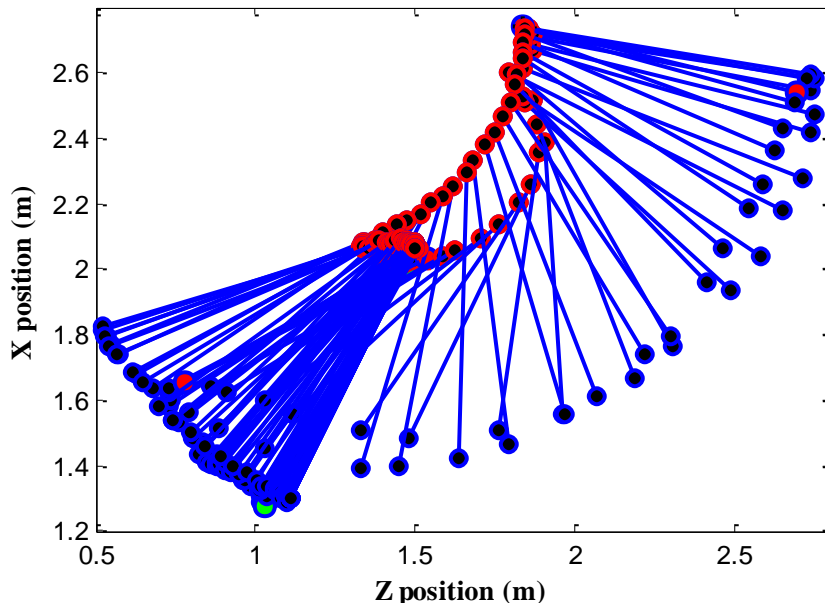


**Fig. 5.40** Trajectories of the bat during entire swing. Upper red circles indicated the top and the lower

blue circles indicated the bottom of the bat. Comparatively larger green, two red circles at the bottom of the bat represent start of back-lift, drive (left red circle), and return (right red circle) respectively.

The two ends of the bat in each video frame were plotted beginning from the start of the back-lift. This provided the full trajectory of the bat in the entire swing range as shown in Fig. 5.40. The dense lines in part of the trajectory indicate very little movement of the bat. The temporal events of different phases of the swing, i.e. the back-lift (as mentioned in the literature), the drive (equivalent to downswing plus follow-through as in Taliep et al. [41]) and the return (reverse drive till the bat touches the ground after the entire swing) were extracted from the video footage.
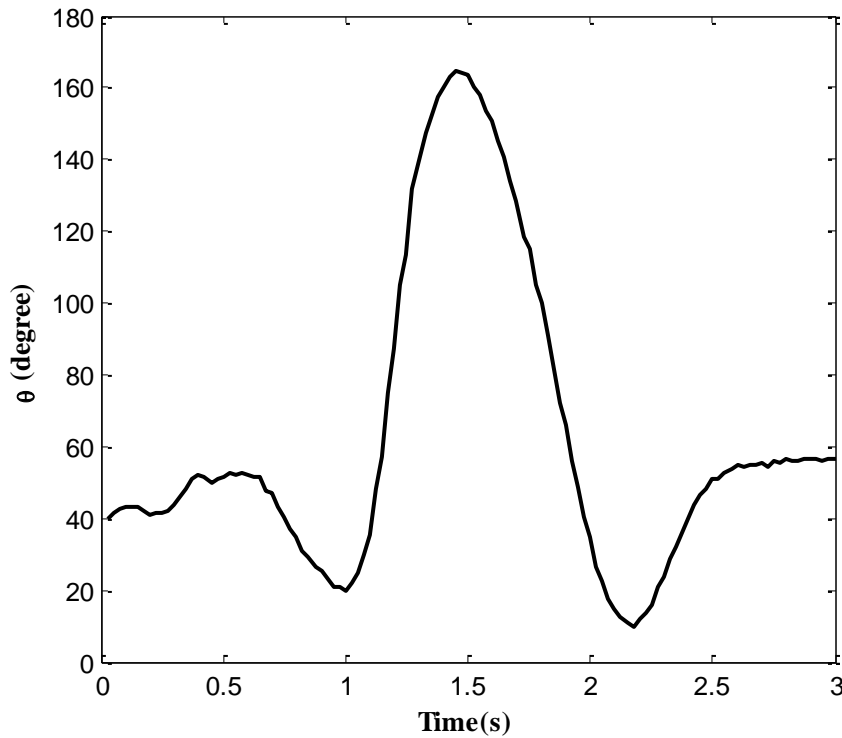


**Fig. 5.41**   Angle of rotation of the bat during entire swing derived from the video data (measured from the direction of negative Z-axis (the back-lifting side of the batter, parallel to the ground)).

To calculate the angle of rotation $\theta$, every fifth frame was chosen, and the arctangent of slope of the image bat (as shown in Fig. 5.40) of those data allowed calculation of the angular velocity. This angle of rotation, $\theta$ measured from the direction of negative Z-axis (the back-lifting side of the batter, parallel to the ground) during the

drive was plotted as a function of time (Fig. 5.41) and the time derivative of the angle of rotation was calculated to determine the angular velocity.

**Table 5.11** Decision codes and total acceleration according to the bat location and orientation from the video.

| $DX_B$ | $DY_B$ | $DX_T$ | $DY_T$ | $A_T$ |
|--------|--------|--------|--------|-------|
| 0 | 0 | 0 | 0 | $A_{TX}=g_x$, $A_{TZ}=g_z$ |
| 0 | 0 | 0 | 1 | * |
| 0 | 0 | 1 | 0 | * |
| 0 | 0 | 1 | 1 | $A_{TX}=g_x-a_{xr}$, $A_{TZ}=g_z-a_{zr}$ |
| 0 | 1 | 0 | 0 | * |
| 0 | 1 | 0 | 1 | $A_{TX}=g_x-\tau_x$, $A_{TZ}=g_z$ |
| 0 | 1 | 1 | 0 | * |
| 0 | 1 | 1 | 1 | $A_{TX}=g_x-a_{xr}-\tau_x$, $A_{TZ}=g_z-a_{zr}-\tau_z$ |
| 1 | 0 | 0 | 0 | * |
| 1 | 0 | 0 | 1 | * |
| 1 | 0 | 1 | 0 | $A_{TX}=g_x$, $A_{TZ}=g_z-\tau_z$ |
| 1 | 0 | 1 | 1 | $A_{TX}=g_x-a_{xr}-\tau_x$, $A_{TZ}=g_z-a_{zr}-\tau_z$ |
| 1 | 1 | 0 | 0 | $A_{TX}=g_x-a_{xr}$, $A_{TZ}=g_z-a_{zr}$ |
| 1 | 1 | 0 | 1 | $A_{TX}=g_x-a_{xr}-\tau_x$, $A_{TZ}=g_z-a_{zr}-\tau_z$ |
| 1 | 1 | 1 | 0 | $A_{TX}=g_x-a_{xr}-\tau_x$, $A_{TZ}=g_z-a_{zr}-\tau_z$ |
| 1 | 1 | 1 | 1 | $A_{TX}=g_x-a_{xr}-\tau_x$, $A_{TZ}=g_z-a_{zr}-\tau_z$ |
| **\*the situation is not possible** | | | | |

Table 5.11 shows a decision chart which categorizes the acceleration components according to the bat position during the swing. As shown in the chart in Table 5.11, $X_B$, $X_T$ represent the abscissa (along $Z^B$-axis direction as shown in Fig. 4.4 in Section 4.1.1.3) and $Y_B$, $Y_T$ ordinate (along opposite to $X^B$-axis direction as shown in Fig. 4.4 in Section 4.1.1.3) of two points (suffices 'B' for bottom near the toe and 'T' for top near end of handle of the bat) in bat in the video footage window mentioned in section 4.1.3.1. Then the variables $DX_B$, $DY_B$, $DX_T$ and $DY_T$ for the codes indicate the differences between the adjacent abscissas and ordinates. In Table 5.11 the zero for these variables (say $DX_B=0$) means no change and one (say $DX_B=1$) means there is a change from one frame to the next frame. A batter was instructed to swing the

bat straight in the ZX-plane without twisting the bat or any bat movement in the Y-direction. The X-axis and Z- axis acceleration and their constituents shown in Fig. 5.42 and Fig. 5.43 were estimated using equation 4.14 and the decision chart in Table 5.11 (the sign differed from that in equation 4.14 is due to sensor's axis orientation and swing direction). In Fig. 5.42 and 5.43 the 'drive' phase is highlighted and discriminated from other phases by the colored shaded bar.
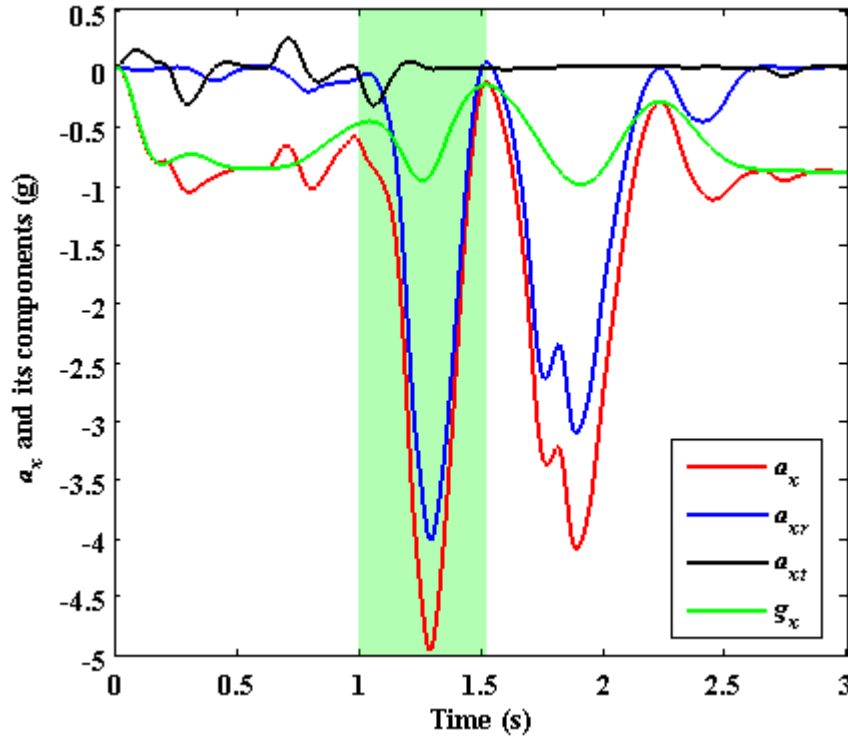


**Fig. 5.42**  Components and total X-axis acceleration profiles obtained from video data.

As shown in Fig. 5.42 and 5.43 the rotational components of the acceleration (centripetal, $a_{xr}$ for X- and tangential, $a_{zr}$ for Z-axis) is calculated using the angular velocity $\omega$ and the angular acceleration $\alpha$ in Equation 4.14, where $|\bar{l}|$ is the instantaneous radius of rotation for all the cases in Table 5.11 except for the last one (when $DX_B$, $DY_B$, $DX_T$ and $DY_T$ all equal to 1) for which the physical length of the bat was used for $|\bar{l}|$. The translational accelerations ($\tau_x$, $\tau_z$) for all the cases except the last one in the Table 5.11 was calculated as the second derivative of $X_B$ and $Y_B$ for $A_{TZ}$ and $A_{TX}$ respectively. The first term in Equation 4.14 served the purpose directly

for the last case. The instantaneous radius of rotation was calculated from the data points of the bottom of the bat ($X_B$, $Y_B$) using the geometry as stated by Cross [65]. To improve the match between video and accelerometer data, the value of the instantaneous radius, $R$ (used for $|\bar{l}|$ in calculating $a_{zr}$ and $a_{xr}$) was adjusted to achieve the best fit to the data.
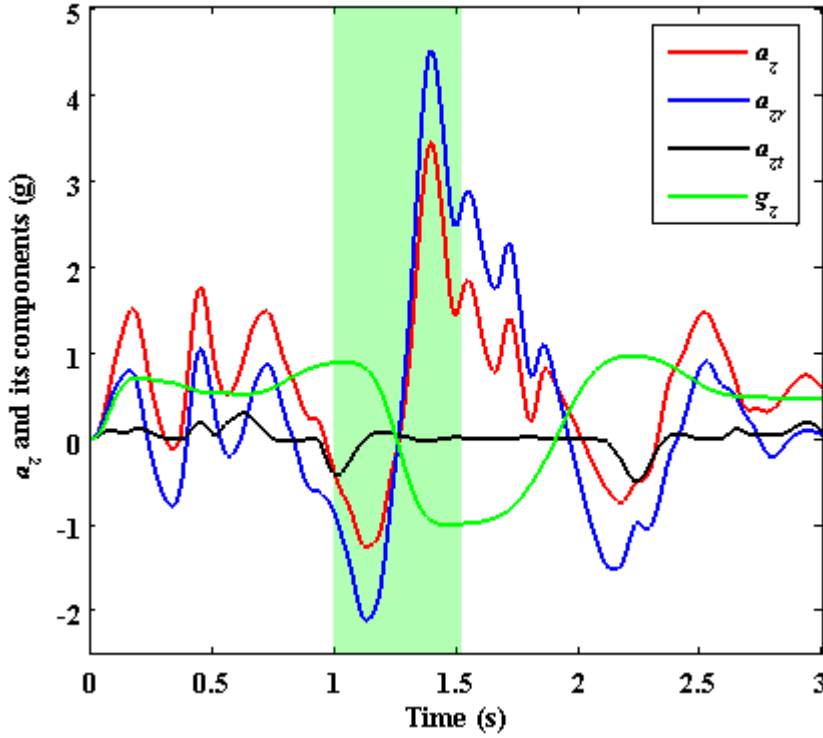


**Fig. 5.43**   Components and total Z-axis acceleration profiles obtained from video data.

*Accelerometer*

Accelerometer data was converted to gravity units (g) after the sensors were manually calibrated. The data are shown in Fig. 5.44 and 5.45 together with video data for comparison. Using the matlab toolbox named ADAT [106] a low pass filter of cut off frequency of 5 Hz was used to smooth the curves. The cut off frequency was chosen after reviewing the spectrum of the acceleration data.

X-axis acceleration calculated from video data and that obtained from sensor during the entire swing duration are shown in Fig. 5.44. The equivalent Z-axis data are shown in Fig. 5.45. It is evident from Fig. 5.44 and 5.45 that the video data matches with the sensor data in magnitude and time with minor variations. From regression analysis a correlation coefficient of 0.92 and 0.87 were found for Z-axis and X-axis accelerations respectively between video revealed and sensor recorded data.
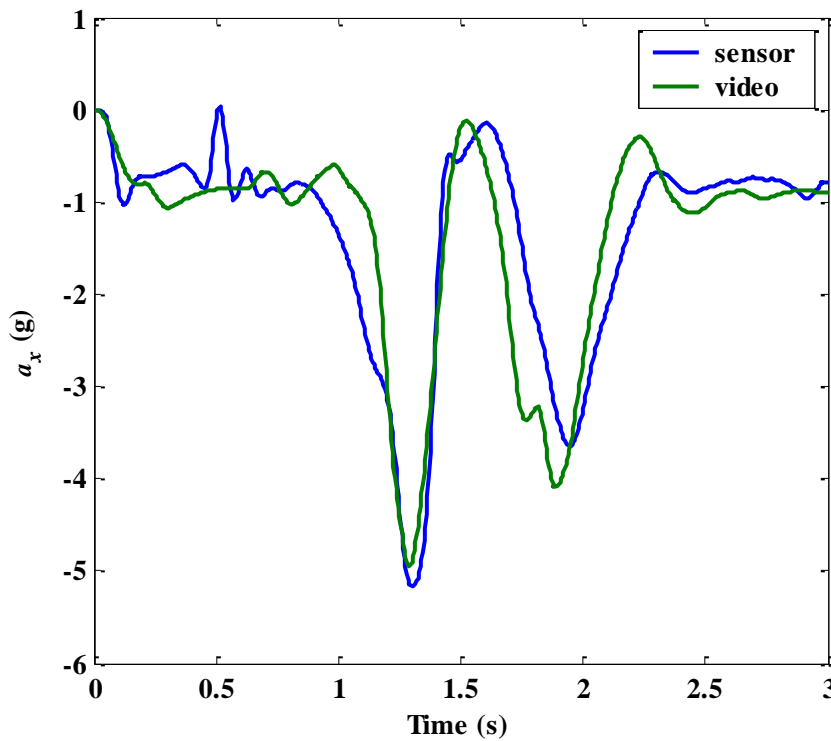


**Fig. 5.44** X-axis acceleration profiles obtained from sensor and video data.

## 5.7.4 Discussion

The drive was started at 1.0s (comparatively larger single red dot at the bottom of the bat trajectory in the left part of Fig. 5.40 or at 1.0s in Fig. 5.41) and ended at 1.52s (comparatively larger single red dot at the bottom of the bat trajectory in the right part of Fig. 5.40 or at 1.52s in Fig. 5.41) with duration of 0.52s (shown by the colored shaded region in Fig. 5.42 and 5.43). The back-lift started at 0.575s

(comparatively larger single green dot at the bottom of the bat trajectory in the left part of Fig. 5.40 or at 0.575s in Fig. 5.41) and its duration was 0.425s.
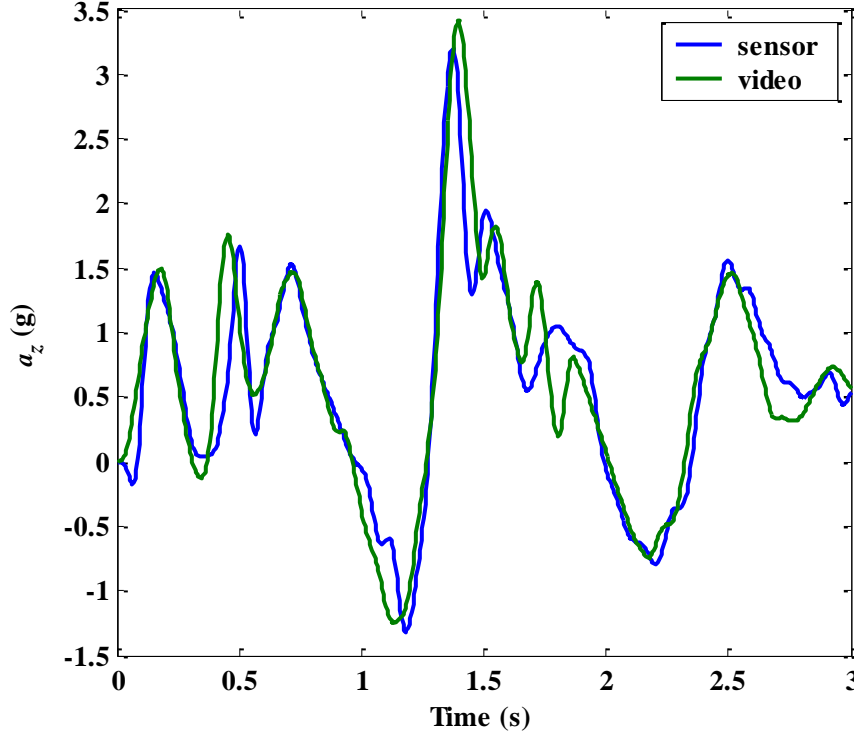


**Fig. 5.45**   Z-axis acceleration profiles obtained from sensor and video data.

Because the accelerometer data is matched with the video (as shown in Fig. 5.44 and 5.45), the duration of the drive is identified between the start of the linear negative slope of $a_x$ before going to a deep minimum to the end of the trough. This is shown in Fig. 5.42 by the shaded region. To match the video data, the radius of rotation ($R$) was varied manually to obtain the best match. The value of $R$ determined for the entire swing was plotted together with $a_x$, $a_z$ and gravity in X-axis ($g_x$) in Fig. 5.46.

The maximum peak of $a_z$ occurred at the maximum value of $R$ in the drive and $a_x$ while absolute magnitude of $g_x$ was maximum and $R$ was close to minimum in the drive shown by the three dots in Fig. 5.46. These observations suggest that for a straight drive the maximum drive velocity in the swing direction occurs when the radius of rotation is maximum (while batter straightening the hand, larger $R$ [22]) and

more control over the bat (by having more centripetal acceleration) occurs when the bat is very close to batter (smaller $R$), and aligned vertically to take advantage of full gravity.
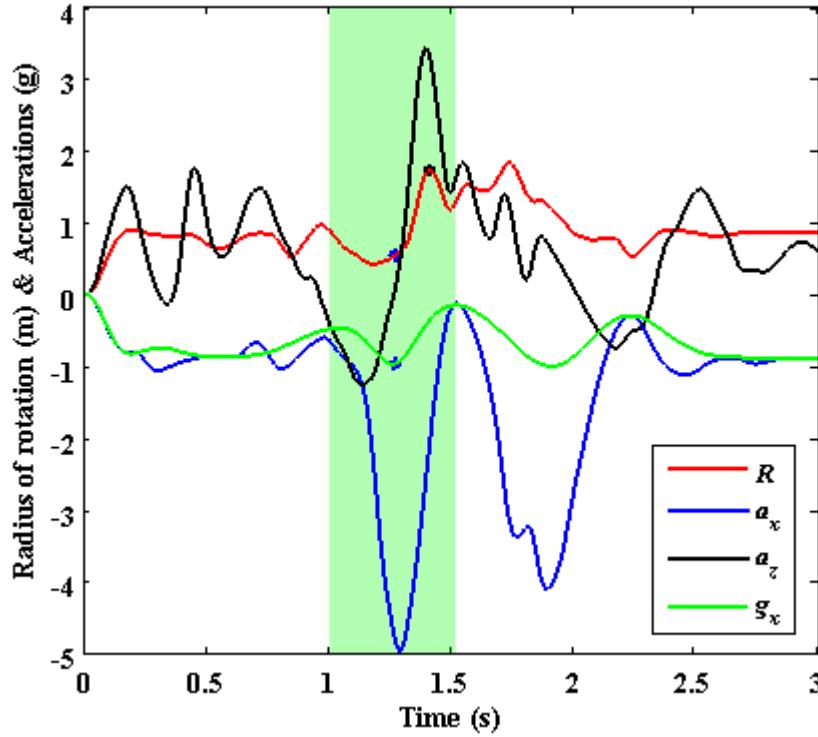


**Fig. 5.46**   Instantaneous radius of rotation during swing, X- and Z-axis acceleration, and gravity of X-axis acceleration.

Inspection of the static, rotational and translation components of the X-axis acceleration ($g_x$, $a_{xr}$, $\tau_x$ respectively) and Z-axis acceleration ($g_z$, $a_{zr}$, $\tau_z$ respectively) shown in Fig. 5.42 and 5.43 revealed the fact that during the drive and return phase (started at 1.52s shown by comparatively larger red dot at the bottom of the bat trajectory in the right part of Fig. 5.40), the rotational component was dominant for both $a_x$ and $a_z$. This finding validates the literature of swinging an implement (Koenig et al. [31]). The analytical model presented in that study assumed pure rotation of the batter/bat system about a vertical axis through the batter's body to predict the effect of moment of inertia on baseball/softball bat swing speed. The assumption proved acceptable as there was reasonable agreement between the model

and the measured speeds. The pure rotation of the bat in the drive and return phase in Fig. 5.42 and 5.43 is evident because the translational components ($\tau_x$, $\tau_z$) are almost zero. However, in case of the $a_z$ rotational component ($\underline{a_{zr}}$) was dominant throughout the drive, whereas before the drive $a_x$ translational component ($\tau_x$) was dominant. The dominant $\tau_x$ indicated the 'on guard' posture of the bat by the batter. In both $a_z$ and $a_x$ at the start of the drive some translation component is observed, and that is evident from the fact that there is little body movement and lifting of the bat at the start of that phase.

### 5.7.5 Conclusions

The feasibility of using tiny, inexpensive accelerometer in cricket batting research was investigated to replace the bulky, expensive motion capture system. Work on ball free straight drives by an amateur batter and a 3-axis accelerometer was validated with video analysis. The accelerometer data was matched to the video data by adjusting the radius of rotation of the bat. A good match was obtained between the sensor and video profiles, regression analysis showed 0.92 and 0.87 correlation coefficient for swing direction and bat axis aligned acceleration respectively. Breaking down these two accelerations into their components (rotational, translational and gravity) to match the data, the rotational component was dominant during the drive and the translational during the back-lift. However at the start of the drive a translational was noticed due to the movement of the body of the batter. The drive time duration, the posture of the bat at maximum gravity, and the instant of maximum swing velocity and its magnitude with respect to radius of rotation can easily be determined from accelerometer profiles. However, further investigation is required on a larger number of subjects with different skill levels to generate concrete decisions on the effect of the radius of rotation on swing velocity and temporal events of straight drives. Future work could be planned for other strokes by professional batters using 3-axis accelerometer to extract the spatiotemporal parameter for a standard template shot measured from bat position.

## 5.8 Relationship between wrist and bat acceleration in cricket batting

In cricket, bat and limb mounted miniature movement sensors could be useful for the assessment and understanding of effective batting.

### 5.8.1 Background

The correct grip and coupling between the hand and bat play a vital role in ball control. An understanding of hand-bat coupling before, at and after contact enables a coach to prepare the batters for improved stroke play. This work examined the use of small, low-cost, three dimensional motion sensors to assess the coupling of the top and bottom hand with the bat in a defensive stroke.

### 5.8.2 Experimental Procedure

Triaxial inertial sensors can be used for cricket shot analysis and bat swing interpretation [55], [114]. Using sensors on the bat, the left and the right wrists of five batters (one sub-elite, two amateurs had grade level playing experiences and two novices who had no sustained match play), the ball-contacts in defensive strokes were recorded. The experimental set up and protocol was the same as in Section 5.4.2. The players were asked to hit the incoming ball along the ground. The ball was delivered using an underarm throw at slow speed and without swing. The bat swing was in the x-z plane of the sensor placed on the reverse face of the bat (the bat face was in the z direction) as shown in Fig. 4.4 in Section 4.1.1.3. The sensor data were recorded in the wrists and bat attached sensors as a 3D form of $a_x$, $a_y$, $a_z$ along each sensor's X-, Y- and Z-axis respectively. The total acceleration for each sensor was calculated using Equation 4.2. The velocity of the wrists and bat was derived by integrating the total acceleration data from each sensor. Before integration the data were passed through a high-pass filter of 1 Hz cut off frequency. The filtering was performed to avoid the integration error hazards due to presence of low-frequency signal components as discussed in Section 4.1.2. The filter frequency was chosen by

observing the dominant frequency components in the FFT of the total acceleration data.

### 5.8.3 Results and discussion

The bat and wrists sensors recorded total acceleration profiles from a defensive stroke played by each of batter-1 to batter-5 (N1: amateur, N2: sub-elite, N3: amateur, N4: novice, and N5: novice) are shown in Fig. 5.47. The total acceleration was calculated one second before and after of ball-contact. Large spikes in the total acceleration indicated the ball-contact, and it is referenced as zero time in the figure. The negative and positive values in the time axis indicate before and after ball contact time respectively. First three batters data sets (first three figures in Fig. 5.47) revealed that the top hand (left hand for a right handed batter) was more strongly coupled with the bat before and after contact having a smaller acceleration difference with bat than the bottom hand. The other two batters showed neither hand was coupled properly with the bat. A second deflection showed inferior quality of ball-contact caused by the jarring. The second deflection occurs at $t = 0.01$ s in Fig. 5.47.
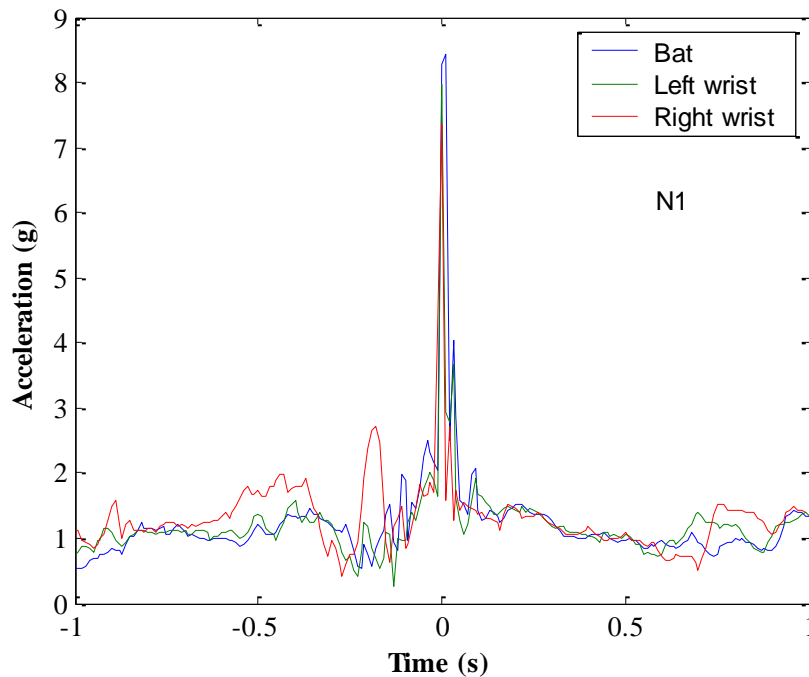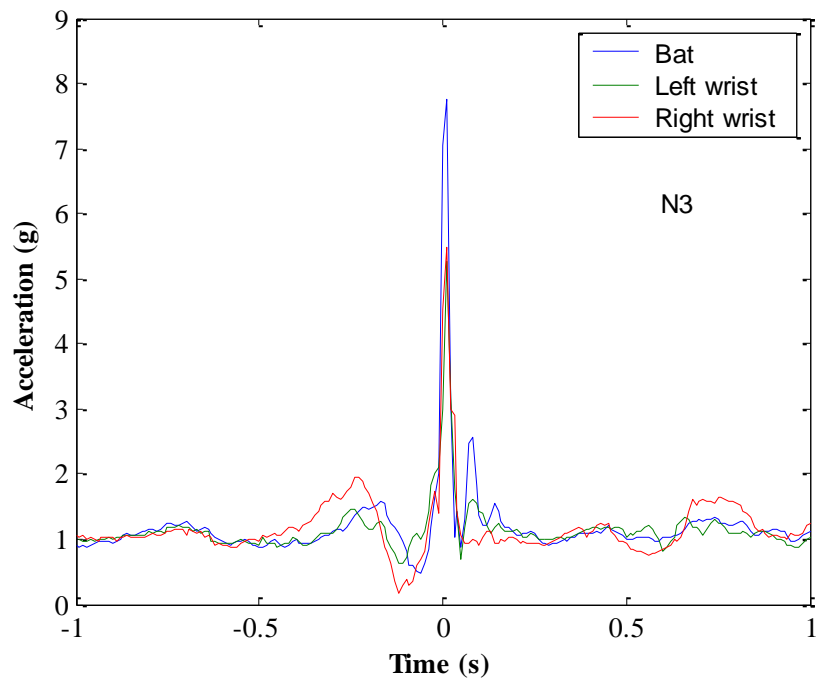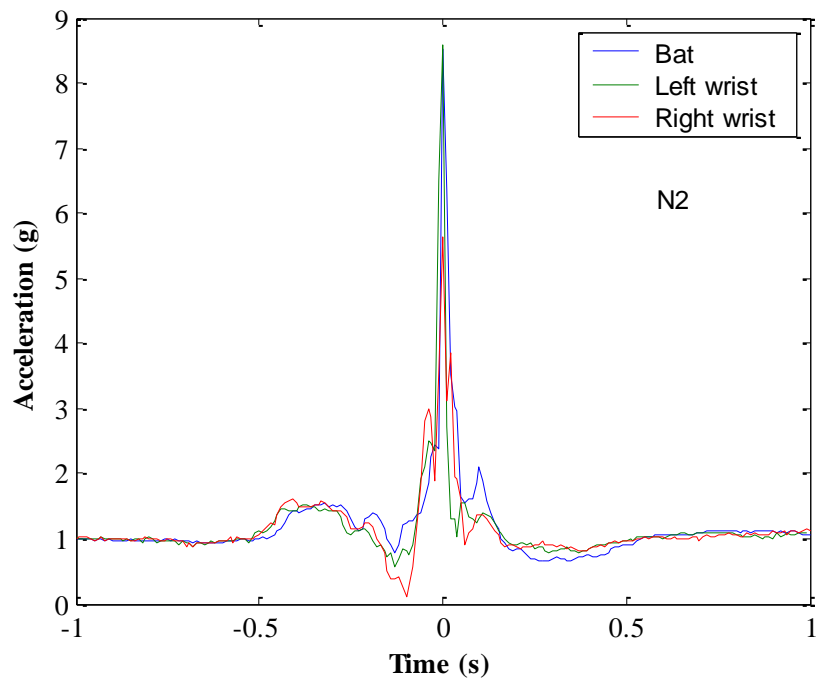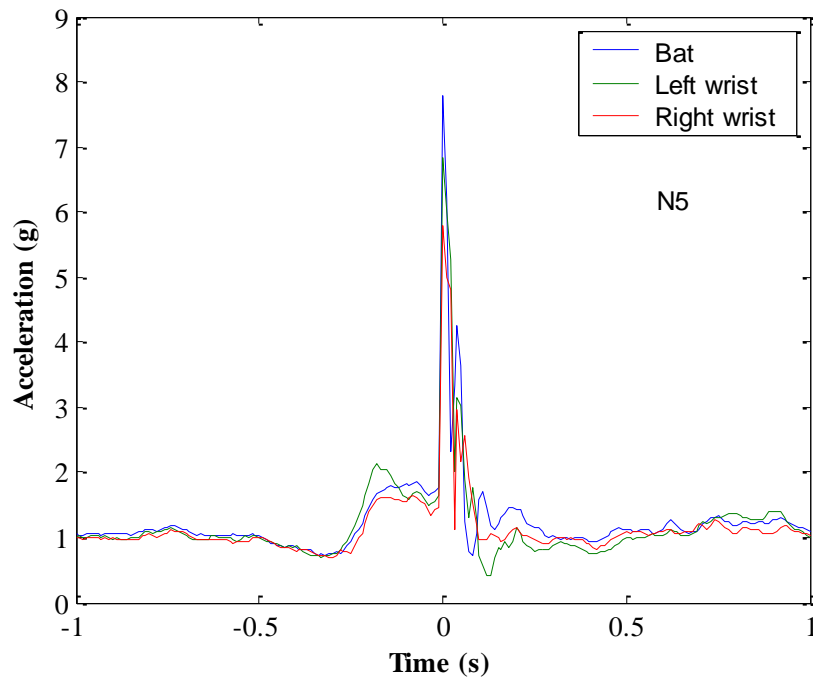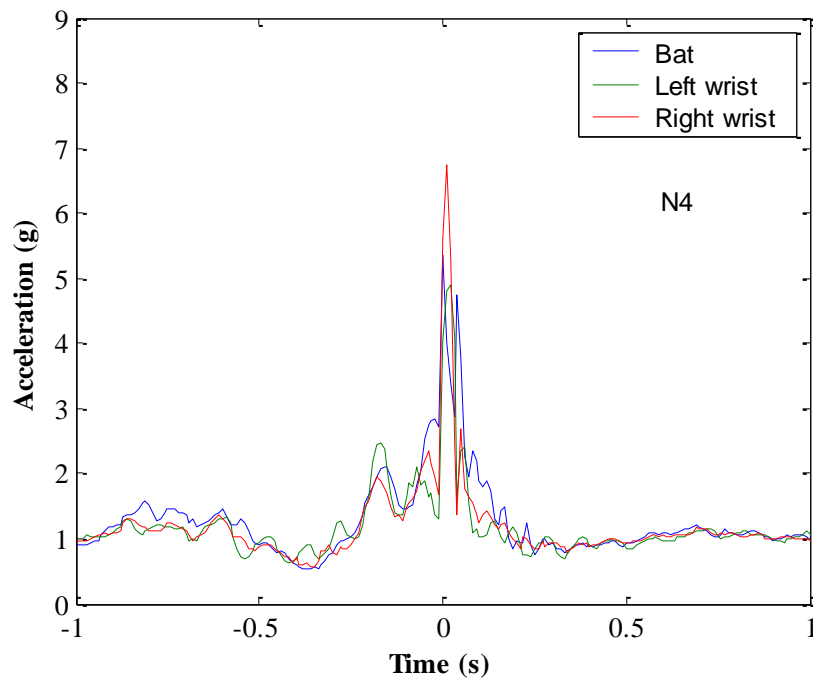
**Fig. 5.47** Total acceleration recorded in bat and wrists attached sensors for batter-1 to batter-5 (N1, N2, N3, N4, and N5) for a defensive stroke played by each. Zero in the time axis refers the ball-contact instant and negative and positive values are for the time before and after contact.

The velocities were calculated from the acceleration data using the method described in Section 5.8.2. The velocity profiles for each of the batters are shown in Fig. 5.48. Similar to the acceleration data in Fig. 5.47, the zero time indicated the ball-contact in Fig. 5.48. The velocity profiles also revealed the same fact as was in acceleration profiles that first three batters' top hand was more strongly coupled with the bat before and after contact than the bottom hand. Because of the top hand was having a smaller velocity difference with bat than the bottom hand. The wrist velocities were plotted against bat velocity for each batter is shown in Fig. 5.49. A linear relationship (slope > 0.64) was found for the left wrist (r>0.88) and slope > 0.44 for right wrists (r > 0.7) shown in the Table 5.12. This shows that the left hand was dominant [22]. On the contrary, the drives of the last 2 novices showed that their bottom hand consistently dominated the action.
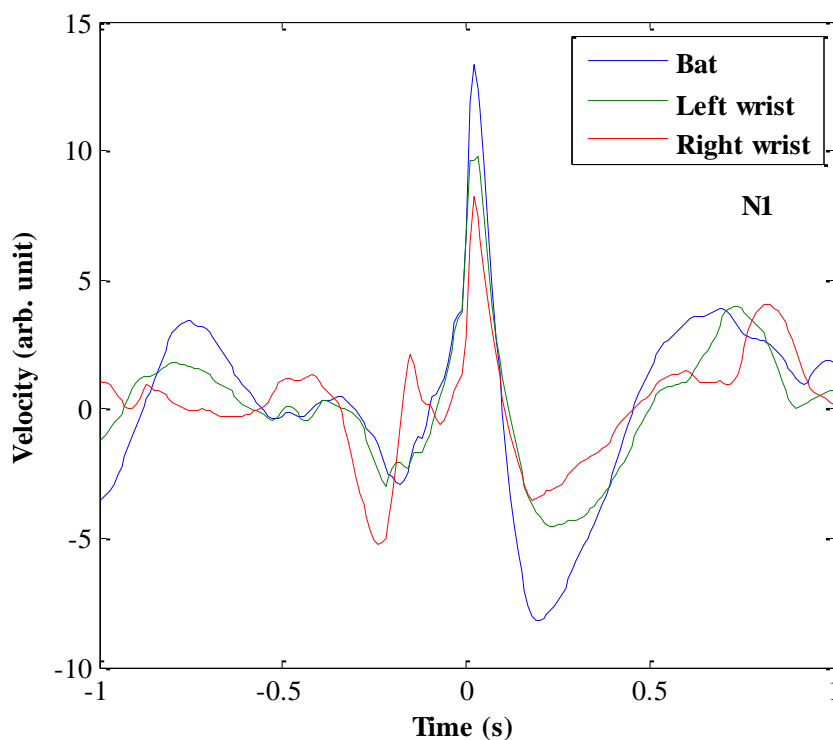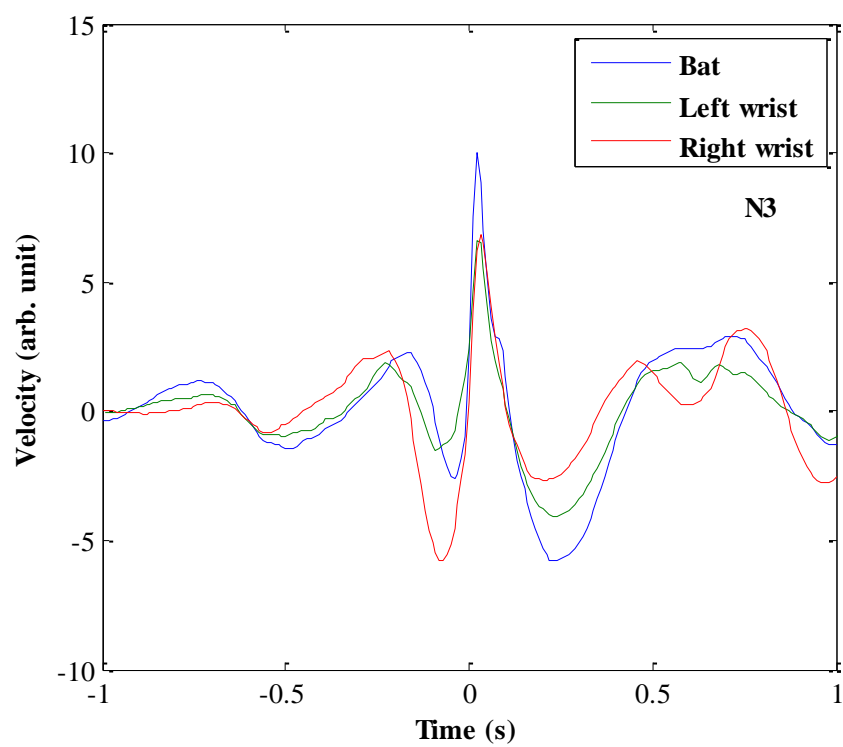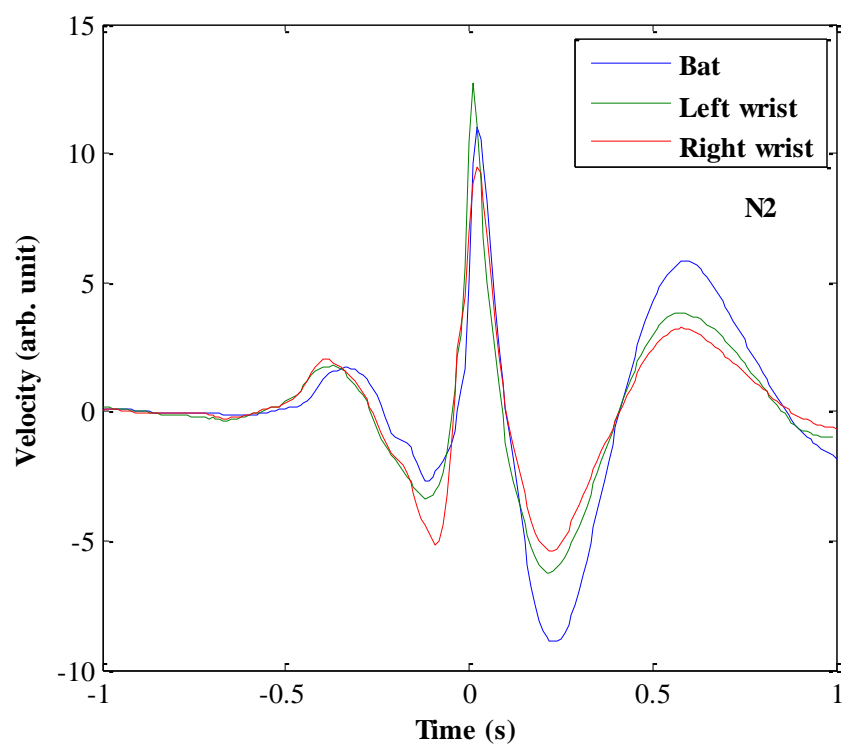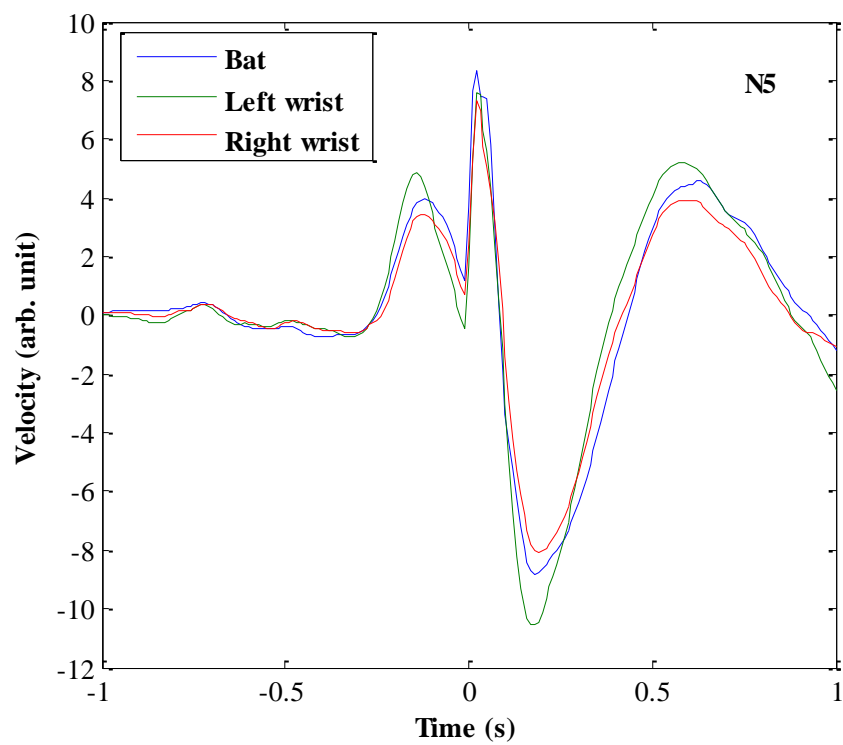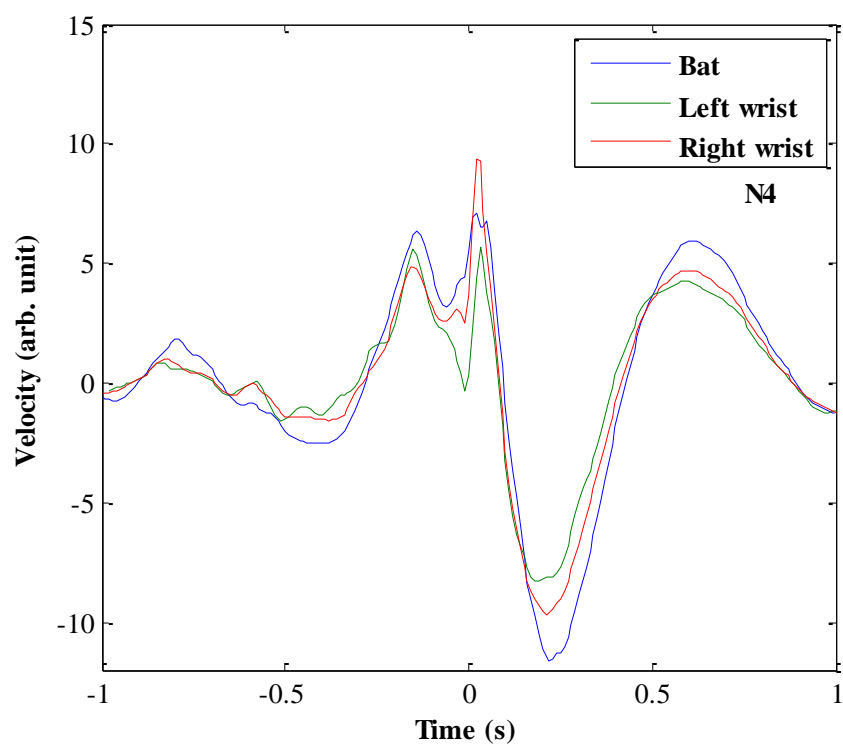
**Fig. 5.48** Velocity profiles derived from the total accelerations profiles shown in Fig. 5.47 from bat

and wrists attached sensor for batter-1 to batter-5 (N1, N2, N3, N4, and N5) for a defensive stroke played by each. Zero in the time axis refers the ball-contact instant and negative and positive values are for the time before and after contact.
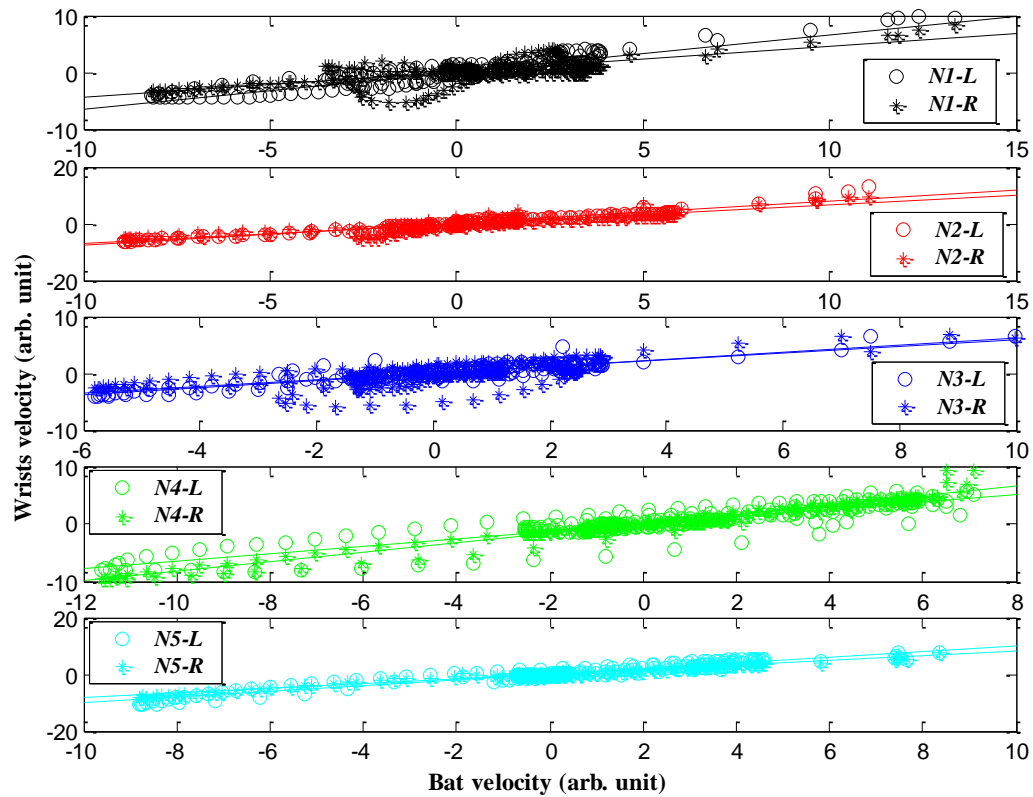


**Fig. 5.49**    Bat velocity versus wrists velocities from five batters strokes (N1~N5). Velocity data were derived from acceleration data recorded in bat, left-, right-wrist attached sensors. L and R stand for left- and right- wrist.

**Table 5.12** The statistical values for the correlation between bat versus wrists velocity shown in Fig. 5.49; r, L, R, Sl stand for regression coefficient, Left wrist, Right wrist and slope of the regression line respectively.

| Batter | r_L | r_R | Sl_L | Sl_R | Intercept_L | Intercept_R |
|--------|-----|-----|------|------|-------------|-------------|
| 1 | 0.9331 | 0.751 | 0.67 | 0.44 | 0.033 | 0.12 |
| 2 | 0.97 | 0.9266 | 0.78 | 0.68 | -0.028 | -0.0082 |
| 3 | 0.9278 | 0.7058 | 0.64 | 0.59 | -0.04 | -0.02 |
| 4 | 0.8891 | 0.9807 | 0.64 | 0.82 | 0.025 | 0.0023 |
| 5 | 0.9663 | 0.9907 | 1 | 0.84 | -0.0015 | -0.032 |

### 5.8.4 Conclusions

Using bat and wrists mounted inertial sensors one defensive stroke of each of five batters (one sub-elite, two amateurs with grade level playing experiences and two novices without regular playing experience) were recorded. The aim was to investigate the relation between bat and wrists accelerations to judge the difference in the two hands to be coupled with the bat before and after ball-contact. Both sensor recorded acceleration data and then converted velocity data showed stronger coupling of the top hand (left hand of a right-handed batter) than the bottom hand for the first three batters. Other two novices' stroke data, neither hand showed coupled with the bat resulted from inferior stroke. Because of a second deflection peak at ball-contact (shows large spike) caused by the jarring proved an inferior quality of ball-contact. However, for all batters a linear relationship (r>0.7) was found between the wrists and bat velocities. The regression line showed greater slope of left-wrist (slope>0.64) and right-wrist (slope>0.4) for first three batters. That means that top hand dominated in the stroke consistent with the literature [22], but last two novices' strokes showed the bottom hand consistently dominated the action. This study showed accelerometer sensors can provide useful information about the grip on the bat during ball contact.

## 5.9   Results summary

The results section includes the followings:

(i)     Pendulum theory was adopted in bat swing in a stroke for parameter seeking to maximize swing acceleration in a batting stroke.

(ii)    The orientation of the bat in swing during different phases of a batting stroke was determined by acceleration data.

(iii)   The impact location of the ball on the bat surface for the sweet spot hits were identified from the acceleration data.

(iv)    An approximation of bat angle equation as a function of cosine square of time was made during straight drive swing and validated by the video. Using the approximated angles the calculated acceleration profile and sensor recorded profile were compared. The angle at the end of a straight drive at different bat height by different batters was correlated with the sensor data and checked the strength of relation by the Bland Altman covariance correlation method.

(v)     Effect of high back-lift in defensive stroke in bat orientation during ball contact was determined using sensor data.

(vi)    Using rigid body dynamics and a decision codes relating to the bat posture during the straight drive, the sensor data was validated by matching the video data with sensor. One of the parameter for the maximum bat swing velocity along the swing direction was determined while matching the two data.

(vii)   The coupling of the hands (top and bottom hand) with the bat during a defensive stroke were discriminated from wrists and bat acceleration and velocity. Experienced and comparatively less-experienced batters were distinguished from the bat-hand coupling differences.

# 6  <u>CONTRIBUTIONS, CONCLUSIONS</u>

# <u>AND FUTURE DIRECTIONS</u>

## 6.1   Contributions and Conclusions

This research was dedicated to an analysis of cricket bat swing using a novel technological tool. It was concluded that tiny inertial sensors can contribute in the following ways:

(1) The limitations of existing cricket batting research methodology (bulk tools of video and opto-graphic systems) was outlined by reviewing the literature including several other sports implement swings.

(2) A miniature sensor methodology in cricket bat swing research is introduced.

(3) Signal processing features on sensor data to extract the key parameters of interest for bat swing analysis was presented. The device level errors and minimization techniques and validation of the sensor data were documented.

(4) Results from the straight drive and defensive strokes were presented. Those results indicated that bat orientation, speed, categorisation of ball-contact on the bat surface, bat-hand couple during drive, bat height at the end of drive, effect of back-lift height over bat control were easily determined using sensor data. A straight bat swing was mathematically represented with a pendulum with a moving pivot and was used to analyse the dynamics of the recorded bat swing acceleration data. The sensor profiles could be produced using the solution of the equation imposing the initial parameters of swing. It facilitates the identification of the variations of initial angular velocity, radius of rotation in sensor profiles. A cosine square function of time could be matched for the bat angle during straight drive bat swing.

The results from this novel technology were validated by using the video confirmation as used by many researchers in cricket batting research and found promising. The proposed methodology of using accelerometers has the advantages of

being small in size, cheap, having easy handling and data analysis features, and has been demonstrated to be a promising vehicle to a cricket coach in training and skill development program. Furthermore, the real-time data outcome features facilitate a feedback aid to the batters and coach about a stroke play. Direct numerical data recording abilities of sensors could facilitate the recording of the elite batters stroke play as standard techniques. This stored information can be used in coaching and to measure skill enhancement, where the existing methodology uses the human memory and video records.

In this research 1 sub-elite, 7 amateur, 14 novice batters were used as subjects. This investigation used more novice batters as participants as their batting movements are not well developed. This results in a much larger variation between batters and between each of their batting movements. The next steps of using elite and sub-elite batters will provide the outcomes of standard techniques for formulating batting template for coaching and training. However, the outcomes using the subjects in this research could be the foundation of level of skills judgment, consideration of variations in techniques, notifying possible errors areas and improvement measures to establish a batting expertise development program.

## 6.2 Future Directions

This research established the foundation of using accelerometer sensors in cricket bat swing analysis and focused on classical batting shots (straight drives and defensive strokes). Integrating accelerometer sensors with gyroscope, magnetometer, and pressure sensors can provide the opportunity to analyze other advanced batting shots. The inclusion of wireless facilities with the sensors can provide feedback to the coach about the quality of stroke play.

This research used the swing mechanics from pendulum theory and outlined the effect of initial angular velocity, radius of rotation on the swing profile. The validation of the sensor profile from straight drive with the pendulum equation

estimated profile laid scopes to quantify the force level of batters using only the sensor data. Different levels of player development could be assessed quantitatively using sensor profiles. The bat angle function validated in this research could be used for calculating force, swing inertia to assess the skills of batters and useful in other swing sports implement swing. The use of acceleration in batting analysis and the mechanics of a shot could be beneficial to coach for setting the attributes for a particular skill enhancement. The data analysis features of these sensors could help coaches to use templates from experienced batters in their coaching skills development.

# 7  <u>SUMMARY</u>

The research in this thesis has established a foundation of using sensor technology in extracting bat swing features. The practical implications have provided by analysing classical straight drive and defensive shots by sensor in several studies. The validation of the results proved sensor methodology a promising investigative tool for the sports scientist. The analysis on a cosine square function for bat angle and mechanics of pendulum with moving pivot provided the insight to include science in bat swing and to validate the sensor method from science perspectives. The entirety of the research presented here was to make an attempt to provide the insight for replacement of the existing bulky methodology of batting research by sensors. This sensor methodology could be advantageous in batting skill development, particularly any training or competition activity. A number of defined areas are identified for future research directions.

# REFERENCES

[1]     M. C. Club. (12-11-2009). *Laws of Cricket*. Available: http://www.lords.org/mcc/laws-of-cricket/

[2]     Rediff.com. (2013). *Puma Iridium Gt Kashmir Willow Cricket Bat*. Available: http://shopping.rediff.com/product/puma-iridium-gt-kashmir-willow-cricket-bat/10823686

[3]     EnglishClub. (11-06-2012). *Cricket*. Available: http://www.englishclub.com/vocabulary/sports-cricket.htm

[4]     R. M. Bartlett, "The science and medicine of cricket: an overview and update " *Journal of Sports Sciences,* vol. 21, pp. 733–752, 2003.

[5]     B. Elliott, "An Overview of Sport Science Literature in Cricket: Where are we at?," in *Conference of Science, Medicine & Coaching in Cricket 2010*, Gold Coast, Australia, 2010, pp. 7–11.

[6]     V. Sarpeshkar and D. L. Mann, "Biomechanics and visual-motor control: how it has, is, and will be used to reveal the secrets of hitting a cricket ball," *Sports Biomechanics,* vol. 10, pp. 306-323, 2011.

[7]     R. J. Clarke. (2005, 16-09-2011). *Research Models and Methodologies*. Available: www.uow.edu.au/content/groups/public/@web/@commerce/documents/doc/uow012042.pdf

[8]     D. F. Gucciardi and S. Gordon, "Development and preliminary validation of the Cricket Mental Toughness Inventory (CMTI)," *Journal of Sports Sciences,* vol. 27, pp. 1293-1310, 2009.

[9]     J. W. Orchard, T. James, M. Portus, A. Kountouris and R. Dennis, "Fast bowlers in cricket demonstrate up to 3- to 4-week delay between high workloads and increased risk of injury," *The American Journal of Sports Medicine,* vol. 37, pp. 1186–1192, 2009.

[10]    J. Weissensteiner, B. Abernethy, D. Farrow, "Towards the development of a conceptual model of expertise in cricket batting: a grounded theory approach," *Journal of Applied Sport Psychology,* vol. 21, pp. 276–292, 2009.

[11]    C. J. Christie, A. I. Todd, and G. A. King, "Selected physiological responses during batting in a simulated cricket work bout: A pilot study," *Journal of Science and Medicine in Sport,* vol. 11, pp. 581-584, 2008.

[12]    M. C. Stuelcken, R. E. Ferdinands, P. J. Sinclair, "Three-dimensional trunk kinematics and low back pain in elite female fast bowlers.," *Journal of Applied Biomechanics,* vol. 26, pp. 52–61, 2010.

[13]    G. R. Dias, R. Ferdinands, "The biomechanics of the Initial Movement in Cricket Batting," in *Conference of Science, Medicine & Coaching in Cricket 2010*, Gold Coast, Australia, 2010, pp. 63–66.

[14]    J. A. Hides, W. R. Stanton, M. Freke. MRI Study of the size, symmetry and function of the trunk muscles among elite cricketers with and without low back pain [Online]. Available: bjsm.bmj.com

[15]    B. Elliott, M. Khangure, "Disk degeneration and fast bowling in cricket: an intervention study.," *Med Sci Sports Exerc.,* vol. 34, pp. 1714–1718, 2002.

[16]    H. D. Visser, C. J. Adam, S. Crozier, M. J. Pearcy, "The role of quadratus lumborum asymmetry in the occurrence of lesions in the lumbar vertebrae of cricket fast bowlers," *Medical Engineering & Physics,* vol. 29, pp. 877–885, 2007.

[17]  M. R. Portus, C. D. Rosemond, and D. A. Rath, "Fast bowling arm actions and the illegal delivery law in men's high performance cricket matches," *Sports biomechanics / International Society of Biomechanics in Sports,* vol. 5, pp. 215-230, 2006.

[18]  R. A. Pinder, I. Renshaw and K. Davids, "Information-movement coupling in developing cricketers under changing echological practice constraints " *Human Movement Science,* vol. 28, pp. 468–479, 2009.

[19]  R. Pinder, K. Davids, I. Renshaw, and D. Araújo, "Manipulating informational constraints shapes movement reorganization in interceptive actions," *Attention, Perception, & Psychophysics,* vol. 73, pp. 1242-1254, 2011.

[20]  R. Davies, R. du Randt, D. Venter, R. Stretch, "Cricket: Nature and incidence of fast-bowling injuries at an elite, junior level and associated risk factors," *South African Journal of Sports Medicine* vol. 20, pp. 115-118, 2008.

[21]  BigCricket. (2010, 12-10-2011). *The Three Phases of Batting*. Available: http://www.bigcricket.com/community/threads/the-three-phases-of-batting.49166/

[22]  R. Stretch, F. Buys, E. D. Toit, G. Viljoen, "Kinematics and kinetics of the drive off the front foot in cricket batting " *Journal of Sports Sciences,* vol. 16, pp. 711–720, 1998.

[23]  I. Renshaw, A. R. H. Oldham, K. Davids, T. Golds, "Changing ecological constraints of practice alters coordination of dynamic interceptive actions " *European Journal of Sport Science,* vol. 7, pp. 157–167, 2007.

[24]  S. Müller, B. Abernethy, "Batting with occluded vision: An in situ examination of the information pick-up and interceptive skills of high-and low-skilled batsmen " *Journal of Science and Medicine in Sport,* vol. 9, pp. 446–458, 2006.

[25]  S. Müller, B. Abernethy, J. Reece, M. Rose, M. Eid, R. McBean, T. Hart and C. Abreu, "An in-situ examination of the timing of information pick-up for interception by cricket batsmen of different skill levels " *Psychology of Sport and Exercise,* vol. 10, pp. 644–652, 2009.

[26]  J. M. T. Penrose, D. R. Hose, "An impact analysis of a flexible bat using an iterative solver," *Journal of Sports Sciences,* vol. 17, pp. 677–682, 1999.

[27]  R. Bower, "The sweet spot of a cricket bat for low speed impacts," *Sports Engineering,* vol. 15, pp. 53-60, 2012.

[28]  D. L. Mann, B. Abernethy, D. Farrow "The resilience of natural interceptive actions to refractive blur " *Human Movement Science* vol. 29, pp. 386–400, 2010.

[29]  R. Cross, "A double pendulum swing experiment: In search of a better bat," *American journal of physics,* vol. 73, pp. 330–339, 2005.

[30]  R. Shapiro, "Three-dimensional kinetic analysis of the baseball swing," Doctor of Philosophy, University of Illinois at Urbana-Champaign, IL, 1979.

[31]  K. Koenig, N. D. Mitchell, T. E. Hannigan, J. K. Clutter, "The influence of moment of inertia on baseball/softball bat swing speed " *Sports Engineering,* vol. 7, pp. 105-117, 2004.

[32]  S. J. MacKenzie, "Club position relative to the golfer's swing plane meaningfully affects swing dynamics," *Sports Biomechanics,* vol. 11, pp. 149-164, 2012.

[33]  G. S. Sawicki, M. Hubbard, W. J. Stronge, "How to hit home runs: Optimum baseball bat swing parameters for maximum range trajectories " *American journal of physics,* vol. 71, pp. 1152–1162, 2003.

[34]  C. I. Egret, O. Vincent, J. Weber, F. H. Dujardin, D. Chollet  "Analysis of 3D Kinematics Concerning Three Different Clubs in Golf Swing," *International Journal of Sports Medicine,* vol. 24, pp. 465-470, 2003.

[35]     D. Delay, V. Nougier, J.-P. Orliaguet, and Y. Coello, "Movement control in golf putting," *Human Movement Science,* vol. 16, pp. 597-619, 1997.

[36]     A. Vena, D. Budney, T. Forest, and J. Carey, "Three-dimensional kinematic analysis of the golf swing using instantaneous screw axis theory, part 1: methodology and verification," *Sports Engineering,* vol. 13, pp. 105-123, 2011.

[37]     A. Vena, D. Budney, T. Forest, and J. Carey, "Three-dimensional kinematic analysis of the golf swing using instantaneous screw axis theory, Part 2: golf swing kinematic sequence," *Sports Engineering,* vol. 13, pp. 125-133, 2011.

[38]     R. A. Stretch, A. Brink, and J. Hugo, "Cricket," *Sports Biomechanics,* vol. 4, pp. 37-45, 2005/01/01 2005.

[39]     D. L. Mann, N. Y. Ho, N. J. D. Souza, D. R. Watson, and S. J. Taylor, "Is optimal vision required for the successful execution of an interceptive task?," *Human Movement Science,* vol. 26, pp. 343–356, 2007.

[40]     M. C. Stuelcken, M. R. Portus, B. R. Mason, "Off-side front foot drives in men's high performance cricket " *Sports Biomechanics,* vol. 4, pp. 17–35, 2005.

[41]     M. S. Taliep, U. Galal, & C. L. Vaughan, "The position of the head and centre of mass during the front foot off-drive in skilled and less-skilled cricket batsmen," *Sports Biomechanics,* vol. 6, pp. 345–360, 2007.

[42]     S. Müller, B. Abernethy, "Validity and reliability of a simple categorical tool for the assessment of interceptive skill," *Journal of Science and Medicine in Sport* vol. 11, pp. 549–552, 2008.

[43]     A. Ahmadi, D. D. Rowlands, D. A. James, "Development of inertial and novel marker-based techniques and analysis for upper arm rotational velocity measurements in tennis," *Sports Engineering,* vol. 12, pp. 179-188, 2010.

[44]     A. Ahmadi, D. D. Rowlands, D. A. James, "Investigating the translational and rotational motion of the swing using acclerometers for athlet skill assessment " presented at the 5th IEEE Conference on Sensors 2006, Daegu, Korea, 2006.

[45]     A. Ahmadi, D. Rowlands, D. A. James, "Towards a wearable device for skill assessment and skill acquisition of a tennis player during the first serve," *Sports Technology,* vol. 2, pp. 129-136, 2009.

[46]     N. Davey, M. Anderson and D. A. James, "Validation trial of an accelerometer-based sensor platform for swimming," *Sports Technology,* vol. 1, pp. 202–207, 2008.

[47]     D. Rowlands, D. A. James, D. Thiel, "Bowler analysis in cricket using centre of mass inertial monitoring," *Sports Technology,* vol. 2, pp. 39–42, 2009.

[48]     A. Wixted, W. Spratford, M. Davis, M. Portus, D. James, "Wearable sensors for on field near real time detection of illegal bowling actions," in *Conference of Science, Medicine & Coaching in Cricket 2010*, Gold Coast, Australia, 2010, pp. 165–168.

[49]     A. Busch, and D. James, "Extraction of virtual acceleration data from motion capture," in *26th International Conference on Biomechanics in Sport*, Seoul, Korea, 2008, pp. 68–71.

[50]     K. King, J. Hough, R. McGinnis, N. C. Perkins, "A new technology for resolving the dynamics of a swinging bat," *Sports Engineering,* vol. 15, pp. 41-52, 2012.

[51]     L. Fallon, J. Sherwood, M. Donaruma, "An Assessment of Sensing Technologies to Monitor The Collision of a Baseball and Bat (P34)," in *The Engineering of Sport 7*, ed: Springer Paris, 2008, pp. 191-198.

[52]    D. A. James, "A biofeedback system for swing skill acquisition in implement sports," in *Joint Symposium on Sports Engineering and Human Dynamics*, Tokyo, Japan, 2008, pp. 171–172.

[53]    A. J. Wixted, D. C. Billing, D. A. James, "Validation of trunk mounted inertial sensors for analysing running biomechanics under field conditions, using synchronously collected foot contact data," *Sports Engineering,* vol. 12, pp. 207–212, 2010.

[54]    K. Ohta, K. Umegaki, K. Murofushi, A. Komine, C. Miyaji, "Dynamics-based force sensor using accelerometers-application of hammer throw training aid- (P37)," *The Engineering of Sport 7,* vol. 1, pp. 207–213, 2008.

[55]    A. Busch, & D. A. James, "Analysis of cricket shots using inertial sensors," *The Impact of Technology on Sport II,* pp. 317–322, 2008.

[56]    Sportplan. (2010). *How to Play the Straight Drive*. Available: www.sportplan.com

[57]    G. J. P. Savelsbergh, R. J. Bootsma "Perception-action coupling in hitting and catching," *International Journal of Sport Psychology,* vol. 25, pp. 331-343, 1994.

[58]    D. Regan, "Visual factors in hitting and catching," *Journal of Sports Sciences,* vol. 15, pp. 533-558, 1997.

[59]    A. M. Williams, K. Davids, & J. G. Williams, *Visual perception and action in sport*. London: E&FN Spon, 1999.

[60]    M. R. Portus, D. Farrow, "Enhancing cricket batting skill: implications for biomechanics and skill acquisition research and practice," *Sports Biomechanics,* vol. 10, pp. 294-305, 2011.

[61]    D. L. Mann, B. Abernethy, D. Farrow, "Action specificity increases anticipatory performance and the expert advantage in natural interceptive tasks," *Acta Psychologica,* vol. 135, pp. 17-23, 2010.

[62]    B. Elliott, J. Baker, and D. Foster, "The kinematics and kinetics of the off-drive and on-drive in cricket," *The Australian Journal of Science and Medicine in Sport,* vol. 25, pp. 48–54, 1993.

[63]    J. Weissensteiner, B. Abernethy, D. Farrow, S. Müller "The development of anticipation: a cross-sectional examination of the practice experiences contributing to skill in cricket batting " *Journal of Sport & Exercise Psychology,* vol. 30, pp. 663–684, 2008.

[64]    M. G. Kelly, K. M. Curtis and M. P. Craven, "Fuzzy recognition of cricket batting strokes based on sequences of body and bat postures   " in *IEEE* Southeastcon 2003, pp. 140-147.

[65]    R. Cross, "Mechanics of swinging a bat " *American Journal of Physics* vol. 77, pp. 36–43, 2009.

[66]    R. Cross, & R. Bower, "Effects of swing-weight on swing speed and racket power " *Journal of Sports Sciences,* vol. 24, pp. 23–30, 2006.

[67]    S. Joseph, R. Ganason, B. D. Wilson, T. H. Teong, C. R. Kumar *A biomechanical analysis of the straight hit of elite women hockey players* London: Taylor & Francis, 2008.

[68]    J. Weissensteiner, B. Abernethy, D. Farrow, "A skill test for examining the development of technical skill in cricket batting " in *Cricket Australia Sport Science Sport Medicine Conference 2007*, Brisbane, Australia, 2007, pp. 32–33.

[69]    P. J. Beek, J. C. Dessing, C. E. Peper and D. Bullock, "Modelling the control of interceptive actions," *Philosophical transactions. Biological sciences,* vol. 358, pp. 1511–1523, 2003.

[70]     S. Müller, and S. Rosalie, "Transfer of Motor Skill Learning: Is it Possible?," in *Conference of Science, Medicine & Coaching in Cricket 2010*, Gold Coast, Australia, 2010, pp. 109–111.

[71]     I. Karliga, and J.-N. Hwang, "Analyzing human body 3-D motion of Golf swing  from single-camera video sequences   " in *International Conference on Acoustics, Speech and Signal Processing*, 2006, pp. V493–V496.

[72]     S. Müller, B. Abernethy, D. Farrow, "How do world-class cricket batsmen anticipate a bowler's intention?," *The Quarterly Journal of Experimental Psychology,* vol. 59, pp. 2162–2186, 2006.

[73]     G. S. Fleisig, N. Zheng, D. F. Stodden, J. R. Andrews, "Relationship between bat mass properties and bat velocity," *Sports Engineering,* vol. 5, pp. 1-8, 2002.

[74]     A. J. Wixted, D. V. Thiel, A. G. Hahn, C. J. Gore, D. B. Pyne, and D. A. James, "Measurement of Energy Expenditure in Elite Athletes Using MEMS-Based Triaxial Accelerometers " *IEEE Sensors Journal,* vol. 7, pp. 481–488, 2007.

[75]     A. M. Sabatini, C. Martelloni, S. Scapellato, and F. Cavallo, "Assessment of Walking Features From Foot Inertial Sensing," *IEEE Transactions on Biomedical Engineering,* vol. 52, pp. 486–494, 2005.

[76]     T. Helten, H. Brock, M. Mu¨ller, H.-P. Seidel, "Classification of trampoline jumps using inertial sensors," *Sports Engineering,* vol. 14, pp. 155–164, 2011.

[77]     M. Schulze, T.-H. Liu, J. Xie, W. Zhang, K.-H. Wolf, T. Calliess, H. Windhagen, and M. Marschollek, "Unobtrusive ambulatory estimation of knee joint angles during walking using gyroscope and accelerometer data - a preliminary evaluation study," in *IEEE-EMBS International Conference on Biomedical and Health Informatics (BHI 201 2)*, Hong Kong and Shenzhen, China, 2012, pp. 559–562.

[78]     J. J. Kavanagh, S. Morrison, D. A. James and R. Barrett, "Reliability of segmental accelerations measured using a new wireless gait analysis system " *Journal of Biomechanics,* vol. 39, pp. 2863–2872, 2006.

[79]     Y. Ohgi, "Microcomputer-based acceleration sensor device for sports biomechanics-stroke evaluation by using swimmer's wrist acceleration," in *Proceedings of IEEE Sensors*, 2002, pp. 699-704.

[80]     H. Ghasemzadeh, V. Loseu, E. Guenterberg, R. Jafari, "Sport training using body sensor networks: A statistical approach to measure wrist rotation for golf swing," in *The Fourth International Conference on Body Area Networks (BodyNets 09)*, Los Angeles, CA, 2009.

[81]     M. Lapinski, E. Berkson, T. Gill, M. Reinold, and J. A. Paradiso, "A distributed wearable, wireless sensor system for evaluating professional baseball pitchers and batters," in *International Symposium on Wearable Computers (ISWC'09)* 2009, pp. 131-138.

[82]     D. A. James, N. Davey, T. Rice, "An accelerometer based sensor platform for insitu elite athlete performance analysis," in *IEEE Sensor*, Vienna, Austria, 2004, pp. 1373–1376.

[83]     M. Sipos, P. Paces, J. Rohac, and P. Novacek, "Analyses of triaxial accelerometer calibration algorithms," *IEEE SENSORS JOURNAL,* vol. 12, pp. 1157–1165, 2012.

[84]     U. X. Tan, K. C. Veluvolu, W. T. Latt, C. Y. Shee, C. N. Riviere, and W. T. Ang, "Estimating displacement of periodic motion with inertial sensors," *IEEE SENSORS JOURNAL,* vol. 8, pp. 1385–1388, 2008.

[85]     Y. S. Suh, "A Smoother for Attitude and Position Estimation Using Inertial Sensors With Zero Velocity Intervals," *IEEE SENSORS JOURNAL,* vol. 12, pp. 1255–1262, 2012.

[86]  R. Cross, "A double pendulum model of tennis strokes," *American Journal of Physics,* vol. 79, pp. 470–476, 2011.

[87]  R. Cross, "Response to ''Comment on 'The sweet spot of a baseball bat' '' [Am. J. Phys. 69 (2), 229–230 (2001)]," *American journal of physics,* vol. 69, pp. 231–232, 2001.

[88]  R. Cross, "The sweet spots of a tennis racquet," *Sports Engineering,* vol. 1, pp. 63–78, 1998.

[89]  R. K. Adair, "Comment on ''The sweet spot of a baseball bat,'' by Rod Cross [Am. J. Phys. 66 (9), 772–779 (1998)]," *American journal of physics,* vol. 69, pp. 229–230, 2001.

[90]  A. W. B. Garner, J. L. Newbery, "CRICKET BAT," 4,186,923, 1980.

[91]  M. F. Land, P. McLeod, "From eye movements to actions: how batsmen hit the ball," *Nature neuroscience,* vol. 3, pp. 1340–1345, 2000.

[92]  A. P. Gibson, & R. D. Adams, "Batting stroke timing with a bowler and a bowling machine: A case study," *Australian Journal of Science and Medicine in Sport,* vol. 21, pp. 3–6, 1989.

[93]  J. Potts. (2011, 7-10-12). *Cricket Batting Tips*. Available: www.mademan.com/mm/cricket-batting-tips.html#vply=0

[94]  Sportplan. (2011, 28-08-2011). *Front foot defence, Batting Mechanics Cricket*. Available: www.sportplan.net/drills/Cricket/Batting-Mechanics/Front-foot-defence-frontdef.jsp

[95]  C. Web. (25-09-12). *Coaching: Batting - Front Foot Strokes*. Available: www.cricketweb.net/resources/coaching/frontfootstrokes.php

[96]  K. M. Curtis, G. M. Kelly, M. P. Craven "Cricket batting technique analyser/trainer using fuzzy logic " presented at the 16th International Conference on Digital Signal Processing, Santorini-Hellas, 2009.

[97]  Y. Ohgi, T. Baba, and I. Sakaguchi, "Measurement of Deceleration of Golfer's Sway and Uncock Timing in Driver Swing Motion," *The Impact of Technology on Sport,* pp. 349-354, 2005.

[98]  V. D. Opfer. (12-03-2012). *Perspectives on Research Methodology - Darleenopfer.com* Available: www.darleenopfer.com

[99]  N. Davey, A. Wixted, Y. Ohgi, D. A. James, "A low cost self contained platform for human motion analysis " *The Impact of Technology on Sport II,* pp. 101–111, 2008.

[100]  A. J. Wixted, "In-situ Athlete Monitoring: Data Collection, Interpretation & Feature Extraction," Doctor of Philosophy, Griffith School of Engineering, Griffith University, Brisbane, Australia, 2007.

[101]  A. Lai, D. A. James, J. P. Hayes, and E. C. Harvey, "Semi-automatic calibration technique using six inertial frames of reference," in *Proceedings of SPIE*, 2003, pp. 531-542.

[102]  D. T. W. Fong, J. C. W. Wong, A. H. F. Lam, R. H. W. Lam, and W. J. Li, "A wireless motion sensing system using ADXL MEMS accelerometers for sports science applications," in *Fifth World Congress on Intelligent Control and Automation, WCICA* 2004, pp. 5635-5640 Vol.6.

[103]  f. s. inc. (2005, 12-7-12). Available: www.freescale.com

[104]  R. Oshana, *DSP Software Development Techniques for Embedded and Real-Time Systems*: Elsevier Science, 2006.

[105]  A. Savitzky, and M. J. E. Golay, "Smoothing and Differentiation of Data by Simplified Least Squares Procedures " *Analytical Chemistry,* vol. 36, pp. 1627–1639, 1964.

[106]    D. A. James and A. Wixted, "ADAT: A Matlab toolbox for handling time series athlete performance data," *Procedia Engineering,* vol. 13, pp. 451–456, 2011.

[107]    M. Meredith, S. Maddock. *Motion Capture File Formats Explained*. Available: http://www.dcs.shef.ac.uk/intranet/research/public/resmes/CS0111.pdf

[108]    D. James, A. Wixted, "Technology in Sports Assessment: Past, Present and Future," in *Conference of Science, Medicine & Coaching in Cricket 2010*, Gold Coast, Australia, 2010, pp. 161–164.

[109]    M. Renardy. *The Pendulum Equation - The Department of Mathematics at Virginia Tech*. Available: www.math.vt.edu/people/renardy/class_home/FromSun/ade_ch2.pdf

[110]    L. Bai, M. G. Pepper, Y. Yan, S. K. Spurgeon, and M. Sakel, "Application of low cost inertial sensors to human motion analysis," in *IEEE International Instrumentation and Measurement Technology Conference (I2MTC)* 2012, pp. 1280-1285.

[111]    R. A. Stretch, R. Bartlett, K. Davids, "A review of batting in men's cricket " *Journal of Sports Sciences,* vol. 18, pp. 931–949, 2000.

[112]    J. M. Bland, D. G. Altman "Calculating correlation coefficients with repeated observations: Part 1-correlation within subjects," *British Medical Journal,* vol. 310, p. 446, 1995.

[113]    R. A. Stretch, "A biomechanical analysis of batting in cricket " Unpublished doctoral dissertation, University of Port Elizabeth, Port Elizabeth, South Africa, 1993.

[114]    A. K. Sarkar, D. A. James, A. W. Busch, D. V. Thiel, "Triaxial accelerometer sensor trials for bat swing interpretation in cricket," *Procedia Engineering,* vol. 13, pp. 232 –237, 2011.

# APPENDICES

## Appendix A: Terminology, notational style and reading and processing of MOCAP data to Chapter 4 (Section 4.1.3)

This appendix defines the terminology used in MOCAP system and outlines the data reading and processing techniques [107].

The different aspects of a motion of a point on a rigid body or an entire limb as the combination of several points is identified and described by some key words or terminology, these are *Skeleton*, *Bone*, *Channel* or *Degree of Freedom* (DOF), and *Frame*.

*Skeleton* is the complete reconstructed linkages of all marker placed in the volume.

*Bone* is the basic entity in the representation of a skeleton and it is subjected to have its individual translation and orientation changes during the animation of the skeleton. A number of bones (usually in a hierarchical structure, as illustrated in Fig. 1) comprise a skeleton, where each bone can be associated with a vertex mesh to represent a specific part of the character, for example the femur or humerus bones.

*Channel* or *Degree of Freedom* are parameters that describe the position, orientation and scale changes of each bone within a skeleton over the course of the animation. The changes in the channel data over time give information about the animation.

*Frame* is the unit of every animation for which the channel data for each bone is defined. Every animation is comprised of a number of frames. High frame rates (frames per second) of animation data can be captured by the motion capture system, for instance, as high as 240 frames per second. In many applications the normal rate is usually 30 or 60 frames per second is sufficient.
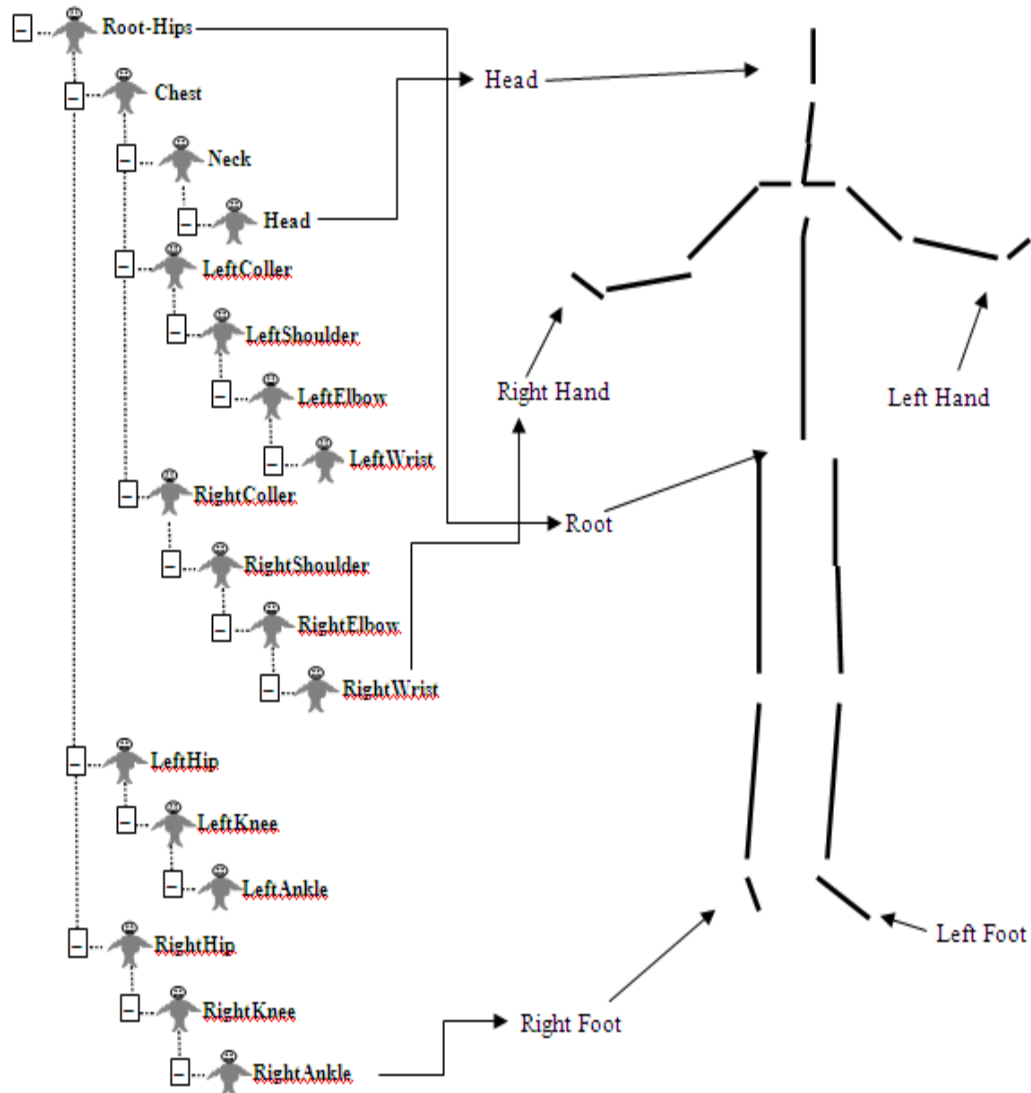
**Fig. 1** Hierarchical structure for a Human Figure used in 3D motion capture systems [107].

Motion capture matrix arithmetic is required to process the captured data to transform the bones to their correct position and orientation. The matrix arithmetic of an individual bone consists of translation, rotation and scale components (depending on the channels defined for the bone), which can be merged together to give an overall transform using homogeneous coordinates. Three separate matrices are required to form the transformation matrix ($M$) needed to express the transformed vertices from the original vertices for an animation. The equation of the

transformation matrix and the relation between original vertices and the transformed vertices are shown in Equation 1.

$$M = TRS, \quad V' = VM \tag{1},$$

where $T$, $R$ and $S$ are translation, rotation, and scale matrices respectively, and $V'$ and $V$ are transformed and original vertices respectively. Equation 1 is used over the traditional left to right approach. The convention is important particularly when the rotation matrix is constructed from its 3 separate Euler angles. The rotation matrix, $R$ is based on the separate rotation matrices about each axis, $R_X$, $R_Y$ and $R_Z$ as a multiplication of them according to the convention of approach (left to right or right to left) on rotation.

The data is presented in a hierarchical manner in most motion capture file formats. The local transformation of a bone is obtained using the first part of Equation 1 that describes its orientation within in its local coordinate system, which in turn is subject to its parent's local orientations. To obtain a global matrix transform for a given bone, the local transform needs to be pre-multiplied by its parent's global transform, which itself is derived my multiplying its local transform with its parent's global transform and so on. Equation 2 expresses this combination sequence, where $n$ is the current bone whose parent bone is $n$ - 1 and $n = 0$ is the bone at the root of the hierarchy.

$$M^n_{global} = \prod_{i=0}^{n} M^i_{local}$$

(2).

Motion capture file formats are imposed by the equipment manufacturers. Several formats includes BVH & BVA (associated company: BioVision), C3D (associated company: Biomechanics, Animation and Gait Analysis), DAT (associated company Polhemous) etc.

The BVH format of the motion capture is (shown below) consists of two parts where the first section details the hierarchy and initial pose of the skeleton and the second section describes the channel data for each frame, that is, the motion section shown below. The explanation of the file format and motion data are outlined next as in [107].

```
HIERARCHY
ROOT Hips
{
    OFFSET 0.00 0.00 0.00
    CHANNELS 6 Xposition Yposition Zposition Zrotation Xrotation Yrotation
    JOINT Chest
    {
            OFFSET 0.000000 6.275751 0.000000
            CHANNELS 3 Zrotation Xrotation Yrotation
            JOINT Neck
            {
                    OFFSET 0.000000 14.296947 0.000000
                    CHANNELS 3 Zrotation Xrotation Yrotation
                    JOINT Head
                    {
                            OFFSET 0.000000 2.637461 0.000000
                            CHANNELS 3 Zrotation Xrotation Yrotation
                            End Site
                            {
                                    OFFSET 0.000000 4.499004 0.000000
                            }
                    }
            }
            JOINT LeftCollar
            {
                    OFFSET 1.120000 11.362855 1.870000

                    CHANNELS 3 Zrotation Xrotation Yrotation
                    JOINT LeftUpArm
```

```
            {
                    OFFSET 4.565688 2.019026 -1.821179

                    CHANNELS 3 Zrotation Xrotation Yrotation
                    JOINT LeftLowArm
                    {
                            OFFSET 0.219729 -10.348825 -0.061708
                            CHANNELS 3 Zrotation Xrotation Yrotation
                            JOINT LeftHand
                            {
                                    OFFSET 0.087892 -10.352228 2.178217
                                    CHANNELS 3 Zrotation Xrotation Yrotation
                                    End Site
                                    {
                                            OFFSET 0.131837 -6.692379 1.711456
                                    }
                            }
                    }
            }
    }
    JOINT RightCollar
    {
            OFFSET -1.120000 11.362855 1.870000
            CHANNELS 3 Zrotation Xrotation Yrotation
            JOINT RightUpArm
            {
                    OFFSET -4.708080 2.034554 -1.821179
                    CHANNELS 3 Zrotation Xrotation Yrotation
                    JOINT RightLowArm
                    {
                            OFFSET -0.263676 -10.428555 -0.061708
                            CHANNELS 3 Zrotation Xrotation Yrotation
                              JOINT RightHand
                            {

                                    OFFSET 0.000000 -10.255345 2.178217
```

```
                                    CHANNELS 3 Zrotation Xrotation Yrotation
                                    End Site
                                      {
                                            OFFSET -0.140882 -6.671274 1.711456
                                      }
                            }
                      }
                }
        }
}
    JOINT LeftUpLeg
  {
        OFFSET 3.910000 0.000000 0.000000
        CHANNELS 3 Zrotation Xrotation Yrotation
        LeftLowLeg
        {
                    OFFSET -0.441177 -17.569450 1.695613
                    CHANNELS 3 Zrotation Xrotation Yrotation
                    JOINT LeftFoot
                    {
                            OFFSET -0.043946 -17.197315 -1.478076
                            CHANNELS 3 Zrotation Xrotation Yrotation
                            End Site
                            {
                                    OFFSET 0.000000 -3.933155 5.233925
                            }
                    }

            }
}
JOINT RightUpLeg
{

        OFFSET -3.910000 0.000000 0.000000
        CHANNELS 3 Zrotation Xrotation Yrotation
```

275

```
                    JOINT RightLowLeg
                    {

                            OFFSET 0.437741 -17.622387 1.695613
                            CHANNELS 3 Zrotation Xrotation Yrotation
                            JOINT RightFoot
                            {
                                    OFFSET 0.000000 -17.140001 -1.478076
                                    CHANNELS 3 Zrotation Xrotation Yrotation
                                    End Site
                                    {
                                            OFFSET 0.000000 -4.038528 5.233925
                                    }
                            }
                    }
            }
}


MOTION

Frames: 2

Frame Time: 0.04166667

-9.533684        4.447926 -0.566564 -7.757381 -1.735414 89.207932 9.763572

            6.289016 -1.825344 -6.106647 3.973667 -3.706973 -6.474916

            -14.391472 -3.461282 -16.504230 3.973544 -3.805107 22.204674

            2.533497 -28.283911 -6.862538 6.191492 4.448771 -16.292816

            2.951538 -3.418231 7.634442 11.325822 5.149696 -23.069189

            -18.352753 15.051558 -7.514462 8.397663 2.953842 -7.213992

            2.494318 -1.543435 2.970936 -25.086460 -4.195537 -1.752307

            7.093068 -1.507532 -2.633332 3.858087 0.256802 7.892136

            12.803010 -28.692566 2.151862 -9.164188 8.006427 -5.641034

            -12.596124 4.366460
```

-8.489557       4.285263 -0.621559 -8.244940 -1.784412 90.041962 8.849357

5.557910 -1.926571 -5.487280 4.119726 -4.714622 -5.790586

-15.218462 -3.167648 -15.823254 3.871795 -4.378940 22.399654

2.244878 -29.421873 -6.918557 6.131992 4.521327 -18.013180

3.059388 -3.768287 8.079588 10.124812 5.808083 -22.417845

-15.736264 18.827469 -8.070700 9.689109 2.417364 -7.600582

2.505005 -1.625679 2.430162 -27.579708 -3.852241 -1.830524

12.520144 -1.653632 -2.688550 4.545600 0.296320 8.031574

13.837914 -28.922058 2.077955 -9.176716 7.166249 -5.170825

-13.814465 4.309433

The first section of the motion file starts with the keyword HIERARCHY, which is followed on the next line by the keyword ROOT and the name of the bone that is the root of the skeletal hierarchy. For instance, hips is the root of the skeleton as shown in Fig. 1 hips. The ROOT keyword indicates the start of a new skeletal hierarchical structure.

The remaining structure of the skeleton is defined in a recursive nature and use of curly brackets, where any children, are encapsulated in braces, which is demarkated on the previous line with the keyword JOINT (or ROOT in the case of the root bone) followed by the bone's name. Within the definition of each bone, the first line, delimited by the keyword OFFSET, specifies the translation of the origin of the bone with respect to its parent's origin (or globally in the case of the root bone) along the x, y and z-axis respectively.

The keyword CHANNELS in the second line of a bone's definition defines the DOFs for the current bone. The order of that is important for two reasons. First, the order that each channel is seen in the hierarchy section exactly matches the order of the data in the motion section of the file. For example, the motion section of the file contains information for the channels of the root bone in the order defined in the hierarchy, followed by the channel data for its first child, followed by the channel

data for that child and so on through the hierarchy. The second reason to state with regards to the channel ordering is that the concatenation order of the Euler angles when creating the bone's rotation matrix needs to follow the order depicted in the CHANNEL section.

After the OFFSET and CHANNEL lines, the next non-nested lines in the bone definition are used to define child items, starting with the keyword JOINT, however in the case of end-effectors, a special label is used, "End Site", which encapsulates an OFFSET triple that is used to deduce the bone's length and orientation.

The second section of a BVH file denoted with the keyword MOTION as shown above contains number of frames in the animation, frame rate (starting with "Frame Time:" followed by a positive float number that represents the duration of each frame) and channel data (for each bone in the order as defined in the hierarchy) of each line of float values represent an animation frame.

To process the motion capture data the first thing require is to determine each bone's local transform using the first part of Equation 1. Since BVH formats do not contain scaling information, only the rotation and translation matrices are considered to construct the local transform. The rotation matrix, $R$ is constructed by multiplying the rotation data for each different channel axis in the order they appeared in the hierarchy section of the file. For instance, considering the following channel description for a bone:

CHANNELS 3 Zrotation Xrotation Yrotation,

then the compound matrix, $R$ is calculated by the following equation

$$R = R_Z R_X R_Y \qquad\qquad (3).$$

Once the composite rotation matrix is calculated, using a homogeneous coordinate system, the translational components are simply the first 3 cells of the 4$^{\text{th}}$ column of the transform matrix, $M$ as shown in the Equation 4. Usually the root is the only bone

that has per-frame translation data, then the translational components are needed to get the each bone's base offset to the local matrix stack through addition. So $T_x$, $T_y$, and $T_z$ in equation 4.17 represent the summation of a bone's base position and frame translation data.

$$M = \begin{bmatrix} R & R & R & T_x \\ R & R & R & T_y \\ R & R & R & T_z \\ 0 & 0 & 0 & 1 \end{bmatrix}$$  (4).

Using Equation 2 and the local transforms, the global positions for each bone origin can be calculated and from the origin, the bone is drawn using the offset information in the hierarchy section of the file. Equation 5 shows this process for the LeftFoot shown in the above BVH file format, where $v0'$ and $v1'$ are the endpoints of the bone whose local orientation is given by $v$ and $M_i$ are the local transforms of the bones involved in the hierarchical chain. The vector, $[0, 0, 0, 1]^T$ on the right of the first expression in Equation 5, is the local origin of the LeftFoot, which is transformed into its global position by the equation

$$v0' = M_{Hipps}M_{LeftUpLeg}M_{LeftLowLeg}M_{LeftFoot}[0,0,0,1]^T$$
$$v1' = M_{Hipps}M_{LeftUpLeg}M_{LeftLowLeg}M_{LeftFoot}v$$  (5)

# Appendix B: Matlab code to extract the peaks of acceleration profile to Chapter 5 (Section 5.1.3)

This appendix documents the matlab code for extracting the values of the positive peaks of $A_z$ profile in Fig. 5.4(a) during the free swing of the pendulum pivot arm.

```
TIME=(14689:17000)*0.01; %  points from where the swing profile starts

test1(1).data=Hz1_5band_filtered_Z; test1(2).data=Hz1_5band_filtered_Y;
test1(3).data=Hz1_5band_filtered_X;
```

```matlab
Peak1_(1).data=[]; Peak1_(2).data=[];  Peak1_(3).data=[];

Time_peak1_(1).data=[]; Time_peak1_(2).data=[];  Time_peak1_(3).data=[];

LL=length(Hz1_5band_filtered_Z);

for mm=1:3

for pp=1:(LL-1)

    switch(test1(mm).data(pp)<0)

      case 1

      diff_n=abs(test1(mm).data(pp+1))-abs(test1(mm).data(pp));

      if diff_n<0

              Peak1_(mm).data=[Peak1_(mm).data;test1(mm).data(pp)];

        Time_peak1_(mm).data=[Time_peak1_(mm).data;TIME(pp)];

          end

       case 0

         diff_p=abs(test1(mm).data(pp+1))-abs(test1(mm).data(pp));

      if diff_p<0

        Peak1_(mm).data=[Peak1_(mm).data;test1(mm).data(pp)];

        Time_peak1_(mm).data=[Time_peak1_(mm).data;TIME(pp)];

      end

    end

end

end

PEAK1_(1).data=[];TIME_PEAK1_(1).data=[]; PEAK1_(2).data=[];TIME_PEAK1_(2).data=[];

PEAK1_(3).data=[];TIME_PEAK1_(3).data=[];

Ylab1_(1).data='Z'; Ylab1_(2).data='Y'; Ylab1_(3).data='X';

for gg=1:3

for dd=1:length(Peak1_(gg).data)-1

sign_PREVdata=sign(Peak1_(gg).data(dd)); signNEXTdata=sign(Peak1_(gg).data(dd+1));
```

```
if (sign_PREVdata~=signNEXTdata) && (abs(Peak1_(gg).data(dd+1))>abs(Peak1_(gg).data(dd)))

    PEAK1_(gg).data=[PEAK1_(gg).data;Peak1_(gg).data(dd+1)];TIME_PEAK1_(gg).data=[TIME_P
EAK1_(gg).data;Time_peak1_(gg).data(dd+1)];

    end

    end

  N=(1:length(PEAK1_(gg).data));
SCPLOT=scatter(N,PEAK1_(gg).data);set(SCPLOT,'LineWidth',1.5);

  xlabel('Peak data point number','Fontsize',10,'FontWeight','bold','FontName','Times New Roman');

  ylabel('Peak value of sensor recorded
acceleration(g)','Fontsize',10,'FontWeight','bold','FontName','Times New Roman');

  title(Ylab1_(gg).data,'Fontsize',10,'FontWeight','bold','FontName','Times New Roman');

  set(gcf,'Units','centimeters'); afFigurePosition=[1 1 12.5
10.5];set(gcf,'Position',afFigurePosition);figure

    end

  SELECTED_points=2:2:(length(PEAK1_(1).data));posi_peaks=PEAK1_(1).data(SELECTED_poi
nts); % TO USE FOR THE VALUE OF EXPONENTIAL CONSTANT in the equation
```

# Appendix C: Matlab code for non-linear equation of pendulum with moving pivot to Chapter 5 (Section 5.2.2)

This appendix documents the matlab codes (the main program and function) for the solution of non-linear equation of pendulum with moving pivot shown in Equation 5.12.

### Main program

```
x0_B = input('Enter initial angle for backlift (degrees) ');

x0_B = (pi*x0_B)/180;

vx0_B=input('Enter intial angular velocity for Backlift (radians/s) ');

Ti_back=input('Enter the back-lift time ');

t0=0.01;
```

```
Num_point_back=Ti_back/t0;  Tspan_B=(1:Num_point_back)*0.01;

womegP=input('Enter the angular frequency of pivot during back-lift ');

 womegPt=womegP*t0;

b_B=womegPt;

A=input('Enter the value of pivot motion magnitude (driving force) during back-lift ');

initial_x_B=[x0_B,vx0_B,b_B]';

[time_x_B,numtheta_B] = ode23s('pendulumWmpt',Tspan_B,initial_x_B);

 le_B=1.5;

C_B=1.0;

RADI_B=le_B*exp(C_B*numtheta_B(:,1));

 TR_B=input('enter the value of TR for backlift ');

WOMEG_BL=numtheta_B(:,2);

Xaccel_B=RADI_B.*(WOMEG_BL).^2-9.8*cos(numtheta_B(:,1))+TR_B;

SWING_BL=-Xaccel_B./9.8;

THETA_BL=(180/pi)*numtheta_B(:,1);

%%&&&&&&&&&&&&&&&&&&&&&&&&&&&&&&&&&&&&&&&&&&&&&

clear A; clear womegP; clear womegPt;

%############################# FOR SWING

x0=-THETA_BL(length(THETA_BL));

x0 = (pi*x0)/180;

vx0 = input('Enter intial velocity for swing (radians/s) ');

Ti_swing=input('Enter the time of forward swing in second ');

Num_point_swing=Ti_swing/t0;

Tspan_swing=(1:Num_point_swing)*t0;

womegP=input('Enter the angular frequency of pivot during forward swing ');

 womegPt=womegP*t0;

b=womegPt;
```

```matlab
A=input('Enter the value of pivot motion magnitude (driving force) during forward swing ');

initial_x=[x0,vx0,b]';

[time_x,numtheta] = ode23s('pendulumWmpt',Tspan_swing,initial_x);

 Hand_le=0.75;

B=input('Enter the value of radius constant ');

TR_SWING=input('Enter the value of thrust force constant for SWING ');

RADI_SWING=(Hand_le+0.85)*exp(B*numtheta(:,1));

WOMEG_SWING=numtheta(:,2);

Xaccel=RADI_SWING.*(WOMEG_SWING).^2-9.8*cos(numtheta(:,1))+TR_SWING;

SWING=-Xaccel./9.8;

 BACKLIFT_SWING=[SWING_BL;SWING];
T_BACK_SWING=[Tspan_B';Tspan_B(length(Tspan_B))+Tspan_swing'];

THETA_SWING=(180/pi)*numtheta(:,1);

 %&&&&&&&&&&&&&&&&&&&&&&&&&&&&&&&&&&&&&&&&&&&&&&&&&&&

clear A; clear womegP; clear womegPt;

% %############################## FOR RETURN

xF0=THETA_SWING(length(THETA_SWING))-180;

xF0 = (pi*xF0)/180;

vxF0 = input('Enter the angular velocity in return(radians/s) ');

Ti_return=input('Enter the time of recovery in second ');

Num_point_return=Ti_return/t0;

Tspan_return=(1:Num_point_return)*t0;

 womegP=input('Enter the angular frequency of pivot during recovery ');

womegPt=womegP*t0;

bF=womegPt;

A=input('Enter the value of pivot motion magnitude (driving force) during recovery ');

initial_xF=[xF0,vxF0,bF]';

[time_x_F,numtheta_F] = ode23s('pendulumWmpt',Tspan_return,initial_xF);
```

TR_return=input('Enter the value of thrust force constant for return ');

BF=input('Enter the value of radius constant for return ');

Hand_le=0.65;

RADI_return=(Hand_le+0.85)*exp(BF*numtheta_F(:,1));

WOMEG_SWING_return=numtheta_F(:,2);

Xaccel_return=RADI_return.*(WOMEG_SWING_return).^2-
9.8*cos(numtheta_F(:,1))+TR_return;

SWING_return=-Xaccel_return./9.8;

THETA_return_SWING =(180/pi)*numtheta_F(:,1);

%%#################################################################

%%TOGETHER BACKLIFT, SWING, RETURN

BL_angle_EQN=THETA_BL+180;   DR_angle_EQN=180-(THETA_SWING);
RE_angle_EQN=THETA_return_SWING +180;

EQN_angles_ALL=[BL_angle_EQN;DR_angle_EQN;RE_angle_EQN];

SW=[SWING_BL;SWING;SWING_return;];

t_BL=Tspan_B;          t_SWING=Tspan_swing';          t_return=Tspan_return';

t1=t_BL;    t2=t1(length(t1))+t_SWING; t3=t2(length(t2))+t_return;

T_bl_swing_return=[t1';t2;t3];

NCORE_x=accelx_S5(51030:51296);   % sensor recorded x-axis acceleration from data file

T_ncore= (1:length(NCORE_x))*0.01;

plot(T_ncore,NCORE_x,'ko',T_bl_swing_return,SW,'ro');legend('Sensor recorded','Equation estimated',0);

xlabel('Time(s)');ylabel('X-acceleration(g)');

## Function

%function pendulumWmpt.m

function uprime = pendulumWmpt(t,u)

g = 9.8; % acceleration due to gravity

L = 1.0; % length of pendulum is 1 meter

```
A=12;

womegP=0.35;

theta = u(1); % u is the state vector (theta and derivs)

thetadot = u(2);

womegPt=u(3);

womegPtdot=womegP;

uprime(1) = thetadot; % define u1' = u2 = thetadot

uprime(2) = (A*(womegP^2)*cos(womegPt-theta)-g*sin(theta))/L; % define u2'

uprime(3)=womegPt;

uprime=[uprime(1);uprime(2);uprime(3)];
```